Enabling Technologies for Smart Grid Integration and Interoperability of Electric Vehicles

Martinenas, Sergejus

Publication date:
2017

Document Version
Publisher's PDF, also known as Version of record

Technical University of Denmark

Sergejus Martinenas

Enabling Technologies for Smart Grid Integration and Interoperability of Electric Vehicles

PhD Thesis, September 2017

Risø, Roskilde, Denmark

Center for Electric Power and Energy
Department of Electrical Engineering

DANMARKS TEKNISKE UNIVERSITET
Center for Electric Power and Energy
DTU Electrical Engineering

Enabling Technologies for Smart Grid Integration and Interoperability of Electric Vehicles

Teknologier til intelligent integration og interoperabilitet af elbiler i elnettet

PhD Thesis by

Sergejus Martinenas

Supervisors:
Associate Professor Chresten Træholt, Technical University of Denmark
Associate Professor Mattia Marinelli, Technical University of Denmark
Senior Researcher Peter Bach Andersen, Technical University of Denmark

DTU - Technical University of Denmark, Roskilde - September 2017

Enabling Technologies for Smart Grid Integration and Interoperability of Electric Vehicles

This thesis was prepared by:
Sergejus Martinenas

Supervisors:
Associate Professor Chresten Træholt, Technical University of Denmark
Associate Professor Mattia Marinelli, Technical University of Denmark
Senior Researcher Peter Bach Andersen, Technical University of Denmark

Dissertation Examination Committee:
Senior Researcher Oliver Gehrke, Technical University of Denmark
Professor Inmaculada Zamora Belver, University of the Basque Country
Professor Ghanim Putrus, Northumbria University

Center for Electric Power and Energy
DTU Electrical Engineering
Frederiksborgvej 399, Building 776
DK-4000 Roskilde
Denmark
www.cee.elektro.dtu.dk

Tel: (+45) 4525 3500
Fax: (+45) 4588 6111
E-mail: cee@elektro.dtu.dk

Release date: August 2017

Class: Public

Field: Electrical Engineering

Remarks: The dissertation is presented to the Department of Electrical Engineering of Technical University of Denmark in partial fulfilment of the requirements for the degree of Doctor of Philosophy.

ISBN: 000-00-00000-00-0

If we were logical, the future would be bleak, indeed. But we are more than logical. We are human beings, and we have faith, and we have hope, and we can work.

— Jacques Yves Cousteau

Dedicated to My Family

Preface

This thesis is prepared at the Department of Electrical Engineering of the Technical University of Denmark in partial fulfillment of the requirements for acquiring the degree of Doctor of Philosophy in Engineering. The PhD project was funded by COTEVOS EU project and Danish NIKOLA project.

This dissertation summarizes the work carried out by the author during his PhD project. It started on August 1st 2014, and was completed on July 31st 2017. During this period, he was employed by Technical University of Denmark as a PhD student at the Center for Electric Power and Energy (CEE).

The thesis is composed of 6 chapters and 9 attached scientific papers, 8 of which have been peer-reviewed and published, and the other is currently under the review process.

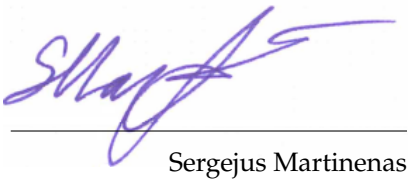

Sergejus Martinenas
August 2017

Acknowledgements

Through the years of this PhD study, I have ventured not alone. Hereby, I would like to thank all of those that accompanied me in this journey.

Firstly, I would like to thank supervisors Prof. Chresten Træholt, Prof. Mattia Marinelli and Dr. Peter Bach Andersen for their trust and opportunity to contribute to transportation electrification research; for all the guidance, productive discussions and constructive feedback. I am especially grateful to Prof. Dr. Don Mattia Marinelli for all the encouragement and everyday help to stay on course, at times when PhD study seemed troublesome.

I want to thank my colleagues Alex, Anders, Andreas, Anna, Antonio, Esteban, Giuseppe, Michel, Venkat, Xue and others. For the interesting discussions, working collaboration, overseas trips to conferences and other fun extracurricular activities :)

Finally, I want to thank my loving family for their unconditional support and patience throughout the years. I owe my success to you.

Sergejus

Frederiksborgvej 399, Building 776
DK-4000 Roskilde
Denmark
August 2017

Table of Contents

Abstract

Conventional, centralized power plants are being replaced by intermittent, distributed renewable energy sources, thus raising the concern about the stability of the power grid in its current state. All the while, electrification of all forms of transportation is increasing the load on the transforming power grid and potentially only contributing to the problem. However, an intelligent integration of EVs into the grid, could not only alleviate potential self induced problems, but also make EVs a vital resource for providing grid services.

This thesis investigates the technical requirements for successful EV integration into the smart grid, as a smart, mobile distributed energy resource. The work is split into three key topics: enabling technologies, grid service applications and interoperability issues.

The current state of e-mobility technologies is surveyed. Technologies and protocols in the full e-mobility architecture, enabling the synthesis between EVs and smart grid, are analyzed for potential gaps. A test system, inspired by the core of the e-mobility architecture, is implemented to enable testing of EVs providing grid services.

The grid services identified in the NIKOLA project, as potentially viable to be provided using EVs, are tested in laboratory- and field experiments. The work shows that EVs can provide a variety of grid services on the distribution- and transmission level, such as improving voltage quality, preventing transformer overloading and frequency regulation.

The issue of interoperability in the field of e-mobility, investigated in the COTEVOS project, is explored. It is concluded, that collective testing of the OEM equipment in testing symposiums, is the best way to ensure interoperability between different OEMs, and to discuss as well as fix the issues in the standard itself.

Altogether, it is demonstrated that the provision of different grid services, using EVs, is technically feasible. While some gaps in standards/protocols still exist, standardization committees are actively listening to inputs from e-mobility research projects to cover them in the new versions. This enables EVs to not only mitigate their own effects on the grid, but also provide value to grid operators, locally as well as system wide.

Finally, it is shown that active integration of EVs into the smart grid, is not only achievable, but is well on its way to becoming a reality.

Resumé

Konventionelle, centrale kraftværker erstattes af de grønne energikilder og det giver store bekymringer for stabilitet af elnettet i dens nyværende form. Samtidig belastningen på det transformerende elnettet øges med stigende tendens til udskift af de konventionalle transport former med de grønne el-transport fx elbiler. Intelligent integration af elbiler i elnettet, kan ikke kun afhjælpe potentielt selvforesagede problemer, men også gøre elbiler mere tilgængelige, i form af deres evne til at tilbyde ydelser til elnettet.

Denne studie har undersøgt de tekniske krav for en vellykket integration af elbiler i fremtidens smart grid, som en smart, mobil distribueret energikilde. Studiet er opdelt i tre hovedemner: elbil teknologier, applikationer til system ydelser i elnettet og interoperabilitetsproblemer.

Den aktuelle tilstand af e-mobility teknologier er undersøgt. Teknologier og protokoller i den fulde e-mobility arkitektur, som muliggør foreningen af elbiler og smarte elnettet, analyseres med henblik på at klarlægge potentielle mangler. Et test setup, der er inspireret af kernen i e-mobility arkitekturen, er implementeret for at kunne muliggøre yderligere tests af elbiler, der leverer ydelser i elnettet.

De systemydelser der er blevet identificeret i NIKOLA projektet, hvor elbiler har vist sig særligt nyttive i relation til elnettet, er testet i laboratorie- og felt eksperimenter. Studiet har påvist, at elbiler kan tilbyde en række ydelser på distribution- og transmissionsniveaue, som for eksempel spændingskvalitet, modvirking af transformator overbelastning og frekvensregulering.

Spørgsmålet om interoperabilitet inden for e-mobility, hvilket blev undersøgt i COTEVOS-projektet, er udforsket. Det er konkluderet, at den kollektive test af OEM-udstyr i test symposier, ikke kun er den bedste måde hvorpå man kan sikre interoperabilitet mellem forskellige OEM'er, også at diskutere og løse problemerne i standarderne.

I det hele taget er det påvist, at levering af forskellige systemydelser til elnettet, ved hjælp af elbiler, er teknisk muligt. Selv om nogle mangler i standarder og protokoller stadig eksisterer, er standardiseringsudvalgene åbne for input fra de forkellige e-mobility forskningsprojekter og dækker emnerne i de nye versioner. Dette gør det muligt for elbiler ikke kun at afbøde deres egne effekter på elnettet, men også give værdi til netoperatører lokalt og system bredt.

Endeligt er det påvist, at aktiv integration af elbiler i smart grid ikke kun er en muligthed, men allerede er i færd med at blive en realitet.

Nomenclature & Acronyms

η	Efficiency
E	Energy
I	Current
P	Active power
Q	Reactive power
t	Time
U	Voltage
AC	Alternating Current
BRP	Balance Responsible Party
CCS	Combined Charging System
CP	Charging Point
CP	Control Pilot
CPO	Charge Point Operator
DC	Direct Current
DER	Distributed Energy Resource
DR	Demand Response
DSM	Demand Side Management
DSO	Distribution System Operator
EMSP	E-Mobility Service Provider
EV	Electric Vehicle
EVSE	Electric Vehicle Supply Equipment
GFCI	Ground Fault Circuit Interrupter
GSM	Global System for Mobile Communications
HP	Heat Pump

HV High Voltage

HVAC Heating, Ventilation, and Air Conditioning

ICE Internal Combustion Engine

ICT Information and Communication Technology

IEC International Electrotechnical Commission

LV Low Voltage

MV Medium Voltage

OCA Open Charge Alliance

OCHP Open Clearing House Protocol

OCPI Open Charging Point Interface

OCPP Open Charging Point Protocol

OEM Original Equipment Manufacturer

OICP Open InterCharge Protocol

OpenADR Open Automated Demand Response

OSCP Open Smart Charging Protocol

PE Protective Earth

PFR Primary Frequency Regulation

PHEV Plugin Hybrid Electric Vehicle

PLC Power Line Communication

PP Proximity Pilot

PV Photo-Voltaic

PWM Pulse Width Modulation

RCCB Residual Current Circuit Breaker

RES Renewable Energy Sources

SGU Smart Grid Unit

SOC State Of Charge

TSO Transmission System Operator

V2G Vehicle to Grid

VUF Voltage Unbalance Factor

Chapter 1
Introduction

1.1 The age of change

The world is facing a threat from accelerating climate change happening due to greenhouse gas from humanity's emissions. These emissions are coming from multiple sectors: energy, transportation, agriculture and manufacturing. The emissions from the energy sector could be eliminated by switching to emission free renewable resources e.g. wind and solar. This is already well underway with current installed wind power capacity of 153.7 GW by 2016 in Europe alone and 486.8 GW in the whole world [1], [2]. The solar - photo-voltaic (PV) power capacity is also on the rise growing by 75 GW in 2016 to a total of around 300 GW of solar power installed in the world [3]. Combining this with transportation electrification, the emissions from transportation sector would also be significantly reduced.

1.1.1 Power grid transformation

There are two main transformation trends happening in the modern electrical power system: distributed renewable energy integration and smart grid roll out. Both of these trends are well depicted in Figure 1.1.

The power grid is transforming from fossil fueled power plants to distributed renewable energy resources. These energy resources are intermittent in nature: PVs are generating energy during daytime and wind generators energy output is rather stochastic. Introduction of renewable energy resources transforms the grid from centralized energy generation to a more distributed one. This is due to distribution of suitable geographical locations for installation of renewable energy power plants and convenience of local installation e.g. rooftop PV. While this change improves ecological situation, it brings new challenges to the power system. As renewable energy resources are so intermittent, their introduction increases the need for ancillary services to maintain the balance between the production and consumption in the power grid.

The other transformation coming to the power grid is a roll out of the smart grid. The main idea of the smart grid is that the whole grid is interconnected, not only with power cables, but also with communication links. It is done by introduction of modern communication technologies to gather information and coordinate the actions of loads and power generation units. This upgrade enables previously uncontrolled large loads to participate in maintaining grid stability by providing Demand Response (DR) as Distributed Energy Resources (DER). These loads could be electric heaters, heat pumps, refrigerators, lighting installations and newly appearing electric vehicles.

Figure 1.1: Smart grid concept [4].

1.1.2 Transportation electrification

In our daily lives, the most obvious source of pollution and greenhouse gas emissions, is transportation. Therefore, all modes of transportation except for rockets are currently being electrified. Diesel trains are being phased out as rail networks are electrified. Aerospace industry is actively researching and developing hybrid and fully electric airplanes [5]. But perhaps the loudest transformation is happening in automotive industry. Under stricter environmental regulations almost every automotive Original Equipment Manufacturer (OEM) is currently producing hybrid and Plugin Hybrid Electric Vehicle (PHEV) versions of their current models. Additionally, most OEMs have announced new fully electric vehicle models coming in the near future. This way conventional gasoline powered vehicles are being slowly replaced by EVs charged with electricity from the power grid. Incentives are already driving EV sales up in some countries, such as Norway - where 9 of 10 best selling vehicles in 2016 were electric or electrified [6]. Other countries announced their commitment to ban ICE vehicle sales in the future.All this makes the automotive companies, traditionally producing ICE vehicles, pledge to switch to only electric and electrified model manufacturing in near future [7].

All in all, the goal is clear - complete electrification of the transportation sector, combined with electrical grid powered by renewable energy sources would ensure emissionless transport.

1.1.3 The fusion of two industries

Transportation and energy are two sectors that generate a large portion of global green house gas emissions [8]. Transition to distributed, intermittent energy sources and additional load of electric

vehicles poses a serious threat to the stability of the electric power grid [9]. These concurrent changes, happening in conservative energy and automotive industries, are bringing them together.

Transportation electrification brings challenges and opportunities to the transforming power grid. On one hand uncontrolled charging of large number of EVs could make grid infrastructure overloading - a daily issue. On the other hand, smart integration of the same EVs into smart grid could alleviate this effect and help grid stability [10–13]. The flexibility and controllability of the EVs, combined with possibility of vehicle to grid (V2G) capability, make them almost ideal Mobile Distributed Energy Resource (Mobile DER).

1.2 Thesis objectives

The main motivation behind the integration of EVs into smart grid operation is their potential ability to provide grid services. The objective of this thesis is to investigate the technologies that enable EVs to effectively become a Mobile DER. The focus of the work, is put on overview, implementation and testing of the technologies. A handful of technologies is chosen for implementation, it is done to identify technical gaps and propose solutions for filling them. Additionally, interoperability issues, in the field of e-mobility, are investigated. The main research question this work strives to answer is: ***What is technically required to convert an EV into a smart mobile distributed energy resource?*** This main question can be divided into components presented as the following sub-questions:

- Which grid services could EVs provide? Provision of grid services is the main motivation for integrating EVs into the smart grid. Implementation and testing of various grid services is done to identify the best suiting candidates for provision by EVs.
- What are technical requirements for EV aggregation? One of the key components to successful EV integration is aggregation. It is essential to identify the communication requirements between EVs and aggregators.
- What is current EV technology development status in relation to grid integration? It is important to assess the status of e-mobility development before proceeding with integration into smart grid.
- Which technical challenges are still present for EV integration? After assessing the current state of technology and its applications, key barriers for future development are identified and solutions are proposed.
- What are prerequisites and current state of EV interoperability? EV interoperability should be considered when integrating EVs for grid applications to enable a greater variety of resources to provide grid services. In this work, interoperability issues are not discussed as part the technical assessment of e-mobility. The issues were investigated as a part of the COTEVOS project, thus the results are presented in a self contained chapter.

1.3 Thesis outline and research contributions

Following this introduction, the thesis is organized into 5 self-contained chapters and 9 papers attached as appendices A through I. Chapters 3, 4 and 5 outline and expand on the contributions of the attached papers and summarize them.

Chapter 2 describes the motivation for EV integration into the smart grid and background on grid power operation. The chapter reasons splitting the work into 3 main parts and why the focus is put on grid services, enabling technologies and interoperability issues. The enabling technologies for EV integration are the main focus of the work. These technologies are then divided into 3 main topics: hardware, communication and control. The topics are briefly outlined and explored in detail in the next chapter.

Chapter 3 reviews the enabling technologies used for smart grid integration of EVs i.e. hardware, communication and software. Each technology is described in detail in a corresponding section with references to the state of art and papers. The requirements for enabling technologies are compared to state of contemporary e-mobility technologies. This comparison allows to identify technical shortcomings in the technologies. Additionally, design and implementation of a test system based on a real e-mobility architecture is presented. The chapter expands on the contents of Pub. A and Pub. B.

Chapter 4 presents the application of previously described technologies to provide grid services. The services are chosen from the grid service catalog developed in the NIKOLA project. The chosen services are implemented in the developed test system. In addition to theoretical description, an experimental validation of multiple services is presented and analyzed. The results presented in papers Pub. C, Pub. D, Pub. E, Pub. F, Pub. G and Pub. H are included in the chapter.

Chapter 5 turns the focus onto the existing and potential interoperability issues in e-mobility infrastructure and possible solutions for it. The chapter is mostly based on the work performed for COTEVOS project. The findings and results e.g. test procedures designed for interoperability testing, are presented and expanded upon. The chapter expands on the contents of the deliverable Pub. I.

Finally, in Chapter 6, conclusions are stated with a summary of thesis contributions and outline for future work.

1.4 Publications

The relevant publications included in this work are the following:

A S. Martinenas, S. Vandael, P.B. Andersen, B. Christensen, "Standards for EV charging and their usability for providing V2G services in the primary reserve market," in *Proceedings of International Battery, Hybrid and Fuel Cell Electric Vehicle Symposium (EVS29)*, Montreal, Canada, IEEE, Jun. 2016.

B S. Martinenas, "Implementation of E-mobility architecture for providing Smart Grid services using EVs," in *International Battery, Hybrid and Fuel Cell Electric Vehicle Symposium (EVS30)*, Stuttgart, Germany, 2017.

C S. Martinenas, M. Marinelli, P.B. Andersen, C. Træholt, "Implementation and Demonstration of Grid Frequency Support by V2G Enabled Electric Vehicle," in *Proceedings of the 49th International Universities Power Engineering Conference (UPEC) 2014*, Cluj-Napoca, Romania, Sep. 2014.

D M. Marinelli, S. Martinenas, K. Knezovic, P.B. Andersen, "Validating a centralized approach to primary frequency control with series-produced electric vehicles," in *Journal of Energy Storage*, Vol. 7, 2016, p. 63–73.

E S. Martinenas, M. Marinelli, P.B. Andersen, C. Træholt, "Evaluation of Electric Vehicle Charging Controllability for Provision of Time Critical Grid Services," in *Proceedings of the 51st International Universities Power Engineering Conference (UPEC) 2016*, Coimbra, Portugal, Sep. 2016.

F M. Rezkalla, A. Zecchino, S. Martinenas, A. Prostejovsky, M. Marinelli, "Comparison between Synthetic Inertia and Fast Frequency Containment Control Based on Single Phase EVs in a Microgrid," in *Applied Energy*, 2017.

G S. Martinenas, K. Knezovic, M. Marinelli, "Management of Power Quality Issues in Low Voltage Networks using Electric Vehicles: Experimental Validation," in *IEEE Transactions on Power Delivery*, IEEE, 2016.

H S. Martinenas, A.B. Pedersen, M. Marinelli, P.B. Andersen, C. Træholt, "Electric Vehicle Smart Charging using Dynamic Price Signal," in *Proceedings of IEEE International Electric Vehicle Conference (IEVC) 2014*, Florence, Italy, Dec. 2014.

I T.M. Sørensen, M.B. Jensen, S. Martinenas, "Analysis of needs for on-going or incipient standards. Design of Round Robin tests and results of the performed tests. Recommendations for existing standards" in *COTEVOS project deliverable*, Feb. 2016

Other publications

In addition to the main publications attached to this thesis, the author, during his PhD study, has contributed to multiple other publications and a patent application. However, these publications were not directly included in the thesis as they are not directly related to the primary objective, or they are partially covered by other presented papers. The following publications have also been written and contributed to during the PhD study:

- A.B. Pedersen, P.B. Andersen, T.M. Sørensen, S. Martinenas, "IPC No. B60L 11/18 A I. Electric vehicle battery charging controller (Patent No. WO2016087150.)", 2016
- A.B. Pedersen, S. Martinenas, P.B. Andersen, T.M. Sørensen, H.S. Høj, "A Method for Remote Control of EV Charging by Modifying IEC61851 Compliant EVSE Based PWM Signal," in *Proceedings of IEEE International Conference on Smart Grid Communications (SmartGridComm) 2015* Miami, Florida, Nov. 2015.
- A. Kieldsen, A. Thingvad, S. Martinenas, T.M. Sørensen, "Efficiency Test Method for Electric Vehicle Chargers," in *Proceedings of International Battery, Hybrid and Fuel Cell Electric Vehicle Symposium (EVS29)*, Montreal, Canada, Jun. 2016.
- A. Thingvad, S. Martinenas, P.B. Andersen, M. Marinelli, B. Christensen, O.J. Olesen, "Economic Comparison of Electric Vehicles Performing Unidirectional and Bidirectional Frequency Control in Denmark with Practical Validation," in *Proceedings of the 51st International Universities Power Engineering Conference (UPEC) 2016*, Coimbra, Portugal, Sep. 2016.
- K. Knezovic, S. Martinenas, P.B. Andersen, A. Zecchino, M. Marinelli, "Enhancing the Role of Electric Vehicles in the Power Grid: Field Validation of Multiple Ancillary Services," in *IEEE Transactions on Transportation Electrification*, 3(1), 201 - 209. DOI: 10.1109/TTE.2016.2616864

- M. Rezkalla, S. Martinenas, A. Zecchino, M. Marinelli, E. Rikos, "Implementation and validation of synthetic inertia support employing series produced electric vehicles," in *Proceedings of CIRED 2017*, Glasgow, Scotland, Jun. 2017.

Chapter 2
Synthesis between EVs and the Smart Grid

In this chapter, the background provision of grid services is presented, which is the core motivation for smart grid integration of EVs. Then the requirements for converting the EV into a mobile DER and reasoning for splitting the thesis into 3 main parts: grid services, technical requirements and interoperability issues, are presented. The topics are then briefly outlined and explored deeper in the corresponding chapters.

2.1 Why integrate EVs into the smart grid?

The reason for integrating EVs into the power grid is their potential ability to provide grid services. Grid services are an essential part of daily grid operation. To better understand the need for these services, the power grid structure, operation and ongoing transformation is explained.

2.1.1 Grid structure and operation

Typical electrical power grid has two levels: transmission and distribution as shown in Figure 2.1.

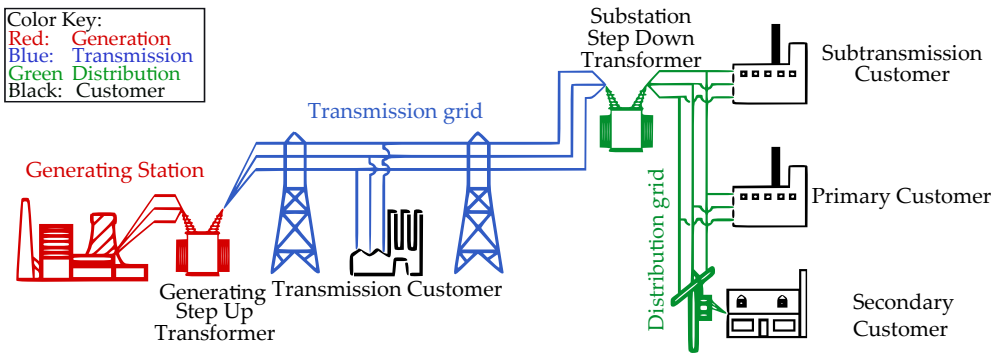

Figure 2.1: Simple diagram of electricity grids [14].

The power produced by the generation plants is fed through the step up transformers to the high voltage transmission lines. These lines are historically designed to cover long distances between centralized generation and remote consumption areas as well as for interconnection between different areas. Once the transmission line reaches the area where the power will be consumed it is transformed into Medium Voltage (MV) distribution lines. Some bigger consumers, such as industrial scale manufacturing plants, are connecting directly to the MV lines. Typical MV lines, distribute the power in the area by transforming down into local Low Voltage (LV) feeders that then connect to individual consumers.

2.1.2 System wide services

The power grid is a balanced system, where generation and consumption are in constant equilibrium. This means that the power produced by the generators should always equal to the power consumed by the grid loads. That is ensured by forecasting the consumption that generators then follow. The predictions of the consumption profile are not always accurate, the bigger power imbalances are accommodated by balancing energy sources. This balancing energy is usually imported from adjacent areas or local power plants that are contracted to increase their power production on demand. The smaller, more immediate fluctuations in the power balance of the grid are resolved by system-wide ancillary services - frequency regulation reserves.

The frequency regulation reserves in the power grid are typically divided into the three levels: primary, secondary and tertiary. An overview of the activation timing of different frequency regulation reserves is shown in Figure 2.2.

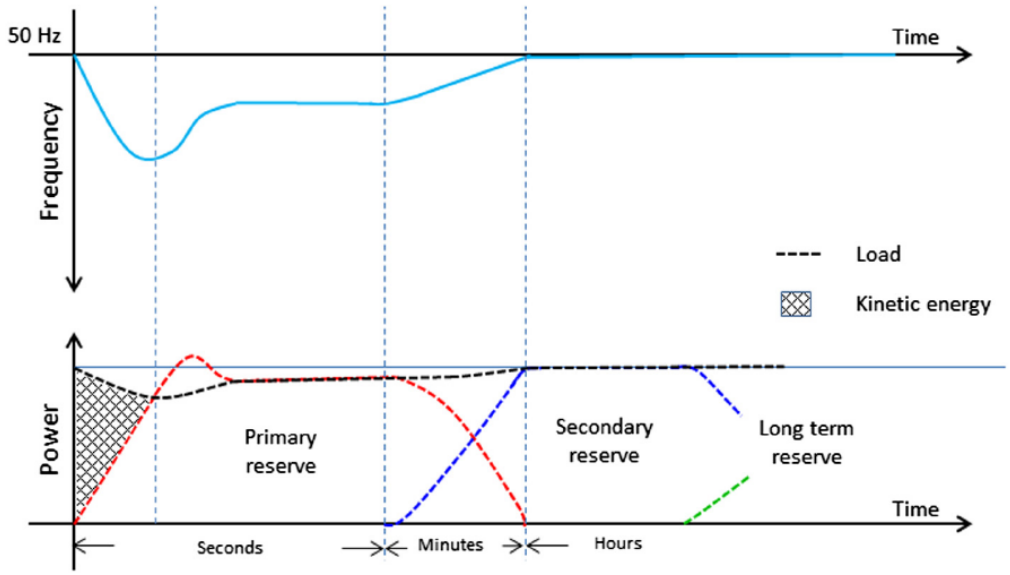

Figure 2.2: Frequency reserve activation timing [15]

Primary reserve is always active and has a short activation period. Secondary reserve is activated to relieve the primary reserve providers and restore frequency to the nominal value. Tertiary reserves are used in exceptionally long and large frequency deviations, to aid the secondary reserve in restoring the frequency to normal operating value.

Typically, each synchronous region ,or even each Transmission System Operator (TSO), has their own definition of the frequency regulation services. A unique feature of the Danish power grid is that it is located in two separate synchronous regions as shown in Figure 2.3.

DK1 region that covers Jylland (continental part of Denmark) and island of Fyn is connected to the rest of continental Europe. DK2 region covers the islands of Sjælland and Bornholm connected to other Nordic countries. Each region has three levels of frequency regulation reserves, defined by a Danish TSO Energinet.DK [16].

DK1 region has frequency regulation reserves like the rest of Europe:

Figure 2.3: Danish power grid areas DK1 and DK2

- Primary Reserve - restores balance between production and consumption, stabilizing the frequency close to 50Hz. The regulation is automatic, power output of the reserve is controlled by frequency deviation, with a small permitted deadband.
- Secondary Reserve - is enabled during major operational disturbance. It is used to indirectly restore frequency to 50Hz followed by stabilization by primary reserve. It also serves the purpose of releasing the activated primary reserve. The regulation is automatic and controlled by a signal from Energinet.dk.
- Manual Reserve - is used to restore system balance, acting as a tertiary reserve. It is activated manually from Energinet.dk's Control Center.

DK2 region also has similar reserves like the rest of the Nordic power system:

- Normal Operation Reserve - ensures that production and consumption equilibrium is restored. The regulation is automatic and controlled by frequency deviation, without deadband.
- Disturbance Reserve - is a fast reserve, activated in the event of major system disturbances. It is started automatically in the event of sudden frequency drop under 49.9Hz and remains active until frequency is restored or manual reserve takes over.
- Manual Reserve - is used to restore system balance, acting as a tertiary reserve. It is manually activated from Energinet.dk's Control Center.

2.1.3 Distribution grid services

Distribution grid have been historically designed for unidirectional power use - bringing electricity to the consumer. Therefore most grids have a radial topology, sometimes with quite long feeder lines. An example distribution feeder topology is shown in Figure 2.4.

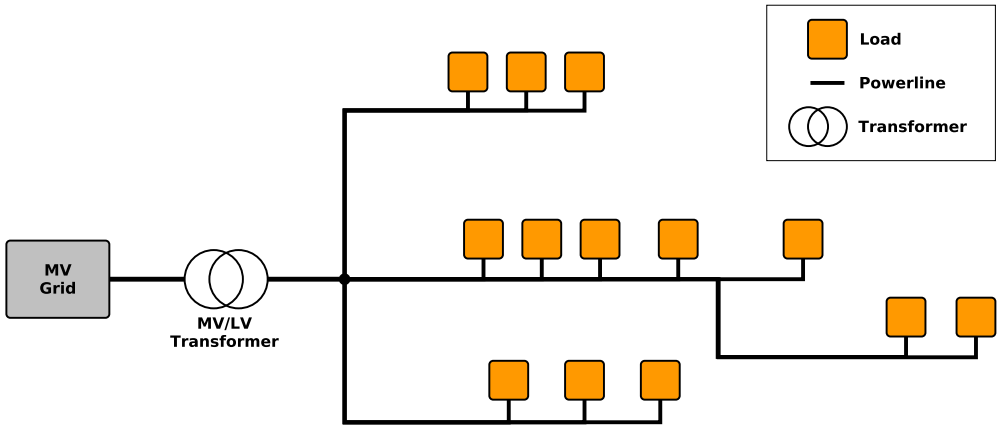

Figure 2.4: LV feeder topology example.

Traditionally, distribution grids are planned and upgraded for increasing customer demand, thus avoiding power supply security issues. While transmission system operators have a well defined set of services they procure to keep the grid stable, the distribution grid operators do not. That however does not mean that distribution grid has no problems or is unregulated. Local distribution grids also suffer from problems usually called power quality issues. Common power quality issues that occur in the local grids are over- and under-voltages, voltage unbalances, transformer and line overloading. These problems are typically created by high loads unevenly distributed among three phases.

Figure 2.5 illustrates the voltage drop that naturally occurs on a long feeder line due to its internal impedance.

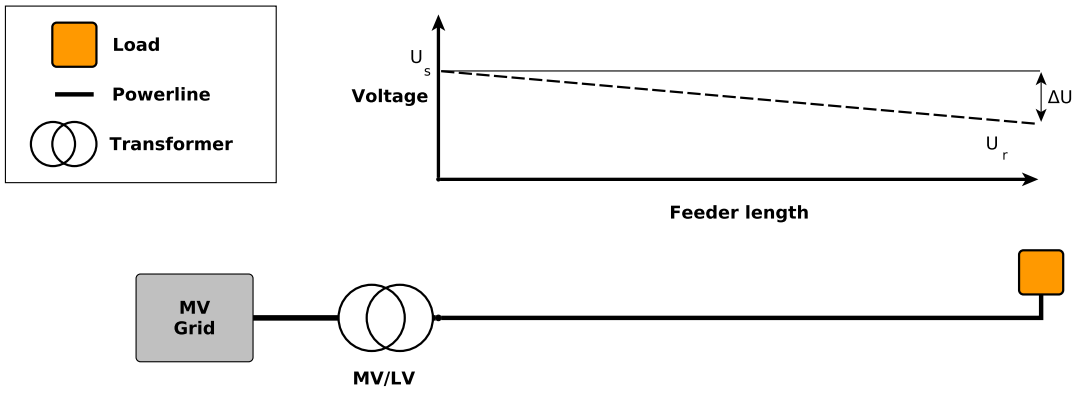

Figure 2.5: Voltage drop on a long feeder line.

The voltage drop on a feeder line can be calculated from:

$$\Delta\hat{U} = (R + jX) \cdot \hat{I} = (R + jX) \cdot \frac{(P + jQ)^*}{\hat{U}_r^*} = \frac{RP + XQ}{\hat{U}_r^*} + j\frac{XP - RQ}{\hat{U}_r^*} \tag{2.1}$$

As the voltage angle between the nodes is very small, the imaginary part can be disregarded and the voltage drop simplifies to:

$$\Delta U \approx \frac{RP + XQ}{U_r} \tag{2.2}$$

As can be seen from the resulting equation the magnitude of the voltage drop is directly proportional to the increasing active power load on the feeder.

In the unbalanced 3 phase systems heavy loading of one or two of the phases might bring under-voltage issues to those phases. At the same time the voltage on the remaining lightly loaded phase is raised and could potentially create over-voltage problem. In Europe the limits of the distribution grid voltages are defined by EN50160 [17].

2.1.4 Smart grid services

Until recently, in the conventional power grid, only large generators and industrial consumers communicated with the grid operators. However, this is recently changing with the transformation into the age of smart grid. The power grid that utilizes communication technologies to communicate with and control the distributed energy resources is called smart grid. Introduction of distributed energy resources and new communication technologies now enable for every consumer to be connected not only to the power grid but also communicate with the grid operators. Such communication and control technology enables the consumers to participate in grid services. In particular the focus is put on the integration of local generation units like rooftop PV and bigger household loads e.g. electric heaters, heatpumps and electric vehicles.

There are several reasons to integrate EVs in the smart grid, making them a sort of a mobile distributed energy resource. Firstly, controlling the charging of large numbers of EVs using smart algorithms would reduce local grid congestion and power quality issues [18, 19]. The issues potentially created by the EVs themselves, being large number of high power loads. Secondly, as a flexible, controllable and fast energy resource, EVs could provide ancillary services for the grid e.g frequency regulation.

An extensive amount of research shows that controllable EVs could be used for lowering the impact on the power system or providing different ancillary services e.g. frequency regulation, congestion reduction, voltage quality improvement [10, 13, 20–24]. Table 2.1 displays some of the chosen grid services that EVs could potentially provide, identified in NIKOLA project [25].

Table 2.1: List of grid services from the NIKOLA service catalog [26].

Service Group	**Name**	**Exist in Denmark**
System-wide	Frequency Regulation	Yes
	Fast Frequency Regulation	No
	Secondary Regulation	Yes
	Tertiary Regulation	Yes
	Synthetic Inertia	No
	Smart Charging	Yes
Distribution grid	Mitigation phase unbalance in LV feeder	No
	Islanded microgrid and black start	-
	MV-LV transformer line overloading	No
	Voltage quality improvement in LV feeder	No

Grid services were divided into two grid levels described earlier. While most system wide services were inspired by their existing counterparts, distribution services were developed from the commonly occurring issues and grid codes.

All services were given an implementation priority, based on available technology as well as relevance to current and near future issues in Danish grid.

Grid services marked with high priority were implemented in experimental validations during this PhD study. Implementations and test results are discussed in detail in Chapter 4 and corresponding attached papers.

2.2 EV as a smart mobile distributed energy resource

Enabling EVs to provide grid services requires converting them into a distributed energy resource. There are technical and regulatory requirements to transform EVs into mobile DER in smart grid. This thesis is focusing on the technical requirements, while regulatory challenges are only mentioned.

Regulatory requirements for EV integration as grid service providers are:

- Permission to provide services by aggregated units - many grid operators currently allow grid service provision only by large centrally located units. Aggregation of large numbers of EVs would allow for providing the same service even with the distributed fleets.
- Revision of distribution grid regulations for EVs. As relatively new household loads EVs have no grid regulation requirements (besides feeder power capacity) to be connected to the grid. As they are large loads and could potentially worsen power quality issues in the local grid, appropriate grid code for EVs should be developed. This grid code could be inspired by existing PV inverter regulations, as they had to undergo a similar process.
- Establishment of incentive schemes for grid service provision, especially relevant for distribution grid services. As it is evident from numerous trials, monetary incentive is the best way to motivate EV users to participate in grid service provision.

On the technical side, to integrate a distributed energy resource, specifically an EV, into the smart grid there are three main technical requirements:

Controllable hardware - EVs have three main components: electric drivetrain, energy storage and auxiliary electronics. The large batteries and high power controllable chargers are the main parts that make EVs interesting for grid integration. Built-in AC chargers and an optional capability to be connected to an external DC charger can be found in every modern EV.

Communication channel - even minimal EV to EVSE communication is a necessary part of the charging standards (e.g. IEC 61851, IEC 15118, CHAdeMO). Majority of modern charge points also have communication links (e.g. GSM, wireless or cable connection) to the charge point operator for maintenance and control purposes. These and other communication links to the higher level actors are vital for EV to grid integration.

Control software - a large number of connected and controllable EVs can be managed by a single centralized entity usually called EV aggregator. It implements the control strategy and sends power set-points for individual vehicles.

These three requirements are discussed in detail in Chapter 3. There, the EV hardware capabilities are overviewed, contemporary e-mobility communication standards are presented and analyzed for compliance. Additionally a controller architecture based on these standards is presented.

The controller is then implemented for a variety of system-wide and distribution grid services, that EVs could provide, in Chapter 4.

Additional requirement that is often overlooked is interoperability. Interoperable equipment and infrastructure greatly increases scale on which the grid integration of EVs could be applied. The issue of interoperability in e-mobility context is discussed in Chapter 5.

Chapter 3

Enabling technologies: hardware, communication and control

Integration of electric vehicles into smart grid raises the need for corresponding technologies. This chapter overviews and describes the technologies used for smart grid integration of EVs. The essential enabling technologies can be divided into three categories: hardware, communication and control. Firstly, physical infrastructure components are described to give the necessary technical background. Secondly, communication infrastructure and requirements identified during the PhD study are presented. This is followed by relevant descriptions of communication protocols. Once all of the relevant protocols are introduced, the results of their analysis to fit for use in EV integration with the grid services is presented. Thirdly, after reasoning about the need for EV aggregation, multiple versions of the control architectures developed during the PhD study are described.

3.1 What are EVs made of?

Before diving into the grid applications of EVs it is essential to familiarise with the design of an electric vehicle. Figure 3.1 shows an grid connected EVSS that is connected to an EV. The diagram is focusing on the power electronics components of the EV.

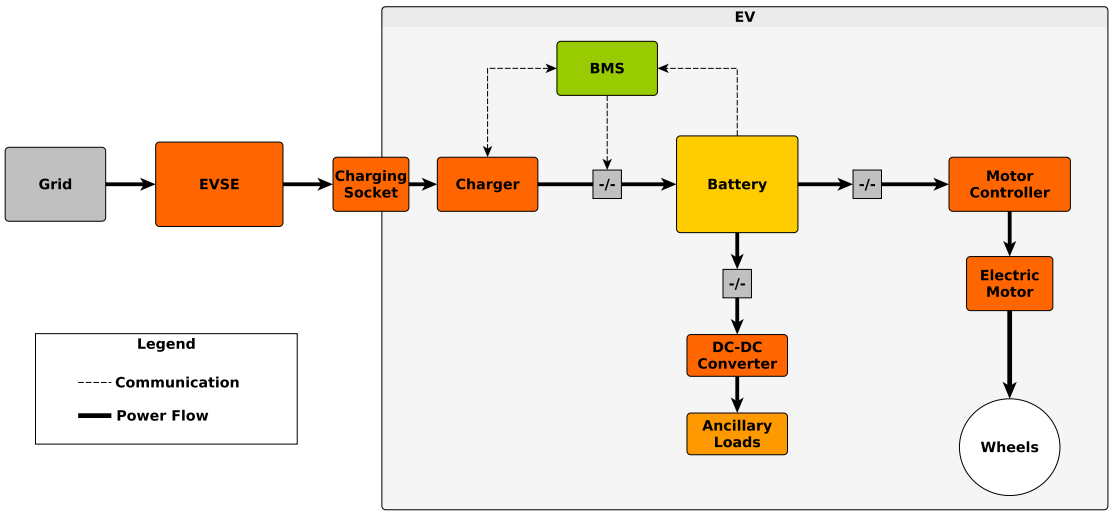

Figure 3.1: EV connected to an EVSE, with detailed view of the EV power electronics components.

The colors in this and following component diagrams depict the function of the component: Green - microcomputer based control electronics aka controllers; Red - power electronics components; Yellow - batteries; Grey - grid and safety breakers.

Electric vehicle powertrain is simple and can be split into 3 main parts: drivetrain power electronics, energy storage and auxiliary power components. Typical contemporary EV uses 3 phase AC motor, which is powered by a motor inverter. The speed and power of the motor is controlled by the inverter via changing the frequency and amplitude of the 3 phase AC signal. The inverter generates this 3 phase AC signal from DC power coming from the vehicle battery.

Vehicle battery is the biggest and heaviest part of the vehicle powertrain, it stores all the energy required for vehicle operation. The battery is monitored and protected by a Battery Management System (BMS) that keeps battery operating in the safe operating area. Typically the battery is charged by a built-in charger that is basically an AC-DC converter. The battery is also charged when vehicle is slowing down, by the effect known as regenerative braking. In this case the electric motor becomes an AC generator and the inverter converts this back to the DC energy that is fed back into the battery.

Auxiliary power electronics are typically powered from an auxiliary 12V battery, that in turn is charged from the main battery via DC-DC converter.

From the perspective of smart grid, EVs are viewed as a mobile distributed energy resource or simply a battery on wheels. Therefore two main components of the EV are of interest: battery and charger, which will be examined closer next.

3.1.1 Battery

Modern EVs typically use high voltage lithium-ion batteries of varying chemistries as a main energy storage. The most common battery chemistries are lithium-manganese with nickel-manganese-cobalt(LMO/NMC) blend and nickel-cobalt-aluminum(NCA). EV battery packs are made of hundreds or even thousands of individual battery cells connected in series and/or parallel configurations. This is done due to the fact that individual lithium-ion cell voltage ranges around 3.7 V, but the motor inverters are designed for input voltage of hundreds of volts. The cells come in different shapes and sizes e.g. cylindrical (18650 or 2170 standard) or rectangular as shown in Figure 3.2.

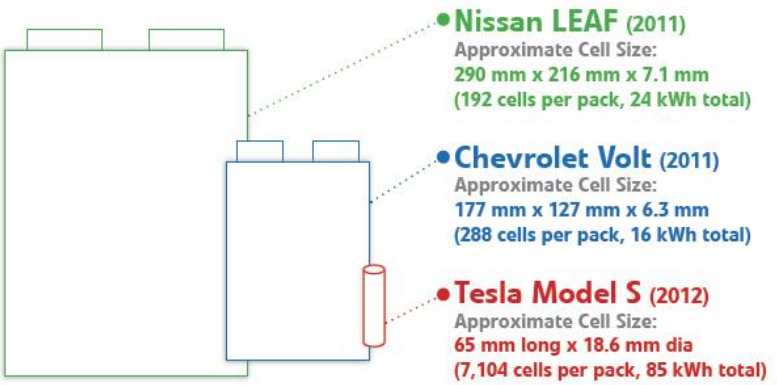

Figure 3.2: Comparison of battery cell sizes [27].

Once the cells are assembled into a battery pack, the voltage range from a few hundred to around 400 V. Future EV models are planning to use battery packs with voltages as high as 800 V to enable higher charging powers without increasing charging current.Contemporary OEM EV battery pack capacities range from 16 to 100 kWh providing from 100 to over 500km range. The battery is managed by a battery management system which tries to keep the battery cells inside safe operating area by monitoring their voltage, current and temperature among other parameters.

3.1.2 Charger

Two types of chargers are typically used for EVs - onboard AC chargers and external DC chargers also called fast chargers. The names of Alternating Current (AC) and Direct Current (DC) charger come from the type of the current that is used in the charging plug.

AC charging

Most electric vehicles currently in the market come with a build-in AC charger that allows the user to charge the vehicle almost anywhere as long as at least a simple electrical socket and cable adapter is available. Figure 3.3 displays a most common EV charging architecture in the e-mobility field - an AC charging setup.

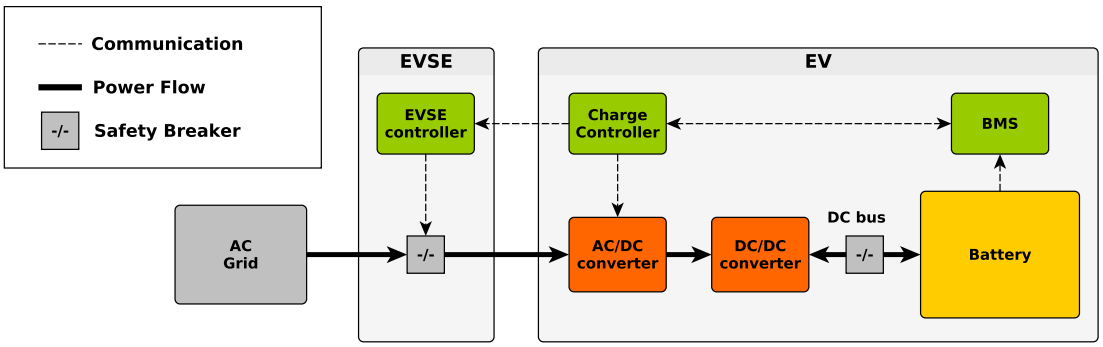

Figure 3.3: Electrical AC charging architecture.

The setup consists of a grid connected EVSE that is connected to an EV via charging cable. Once the EV is connected and ready to charge, the grid breaker inside the EVSE is closed. The AC power then flows to the vehicle where it is converted to DC current that charges the battery. The charging cable between the EV and EVSE has a simple communication link for ensuring safe charging process. This link uses a simple analog signal based communication from IEC 61851 standard or more advanced Power Line Communication (PLC) according to IEC 15118 standard. Finally, an EVSE typically has a communication channel to a Charge Point Operator (CPO).

Figure 3.4 shows a charging point made by DTU, mostly from available industrial components.

This charging point is using Phoenix Contact EVSE Controller to support IEC61851 standard and a Beaglebone Black microcomputer as a communication controller that connects the EVSE to CPO using OCPP protocol. Typical charging spot also includes electrical protection components like short circuit breaker/fuse, a residual-current circuit breaker (RCCB) (also known as ground fault circuit interrupter (GFCI)) and an EVSE controlled relay that connects the EVSE charging socket to the grid. It should be noted that it is common to use EVSE and Charging Point as interchangeable terms, although they do not mean exactly the same thing. An EVSE represents a single supply equipment interface, therefore a Charging Point contains one or more EVSEs in it.

Figure 3.4: Example Mode 3 charging point.

DC charging

In addition to onboard charger, most EVs also support one of a few of DC charging standards. DC chargers place the actual charging power electronics outside the car, thus allowing it to be bigger and support higher charging powers. Therefore DC chargers are often called DC fast chargers. All DC chargers connect directly to the battery and provide DC power flow controlled by a BMS. Three most popular DC charging standards are: CHAdeMO, Combined Charging System (CCS) and Tesla Supercharger.

Figure 3.5 shows a common DC fast charging setup.

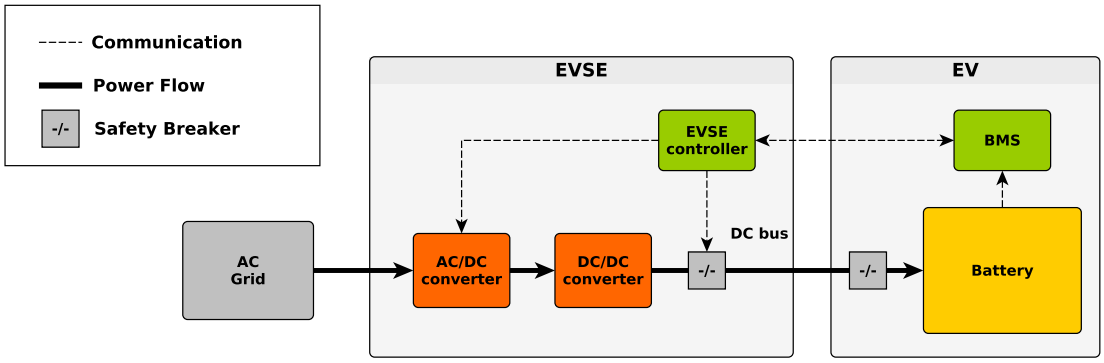

Figure 3.5: Electrical DC charging architecture.

Similarly to the AC charger, this setup also consists of the grid connected EVSE. However, the AC to DC power conversion happens in the EVSE, instead of the EV. Once the EV and EVSE are connected by a charging cable and the secure connection is confirmed by the high level communication as well as multiple safety pins on the connector, the charging of the battery starts. In the DC fast charging case the EVSE connects directly and charges the EV battery under supervision from the vehicle BMS. This entails exchange of charger and vehicle battery parameters as specified by IEC 61851-23 and IEC 61851-24.

V2G

Vehicle to Grid (V2G) is an ability of an electric vehicle to supply power back to the power grid. Just like with charging technologies, there are two main ways to enable vehicle to grid capability in the EV: AC and DC.

AC V2G requires built-in inverter capability inside the vehicle charger, where DC V2G requires the use of an external bidirectional DC charger that just directly connects to vehicle battery using fast charging DC connector. The following are three (two AC and one DC) V2G architectures currently used in EV grid applications.

Vehicle to grid implementation inside the vehicle also known as AC V2G is more complicated to implement. Figure 3.6 shows an AC V2G architecture, where bidirectional charger is built into the vehicle.

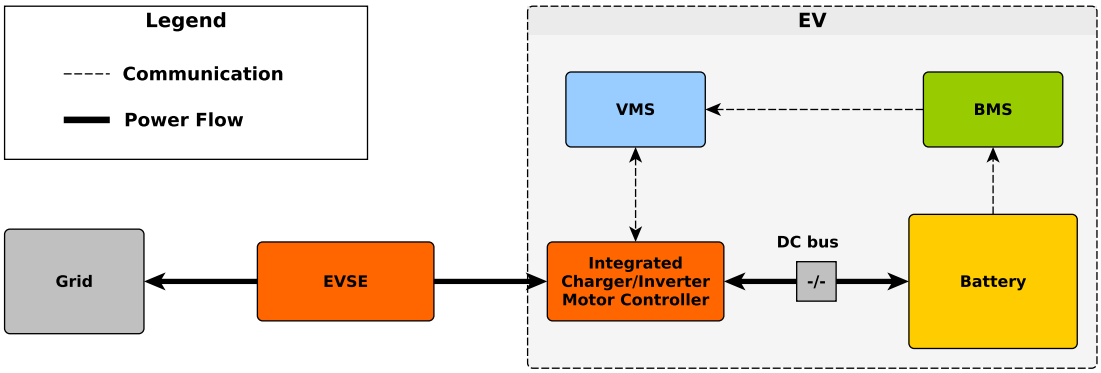

Figure 3.6: V2G architecture for integrated charger/inverter e.g. AC Propulsion eBox.

Here the EV powertrain is more complex as it was designed with bidirectional grid power flow in mind. This approach allows for a compact power electronics unit (PEU) size, but more complicated electronics and increased production costs. One could also notice a vehicle management system (VMS) on the figure, it is responsible for coordinating the actions between user, BMS and PEU. Example vehicles with such powertrain produced by AC propulsion are AC propulsion eBox and BMW Mini-E [28]. Both of these vehicles were used in University of Delaware grid integrated vehicle studies [29].

Figure 3.7 shows another AC V2G architecture where charger and inverter are separate, thus relying on relays to switch between charging and discharging modes.

This way almost any EV could be retrofitted to enable AC V2G capabilities, by adding an inverter and Inverter Management System (IMS). This solution requires sacrificing some storage space to

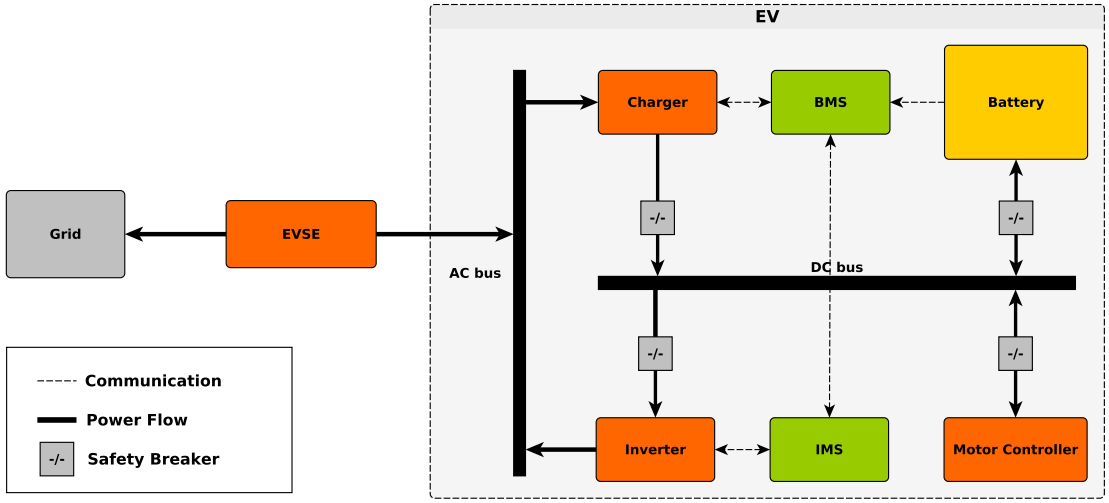

Figure 3.7: V2G architecture for retrofitted EV, adding the inverter for V2G capability.

fit an inverter and extra switching relays. Such method is not currently used in any commercial vehicles but implemented in an experimental converted Citroen C1 EVs used in NIKOLA project.

Figure 3.8 shows a common V2G architecture utilizing a bidirectional DC charger as a V2G interface.

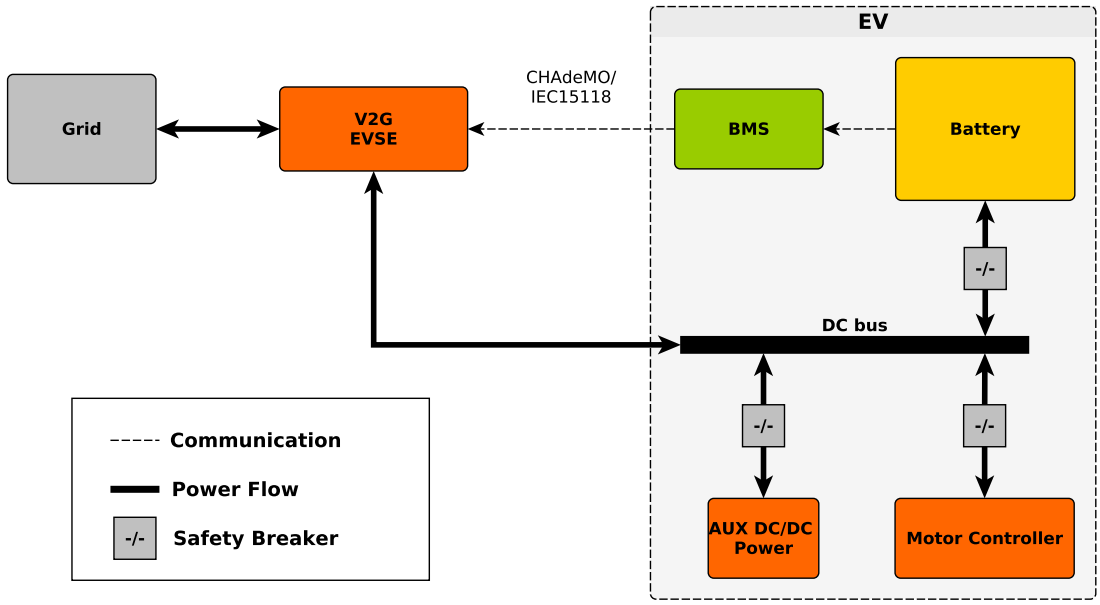

Figure 3.8: V2G architecture for bidirectional off-board DC charger e.g. ENEL V2G charger (CHAdeMO)

In this case, the vehicle only plays a role of a battery which DC charger directly connects to.

Having a charger outside of the vehicle also allows for easier implementation of V2G technology. This way there is no need to add or modify the hardware inside the EV, but merely update the

BMS firmware to allow reverse power flow on a DC charging connector. This approach is already implemented in CHAdeMO protocol as a part of CHAdeMO V2X technology [30]. V2X means vehicle to anything, allowing vehicles to supply power to stand-alone loads or islanded houses.

Figure 3.9 is showing 10kW bidirectional ENEL DC fast charger from Parker project, connected to PSA iOn and providing primary frequency regulation to DK2 grid.

Figure 3.9: 10kW ENEL DC V2G charger connected to PSA iOn EV providing frequency regulation for DK2 grid.

As discussed previously, DC fast chargers connect directly to the EV battery, so the process of using V2G charger is identical to using any other DC fast charger. Therefore every vehicle that supports DC fast charging e.g. using CHAdeMO protocol, can be used for V2G services after a BMS firmware update.

Important characteristics of chargers for grid service provision are: response time, efficiency, power step and ramping rate [18, 31].

Wireless charging

Another type of charging that is currently being actively developed and would free EV users from fiddling with cables is wireless charging. There are two main development paradigms in wireless charging: dynamic and static. Dynamic wireless charging enables vehicle to recharge while it is moving over a series of coils integrated under the road surface [32]. Static wireless charging is meant for vehicle recharge while it is parked [33].

Wireless charging has rather obvious pros:

- Does not require any cables - park and charge, which greatly simplifies charging process.
- Reduces the battery size requirement - in case of dynamic wireless charging, as the vehicle is constantly being recharged while driving.
- Future proof - easy to automate using self driving EVs. Integration of robotic actuators in the conventional cabled charging points is much more complicated than just parking in a precise position.

Unfortunately, with the current state of technology it also has a few cons:

- Low efficiency - requiring precise positioning.
- Limited power - due to coil size limitations and available power electronics [34].
- Safety concerns - nearby humans and animals could be affected by strong EM fields.
- High installation costs - especially for dynamic charging systems.
- Lack of standards - a few communication and hardware safety standards are being developed, but none have been completed yet.

Wireless charging is still in the early development stages, but it is already considered a future of e-mobility. Additionally, it is investigated if static bidirectional wireless charging could be used to provide grid services [35–37].

3.2 Communication in e-mobility

E-mobility is a very broad term that includes all of the electric transportation means. In this work, e-mobility is focusing on the particular type of electric vehicle - electric car. First charging points for EVs were mostly stand alone, later on with the advent of public charging infrastructures charging point operators came into play. Maintenance and control of large, spread out charging infrastructure required communication channels to each charging point. This development in the charging infrastructure also brought opportunities for integration between EVs and the power grid. Therefore, communication in e-mobility is becoming a very important topic.

3.2.1 E-mobility architecture

Figure 3.10 shows the e-mobility architecture inspired by the results of the COTEVOS project [38]. In the figure, e-mobility infrastructure and high level actors are depicted in blue and green respectively. The power grid and energy market related actors are depicted in grey and orange respectively. The hexagonal shapes represent the physical actors e.g. EV, EVSE and grid.

The diagram shows the communication and interaction links between the individual actors. The highlighted part in red shows the essential e-mobility structure for grid integration of EVs. Here the EV and EVSE pair is the device providing a grid service. The CPO and EMSP in this case operate and facilitate the aggregation of the vehicles as well as interface to the grid operator.

3.2.2 Actors in e-mobility architecture

As shown in the Figure 3.10, there are many actors in e-mobility architecture. The roles of these actors are described below.

EV, OEM and User

Perhaps the most important actor in the whole infrastructure is the electric vehicle together with the user. The EV provides transportation to the user and potential service to the grid. The services are enabled by the flexibility of the user coming from his/hers daily habits. The Original Equipment Manufacturer (OEM) of the vehicle plays important role as a technology enabler. The OEM is making and servicing the machine that is both comfortable to use and including the features that could aid the grid.

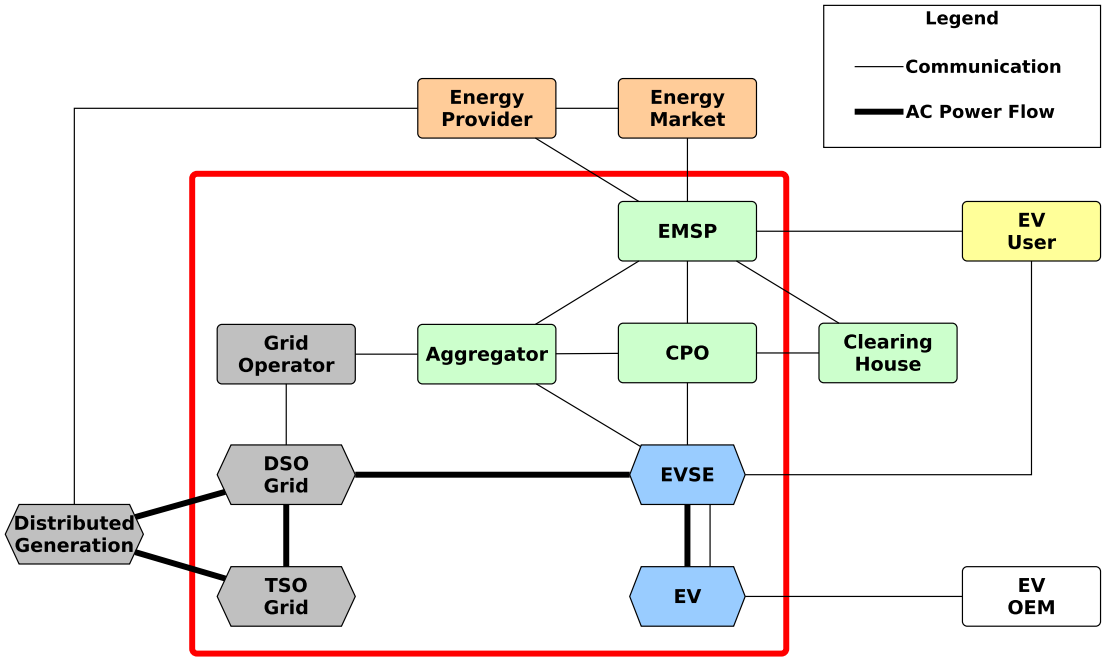

Figure 3.10: E-mobility architecture.

EVSE

Electric Vehicle Supply Equipment (EVSE) plays the role of the physical interface between the EV and the power grid. It also often includes a communication channel to the CPO and a grid operator.

CPO

The role of the Charge Point Operator (CPO) is to operate and maintain a network of charging points.

EMSP

While a CPO and E-Mobility Service Provider (EMSP) is often the same entity in the current e-mobility applications, it is important to distinguish their difference. EMSP is meant to handle communication and billing towards the EV user and clearing house.

Clearing House

The role of the Clearing House is to facilitate automatic clearing of billing processes produced by charging at different charging service providers. The actor is inspired by the clearing house present in mobile telecommunication industry.

Energy Market

Energy market is a commodity market where energy trading is happening. In the context of e-mobility, it refers to electricity market.

Energy Provider

Also known as energy supplier or energy utility, it often shares the responsibility as a local grid operator.

Grid Operator, Generation and Grid

The entity that operates and maintains the grid. Transmission grids and grid stability are usually maintained by a TSO, whereas local distribution grid and power quality is usually maintained by a DSO.

Aggregator

An actor that is not explicitly shown on the e-mobility architecture, but is very important for integration between EVs and the grid. EV aggregator is responsible for aggregating large numbers of EVs, into a virtual power plant or virtual battery, to provide grid services.

3.2.3 Communication in e-mobility architecture

As mentioned before, a vital technical requirement for EV integration in a distributed smart grid is communication. All the communication links between e-mobility and grid operation actors were presented in Figure 3.10. There are a few mainstream communication standards and specifications that enable EV integration as a DER [39]. These standards/specifications are reviewed for relevant communication links shown in the e-mobility architecture. Figure 3.11 shows only the main actors of e-mobility architecture with communication protocols between them.

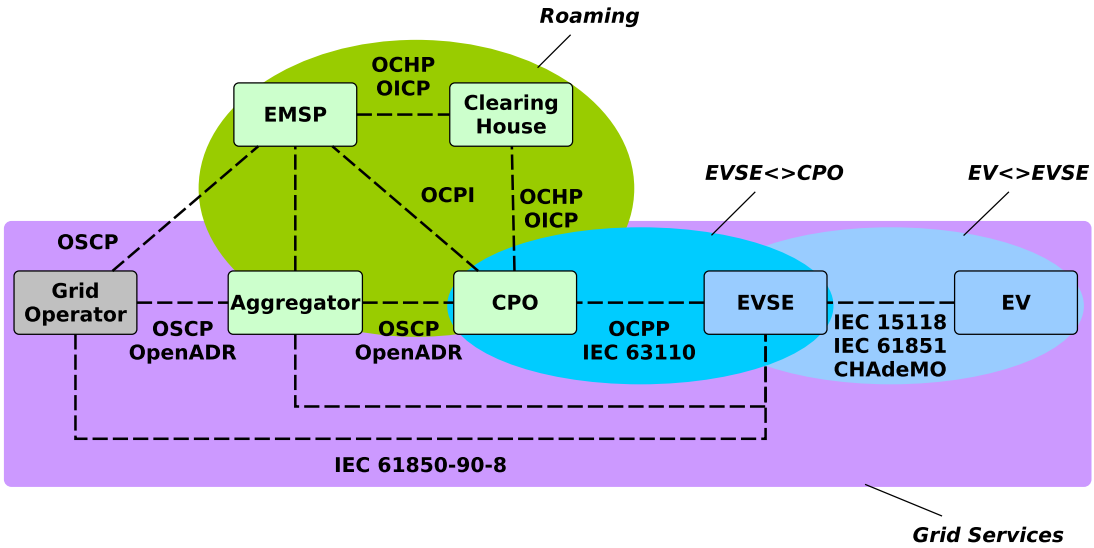

Figure 3.11: Main e-mobility architecture with communication protocols.

The diagram highlights the main areas of the communication protocol analysis:

EV-EVSE - communication between the vehicle and the charging point.

EVSE-CPO - communication between the charging point and the charge point operator.

Roaming - communication protocols enabling roaming services for EV users. Involved actors are: EMSP, Clearing House and CPO.

Grid service communication - communication protocols essential for grid service provision, focusing on grid operator and aggregator communication. Involved actors: EV, EVSE, CPO, Aggregator, Grid Operator.

As can be seen in the diagram, an EV aggregator has been added to the picture to clarify its location and communication links.

3.2.4 Communication requirements

For implementation of intelligent control (for grid services or smart charging) the aggregator needs to gather as much information as possible from individual EVs. The parameters can be divided into three groups: essential, quality-improving and optional parameters. The essential parameters are necessary to provide any kind of grid service. Essential parameters are:

(Dis)Charging power limits - in kW usually the numbers are symmetrical in V2G case

Available energy in the battery - in kWh or state of charge in % could also work if the battery size is known

Indication of plugged-in car - helps determining if the charging point is occupied

Vehicle Identification Number - or any other unique user/vehicle identification

Quality-improving parameters mostly improve the user experience and service availability predictions of the aggregator. Quality-improving parameters are:

Required energy for driving - essential parameter for user comfort and flexibility estimation

Departure time - greatly improves available flexibility estimation

Optional parameters are could be to enable future functionality like driving pattern prediction or battery degradation estimation. Optional parameters are:

Car make and model - useful in estimating battery size and charging power limitations

Odometer reading - for driving pattern identification

Battery temperature - for minimizing battery degradation

Additionally, to provide grid services an aggregator needs information about the local grid, that service providing EVs are connected to:

Voltage - at the EVSE, preferably with knowledge of the EVSE location on the feeder

Charging current - actual charging current of the EV for a feedback loop

Line current limit - essential for providing congestion management

Frequency - as input for a frequency regulation service, could be measured by a centralized measurement device as long as all the vehicle are in the same synchronous area

Now the communication protocols for each area will be described and analyzed for fulfillment of communication requirements.

3.2.5 EV to EVSE communication

While the history of modern EVs is just over a decade old, multiple disagreements about charging plug design also led to quite a few communication standards between EV and EVSE.

IEC 61851

The IEC 61851 is considered to be the main EV to EVSE communication standard for AC charging, the US counterpart of this standard is called SAE J1772. It defines the basic physical and safety requirements to enable EV charging. A typical Type 2 EV connector is shown in Figure 3.12.

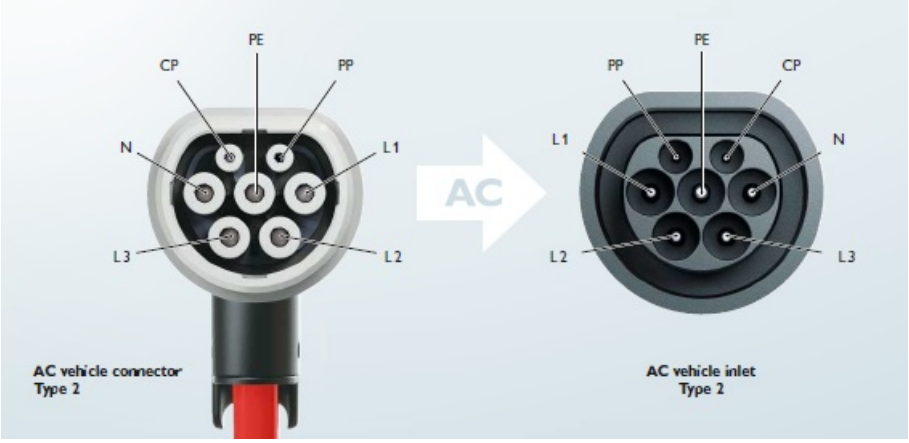

Figure 3.12: Type 2 EV plug [40].

This plug contains 3 phase power pins: L1, L2 and L3; a neutral pin N; protective earth pin PE; proximity pilot pin PP for cable identification; and a control pilot pin CP for communication.

The standard uses one pin, called control pilot (CP) to communicate between the vehicle and EVSE. The communication is analog - simple low level pulse width modulation (PWM) signal and voltage levels. Figure 3.13 illustrates signaling on CP pin between EV and EVSE during a typical IEC 61851 charging session.

It also shows the relevant events in the sequence and timing constrains for those events.

The sequence of events presented by numbers in Figure 3.13 is described as follows:

1. Before the vehicle is connected, an EVSE sets a +12V constant signal on the pilot pin. This state is called A.
2. After the vehicle has connected, the voltage on the pin drops to 9V due to a resistor in the vehicle, that creates a voltage divider with the EVSE. This state is called B.
3. The EVSE start a PWM signal generator of 12V and 1kHz frequency. The duty cycle of the PWM signal is indicating the maximum charging current in amperes the EV can charge with.
4. Vehicle indicates its readiness to charge by closing a switch S2 which connects another resistor inside an EV, thus dropping the CP signal voltage to 6V. This indicates the transition to state C. If the voltage drops to 3V, that means the vehicle is requesting ventilation for charging, due to possible fumes coming from the battery. The vehicle ready state with ventilation is called state D.

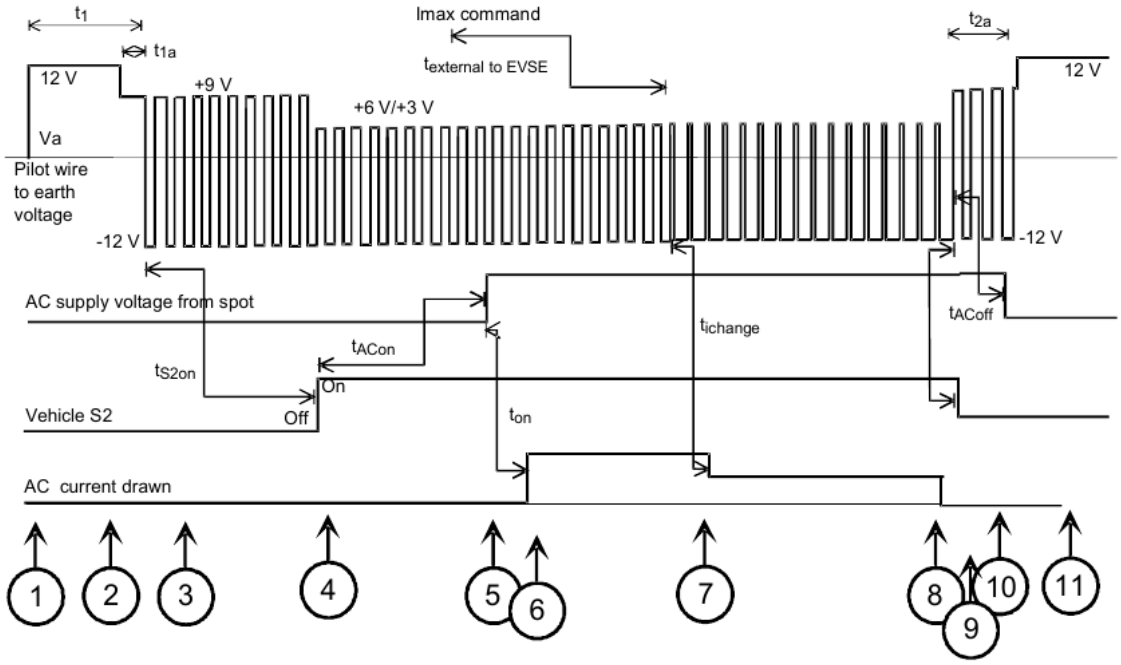

Figure 3.13: IEC 61851 signaling diagram from [41].

5. EVSE closes the grid contactor, enabling the vehicle to charge. If the vehicle is in state D, the contactor is only closed once the ventilation is started.
6. The EV starts drawing current from the grid.
7. The charging current limit can be dynamically adjusted by changing the duty cycle of the signal and the vehicle has to respond within 5 seconds. The conversion between charging current and duty cycle values is described in Table 3.1.
8. Vehicle finishes charging.
9. Vehicle switches to state B indicating readiness to disconnect from the EVSE.
10. The grid contactor is opened after EVSE detects vehicle request to disconnect (state B).
11. Vehicle is disconnected from the EVSE. The CP signal returns to 12V - state A.

The important timing considerations in the Figure 3.13 are the following:

t_{ACon} - beginning of AC power supply top the EV after detecting state C or D, maximum 3 s.

$t_{externaltoEVSE}$ - modification of PWM signal duty cycle in response to an external command to the EVSE, maximum 10 s

$t_{ichange}$ - change of charging current following the change in the duty cycle of the PWM signal on CP line, maximum 5 s.

t_{ACoff} - stop charger current draw, maximum 3 s.

Table 3.1: Maximum charging current conversion table

Duty cycle	Maximum current
Value < 3%	Not allowed
3% ≤ value ≤ 7%	Digital communication
7% < value < 8%	Not Allowed
8% ≤ value < 10%	6A
10% ≤ value ≤ 85%	Current = value x 0.6A
85% < value ≤ 96%	Current = (value - 64) x 2.5A
96% < value ≤ 97%	80A
Value > 97 %	Not Allowed

Other timing constrains are not considered as most of them have no maximum limit and are not important to EV charging process from grid service perspective.

Figure 3.14 illustrates a visual representation of a PWM duty cycle conversion to a maximum charging current described in Table 3.1.

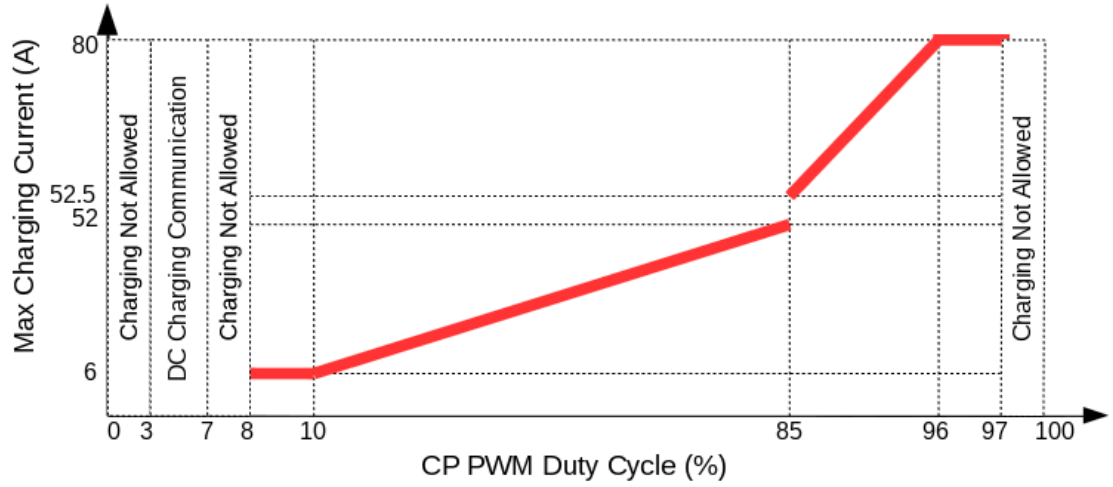

Figure 3.14: IEC 61851 PWM duty cycle to maximum charging current conversion graph [41].

The pin in the charging cable indicating the presence of the plug - it is called plug present (PP) pin. This pin contains a resistor connecting to protective earth (PE) pin. The value of this resistor indicates the maximum current rating for that cable e.g. 16A, 20A, 32A or 63A.

Initial design of the standard did not enable high level digital communication, an extension of this standard was made - IEC 61815-1 Edition 3 Annex-D. This annex extends the physical layer of the standard on EV and EVSE sides and adds minimal higher level communication descriptions [42].

IEC 61851 has been described in such detail due to its importance in the implementations of experimental validations presented in Chapter 4.

ISO/IEC 15118

The need for proper high level communication standard for EV to EVSE communications has fueled the development of IEC 15118 standard. It closes the gap in communication requirements

between EV and EVSE, creating a digital information transfer channel between EV and EVSE. The standard builds on top of the IEC 61851, which is used as a fallback option if either party does not support the new protocol. A major part of the IEC 15118 is based on, and is interoperable with the German DIN 70121 specification. The support for digital communication is indicated by the EVSE with 5 % duty cycle in the IEC 61851 initialization state. The communication link is then established using powerline communication (PLC) on top of the PWM signal running on the CP pin [43]. This enables high level communication to take place, which is based on TCP/IP network setup with possible security features like transport layer security (TLS). The standard enables a plug and charge mode, which does not require user interaction with the charging spot, besides just plugging in the vehicle.

Figure 3.15 shows the 5 layers of the standard.

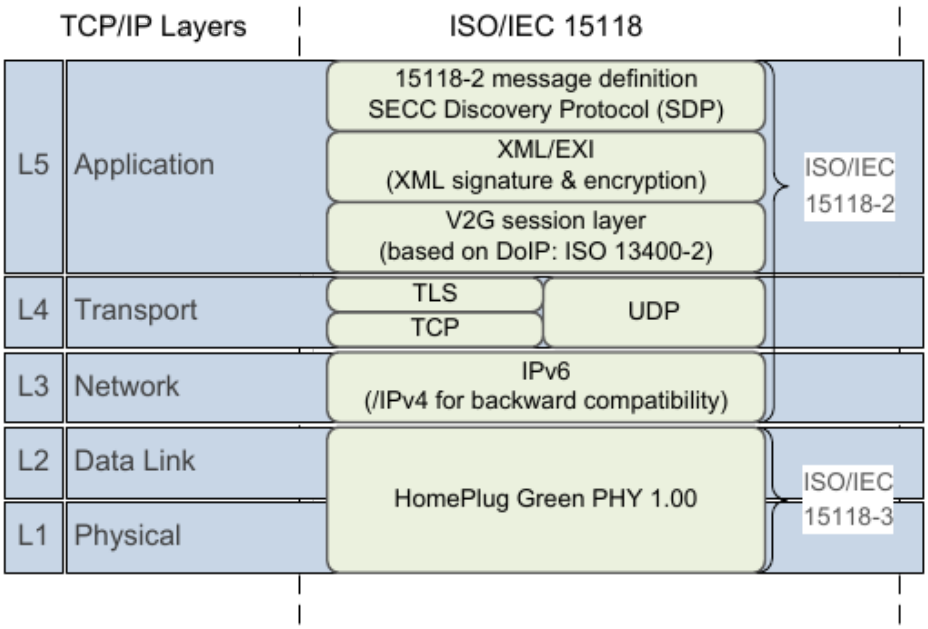

Figure 3.15: IEC 15118 layers [44].

As can be seen in Figure 3.15, the physical layer of the standard (described in IEC 15118-3) is based on HomePlug Green PHY specification used in household range extending WiFi power sockets [45], [46]. On top of the physical layers lies a fairly common IP network stack with options for secure communication i.e. TLS encryption. Finally, topmost is the application layer (described in 15118-2) that enables the main functionality of the standard (described in 15118-1) [47, 48]. IEC 15118 application layer includes the exchange of many information objects that are missing from other communication protocols e.g. state of charge. Although many of them are optional, they have potential to support existing and future e-mobility and grid services. Current implementations of the standard include such features as charging scheduling and identification for automated billing. Use cases of the standard (described in 15118-1) describe important features for grid service provision such as reactive power compensation and V2G support, to be implemented in the future revisions of the standard.

Figure 3.16 shows the typical message exchange between an EV and EVSE during a normal charging session.

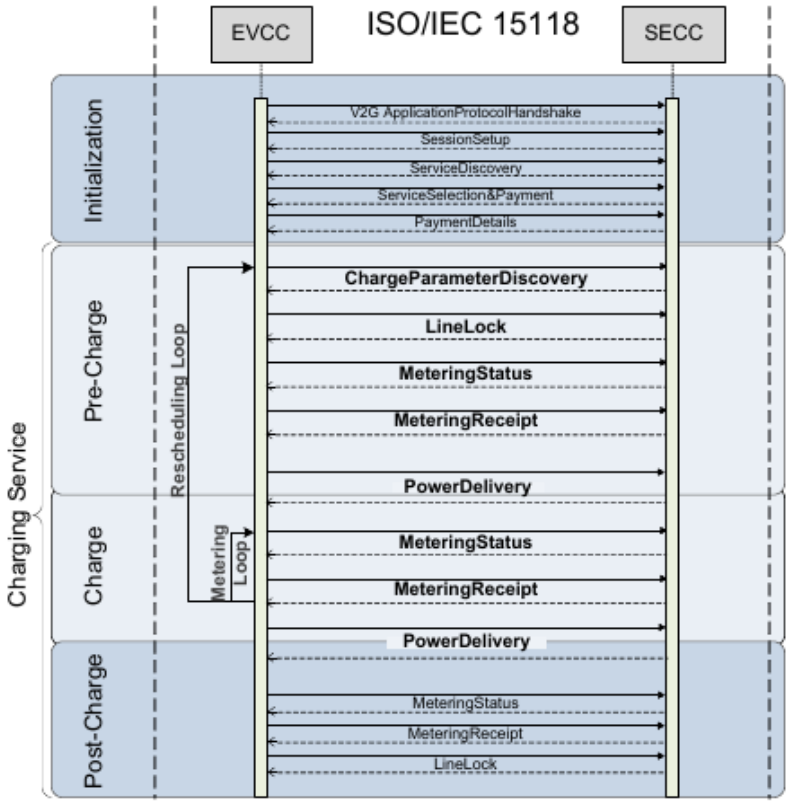

Figure 3.16: IEC 15118 messages during a normal charging session [44].

As seen in the sequence diagram, every interaction is initiated by the EVCC. Such communication paradigm, combined with the relatively long timing limits between rescheduling requests create a barrier for using IEC 15118 for time sensitive grid service provision.

Figure 3.17 shows the design schematics for IEC15118 testing and development system.

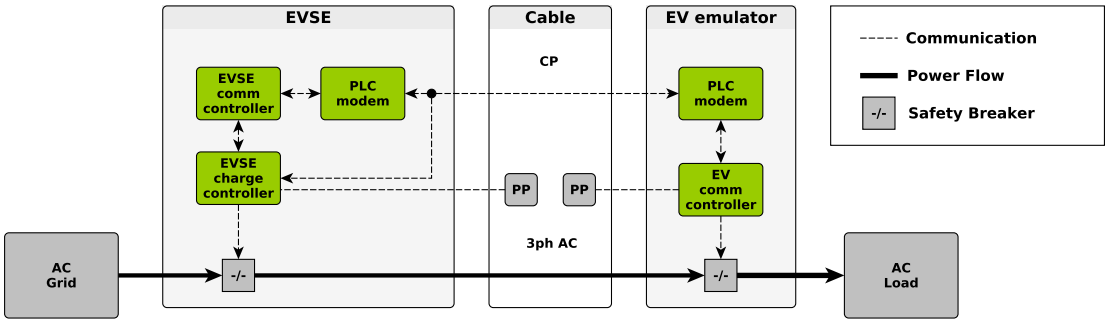

Figure 3.17: IEC 15118 testing hardware schematics.

It closely resembles a typical IEC 61851 based AC charging setup presented earlier.

The DTU IEC 15118 development system is based on INSYS Powerline GP PLC modems that use Qualcomm QCA7000 chip that enables PLC link. The EVSE box contains Phoenix Contact

EVSE controller that is set to digital communication mode. This means that on vehicle plug in and charge initialization, it indicates to the EV that digital communication is available by 5 % PWM signal on CP pin. Each INSYS PLC modem is connected to a Beaglebone black microcomputer via ethernet cable. The microcomputer runs the IP network stack and IEC 15118 application layer implementation based on OpenV2G platform [49]. The developed software is freely available online [50].

Figure 3.18 shows the IEC15118 development system, based on two boxes (EV and EVSE), made by following the schematics from Figure 3.17.

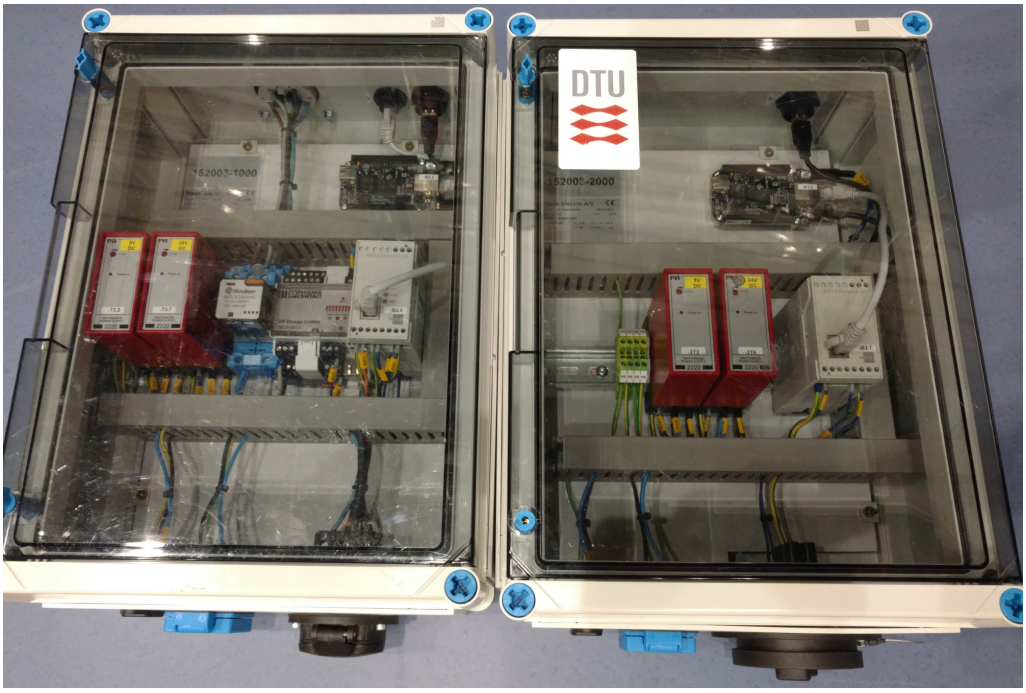

Figure 3.18: IEC 15118 development and testing kit made for COTEVOS project - EVSE (left) and EV (right).

The test system was put to test, by the author, at the IEC 15118 testival in TU Dortmund and at COTEVOS V2G plug-test event against other IEC 15118 implementations.

All in all, IEC 15118 use cases promise a lot of new and necessary functionality for grid integration [48]. However, current edition of the standard does not implement some of the grid service related use cases into the specification, making it difficult to use IEC 15118 for EV to grid integration.

CHAdeMO

Another charging specification developed in Japan for DC fast charging of EVs is CHAdeMO. The chargers supporting this specification can charge compatible vehicle at powers up to 150 kW. This specification is currently the most widely deployed DC (charging mode 4) fast charging protocol in the world [51]. The communication according to this specification is done using a commonly used in automotive industry control area network (CAN) bus. Updated CHAdeMO v2.0 specification recently added a possibility for bidirectional power transfer also known as V2G support. The chargers with CHAdeMO V2G support are already produced and most of the latest CHAdeMO compatible vehicles also support bidirectional power flow from their batteries to the grid.

While CHAdeMO is a proprietary specification, main requirements for its implementation are outlined in IEC61851-23 and IEC61851-24 [52], [53].

As IEC 61851 was originally designed to just enable safe operation of EVs and EVSE while charging, it is only able to dynamically indicate the maximum limit of the charging current from EVSE to the EV. CHAdeMO CAN bus support allows for bidirectional high level communication, which enables all the necessary information exchange to ensure charging safety and extended features for grid service provision. Specifically, CHAdeMO protocol allows for exchange of a mandatory charging parameter that enables charging flexibility assessment, namely State Of Charge (SOC), charging power limit and indication of the plugged in vehicle. While that is a big step forward compared to other EV-EVSE communication protocols, CHAdeMO still lacks identification (e.g. VIN) and secure communication features as well as all the quality improving parameters. These findings were communicated to representatives of CHAdeMO association, so the technical implementation of these features is currently under consideration. Meanwhile, the future version of IEC/ISO 15118 are also promised to be expanded with the same functionality. Finally, all these features should be matched by the communication links in the higher layers of the e-mobility architecture.

3.2.6 EVSE to CPO communication

Although EV charging points exist as long as modern EVs the communication between the charging point and charging point operator (CPO) is not standardized yet. However, a de-facto industry standard this communication link exists.

OCPP

It is called open charging point protocol (OCPP), and is currently a most popular specification for EVSE to CPO communication link. OCPP specification is developed by Open Charge Alliance (OCA) [54]. The specification is primarily developed for charging point maintenance and operation. Early editions of the specification were based on well established Extensible Markup Language (XML) and Simple Object Access Protocol (SOAP) for data encoding and transfer. Latest edition v1.6 adds more modern JavaScript Object Notation (JSON) and Websocket support.

The main functionality of the OCPP specification is:

Charging session authorization - allows a EV user to charge at the charging point after identification.

Collecting billing information - provides charge detail records for billing of EV user.

Grid management - allows to adjust charging according load signal, enabled by charging schedules.

CP operation - upgrading firmware, setting the state to available or unavailable or reserved, configuring charge points, reading and repairing errors.

CP Reservation - functionality needed for EV user to reserve a charging spot e.g. setting charging point to reserved state

Smart charging - adjustment of charging pattern, enabled by charging schedules

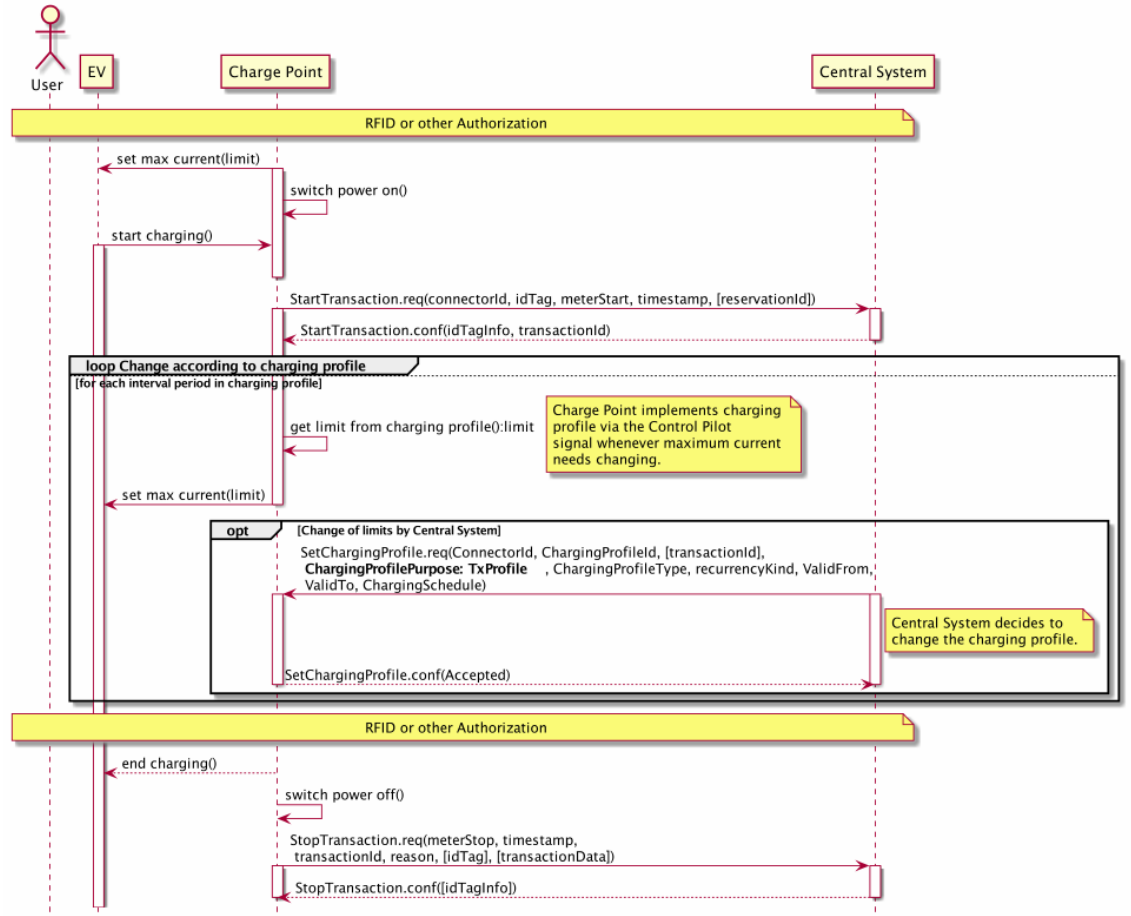

Figure 3.19: OCPP sequence diagram for smart charging using central system controller [55]

Figure 3.19 shows a sequence diagram and a message exchange between the charging point and the CPO while performing smart charging.

Here the charging session between EV and EVSE is already initialized and EV has started charging. Then EVSE initializes new charging session communication with a CPO using OCPP start transaction request. Firstly, transaction details such as user id, start time and transaction id are exchanged. Afterwards a charging schedule is sent to the EVSE. If EVSE accepts the schedule it notifies the CPO and starts following it by adjusting charging current limit for the EV. If the grid situation changes, a new charging schedule could be sent in from the CPO. While the charging session is running, EVSE sends energy meter reading to the CPO at predefined intervals. Finally, once the charging is finished, EVSE sends a stop transaction request with the final energy meter reading for billing. Overall, the specification is missing such essential parameters as vehicle identification and SOC as well as security features.

IEC 63110

Recently, it was decided to standardize the communication between EVSE and CPO [56]. A newly emerging standard that is supposed to take place of OCPP is being developed by IEC, and called IEC 63110. The development of this standard will be based on OCPP v2.0 and aligned with IEC 15118.

3.2.7 Grid Service Communication

This section addresses the communication links in e-mobility infrastructure that are relevant to providing grid services and not covered by previous sections. As was shown in Figure 3.11 these communication links are mostly related to grid operator and aggregator communication. Communication between EV aggregators/charging point operators and grid operators is a relatively new link, not yet covered by a standard.

OpenADR

Similarly to OCPP, one of the de-facto standards in the area of DER communications is Open Automated Demand Response (OpenADR) [57]. The purpose of OpenADR is to provide standardized communication protocol between grid operators and demand response (DR) providers to facilitate automated demand response. While, it is not specifically designed for applications in e-mobility, it is generic enough to support a variety of DR resources, including EVs.

Functionality of the OpenADR specification:

Handle registrations - addition of new DER units to the aggregated nodes

Manage the grid - adjust charging according load signal

Smart charging - adjust charging according to price

Sending price and load control signals - for controlling the power consumption of the DER

Reporting - the metering data and usage times to the grid operator or an aggregator

As the protocol is designed with provision of demand response in mind it has the essential features for supporting grid integration of large aggregated EV fleets as virtual power plants.

OSCP

Open Smart Charging Protocol (OSCP) is also developed by OCA and is one of the first specifications that define the communication between CSO and grid operator e.g. distribution system operator (DSO). The DSO indicates the available grid capacity as a 24 hour prediction to the Charging Point Operator, which then distributes it by adjusting the charging rates. The main functionality of OSCP includes:

Handling capacity budgets

Managing grid capacity

Smart charging using capacity forecasts

It is quite obvious that OpenADR and OSCP overlap. Where OSCP is solely targeted at reducing feeder congestion, OpenADR covers much broader area allowing for applications with various grid services.

IEC 61850-90-8

An extension of a substation automation standard IEC 61850, that defines the additional information objects necessary to control EV charging via the EVSE [58]. A part of IEC 61850 and IEC 61850-7-420 already covers e-mobility domain. The IEC 61850-90-8 brings missing information objects such as EV and the EVSE nodes and means for charging scheduling. The main functionality of the IEC 61850-90-8 is an ability to directly control the charging point by the grid operator [59]. This functionality overlaps with OCPP [60]. However, the extended function set of OCPP is meant for CPOs and technically sharp IEC 61850-90-8 information model is designed for direct grid operator control of EVSEs in abnormal grid conditions.

3.2.8 Roaming communications

A big area in e-mobility communication that is on the side of the essential grid service enabling communication is roaming. Although not directly relevant for grid service provision, but described for completeness of e-mobility architecture. Roaming in e-mobility is very similar to the one in telecommunications, it ideally allows EV users to charge their vehicles at any charging service provider. To enable such functionality communication links and protocols have to be established between Charge Point Operators (CPOs), E-Mobility Service Providers (EMSPs) and clearing houses. Multiple specifications are emerging to cover those missing links in e-mobility back-end communications.

OCPI

Open Charge Point Interface (OCPI) protocol is developed for exchanging information about charging points between CPO and EMSP [61].

The main functionality of OCPI includes:

Authorizing charging sessions - involves allowing a user/EV to charge at the charging point after identification

Billing - providing charge detail records for billing of EV user

Providing charge point information - static and dynamic charge point information e.g. location, availability, tariff

Reservation - functionality needed for EV user to reserve a charging spot

Handle registrations - adding new users to a EMSP

Roaming - information exchange enabling EV user to charge at multiple charging points using a single identification token

OICP

Open InterCharge Protocol (OICP) is also meant for CPO to EMSP communication [62]. It is meant for roaming application e.g. to communicate with Hubject B2B Service Platform. The main functionality of OICP includes:

Authorizing charging sessions - involves allowing a user/EV to charge at the charging point after identification

Billing - providing charge detail records for billing of EV user

Providing charge point information - static and dynamic charge point information e.g. location, availability, tariff

Reservation - functionality needed for EV user to reserve a charging spot

Roaming - information exchange enabling EV user to charge at multiple charging points using a single identification token

OCHP

Open Clearing House Protocol (OCHP) is meant for exchanging charging information relevant to reservation and billing between CPO, EMSP and Clearing House for roaming purposes [63]. The main functionality of OCHP includes:

Authorizing charging sessions - involves allowing a user/EV to charge at the charging point after identification

Billing - providing charge detail records for billing of EV user

Providing charge point information - static and dynamic charge point information e.g. location, availability, tariff

Reservation - functionality needed for EV user to reserve a charging spot

Roaming - information exchange enabling EV user to charge at multiple charging points using a single identification token

Smart Charging (only in OCHPdirect) - only meant for setting limits but not for dynamic smart charging

OCHP is the only notable communication protocol for communicating with e-mobility clearing houses.

3.2.9 Gaps in communication protocols

Over the course of this study, many gaps in communication protocols have been closed by new/updated specifications, thus covering most normal charging scenarios. However, a few issues still remain:

Timing delays - only a few communication standards define the timing requirements for their communication

Missing information objects - majority of the communication protocols are well suited to support normal charging operation. However, grid services require additional information objects (mostly SOC and vehicle identification), outlined in 3.2.4 to be communicated from the EV all the way to the aggregator.

Security risks - only one communication protocol proposes establishment of a secure communication link - IEC 15118 plug and charge mode using TLS. While OCPP is promising to improve the cyber security reqirements in the upcoming OCPP version 2.0 [64]. Almost all discussed communication protocols do not require any security measures, thus allowing for monitoring and possible man in the middle attacks.

3.2.10 Future standards

Current communication standards and specifications have already evolved to the level supporting basic grid services. CHAdeMO and IEC15118 have already implemented some of the features designed to support smart grid applications such as V2G support and required information objects. Formation of IEC 63110 standard to replace OCPP in alignment with IEC 15118 development, and recent developments in all of the e-mobility communications shows adjustment of the standardization area towards better grid integration. The support of the communication standards is crucial, as they are a backbone of the e-mobility control architecture.

3.3 Control

Hardware, e-mobility actors and communication standards are essential building blocks of the control architecture that enables grid service provision using electric vehicles. The final technical requirement for grid integration once hardware is in place and appropriate communication links are available is a controller.

3.3.1 Aggregators

While an EV is a biggest electrical load in the household, a single EV has a very little impact on the power grid. Once aggregated in tens, hundreds and thousands, a real impact on distribution and transmission grids can be established. Such combination of single EVs is enabled by using EV aggregators [65–67]. However, different services could benefit from different kinds of control strategies i.e. centralized, distributed or mixed [68].

3.3.2 Control architecture

Figure 3.20 shows a first version of the control architecture, developed by the author and used in most experiments in NIKOLA project. This experimental architecture is applied in most of the experimental activities described in Chapter 4.

Here, the controller plays multiple roles of: aggregator and a grid operator. The control architecture consists of the software and hardware components as follows:

Controller - contains the main controller logic - control algorithm that actuates the charging of the EVs according to data from measurement devices. Implemented control algorithms include: droop control based frequency and voltage regulation, congestion limiting, secondary frequency regulation, synthetic inertia control. The controller also includes data logging and visualization interface.

ZMQ message bus - a messaging bus implemented using ZeroMQ publish-subscribe pattern to enable communication between multiple components of the controller (mostly as data channel from sensors to the controller and logger) in the control architecture [69].

EVSE interface - communication interface to the Phoenix Contact EVSE controller, implemented using push-pull pattern in ZeroMQ.

SGU poller - communication interface to the smart grid unit measurement device.

MTR3 poller - communication interface to the DEIF MTR3 frequency measurement device.

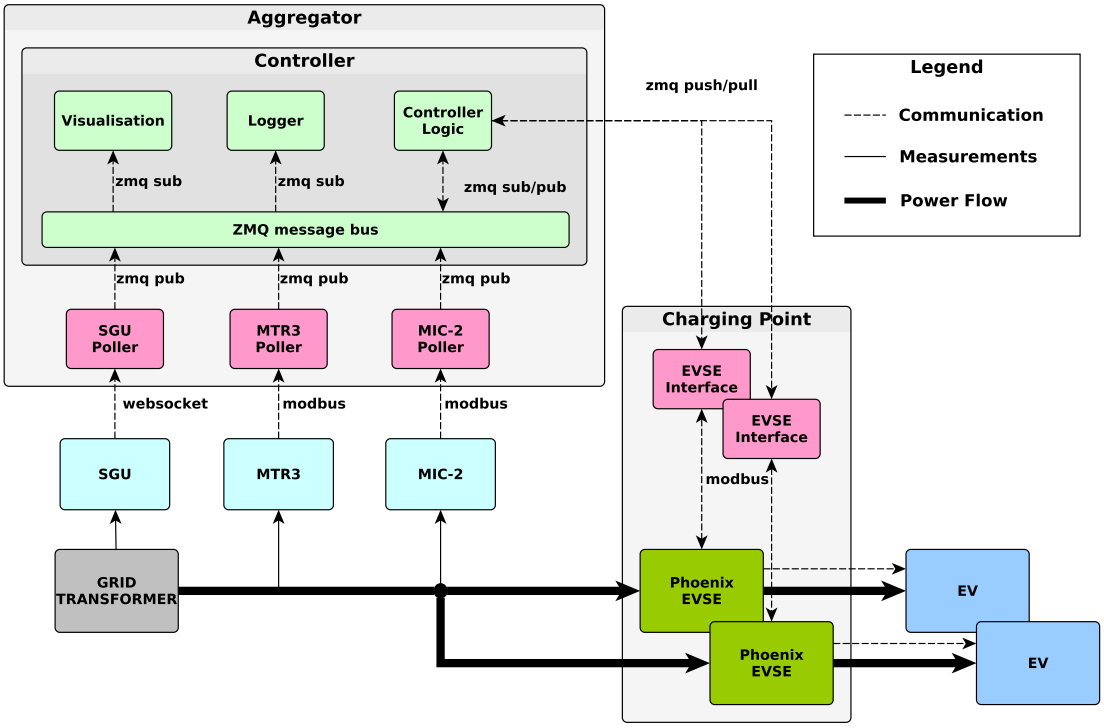

Figure 3.20: Control architecture used in experimental validations.

MIC-2 poller - communication interface to the DEIF MIC-2 multi-instrument measurement device.

SGU - smart grid unit, a measurement device mounted in the MV/LV transformer to measure voltage, current and frequency on LV and MV sides.

DEIF MTR3 - multi-instrument measurement device used for frequency measurements due to its precision to 10mHz as specified by ancillary service provision requirements [16]

DEIF MIC-2 - multi-instrument measurement device used for voltage, current and power quality measurements.

Charging point - a charging point that includes 3 EVSEs.

EVSE - based on Phoenix Contact EVSE controller, implements IEC 61851 support for EV charging.

EV - usually unmodified OEM vehicles: Nissan eNV200/Leaf, Peugeot iOn or Renault Kangoo.

As can be seen from in the figure the controller represents a CPO and an aggregator at the same time. The purpose of this control architecture is to test the technical specifications of the potential grid services. This means that the controller is not designed to include EV user requirements, such as departure time and desired state of charge.

To include real EV users in the testing of the EV grid services, the technical implementation has been redesigned to incorporate user services. The author has developed the second iteration of the control architecture to be implemented in future experiments. The experimental architecture from Figure 3.20 has been expanded to fit into e-mobility architecture from Figure 3.10. The result is a detailed control architecture for e-mobility and grid integration developed at DTU based on open

standards, shown in Figure 3.21. Here, the software controllers are depicted in light green and software interfaces to hardware devices in purple.

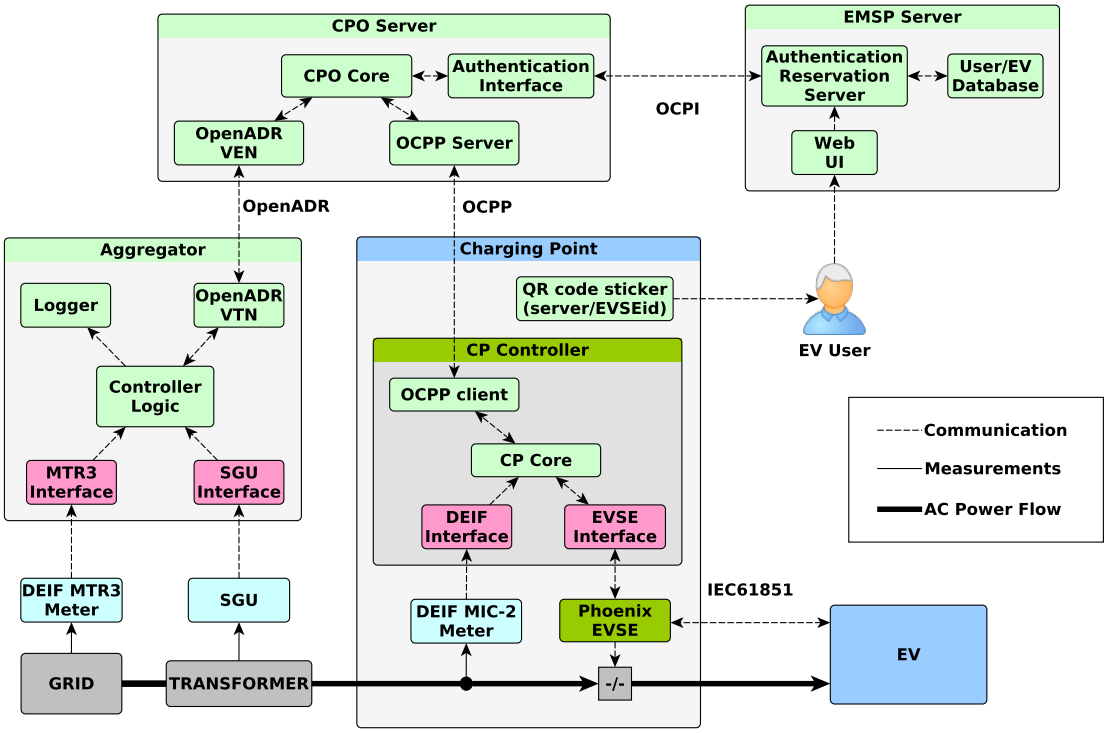

Figure 3.21: Control architecture for commercial applications based on open standards

As seen in the figure, custom communication to the charging spot has been replaced by OCPP, thus enabling interoperability between a CPO and different EVSEs.

The following communication standards are used in the implementation:

IEC 61851 - for EV to EVSE link - used as unmodified OEM vehicles, which at the time of writing, only support IEC61851 standard for AC charging. The IEC61851 on the EVSE side is implemented by using Phoenix Contact EVSE controller.

OCPP 1.6 - for EVSE to CPO link - used as it is a de-facto standard for this link. Implemented in the microcomputer mounted inside the EVSE. It will be replaced by OCPP 2.0, once it is available.

OCPI 2.1 - for CPO to EMSP link - chosen for the openness and maturity of the specification that covers the needs of the communication link. Implemented in the dedicated server, that also provides web interface for authorized EV users to login and enable the charging spot.

OpenADR 2.0b - for CPO to Aggregator link - chosen for maturity, openness and generic application capability. This allows for the aggregator to potentially combine EVs with other DERs to provide larger and more diverse grid services. The aggregator implements the role of the virtual top node (VTN) and the CPO implements the virtual end node (VEN). Another specification potentially fitting this link is Open Smart Charging Protocol (OSCP) [70]. However, it is mostly targeted at feeder capacity control thus limiting its application for other grid services.

Additionally, the CPO and EV aggregator roles have been separated and EMSP role has been added. The EMSP enables public DTU EVSEs to be reserved and require charging authorization for the EV user. Such communication scheme allows for identification of the user and possibly the model of the vehicle by user input via web interface. The interface is accessed by scanning a QR code on the charging point.

3.4 Conclusion

The chapter outlined and explored the three main technologies for EV integration into the smart grid: hardware, communication and control mechanisms. Controllable hardware has been available already for a number of years, and the recent introduction of modern V2G chargers only makes it better. While gaps in the communication protocols still exist, they are covered by alternative solutions and new revisions of the protocols. However, there is still some way to go to achieve widespread adoption of aggregated EVs as ancillary service providers. As seen in the currently used and proposed e-mobility architectures there is a difference in design and implementation. The roles of the e-mobility actors are fairly new and are not yet firmly established. This leads to merging of actor e.g. CPO and EMSP, CPO and aggregator and possible rearrangement of communication links in the e-mobility architecture. That however does not stop the development of different e-mobility control architectures. All in all, most technical requirements for EV integration into smart grid are being implemented, as shown in developed control architectures that are employed in experimentally validating actual grid services in Chapter 4. Furthermore, a pilot demonstration project, inspired by the findings of the NIKOLA project, is already providing actual grid services to real grid operators.

3.5 Contribution summary

The author has identified technical and communication requirements for EV grid integration. Actors, from e-mobility architecture developed in COTEVOS project, necessary for supporting EV grid integration were studied. Existing communication standards and specifications between the actors were analyzed for ability to support grid services. A smart charging controller was developed to enable the implementation of the grid services using OEM EVs. It was used in experimental validation of grid services presented in Chapter 4. The controller was expanded and converted into a system resembling a part of the e-mobility architecture. The implementation is based on the open standards thus providing maximum interoperability with potential future commercial partners. That allows for implementation of grid service provision in real life like conditions with 3rd party EVs and interaction with EV users. It should be noted that the full implementation of the developed control architecture is still work in progress.

3.6 List of publications

The relevant publications are listed as follows:

A S. Martinenas, S. Vandael, P.B. Andersen, B. Christensen, "Standards for EV charging and their usability for providing V2G services in the primary reserve market," in *Proceedings of International Battery, Hybrid and Fuel Cell Electric Vehicle Symposium (EVS29)*, Montreal, Canada, IEEE, Jun. 2016.

B S. Martinenas, "Implementation of E-mobility architecture for providing Smart Grid services using EVs," in *International Battery, Hybrid and Fuel Cell Electric Vehicle Symposium (EVS30)*, Stuttgart, Germany, 2017.

Chapter 4
Grid service applications

This chapter describes the implementations of grid services EVs could provide. In addition to theoretical description, an experimental validation of each service is presented and analyzed. Most of the experimental results presented in this section are made as contributions to a Danish research projects NIKOLA and Parker focusing on the integration of EVs into contemporary and future power systems [25] [71]. The experiments were performed in SYSLAB (part of PowerLabDK) which is a flexible laboratory for distributed energy resources, that consists of real power components paralleled with communication infrastructure and control nodes in a dedicated network [72]. All of the work presented in this chapter is original and based on the authors publications.

Typically, two levels of grid services are considered, they correspond to transmission and distribution grid operation areas also known as system wide and local. Firstly, the applications of system wide services are presented namely frequency regulation and synthetic inertia. This is followed by the distribution grid service for local power quality improvement. Finally, smart charging service that takes user comfort into account is shown. All of these services are enabled by the technical requirements presented in Chapter 3.

4.1 Frequency services

In multiple experimental validations mostly primary and normal reserves from DK1 and DK2 as well as adjusted versions for microgrid control were implemented and tested. These services were chosen for implementation due to: ease of acquiring the control signal i.e. measured grid frequency deviation; low energy use with short duration and quick required response time that is ideal for fast inverter based EV chargers. The experimental validation for system-wide services is presented in steps from proof of concept, through microgrid validation, all the way to the pilot project.

Proof of concept

Firstly the DK1 primary reserve was implemented as a proof of concept. It was tested using AC V2G capable EV - AC Propulsion eBox connected via 32A charging point to the Danish grid.

The controller is running with the following frequency regulation algorithm:

The droop controller was designed by following the technical specification of tender conditions for ancillary services in Danish power grid, see [16].

Firstly, the grid frequency is measured and the deviation from nominal frequency is calculated:

while *true* **do**
  f = measure grid frequency;
  e = calculate the frequency error;
  P_{out} = calculate corresponding output power using preset droop;
  actuate the power for the EV (P_{out});
  wait for the next frequency measurement
end

Algorithm 1: Frequency Droop Control

$$e = f_{nom} - f_m. \tag{4.1}$$

Here the e is the frequency deviation i.e. the difference between nominal and measured frequency values. f_{nom} is a nominal grid frequency in Europe, equal to $50.00Hz$. The f_m is the measured grid frequency, with $10mHz$ accuracy. The power output of the droop controller is calculated as shown in (Equation 4.2).

$$P_{out} = \begin{cases} 0 & , |e| < \Delta f_{db} \\ P_{max} \cdot e \cdot \dfrac{100}{d_{pct}} & , \Delta f_{max} > |e| > \Delta f_{db} \\ P_{max} & , |e| > \Delta f_{max} \end{cases} \tag{4.2}$$

Here P_{out} is output power of the vehicle to the grid. P_{max} is the maximum (dis)charging power of the vehicle, for a $32A$ charging point at one phase it is $7kW$. Δf_{db} is a deadband width used, in this case $20mHz$. d_{pct} is a droop value in percent. Δf_{max} is a maximum frequency deviation, at which the maximum power should be output to the grid, in this case it is $200mHz$. The resulting droop control curve is shown in Figure 4.1.

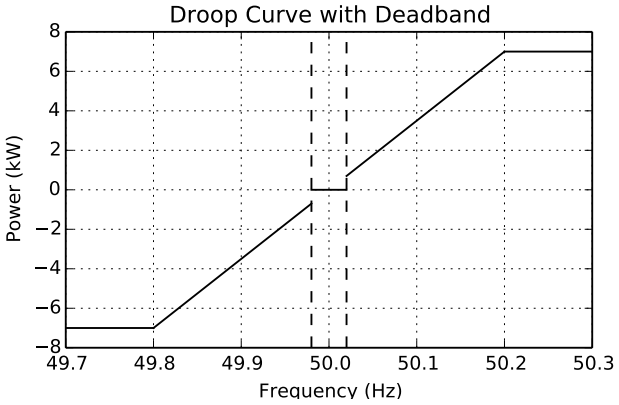

Figure 4.1: Droop curve with deadband (DK1 primary regulation) used in proof of concept frequency regulation experiments

Once the control algorithm was implemented in the controller, a longer experiment was also performed with frequency regulation being active for 22 hours. The results are shown in Figure 4.2.

The average frequency value for the test period was $49.997Hz$. This indicates that the frequency was almost symmetric. The SOC of the vehicle changed from 85% at the start, to around 53% at the end of the test. Such large SOC change can not be explained by slight bias of the frequency,

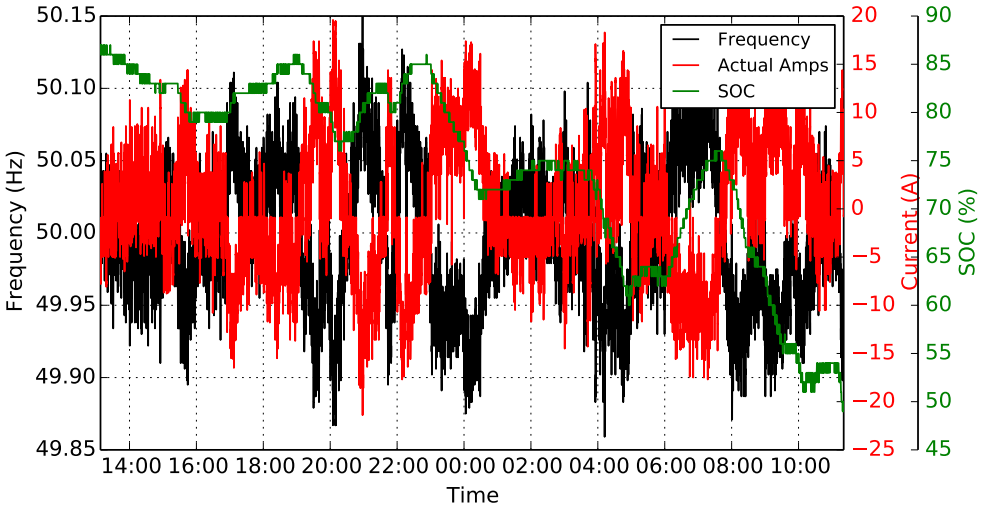

Figure 4.2: Frequency regulation results for 22 hours

but is mainly caused by the V2G inverter roundtrip efficiency. The measured efficiency of vehicle PEU in V2G mode at these low current values is around 0.8, this makes roundtrip efficiency to be around 0.64. That closely matches the ratio of the end to start value of battery SOC in the example from Figure 4.2.

The close up from the 22 hour frequency regulation process is shown in Figure 4.3.

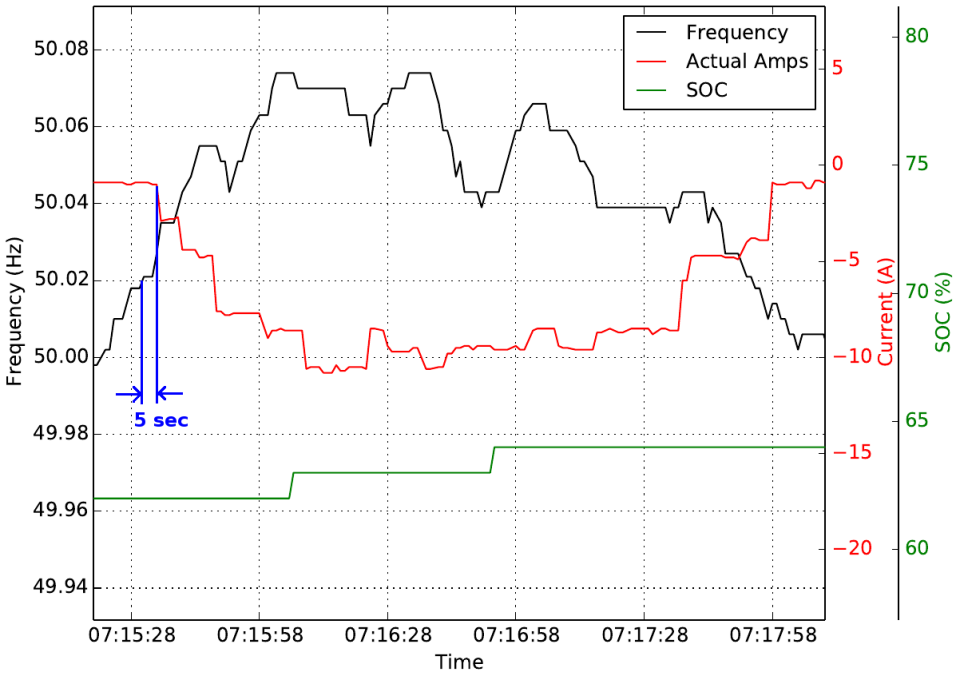

Figure 4.3: Frequency regulation results close up with response delay

Here the delay between the frequency measurement and response by the vehicle can be appreciated. Generally, the vehicle is able to respond to the frequency event in about 5 to 6 s. The delay can be approximately decomposed into the following components: <1 s delay for frequency sampling

time and control action in the controller, <1 s delay for communication and control parameter update in the controller, 3 to 4 s for PEU ramping time and <1 s delay for response data sampling in the measurement device.

Experimental validation in a microgrid

After the proof of concept setup was successfully tested, contemporary unmodified OEM vehicles were selected for testing in a microgrid scenario to better asses their performance. Microgrid environment allows for the scale where the impact of the regulation provided by EVs is tangible.

No contemporary OEM vehicle is able to provide V2G without external charger. Therefore, experimental validation had to rely on unidirectional chargers. To provide the up and down regulation the neutral charging setpoint is set to the middle of the charging rate range.

The connection diagram of the experimental setup is shown in Figure 4.4.

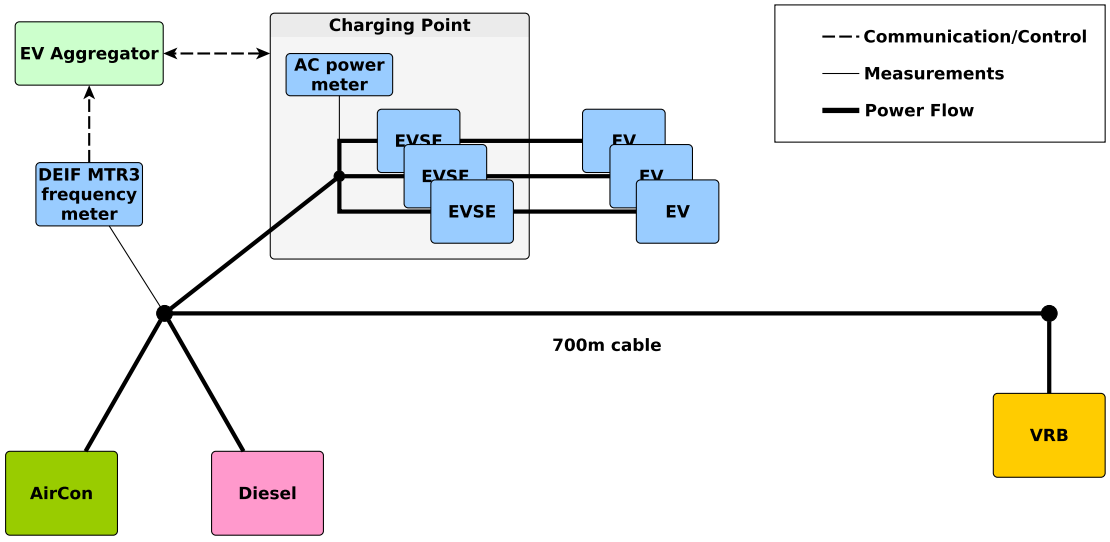

Figure 4.4: Experimental setup for primary frequency regulation in a microgrid scenario

The microgrid experimental setup consisted of:

Diesel generator - base power generator and main inertia source in the microgrid.

Vanadium battery - main and variable load in the microgrid.

AirCon wind turbine - stochastic generation which EVs should balance out when providing frequency regulation service.

Charging Point - charging point with 3x 16 A EVSEs.

EV - 3x Nissan Leaf EVs used as a primary frequency regulation load. Such number of EVs was required as the microgrid is 3 phase and each EV has only a single phase charger.

Grid - use to setup and establish the microgrid, then disconnected once the microgrid was balanced and ready for the experiment, thus not shown in the figure.

The experimental validation was performed in 3 stages.

Firstly, a test to verify that internal frequency controller in the diesel generator is turned off was performed. A balanced microgrid was created with the diesel generator as a power source and VRB and EVs as loads. Then the consumption of VRB was increased by 1 kW, frequency in the microgrid started to steadily drop. After about 120 s the under-frequency protection in the generator has tripped at 47.5 Hz. This proves that no frequency regulation was present in the system.

Secondly, a test to verify the EVs ability to provide the primary frequency regulation in the microgrid scenario was done. A balanced microgrid was established once again, this time VRB was used as base consumtion of 2 kW and EV primary frequency controller active. Then an unbalance was created in the microgrid by varying the VRB power consumption in steps of ± 3 kW.

The primary frequency regulation controller was based on a traditional droop control. The actual droop characteristic used in the experiment is shown in Figure 4.5.

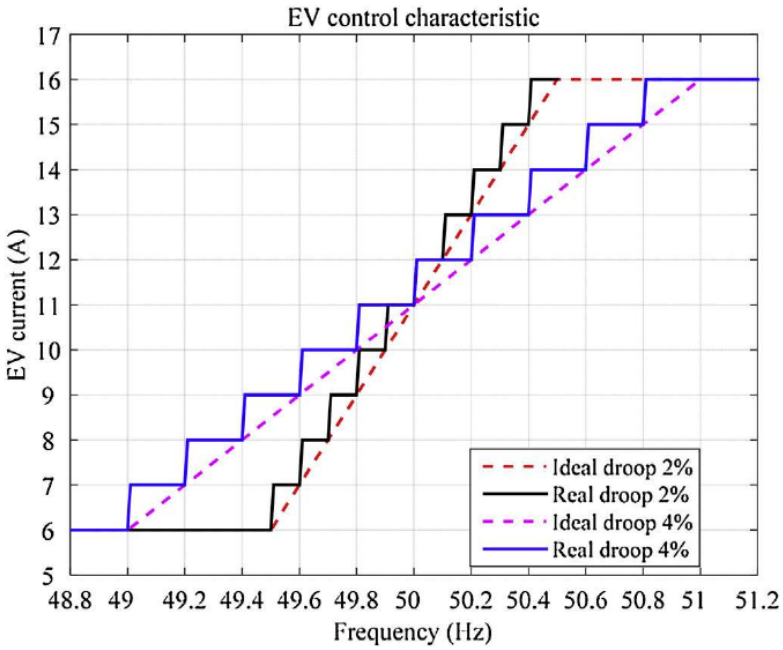

Figure 4.5: Droop curves used in the PFR controller

As shown in Figure 4.6 the EVs have successfully balanced the grid.

As load steps were performed up and down from a nominal 2kW load value, the system frequency started to drift. Primary frequency regulation (PFR) from EVs immediately responded to the disturbance, which slowed and stopped the frequency drift. However, it is evident that, while performing frequency regulation service, EVs also introduce some frequency oscillations. These oscillations are caused by a combination of EV power setpoint accuracy and pure proportional control of PFR. As EVs are controlled by limiting their charging power, their response might differ from the setpoint by up to 1A per phase, that adds to a total of almost 600W. Such power imbalance affects the frequency, which in turn affects the PFR setpoint and the oscillations start. These oscillations disappear when the PFR setpoints reach and exceed boundary values 6A and 16A. The problem of oscillations could be mitigated by adding an integral action to the controller or using equipment with finer power steps.

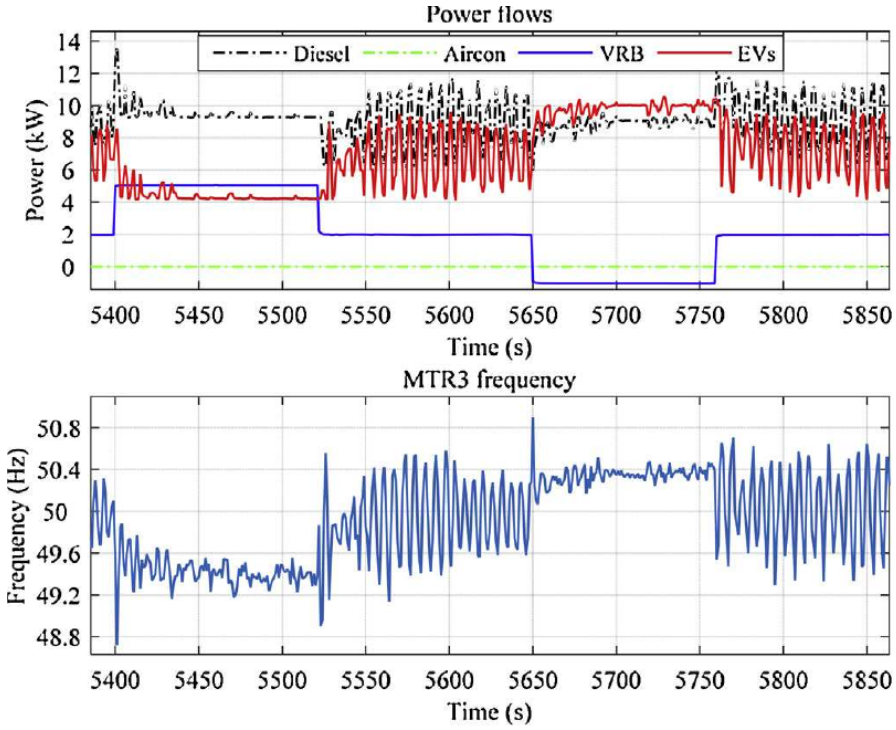

Figure 4.6: Power flow and measured frequency when performing ±3 kW steps with VRB with EV PFR enabled

Lastly, a test where EVs would provide frequency regulation to the microgrid with stochastic power generation was performed. Again a balanced microgrid was established, but this time an additional power source was connected - AirCon wind turbine. VRB power consumption was increased to 4 kW to account for average power production of the wind turbine. However, the wind power production was fluctuating from 4 kW to 7 kW. Therefore, the EV primary frequency regulation was enabled to stabilize the microgrid.

As shown in Figure 4.7 the EVs have successfully balanced the microgrid with an intermittent energy resource.

Here, EVs have precisely followed the fluctuating power output from the AirCon wind turbine, thus not allowing the system frequency to run off. Such challenging balancing scenario was enabled by the very fast response of EVs <3 s. Additionally, the base load setpoint has been appropriately adjusted so that EVs could approximately balance out the predicted amount of power produced by the wind turbine. Overall, even in a such demanding scenario and without V2G capability, the EVs are capable of stabilizing the frequency deviations in the microgrid.

During experimental validations of frequency regulation services, it has been noticed that EVs in general are fast to respond to the control signals. It has been decided to investigate the timing of the EV response to an external stimulus.

4.1.1 EV charging controllability

The typical timing sequence in the control loop for a frequency regulation service is shown in Figure 4.8.

In this figure the different segments are the following:

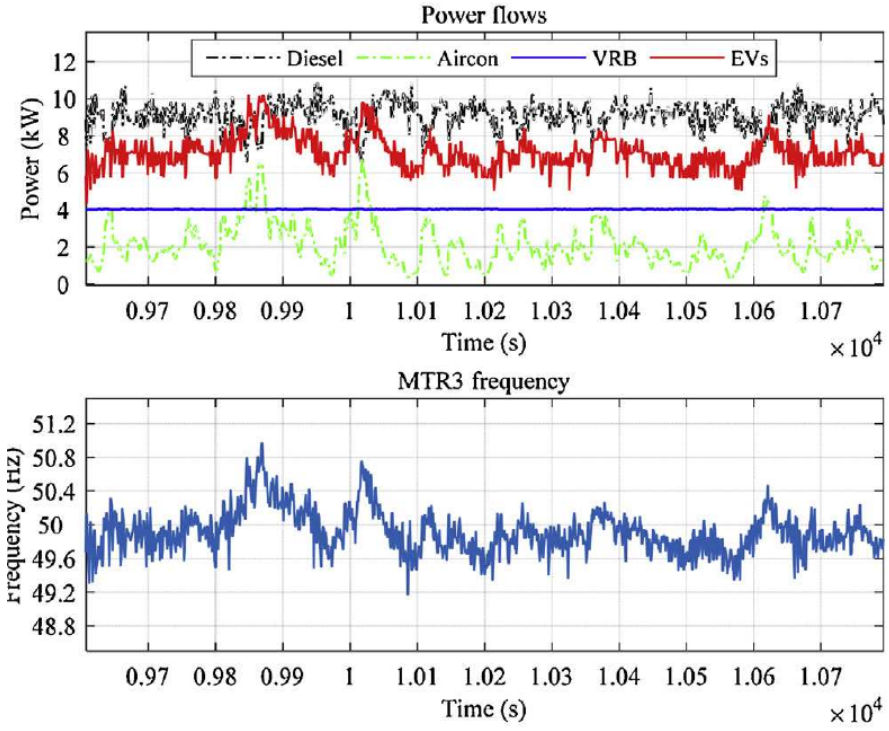

Figure 4.7: Power flow and measured frequency when EV PFR is used to balance stochastic wind turbine power production

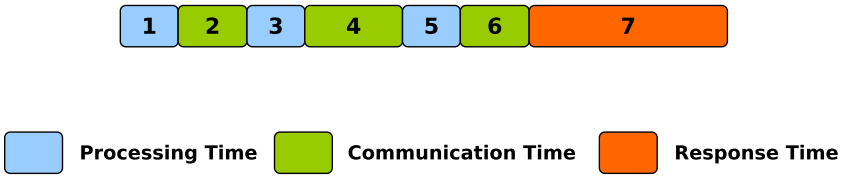

Figure 4.8: Timing sequence for a

1. Measurement acquisition at the frequency measurement device
2. Communication between measurement device and aggregator
3. Aggregator calculating the control response
4. Communication delay between aggregator and EVSE
5. Processing time in the EVSE
6. Communication delay between EVSE and EV
7. Processing and ramping time in the EV charger

Typically, the slowest part of the whole communication-control loop is the EV power response time. In most modern EVs, communication between a vehicle and a charging point is defined by IEC 61851 standard. The standard states that in case a charging current limit is changed, the

vehicle should respond within 3 seconds. Additionally, the standard specifies the lowest current limit is $6A$ with a step of $1A$, while upper current limit is defined by a minimum function of the charging cable and the fuse rating of the EVSE.

The charging power adjustment response time and precision of multiple commercially available EVs are compared. The EVs used in the test are EV I - Peugeot Ion (2011 model), EV II - Nissan Leaf (2015 model), and EV III - Renault Kangoo (2012 model). All of these EVs are equipped with 3.7 kW AC chargers which can be controlled between 6 to $16A$ - providing a $2.3kW$ flexibility window. This window is split in half, by setting nominal EV charging rate to $11A$ at the frequency of $50.00Hz$. This way EVs can provide symmetrical up and down regulation as detailed in Section 4.1.As the grid frequency from real grid is rather stable, a symmetrical, randomized input frequency was designed that would force the controller to change the set-point at each iteration. This way the controllability of each EV is pushed to the limit and the ramping rates can be assessed.

Here the response of the full control loop, with focus on EV power adjustment time and precision are evaluated and compared. Technically, response time is the major factor for grid service provision as response precision always improves with aggregation of multiple vehicles. Typical inaccuracy of the response from each charger is less than the step of $1A$, which only corresponds to approximately $200W$ in power per EV. Such error is below the accuracy limit of typical multi-hundred kilowatt response power for an ancillary service and can be easily corrected by adjusting the charging current for the part of the aggregated EVs.

The control signal and response of the vehicle to the changes in the charging current limits are shown in Figure 4.9, Figure 4.10 and Figure 4.11. The graphs are showing only the first 2 minutes of the experimental data to better appreciate the difference between the control and response.

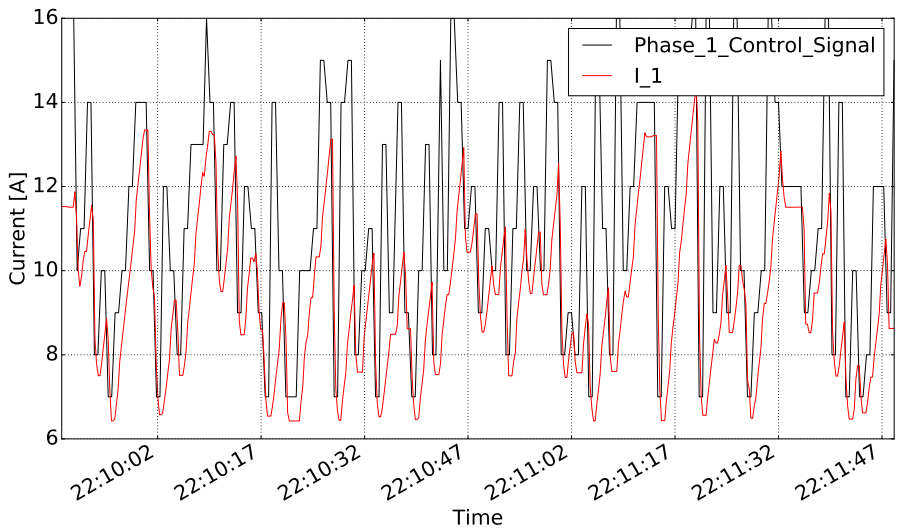

Figure 4.9: Response precision and timing of EV I

As can be seen in Figure 4.9, ramping speeds of the EV I on phase 1 are different for up and down modulation. While increasing the charging current to the new higher limit might take up to 2 seconds, decreasing the charging current to the lowered limit only takes up to 1 second.

As shown in Figure 4.10, the EV II on phase 2 has much faster ramping rates. Both up and down modulation of charging current is performed in less than around 0.5 seconds.

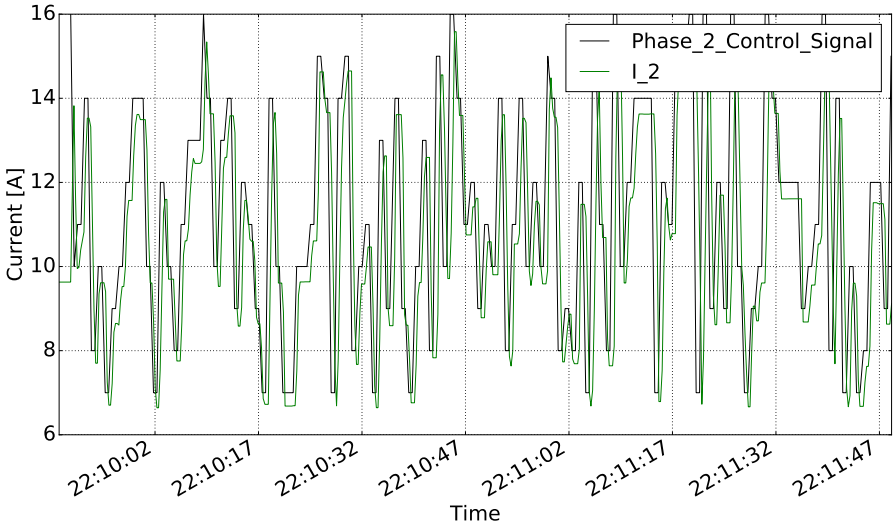

Figure 4.10: Response precision and timing of EV II

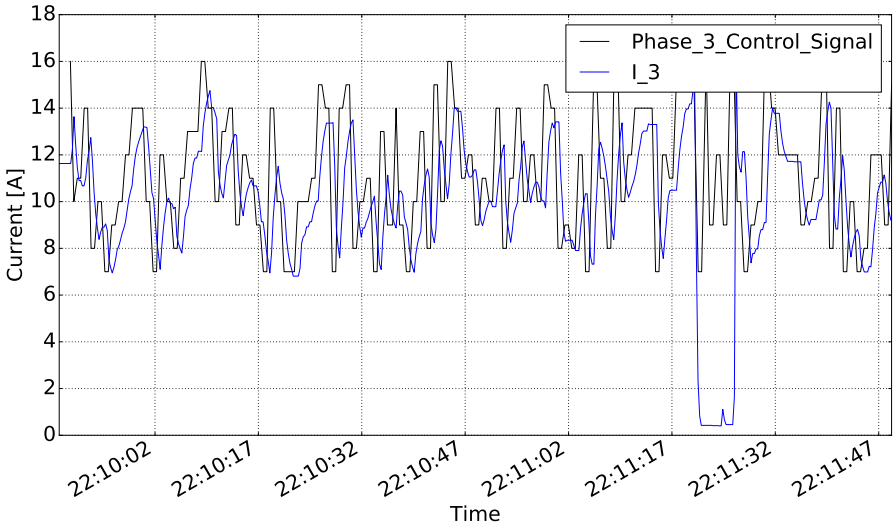

Figure 4.11: Response precision and timing of EV III

Response plot in Figure 4.11, shows that the EV III on phase 3 has a bit slower ramping rates for up and down modulation. It takes up to 1 second to lower the charging current and up to 2 - 3 seconds to increase the charging current to the higher limit. Additionally, the EV also shows occasional current drop to under $1A$ for a about 5 seconds, which could affect the quality of the provided service. This drop could be caused by the battery management system balancing the battery cell voltages or for passive battery cooling.

To better compare the responses of three EVs, zoomed in plot of the first minute of the experiment with control signal and response of all three vehicles is shown in Figure 4.12.

Such difference in timing and response precision can be explained by advancement in power electronics of the EV chargers as EVs I and III are 5 years old and EV II is a recently produced 2015

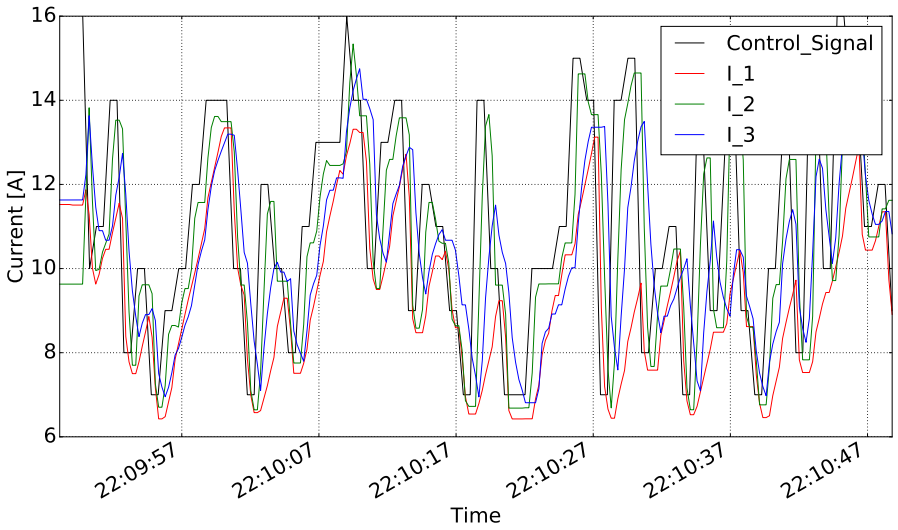

Figure 4.12: Control and response comparison of all three EVs

model.

The timing performance and response precision of the three EVs is summarized in Table 4.1.

Table 4.1: Summary of EV response timing and precision

EV nr.	Minimum delay	Average delay	Maximum delay	Average Response Error
I	0.4 s	1.1 s	2.0 s	0.8 A
II	0.2 s	0.3 s	0.6 s	0.4 A
III	0.5 s	1.5 s	2.5 s	1.0 A

While all EVs are well within the timing limits of the IEC 61851 standard for charging current regulation, EV I and III have similar response times closer to a few seconds, where EV II stands out by having sub-second response time.

This sub-second response enables the EV II to potentially provide synthetic inertia [73]. Therefore it was decided to conduct an experimental validation of a synthetic inertia service. The validation was done using 3 EVs from 2015 and 2016 models each capable with responding to a changing control signal at sub-second rates.

4.1.2 Fast frequency regulation and synthetic inertia

Since synthetic inertia is a new potential service, it was decided to compare its effects to a fast frequency regulation service, based on primary frequency regulation service presented earlier. The fast frequency control and sythetic inertia are both using droop controllers shown in Figure 4.13.

The fast frequency regulation droop is identical to the one used in experimental validation of primary frequency regulation service. The synthetic inertia droop curve has a wide deadband

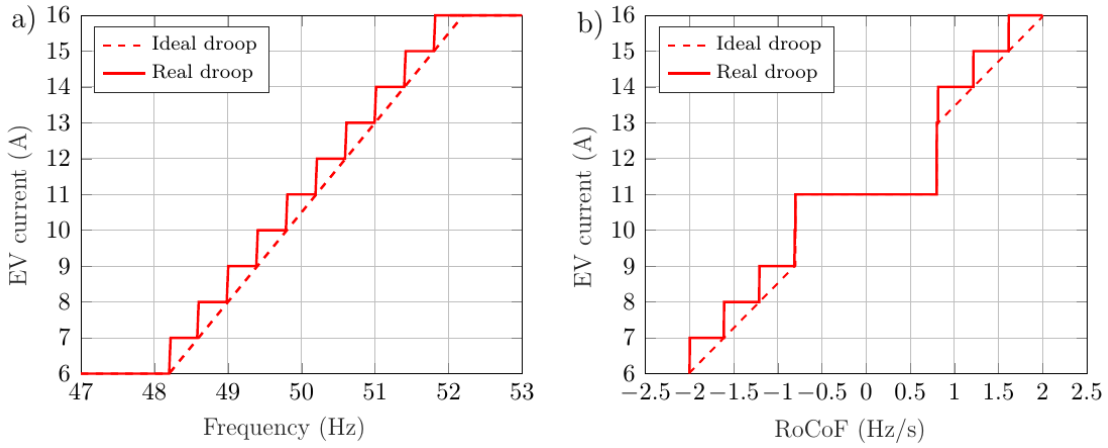

Figure 4.13: Droop curves used in the controllers: a) Fast frequency regulation droop; b) Synthetic inertia droop

to avoid trigerring the synthetic inertia response on minor rate of change of frequency (RoCoF) events.

While frequency regulation service uses the frequency as an input to the controller, synthetic inertia droop controller is based on RoCoF. This makes the synthetic inertia an equivalent of differential component in the PID control. It should be noted, that a minor improvement in the charging point controller has been done to enable faster system response.

The experimental setup used for this comparison is shown in Figure 4.14.

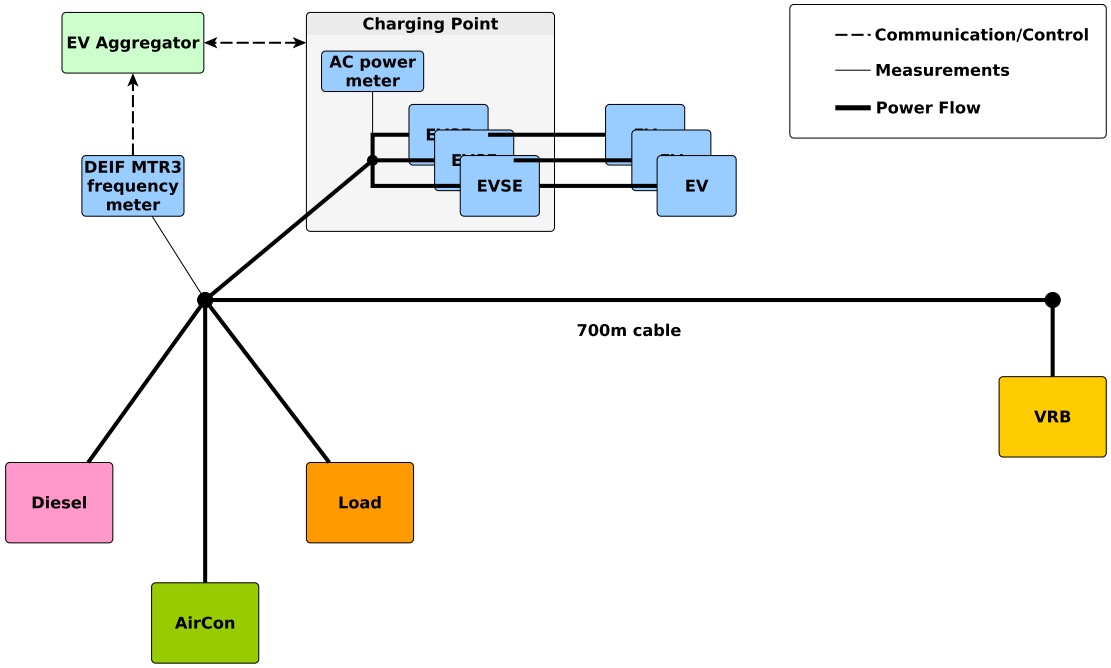

Figure 4.14: Experimental setup for fast frequency regulation vs synthetic inertia comparison

The microgrid experimental setup consists of:

Diesel generator - used as a base power generator and main inertia source in the microgrid.

Vanadium battery - used as a main and variable load in the microgrid.

Dumpload - a resistor load bank

AirCon wind turbine - used as a stochastic generation which EVs should balance out when providing frequency regulation service.

Charging Point - a charging point with 3x 16 A EVSEs.

EV - 3x EVs: 2016 Nissan Leaf, 2014 Nissan eNV200, 2015 eNV200, used to provide fast frequency regulation and synthetic inertia. Such number of EVs was required as the microgrid is 3 phase and each EV has only a single phase charger.

A dumpload has been added as a main source of the variable load for its pure resistive properties.

The same scenarios have been tested in this comparison study: response to a load step and balancing of the stochastic power generation from a wind turbine.

Figure 4.15 shows a closer look on the RoCoF and current response of each controller to a load step.

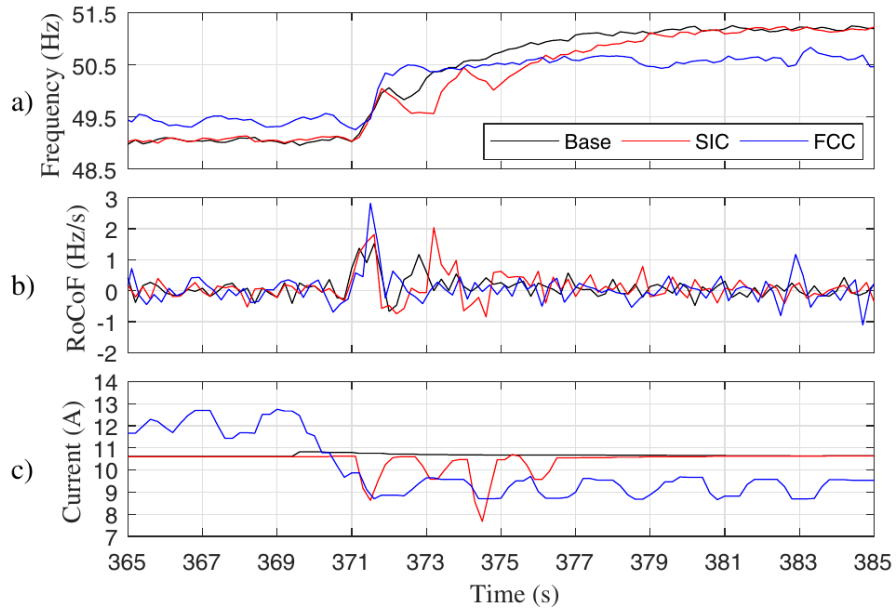

Figure 4.15: Comparison of Fast Frequency control and synthetic inertia: frequency and current

As expected, synthetic inertia controller curtails the RoCoF at the frequency event, slowing down the frequency offset. Meanwhile, fast frequency regulation controller amplifies the initial RoCoF but reduces the frequency offset.

These controllers should be merged and tested together as a single PD controller, thus potentially improving both RoCoF and frequency offset.

4.1.3 Pilot project

It is proven that using V2G capability, EVs could provide ancillary services with higher power and for much longer periods of time, thus increasing the value of the provided service [74]. Therefore, OEM vehicles compatible with bi-directional DC chargers were selected for the real trial. A fleet of 10x EVs are aggregated using 10x bi-directional CHAdeMO chargers with $\pm 10kW$ active power control capability in 1A steps. These aggregated units are used to provide normal frequency regulation service for Energinet.dk under standard tender conditions.

Figure 4.16 shows an existing control architecture for FCR-N ancillary service provision in DK2 used with DC V2G chargers in Parker project.

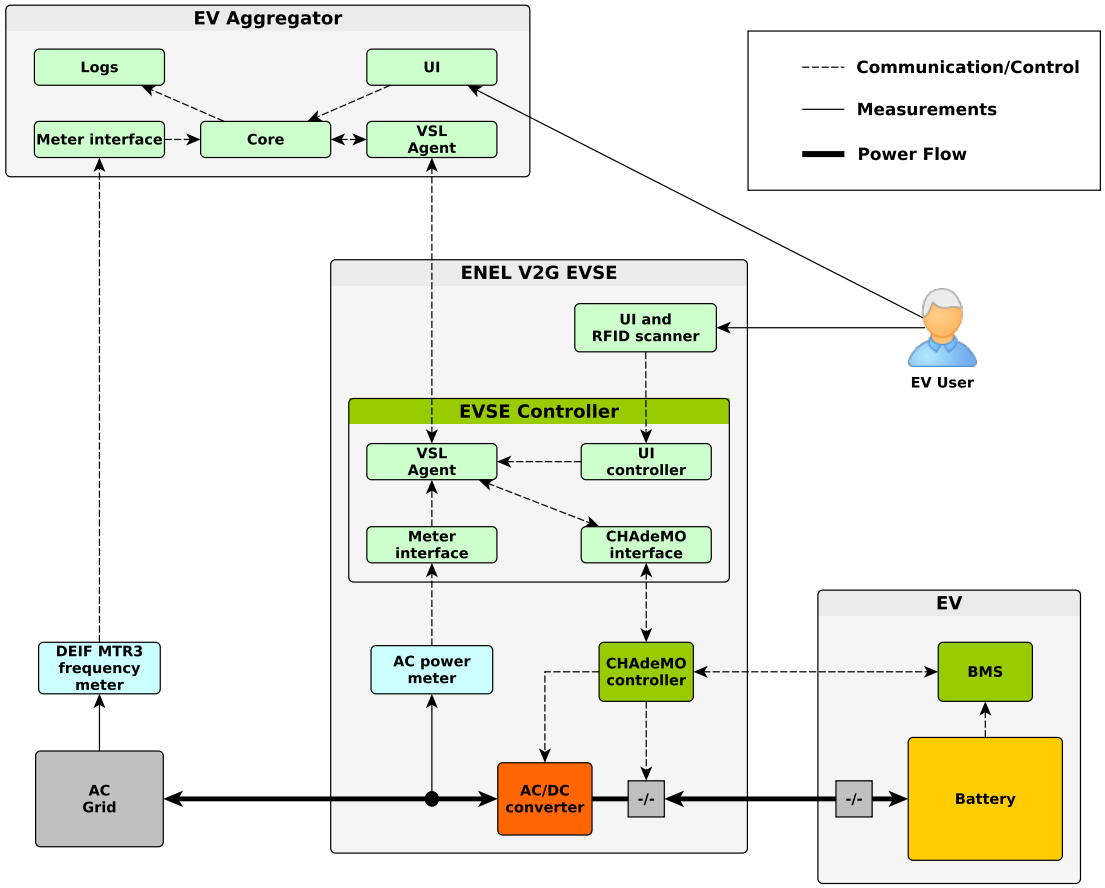

Figure 4.16: Control architecture used in Parker project for frequency regulation - normal, ancillary service provision in DK2 grid area

In this architecture an EV is connected to the grid through a V2G capable EVSE via CHAdeMO DC charging connector. As shown in the diagram EVSE acts as a bidirectional AC/DC converter connecting directly to EV battery. EVSE and EV are communicating using CHAdeMO v2.0 protocol. VSL agent is installed on the EVSE control computer. It receives data and sends control commands to CHAdeMO controller that controls the power electronics. VSL also reads data from the power meter and processes UI start/stop commands. The agent communicates to the EV aggregator using proprietary OCPP inspired protocol. In this case CPO, EMSP and aggregator roles are all merged and provided by a single server. Such implementation reduces the communication overhead and

potential interoperability issues between multiple actors. However, such monolithic structure makes possible integration with other CPOs and EMSPs much more difficult.

Figure 4.17 shows an example aggregator interface. In this case it shows the NUVVE aggregator used in Parker project.

Car Name	EVSE Name	ISO	Power Capacity Up (kW)	Power Capacity Down (kW)	Power Requested (kW)	Power Provided (kW)	Energy Charge (kWh)	Energy Empty (kWh)	POP (kW)	Power Flow (kW)	Volts (V)	Amps (A)	Status
EV@FF03	FF03	Energinet.dk	9.25	-9.25	4.55	5.11	13.86	7.14	-0.75	4.36	383.0	14.0	GI:V2G

Figure 4.17: NUVVE EV aggregator interface

The graphs show aggregated (left) and individual vehicle (right) response power response to a control signal. Below the graphs, the operator sees a list of aggregated vehicles with their actual status parameters.

4.2 Voltage quality in low voltage networks

EVs can not only support system wide TSO services like frequency regulation but also help local DSO grid by improving local power quality [75–78]. The modern three-phase distribution systems supply a great diversity of customers creating a permanent unbalanced running state. Contrary to other disturbances in the power system which have immediate effects on the ordinary customers, voltage unbalance belongs to those disturbances whose perceptible effects are mostly produced in the long run. Unsymmetrical consumption and production lead to voltage and current unbalances which imply greater system power losses, interference with the protection systems, components' performance degradation and possible overheating to the point-of-burnout [79].

The acceptable limits for the several grid parameters, including voltage unbalances, is defined in the European standard EN50160 [17]. The standard defines root mean square (RMS) limits for phase-to-neutral voltage magnitude $|U_{pn}|$ and the VUF as follows:

$$0.9\,U_{nom} \leq |U_{pn}| \leq 1.1\,U_{nom} \tag{4.3}$$

$$VUF \leq 2\%, \tag{4.4}$$

for $> 95\%$ of all weekly 10 minute intervals, and

$$0.85\,U_{nom} \leq |U_{pn}| \leq 0.9\,U_{nom}, \tag{4.5}$$

for $< 5\%$ of all weekly 10 minute intervals. In addition, the standard defines the VUF as:

$$VUF[\%] = \frac{|U_{inverse}|}{|U_{direct}|} \times 100. \tag{4.6}$$

where $|U_{direct}|$, and $|U_{inverse}|$ are the direct (positive) and the inverse (negative) voltage symmetrical component respectively. Since the definition described in (4.6) involves voltage magnitudes and angles, i.e., complex algebra for calculating the positive and negative components, equations (4.7) and (4.8) give a good approximation while avoiding the use of complex algebra [80].

$$VUF[\%] = \frac{max\{\Delta|U_a^i|, \Delta|U_b^i|, \Delta|U_c^i|\}}{|U_{avg}^i|} \times 100 \tag{4.7}$$

$$|U_{avg}| = \frac{|U_{an}^i| + |U_{bn}^i| + |U_{cn}^i|}{3}, \tag{4.8}$$

where $\Delta|U_a|, \Delta|U_b|, \Delta|U_c|$ are deviations of the respective phase-to-neutral voltage magnitudes from the average phase-to-neutral voltage magnitude $|U_{avg}|$, for the observed time window i. These equations will be used later on for assessing the voltage unbalances in the tested study case.

The used droop controllers have been inspired by the aforementioned standard [81]. Firstly, an upper threshold for the droop controlled voltage is set to 0.95 U_{nom}, above which EVs charge at the maximum current I_{max} of 16 A. Secondly, they can either charge at minimum current I_{min} of 6 A or stop the charging process if the voltage drops below 0.9 U_{nom}, corresponding respectively to the *real droop 1* and *real droop 2* seen in Figure 4.18a. The values in-between the EV charging limits would ideally be linear according to the voltage measurement. However, the current controller has the minimum charging current limit of 6 A and the steps of 1 A as defined in the IEC 61851[41]. Therefore using a typical 3.7 kW EV charger, there are 10 current steps in total. In the implemented controller, these steps are equally distributed between 0.9 and 0.95 U_{nom}. In addition, a steeper droop control corresponding to *real droop 3* in Figure 4.18b has also been tested. Similarly to the first droop control, this control also has 10 current steps equally distributed between the charging limits, but the lower voltage limit is set to 0.925 U_{nom}.

Defining an exact droop value for EVs or loads in general, may not be straightforward as it may not be clear what is the nominal power of the load. In this case, it has been considered that the available range of regulating power (i.e., 2.3 kW) is equal to the EV's nominal power instead of the overall EV charging power which amounts to 3.7 kW. The following parameters have been defined for the described droop controls, i.e., (Equation 4.9) for the droop control seen in Figure 4.18a and (Equation 4.10) for the droop control seen in Figure 4.18b:

$$\begin{cases} \Delta U = 11.5V; U_{nom} = 230V \\ \Delta P = 2.3kW; P_{nom} = 2.3kW \\ k_{droop} = \frac{\Delta U/U_{nom}}{\Delta P/P_{nom}} = 5\% \end{cases} \tag{4.9}$$

$$\begin{cases} \Delta U = 5.75V; U_{nom} = 230V \\ \Delta P = 2.3kW; P_{nom} = 2.3kW \\ k_{droop} = \frac{\Delta U/U_{nom}}{\Delta P/P_{nom}} = 2.5\% \end{cases} \tag{4.10}$$

Droop controller calculates the EV charging current limit I_{droop} using the following formula:

$$I_{droop} = \frac{(U_{meas} - U_{nom}) * (I_{max} - I_{min})}{(U_{nom} * k_{droop})} + I_{base} \tag{4.11}$$

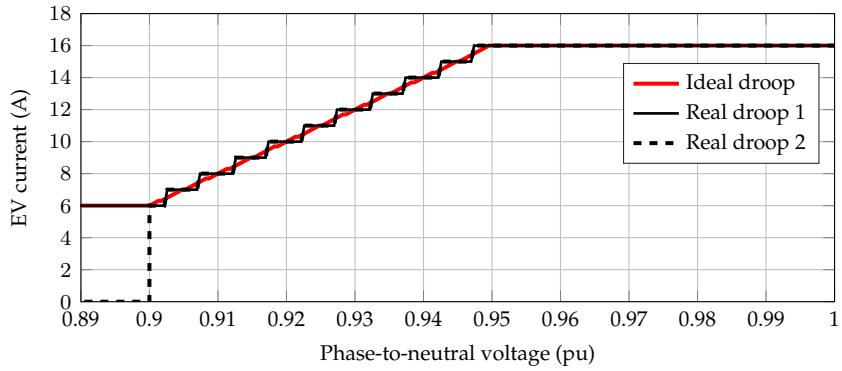

(a)

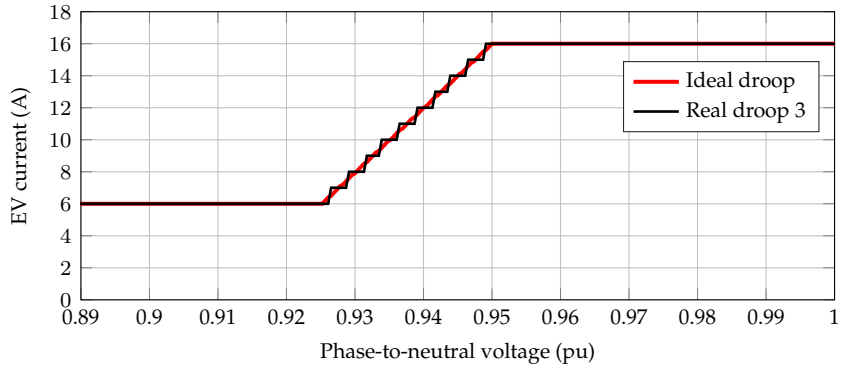

(b)

Figure 4.18: Implemented droop controls: (a) k=5%, and (b) k=2.5%

where U_{meas} is the actual voltage measurement and I_{base} is a base EV charging current when voltage is at the nominal value and corresponds to 11A.

$$I_{EV} = \begin{cases} I_{droop}, & I_{min} \leq I_{droop} \leq I_{max} \\ I_{max}, & I_{droop} > I_{max} \\ I_{min}, & I_{droop} < I_{min} \end{cases} \tag{4.12}$$

I_{max} value represents the available power connection current rating at the consumer site, which is typically 16A, and can be further upgraded to 32A or higher. While I_{min} is chosen from lower charging current limit from IEC 61851 standard.

To validate the previously described controller in real EV charging processes, typical low voltage distribution feeder has been recreated in a laboratory environment. The feeder is grid connected through a typical MV/LV 200 kVA distribution transformer, whereas the EVs are connected in the end of the feeder next to the resistive load, representing a common home charging setup. Additionally, the feeder includes a set of renewable sources such as a wind turbine along with a controllable resistive load capable of modulating the consumption independently per phase.

The EV voltage support can theoretically be done by modulating the active and/or the reactive power. However, since the reactive power control is currently not available in commercial EVs, this experiment focuses on active power control for voltage support. Each electric vehicle supply

equipment (EVSE) is equipped with a local smart charging controller which adjusts the EV charging power according to the droop control described above. Since the controller is independent for each vehicle, the charging current is calculated based only on local voltage measurement meaning that the EVs connected to different phases will react differently. Therefore, the vehicles connected to heavy loaded phases will provide more voltage support due to lower measured voltages resulting in being a less burden to the already unbalanced grid.

The complete test setup is distributed over the SYSLAB grid at the Risø Campus of Technical University of Denmark. The studied experimental setup is depicted in Figure 4.19.

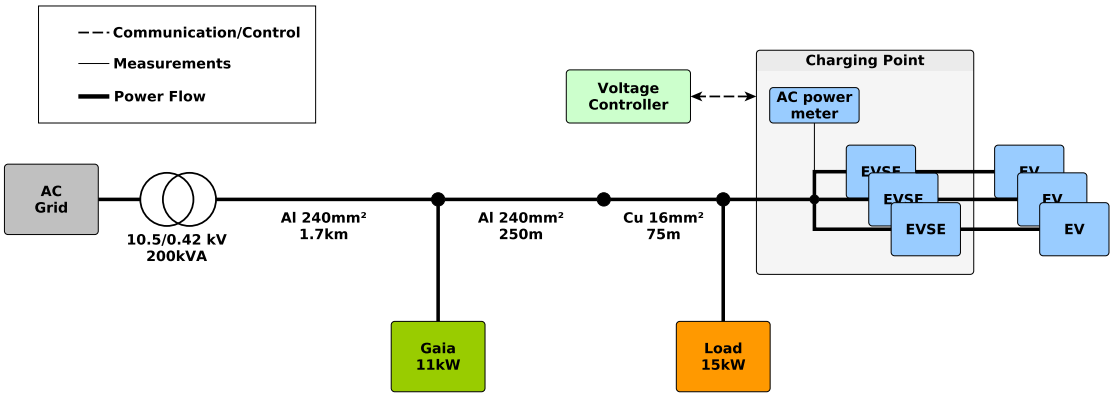

Figure 4.19: Schematic overview of the experimental setup

As seen in the figure, the setup consists of the following components:

- 3 commercially available EVs (Nissan Leaf) with single phase $16\ A\ (230\ V)$ charger and $24\ kWh$ Li-Ion battery.
- 2-blade wind turbine Gaia with rated power $P_n = 11\ kW$.
- $45\ kW$ resistive load ($15\ kW$ per phase) controllable per single-phase in $1\ kW$ steps.
- set of $Al\ 240\ mm^2$ underground cables approximately $1.95\ km$ in length with AC resistance at $45^oC\ R_{AC} = 0.14\Omega/km$ and series reactance $X = 0.078\Omega/km$
- $75\ m$ of $Cu\ 16\ mm^2$ cable with AC resistance at $45^oC\ R_{AC} = 1.26\Omega/km$ and series reactance $X = 0.076\Omega/km$
- $10/0.4\ kV,\ 200\ kVA$ transformer.

The wind turbine connected to the test grid, although not significantly large as active power source, provides stochastic active and reactive power variation to the system. Additionally, it makes the test grid closer to a possible realistic distribution grid with more diverse components than just pure resistive loads.

From the line parameters above, the X/R ratio is calculated to highlight the impedance characteristic of the grid: X/R equals to 0.43. The X/R ratio of the test system is quite low i.e., in the range of the typical LV system and is comparable to CIGRE network [82] as well as other benchmark systems.

Therefore, active power modulation is the most effective way to control voltage levels although reactive power control could also be effective to a certain extent as shown in reference [21].

Firstly, the droop controller with a 5% droop and minimum charging current of 6 A, shown as *real droop 1* in Figure 4.18a, is applied to the EV charging. Measured voltage at the EVSE, load increase steps and corresponding EV charging currents can be seen in Figure 4.20, whereas Figure 4.21 shows the correlation between the measured phase-to-neutral voltage and the measured EV response for each of the phases. The correlation plot closely resembles the droop characteristic shown in Figure 4.18a.

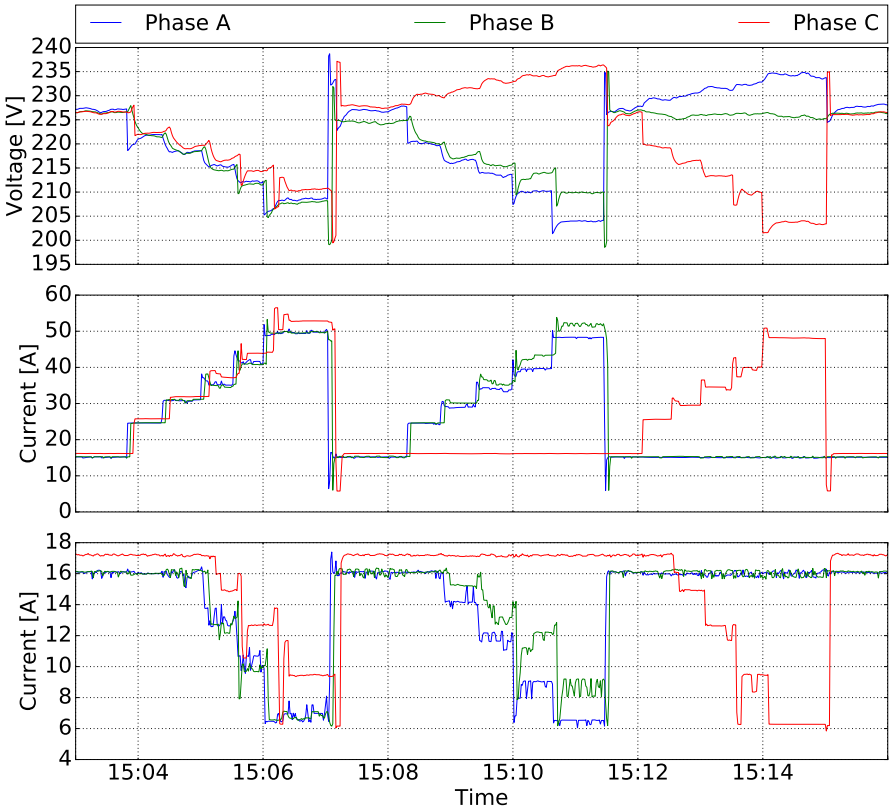

Figure 4.20: Voltage, load and charging current measurements for EV smart charging test scenarios: II - 15:03 to 15:08, III - 15:08 to 15:12 and IV - 15:12 to 15:16

It can be observed that the EVs already start responding at the second load step since the voltage exceeds the droop control boundary of 0.95 U_n. Even for the maximum loading, the voltages are kept above 0.9 U_n as EVs are reducing the charging currents to a minimum value of 6 A. Another interesting phenomena to notice is that the phase-to-neutral voltage on the unloaded phase is rising when the load is increased on the other phases. That is due to a floating, not grounded, neutral line, which introduces a greater voltage unbalance.

Controlled EV charging according to IEC61851 also has the ability to stop and restart the charging of the vehicle. This function could potentially further improve the power quality in the system as the load from the EV could temporarily be removed. Therefore, the same droop controller with 5% slope, but minimum charging current of 0 A is studied. The modification of the droop curve is done as shown in Figure 4.18a as *real droop 2*.

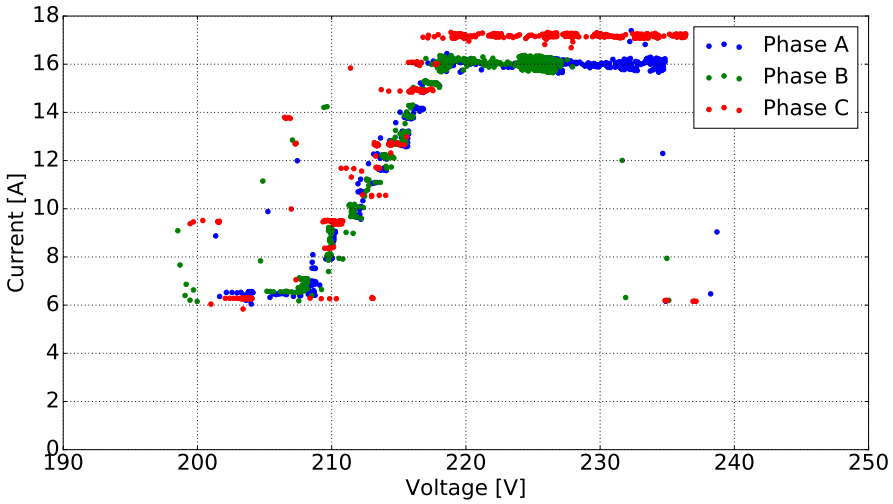

Figure 4.21: Correlation plot between measured phase-to-neutral voltage and EV current for test scenarios II to V

Similarly to previous scenarios, Figure 4.22 shows the measured voltage at the EVSE, load increase steps and corresponding EV charging currents.

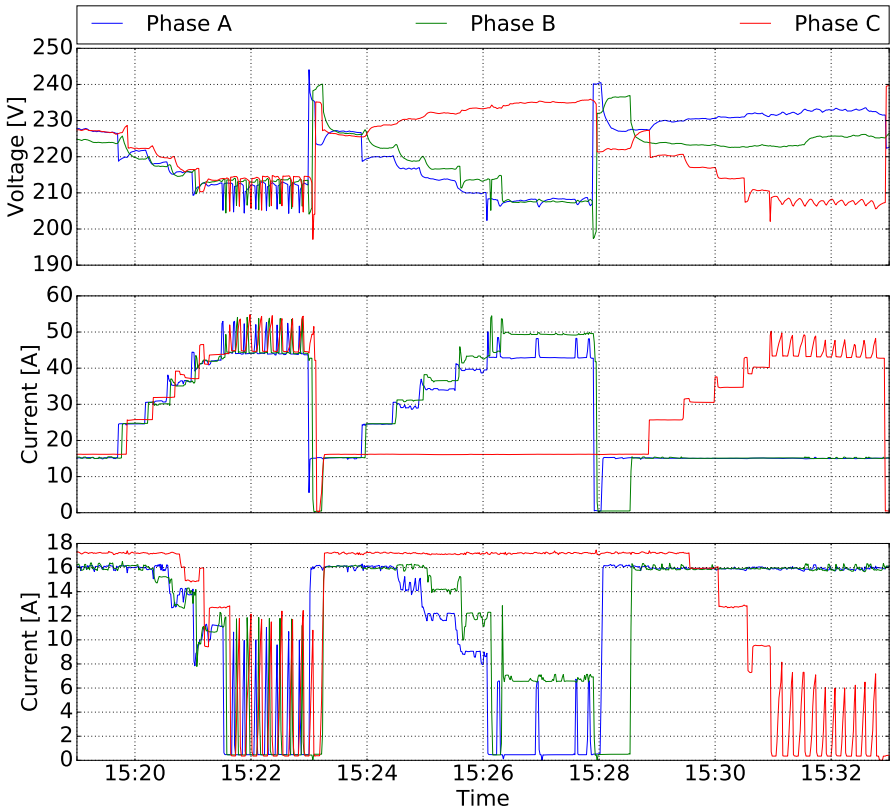

Figure 4.22: Voltage, load and charging current measurements for EV smart charging test scenarios: V - 15:19 to 15:24, VI - 15:24 to 15:28 and VII 15:28 to 15:33

Figure 4.23 presents the correlation between the controller's input voltage and the measured EV

response. The relation pattern is partly resembling the curve shown on Figure 4.18a as *real droop 2*. Although, unlike in the droop curve two clear drops at 6 and 10 A are present. The second drop appears due to controller induced oscillation, which will be explained further.

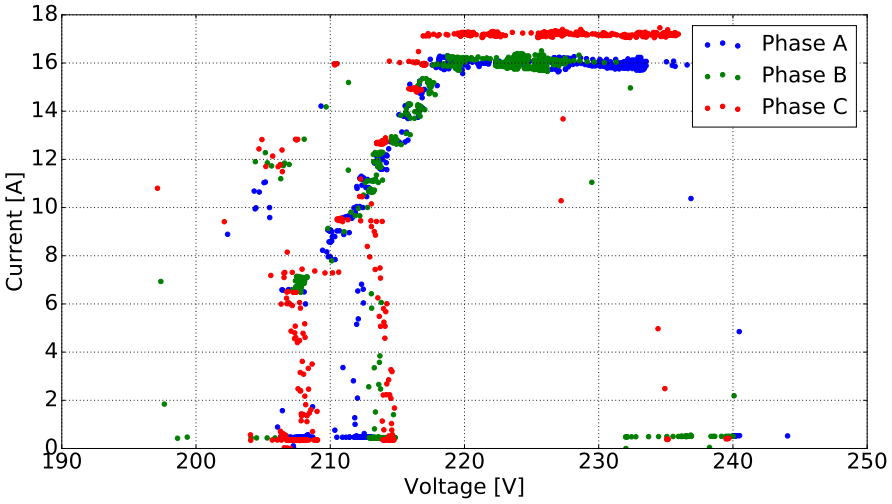

Figure 4.23: Correlation plot between measured voltage and EV current for test scenarios V to VII

Figure 4.22 shows that the system response is almost identical to the test scenarios II to IV, besides in the maximum loading case. At that point, one can notice oscillations in test scenario V and VII which occur due to the brief voltage dip for the last load step. This step briefly puts the voltage under 0.9 U_n, which triggers the controller to stop the charging of the EVs. As the EVs stop charging, the voltages rise to about 0.93 U_n, which makes the controller restart the EV charging since the voltage is now high enough. The restarting process takes about 8 seconds. However, as the EVs restart the charging, the voltage briefly dips under 0.9 U_n again making the controller to stop the charging. This instability repeats as long as the voltage level stays close to 0.9 U_n. In scenario VI, EV on phase a stably mitigates the voltage unbalance by stopping the charge. At the same time, EV on phase b also stabilises the charging current at 7 A, right at the lower limit of stopping the charge. The aforementioned oscillation issues could be solved by modifying the controller to detect the voltage transients and only react for the steady state voltage measurements. However, this has been omitted from the conducted study and left for future work.

Table 4.2: Maximum VUF, steady state voltage values and voltage drop from grid connection to the EV connection point

Scenario	I	II	III	IV	V	VI	VII	VIII
Load	3 phase	3 phase	2 phase	1 phase	3 phase	2 phase	1 phase	3 phase
Droop Control	-	5%	5%	5%	5%	5%	5%	2.5%
Min EV Current	16A	6A	6A	6A	0A	0A	0A	6A
$\mathbf{VUF_{max}}$[%]	1.3	0.8	9.0	7.9	0.6	8.4	6.4	1.0
$\mathbf{U_{an_{maxloadss}}}$[V]	202.8	208.4	203.6	234.5	212.5	208.0	233.0	209.0
$\mathbf{U_{bn_{maxloadss}}}$[V]	202.6	207.9	209.6	225.7	213.5	207.5	225.0	210.5
$\mathbf{U_{cn_{maxloadss}}}$[V]	206.6	210.5	235.9	203.5	214.0	235.0	208.5	212.6
$\mathbf{\Delta U_{an}}$[V]	33.0	27.4	32.1	1.6	23.5	27.8	3.0	27.0
$\mathbf{\Delta U_{bn}}$[V]	30.3	25.1	23.1	7.3	20.7	25.4	7.2	22.6
$\mathbf{\Delta U_{cn}}$[V]	28.3	24.4	-1.2	31.3	19.7	-0.1	27.5	22.3

Firstly, one should note that smart charging when all 3 phases are evenly loaded (test scenarios I, II, V and VIII) improves the voltage unbalance factor (VUF). Secondly, VUF in heavily unbalanced scenarios is much beyond the standard limit for scenarios III, IV, VI and VII. Here, the controller tries to minimise the unbalance by setting EV charging current to the minimum value specified for each scenario. However, vehicles alone can not eliminate the unbalance in the case of maximum loading, since controllable EVs represent only 17 % of the total load. This flexibility could be extended to 25 % if the charging is stopped. It should be noted that values of smart charging scenarios V, and VII were calculated from the measurements of the steady states between the oscillations. Nevertheless, greater controllable power amount results in significant improvements in power quality for scenarios V to VII.

It has been shown that local smart charging controllers can improve power quality in the distribution systems even in extreme cases. Consequently, this allows the integration of higher EV amount in the distribution grids without the need for unplanned and costly grid reinforcements. As the controller and the supporting infrastructure is made from standardised components, such control schemes could potentially be integrated in the EVSE with minimal development effort which makes such solution economically attractive.

4.3 Price based smart charging

All previous grid services were implemented without regard to EV user comfort i.e. estimation of available EV flexibility was not applied. The available flexibility of an EV could be estimated by knowing actual and desired SOC together with departure time. Charging according to external control signal while accounting for available flexibility is commonly known as smart charging.

One typical application of smart charging is to minimize the charging cost in the areas where electricity prices are dynamic. Here smart charging is implemented according to EcoGrid price signal. EcoGrid prices are generated based on the amount of renewable energy production in the area. As can be seen from Figure 4.24, the controller is getting price updates from a prerecorded price database. In this interface live price update is emulated by extracting new values from the price history using the moving window.

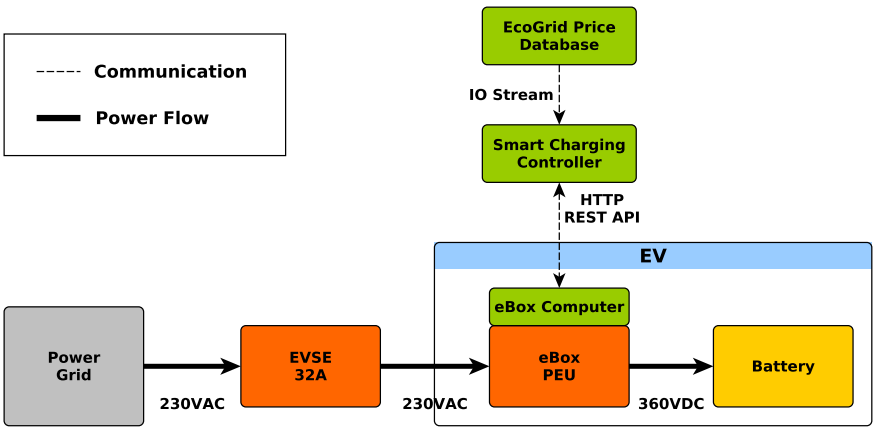

Figure 4.24: Smart charging experimental setup

The EcoGrid price stream consists of three prices series:

- **Real-time price** - the actual electricity price, used for calculating the electricity bill, updated every 5 minutes
- **Hour ahead price** - a collection of 5 minute electricity price predictions for the next hour, updated once an hour
- **Day ahead price** - a collection of hourly price predictions for next 24 hours, updated once a day

Figure 4.26 shows a closer view on price update frequency and accuracy of the predicted price streams compared to real-time price.

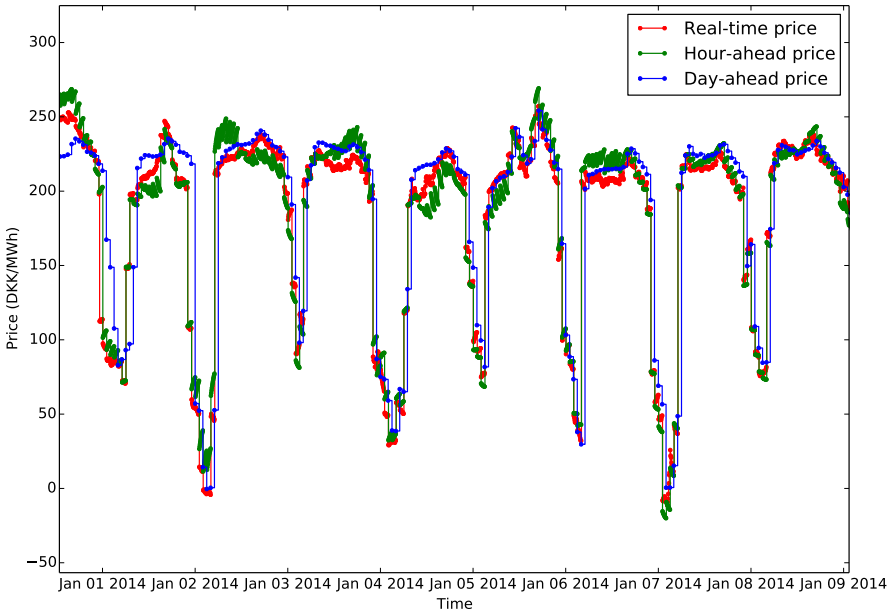

Figure 4.25: EcoGrid price streams

Since the prices are provided for different time slots, the aggregated price for the next 24 hours is composed as shown in Figure 4.27.

This way each price occupies the time slot closest to real time.

The smart charging controller is running with the following algorithm:

while *true* **do**
    read and process price stream data;
    read the actual EV SOC;
    calculate the optimal charging schedule;
    actuate charging power for the EV (P_{ch});
    wait for 5 minutes
end

Algorithm 2: Smart Charging Control

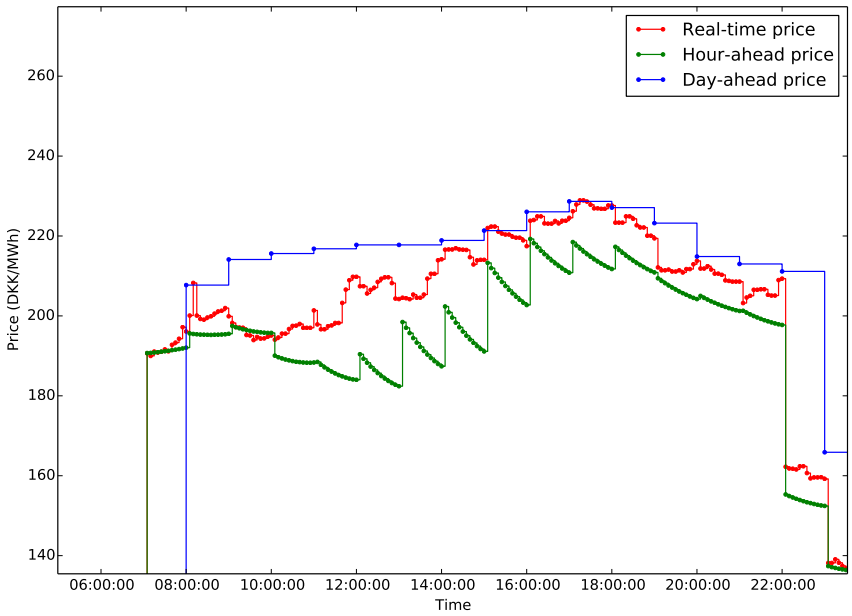

Figure 4.26: Ecogrid price stream close up view

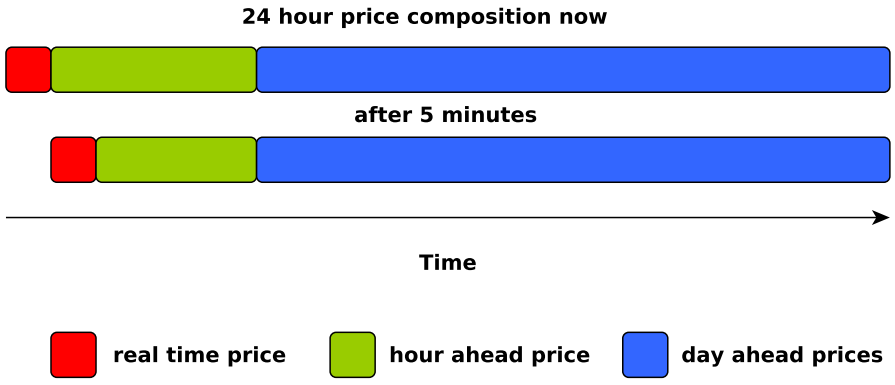

Figure 4.27: Ecogrid price timing

Prices for charging period read from the database with the structure presented in Figure 4.27. Charging cost is formulated as a linear programming problem for minimization, see Equation 4.13 with constraints, see Equation 4.14 and Equation 4.15.

$$TotalPrice_{charge} = \sum_{i=1}^{N} \left(\frac{5}{60} \cdot power_i \cdot price_i \right) \tag{4.13}$$

$$E_{start} + \sum_{i=1}^{N} \left(\frac{5}{60} \cdot P_i \cdot \eta \right) \leq E_{capacity} \tag{4.14}$$

$$E_{end} + \sum_{i=1}^{N} \left(\frac{5}{60} \cdot P_i \cdot \eta \right) \geq E_{target} \tag{4.15}$$

where E_{start} and E_{end} are energy in the battery at the plug-in and plug-out times. E_{target} is a energy target for the battery by plug-out time. P_i is the charging power for the time interval i. N is number of 5 minute intervals from plug-in to plug-out. A linear battery model is used as the operational state of charge will be from 30 to 90%, in which the battery can be charged with constant power [83].

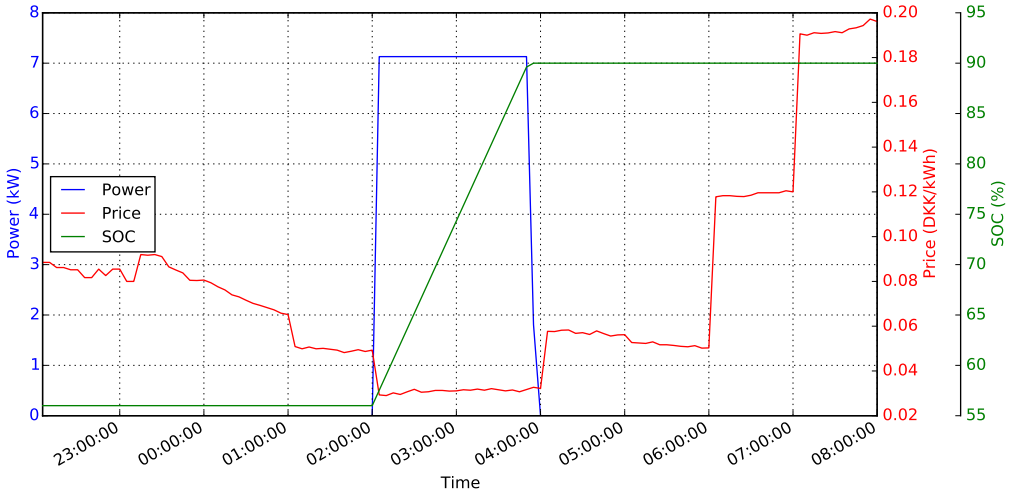

Figure 4.28: Smart Charging simulation results

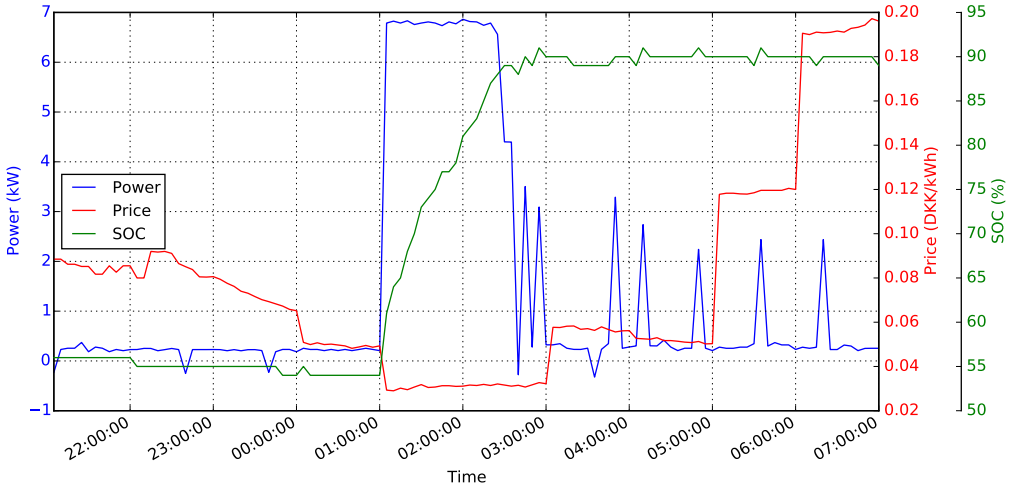

Figure 4.29: Smart Charging experiment results

In the simulation Figure 4.28 and experiment Figure 4.29, the charging is happening during the cheapest time slots, which closely resembles the simulated case. Meanwhile, in Figure 4.29 the small charging peaks present after the vehicle has reached target SOC, is the controller trying

to maintain the battery at the target SOC. The reason for the drops, are the same as previously mentioned regarding PEU idle consumption and active cooling system.

The energy and charging cost results are summarized in the Table 4.3 .

Table 4.3: Smart Charging cost summary

Case	Energy Needed	Energy Consumed	Total Charging Cost
Dumb	13.22 kWh	13.22 kWh	1.060 DKK
Smart	13.22 kWh	14.01 kWh	0.556 DKK

The first thing to notice, is that smart charging reduces the cost of charging with more than a factor two. The other noticeable thing is that charging in general is rather cheap. That is due to the fact that these prices are derived from bulk electricity prices, and therefore do not include various taxes. In Denmark a large part of the electricity price consists of taxes. However, even after adding taxes, the economic benefit of smart charging versus regular charging, would be still noticeable.

This smart charging experiment also serves as a proof of concept. Intelligent integration of grid service provision into a smart charging process could yield additional benefits to the power grid and the EV user.

4.4 Conclusion

While many previous works have tried to prove EVs ability to provide certain grid services, there is no better way than to confirm that than experimental validation. The control architecture from Chapter 3 has been implemented to enable the experiments. The conducted experimental validations show that EV are more than capable of providing multiple grid services. Active power adjustment of EV chargers, combined with fast communication links provide superior performance to any contemporary frequency regulation specification. Addition of reactive power control to external and on board EV chargers could even further improve its value in the local grid. Unfortunately, due to non existing local grid service markets and thus missing financial incentives such devices are not yet manufactured. It is important to note that, to gain user acceptance, all the practical implementations of the grid services should include incentives and account for available EV user flexibility.

4.5 Contribution summary

The author has implemented the control architecture, described in Chapter 3, in a laboratory environment to experimentally validate a set of grid services. Frequency regulation services have been implemented on many levels: the proof of concept with a single vehicle showed that EVs are controllable and fast. Experimental validations in the microgrid showed with significant share of controllable EVs in the grid they could provide even fast frequency regulation services. Similarly, the author used the same control architecture to prove that EVs could also be useful in the local grid, by implementing a decentralized voltage quality controller. Lastly, a proof of concept of electric vehicle smart charging based on the dynamic electricity price signal has also been simulated and experimentally validated.

4.6 List of publications

The relevant publications are listed as follows:

C S. Martinenas, M. Marinelli, P.B. Andersen, C. Træholt, "Implementation and Demonstration of Grid Frequency Support by V2G Enabled Electric Vehicle," in *Proceedings of the 49th International Universities Power Engineering Conference (UPEC) 2014*, Cluj-Napoca, Romania, Sep. 2014.

D M. Marinelli, S. Martinenas, K. Knezovic, P.B. Andersen, "Validating a centralized approach to primary frequency control with series-produced electric vehicles," in *Journal of Energy Storage*, Vol. 7, 2016, p. 63–73.

E S. Martinenas, M. Marinelli, P.B. Andersen, C. Træholt, "Evaluation of Electric Vehicle Charging Controllability for Provision of Time Critical Grid Services," in *Proceedings of the 51st International Universities Power Engineering Conference (UPEC) 2016*, Coimbra, Portugal, Sep. 2016.

F M. Rezkalla, A. Zecchino, S. Martinenas, A. Prostejovsky, M. Marinelli, "Comparison between Synthetic Inertia and Fast Frequency Containment Control Based on Single Phase EVs in a Microgrid," in *Applied Energy*, 2017.

G S. Martinenas, K. Knezovic, M. Marinelli, "Management of Power Quality Issues in Low Voltage Networks using Electric Vehicles: Experimental Validation," in *IEEE Transactions on Power Delivery*, IEEE, 2016.

H S. Martinenas, A.B. Pedersen, M. Marinelli, P.B. Andersen, C. Træholt, "Electric Vehicle Smart Charging using Dynamic Price Signal," in *Proceedings of IEEE International Electric Vehicle Conference (IEVC) 2014*, Florence, Italy, Dec. 2014.

Chapter 5
Interoperability issues and integration challenges

This chapter focuses on the concept of interoperability applied in the field of e-mobility. The work looks deeper into the existing and potential interoperability issues in e-mobility infrastructure and possible solutions for it. Most of the work is based on findings and results of the COTEVOS project that the author participated in [38].

5.1 What is interoperability and why is it needed?

Interoperability is the characteristic of the system to be able to function when system components are changed. In the field of e-mobility, fully interoperable charging systems would enable seamless charging of any electric vehicle with any charging station.

A few reasons to have interoperable systems in e-mobility are:

- User comfort - allow users to charge anywhere, enabling seamless roaming across large areas.
- Economic benefits - interoperable systems are much easier to maintain, as operation costs are reduced by lack of conflicts and smaller integration overhead.
- Larger fleet availability for grid service provision - more vehicles could provide the same services, thus increasing redundancy and flexibility.

5.2 What interoperability problems exist in e-mobility?

While e-mobility is a relatively young field, it is already plagued by the interoperability issues [84]. Current interoperability problems in e-mobility are:

- Mismatch of the hardware interfaces
- Multiple versions of different protocols that cover the same communication link
- Low level of standardization between high level actors

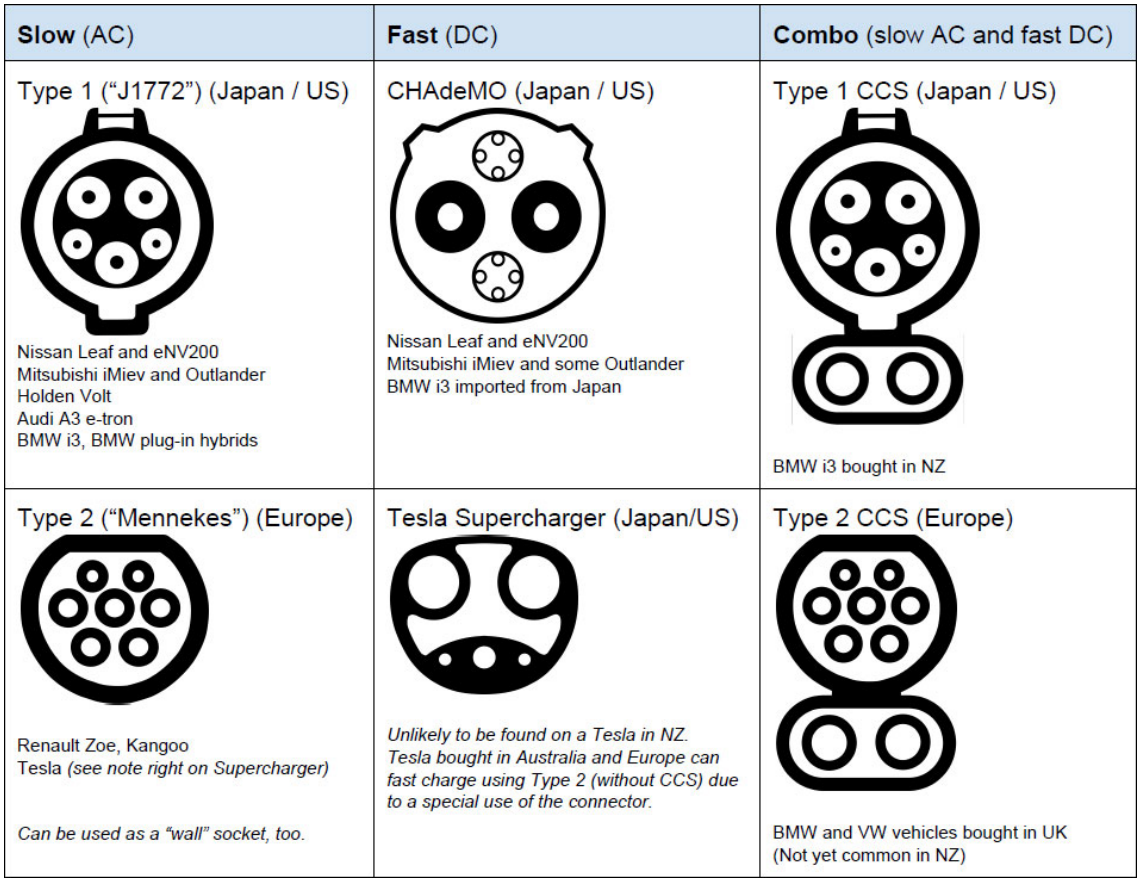

Figure 5.1: Different EV plug types for AC and DC charging [85].

Mismatch of the hardware interfaces is perhaps the most evident problem in e-mobility. Every EV owner is familiar with the issue of the charging spot plug not fitting their EV socket because of different plug type.

An overview of all the common AC and DC charging plugs for EVs is shown in Figure 5.1.

It should be noted that Tesla vehicles in USA use a proprietary Tesla Supercharger plug, but in Europe, due to regulation, they have to use the Type 2 plug. All Tesla Superchargers in Europe use the same Type 2 plug. Engineering decisions by Tesla have maximized the utility of the Type 2 plug to support both AC and DC charging without the need for adding extra pins, such as in Type 2 CCS plug. The way, that Tesla has managed to utilize the simple Type 2 plug, is by using 2 of the power pins (L1 and L2) for + (positive side) and two other power pins (L3 and N) for - (negative side) of the DC connection, when the car is charging at the Tesla Supercharger. The problem of high current running trough the Type 2 plug (AC charging station are rated up to 80A, whereas DC fast chargers could reach around 300A) was solved by making the pins in the plug a bit longer, thus increasing the contact area, while maintaining backwards compatibility with Type 2 plugs used in common AC charging stations.

Looking at some of the most popular EVs on the market, one can notice a variety of supported charging standards, shown in Table 5.1.

It is evident that Japanese manufactured vehicles are all supporting type 1 plugs for AC charging and CHAdeMO standard for DC. On other hand, European vehicles are mostly made with type 2

Table 5.1: Charging standards supported by most popular EV models

EV model	AC charging	DC charging
Nissan leaf	Type 1	CHAdeMO
Mitsubishi i-MiEV	Type 1	CHAdeMO
Renault Kangoo	Type 1	-
Tesla Model S/X	Type 2	Supercharger and CHAdeMO (with adapter)
Renault Zoe	Type 2	-
BMW i3	Type 2	CCS

plugs that support 3 phase charging. The difference between type 1 and type 2 plugs can usually be mitigated by using a different cable, which most EV owners carry with them. That however is only true for the AC charging points with sockets for user owned cables. All of the DC charging stations have fixed cable assembly installed. Additionally, CCS and CHAdeMO use different communication media and protocols for EVSE to EV communication i.e. PLC and CAN bus respectively. Therefore, CCS and CHAdeMO stations are absolutely not interoperable.

EV to EVSE connection is only the first of many communication links that should be interoperable in the field of e-mobility. Figure 5.2 presents an e-mobility reference architecture developed in the COTEVOS project [86]. In the figure, e-mobility infrastructure and high level actors are depicted in blue and green respectively. The power grid and energy market related actors are depicted in grey and orange respectively. The hexagonal shapes represent the physical actors e.g. EV, EVSE and grid.

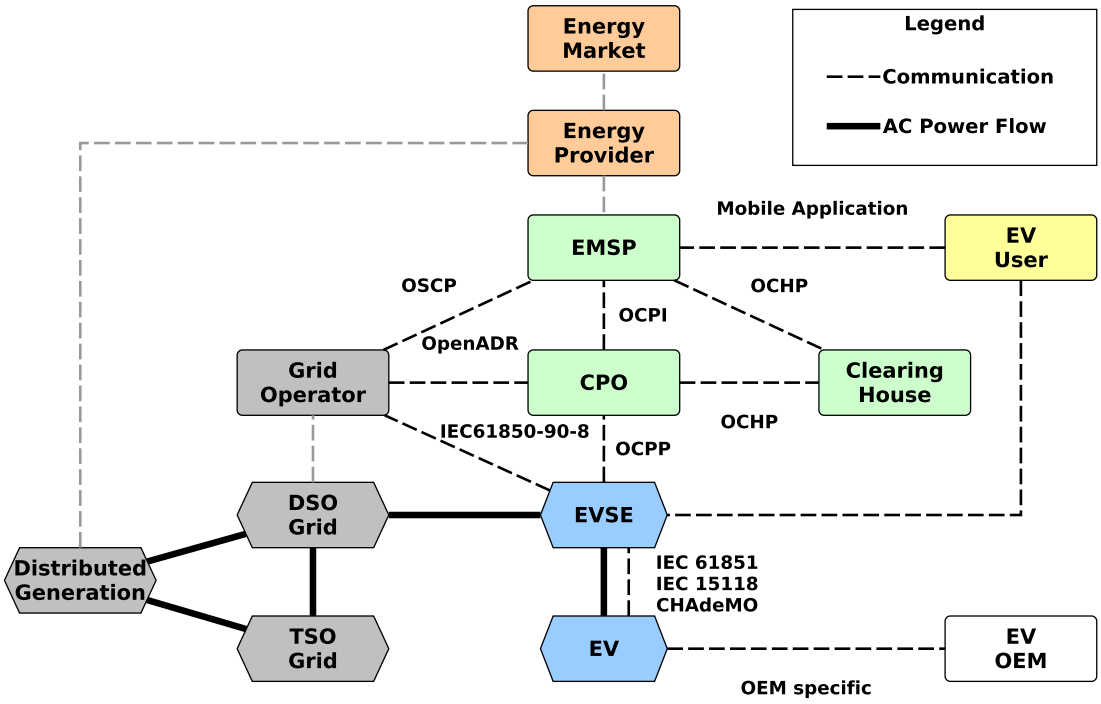

Figure 5.2: E-mobility architecture developed in the COTEVOS project [86].

The actors and their roles were described in Chapter 3. It is evident that a separate role of the EV

aggregator is missing from this architecture, instead it is distributed between grid operator, EMSP and CPO.

In the COTEVOS project all the communication links between actors were divided into the following groups:

EV charging and operation - focusing on testing the interoperability between EV and EVSE.

EVSE operation - focusing on interoperability between EVSE and CPO back-end.

EV/EVSE user services - meant for testing interoperability issues that directly involve the user.

EMSP-CPO services - meant for testing interoperability between different CPOs and EMSPs.

Adaptive charging - meant for testing interoperability issues in adaptive charging scenarios.

V2X and grid services - meant for testing interoperability issues in grid service provision scenarios.

Wireless charging - focusing on testing the interoperability between EV and EVSE when using wireless charging.

5.3 How is interoperability ensured?

Interoperability could be ensured by creating a testing framework [87]. The COTEVOS project attempted to create interoperability testing procedures for entire e-mobility architecture. While this seems like a good idea, such task is too large to comprehensively cover all the interfaces of the architecture in one project. However, firstly all the use cases for the e-mobility operation were written up. Then all of these use cases were converted into test procedures presented in the full version of Pub. I. The full version of Pub. I is 462 pages long as it contains all the test procedures in its appendix. Therefore only a summary and table of contents of this deliverable is attached to the thesis, the full publication can be found online here [88].

5.3.1 Interoperability testing

An example of test procedure from EV charging and operation group can be seen in Table 5.2. The example is filled in with realistic test data that would result from a test performed in the laboratory, presented in italic. Each test procedure is structured in three main parts. Firstly, a brief summary of the procedure is presented on the top. It contains name, test group, short description, objective and relevant standards. Secondly, the fields to be filled with testing equipment specifications are in the middle. Lastly, the steps for the procedure with expected outcome and comment fields ,to be filled, are in the bottom.

As can be seen in the procedure, the test case is closely following the charging process defined in IEC 61851-1. The vehicle under test is the Nissan Leaf EV which supports this standard, thus the test results in nominal performance as expected.

Most testing procedures like the one shown in Table 5.2 are based on the existing standard or specification that covers that link. However, some test cases especially in the higher levels of the reference architecture were quite generic as shown in Table 5.3.

As can be seen here the test case is based on a generic frequency regulation service, thus testing the whole communication chain from the grid operator, trough the e-mobility infrastructure all the

Table 5.2: Test procedure from EV charging and operation group.

Author	**Version**		**Date**
DTU	1.1		2015-04-08
Test Group	EV charging and operation		
Test Case	EV Charging using IEC61851		
Test ID	TC-1.3-EV-001		
Description	EV charging using IEC61851 compatible EVSE		
Objective	Charge the EV using IEC61851 standard		
Relevant standards	IEC61851		
Equipment specifications			
EV	Model: *Nissan Leaf* Battery size: *24kWh* Phases: *1* Max charging current per phase: *16A*		
EVSE	Model: *DTU EVSE* Phases: *3* Maximum current per phase: *32A*		
Cable	Rated current: *16A*		
Test procedure			
Nr	**Action**	**Expected Result**	**Actual Result**
Preconditions	EV SOC below 50%	<50%	*48%*
1	Plug cable into the EVSE	true	*true*
2	Plug cable into the EV	true	*true*
3	Observe CP line state change from B to C	true	*true*
4	Enable PWM	true	*true*
5	CP line PWM set to 16A	true	*true*
6	Close the EVSE contactor	true	*true*
7	EV charging starts	true	*true*
8	Charging voltage at EVSE	value	*225.7V*
9	Charging current at EVSE	value	*15.4A*
10	End charge - unplug cable	true	*true*
11	Charging SOC at start/end %	value/value	*48%/51%*
Post conditions	-		
Comments	*Test for 16A, 32A, 63A and a chosen current limit setting in between*		

way to the EV. In the example case an unmodified unidirectional EV has been used to provide a primary frequency regulation service just like one presented in Chapter 4. The test case is standard agnostic and allows for testing almost any functional grid service setup based on e.g. IEC 61851 or IEC 15118 or CHAdeMO. Additionally, it relies on the compatible communication links in the higher layers of e-mobility infrastructure e.g. OCPP, IEC61850-90-8 or OpenADR.

5.3.2 Recommendations for ensuring interoperability

To ensure interoperability in the e-mobility infrastructure, the following recommendations are identified:

- Harmonization of charging plugs - currently multiple types of charging plugs exist for AC and DC charging, which sometimes creates a problem for EV users to find a compatible charging station.

Table 5.3: Test procedure from V2X and grid services group.

Author	**Version**		**Date**
DTU	1.0		2015-08-04
Test Group	V2X and Grid Services		
Test Case	Primary Frequency Regulation		
Test ID	TC-6.1-EV-001		
Description	Primary frequency regulation using an EV		
Objective	Testing EV ability to provide grid frequency regulation service		
Relevant standards	IEC61851, IEC15118, IEC61850-90-8, OCPP		
Equipment specifications			
EV	Model: *Nissan Leaf* Battery size: *24kWh* Phases: *1* Max charging current per phase: *16A*		
EVSE	Model: *DTU EVSE* Phases: *3* Maximum current per phase: *32A*		
Cable	Rated current: *16A*		
Test procedure			
Nr	**Action**	**Expected Result**	**Actual Result**
Preconditions	V2X is supported by the EV and EVSE EV is connected to the EVSE Charging session is initiated Neutral current setpoint is set	true true true 0kW	*false* *true* *true* *11A*
1	Aggregator measures grid frequency	value	*50.2Hz*
2	Aggregator calculates the power setpoint	value	*16A*
3	Setpoint is sent from aggregator to CPO	true	*true*
4	Setpoint is sent from CPO to EVSE	true	*true*
5	EVSE and EV renegotiate the charging schedule	true	*NA*
6	EV accepts the new charging schedule	true	*NA*
7	EV (dis)charging power changes	value	*16A*
Post conditions	EV power is corresponding to the setpoint set by the aggregator		
Comments	*EV with IEC61851 is used, no V2G support*		

- Open and easily accessible specifications/standards - the process of acquiring a copy of the specification and a possibility to give feedback should be straight forward.

- Strict protocols with detailed and clear communication description - concrete definitions in the protocol design, that do not leave room for misinterpretation, are a key component of interoperable communication protocol.

- Available testing tools - the implementations should be tested with testing tool approved or developed by the organization that is developing the standard/specification.

- Establishment of certification bodies - while testing tools should provide a basic level of interoperability, each implementation should be fully tested by an official certification body that ensures same level of testing for each implementation, providing consistency.

- Application workshops and testing symposiums - just like IEC15118 testing symposiums, such workshops would not only help companies to improve their implementations but also provide feedback to standardization bodies on the needs for future improvements in the standard.
- One link, one specification - each communication link in the e-mobility infrastructure should preferably be covered by one specification/standard avoiding overlap or a gap.

5.4 Conclusion

Although, it might be difficult to fit the study on the interoperability issues into academic context, the practical application of this work is immediate. At the start of the work on assessing and ensuring the interoperability in e-mobility infrastructure very few standards/specifications existed. During past few years, the gaps in the communication links were covered by one or more specifications. Most of these specifications do follow the recommendations identified in the project and thus are highly interoperable. However, there is still a long way to go to ensure the full interoperability of each communication link in the e-mobility architecture. The main findings of the COTEVOS project were summarized by project participants in the white book on "Business Opportunities for Interoperability Assessment of EV Integration" [89].

5.5 Contribution summary

Most results in this chapter are building on top of the work performed in the COTEVOS project, that the author has participated in. The main contributions of the author in the topic of e-mobility are threefold. Firstly, survey of the current state in interoperability issues. Secondly, development and coordination of the test procedures and their execution. Lastly, formulation of the recommendations to ensure interoperability.

5.6 List of publications

The relevant publications are listed as follows:

I T.M. Sørensen, M.B. Jensen, S. Martinenas, "Analysis of needs for on-going or incipient standards. Design of Round Robin tests and results of the performed tests. Recommendations for existing standards" in *COTEVOS project deliverable*, Feb. 2016

Chapter 6
Conclusion

This chapter summarizes the presented thesis by reflecting on the formulated research questions. Additionally, different e-mobility development perspectives are elaborated on and outline of the future work is presented.

6.1 Research conclusions

The main motivation for EV integration into the smart grid is their potential ability to provide grid services as distributed energy resources. The work focused on answering the question:***What is technically required to use an EV as a smart mobile distributed energy resource?*** This main question was divided into sub-questions, here are the answers to the those questions:

- ***What grid services could EVs provide?***
  In Chapter 2 the arguments for grid integration of EVs and their potential benefit for the grid services were outlined: EVs could provide a variety of grid services on distribution and transmission levels. These arguments then were experimentally proven in Chapter 4 by showing that EVs could provide different grid services such as fast frequency regulation, local power quality improvement and smart charging. Even though the frequency regulation service has been experimentally validated just two years ago, it is already implemented in a pilot project in Copenhagen [90]. Possible future services such as very fast frequency regulation or even synthetic inertia are definitely achievable as inverter based chargers have an almost instantaneous response, that is only limited by the controllers. Local grid power quality improvement services i.e. voltage and congestion control were proven to be also feasible. However, clear regulation and compensation schemes for such local services should be established. The grid regulation could be inspired by the solutions from local PV integration experience. Finally, while providing grid services, user comfort should not be forgotten. Therefore, smart charging should be incorporated as part of the grid service provision to ensure maximum benefit for the grid and the EV user.

- ***What are ICT requirements for EV aggregation?***
  EV aggregators are becoming an integral part of e-mobility infrastructure. Therefore, clear information exchange models all the way from EV to the aggregator should be established. In the process of this study essential, quality improving and optional parameters have been identified. These can be further divided into dynamic and static information objects. The essential dynamic information objects passed on are: SOC, power set-point, identification, grid parameters (frequency, voltage). Quality improving dynamic information objects: departure

time and desired SOC (defining available flexibility). The essential static information is: nominal battery capacity, power connection limitation, location on the grid. All of the mentioned parameters are essential to be implemented in the communication links from the EV, trough the e-mobility infrastructure, to the aggregator.

- ***What is current EV technology development status in relation to grid integration?***
  The survey of e-mobility technologies in Chapter 3 has shown that EVs are technically ready to integrate into the grid. The charging hardware devices are controllable, while battery degradation arising from V2G activities, investigated in the PhD study, is acceptable due to low cycling of the battery and much lower power levels compared to driving duties [91–93]. Contemporary standards and communication protocols are largely ready to support the EV grid integration requirements and are constantly developing in that direction. More specific improvements that standardization bodies should focus on are: adding missing information objects, stricter requirements for communication timing and implementation communication security requirements. These improvements are essential to make EVs an active part of the smart grid.

- ***What technical challenges are still present for EV integration?***
  Most major technical problems seem to be solved and multiple demonstration projects are already successfully integrating EVs to provide grid services and alleviate congestion issues. However, some minor issues still remain, such as e-mobility communication standards, that are lacking behind by not including vital information objects for EV grid integration in their current versions. Meanwhile, these missing information objects are acquired using alternative methods and custom extensions to the protocols. This methodology, increases fragmentation of standard implementations and could bring severe interoperability issues in the future. Most organizations behind the standards/specifications are promising the inclusion of needed features in the next releases. Perhaps the biggest barriers to the active EV spread and integration into the grid are not technical, but outdated regulations and policies that were developed for conventional power sources. This is slowly changing, as some grid operators are starting pilot projects with relaxed regulatory entry conditions to investigate the services, that various DERs could provide, for the future power grid. Additionally, lack of incentives does not allow for proper acceleration of the technological innovation in EV grid integration e.g. missing chargers with reactive power control.

- ***What are prerequisites and current state of EV interoperability?***
  In Chapter 5 current interoperability problems in e-mobility field are identified and their solutions are proposed. These findings are largely based on the work that the author has performed during the COTEVOS project. The main problems with EV interoperability remain in the physical variety of charging plugs. AC charging of EVs has been largely unified besides the minor issue of 1 phase vs 3 phase connector. DC charging still remains an active battleground where two big standards are competing: CHAdeMO and CCS. Meanwhile the third contender seems to stay out and develop their own solution - Tesla Supercharger. Current remedies for existing market division into different charging standards are adaptor cables and multi-standard plug EVSEs.

  The prerequisites for fully interoperable charging experience are unified charging interfaces for AC and DC charging and compatible roaming protocols in e-mobility back-ends. This all can be ensured by extensive OEM testing and certification at regular test events. The first

interoperability testing procedures have been developed for entire e-mobility architecture in Pub. I.

6.2 E-mobility development perspective

This work has analyzed current trends in the field e-mobility with regards to integration with the smart grid. Meanwhile, seemingly unrelated social, economic and some technical development trends have not been accounted for. The purpose of this section is to try to identify those trends and predict/speculate their impact on grid integration of EVs.

An important trend currently developing in bigger cities is ride and car sharing also known as mobility as a service. This enables anyone with a right membership to have a vehicle at any time of the day without a need to pay for parking, fuel, vehicle registration fees and other taxes related to vehicle ownership. That plays well together with the needs of current generations of city dwellers, who just want mobility without the hassles of vehicle ownership. An important trend in automotive industry that could have big effects on the way cars are used today is autonomous vehicle. This trend, together with car sharing, could eliminate the need for car ownership as a vehicle could be immediately available on request. This way most vehicles would be almost constantly moving on the road thus greatly reducing the current trend of vehicles just standing around 95% of the time [94]. That would greatly decrease the flexibility, needed for grid service provision, expected from electrification of personal transportation.

Decreasing battery prices, resulting from technology development for transportation electrification, would make the large battery storage facilities for backup power and grid services much more common. These stationary battery solutions would be the biggest competitor to EVs in the grid service provision market.

Current overall need for the primary frequency regulation reserves in continental Europe is around $\pm$ 3000MW. Considering current state of the art V2G chargers or $\pm$ 10kW, theoretically already 300000 EVs connected to those bidirectional chargers could saturate the market. If industrial scale batteries and other large DERs also enter this market, EVs are facing some serious competition. This raises a question, are EVs really the best solution for providing grid services? In the short term, probably yes, as current state of technology and user behavior allows for enough flexibility to provide grid services using EVs. However, this could change by the time personal transport is fully electrified. Therefore, we will have to see about the role of e-mobility in grid operation in a long term.

6.3 Future work

Further research topics and possible upgrades to the developed experimental systems are:

- While bidirectional chargers are already used in a primary frequency regulation service, their design might not be most optimal. Therefore, deeper research into charging hardware technologies should be done. One way to implement it is to build custom V2G chargers with active, reactive power support and possible integrated battery. This would also allow their immediate testing in the laboratory conditions without the need for long waiting times of OEMs to produce and test their hardware.

- There are many electric vehicles from different manufacturers in the field. Each model of the vehicle usually has different power electronic components which result in a different power response to a control signal. Therefore, a response from a hybrid set of vehicles where power electronic unit response patterns are mixed should be investigated. Additionally, the research could be expanded with differences in response from a single (small set) and large aggregated set of vehicles.
- Autonomous vehicles could take over the mobility market faster than expected. Therefore, to future proof current research activities, the use cases of autonomous EV for grid service provision should already be considered. Furthermore, a study into aggregation of autonomous vehicles for grid service provision should investigate if the flexibility/availability of the service would be reduced by such vehicles.
- Wireless charging is likely a de-facto charging mode of the future EVs. Therefore, a possibility of providing grid services using bi-directional wireless charging should be investigated. This topic presents mostly a technical and regulatory challenge to develop an efficient bidirectional wireless charger.
- While some grid services have a predefined control behavior e.g. frequency regulation using droop control, more advanced versions involving PID, MPC, etc. should be investigated for newly identified services as they could bring improved performance. Application of more advanced control strategies for grid services should be researched, especially for undefined services like local power quality improvement and synthetic inertia.
- The second iteration of the control architecture for grid service provision, based on open e-mobility standards, is developed. However, the implementation of this architecture is not yet finalized and tested with real grid services. This is the most immediate future work task.
- Many grid services were experimentally demonstrated in this work. However, most of them were only focusing on the grid relevant aspects of the service. In the real world conditions, the service would likely be provided using a vehicle owned by an individual. Therefore, embedding of smart charging control algorithms into the grid service provision controllers should be investigated to provide a realistic and user friendly service.

Bibliography

[1] Installed wind power capacity in Europe, 2016. https://windeurope.org/about-wind/statistics/.

[2] Installed global wind power capacity, 2016. http://www.gwec.net/publications/global-wind-report-2/global-wind-report-2016/.

[3] IEA PVPS annual report 2016. http://www.iea-pvps.org/index.php?id=6&eID=dam_frontend_push&docID=3951.

[4] Smart grid concept diagram. http://www.ecnmag.com/sites/ecnmag.com/files/legacyimages/ECN/Articles/2011/04/SmartGridDiagram-web.jpg.

[5] Airbus e-fan electric aircraft. http://company.airbus.com/responsibility/airbus-e-fan-the-future-of-electric-aircraft.html.

[6] EV sales in Norway in 2016. http://insideevs.com/ev-sales-norway-2016/.

[7] Volvo Cars to go all electric. https://www.media.volvocars.com/global/en-gb/media/pressreleases/210058/volvo-cars-to-go-all-electric.

[8] IPCC. Climate Change 2014: Mitigation of Climate Change. https://www.ipcc.ch/report/ar5/wg3/.

[9] Dansk Energi, Dong Energy, and Energinet.dk. Analysis no. 5 – Scenarios for the deployment of electric vehicles (in Danish). Technical report, 2013.

[10] W. Kempton and J. Tomic. Vehicle-to-grid power implementation: From stabilizing the grid to supporting large-scale renewable energy. *Journal of Power Sources*, 2005.

[11] J. A Peças Lopes, F. J. Soares, and P. M. R. Almeida. Integration of electric vehicles in the electric power system. *Proc. IEEE*, 99(1):168–183, 2011.

[12] C. Madina, E. Zabala, R. Rodríguez-Sánchez, E. Turienzo, J. Antonio López, et al. Economic Impact of Distribution Grid Operation Scenarios for the Integration of Electric Vehicles. 2014.

[13] K. Knezović, M. Marinelli, P. Codani, and Y. Perez. Distribution grid services and flexibility provision by electric vehicles: A review of options. In *Power Engineering Conference (UPEC), 2015 50th International Universities*, pages 1–6. IEEE, 2015.

[14] Final report on the August 14, 2003 blackout in the United States and Canada. Technical report, U.S.-Canada Power System Outage Task Force , 2008. http://energy.gov/oe/.

[15] V. Lakshmanan, M. Marinelli, J. Hu, and H. W. Bindner. Provision of secondary frequency control via demand response activation on thermostatically controlled loads: Solutions and experiences from Denmark. *Applied Energy*, 173:470–480, 2016.

[16] Ancillary services to be delivered in Denmark Tender conditions. Technical Report October, 2012.

[17] European Committee for Electrotechnical Standardization. EN50160:Voltage characteristics of electricity supplied by public electricity networks, 2010.

[18] K. Knezović, C. Træholt, M. Marinelli, and P. B. Andersen. *Active integration of electric vehicles in the distribution network - theory, modelling and practice*. PhD thesis, 2017.

[19] J. García Villalobos. *Optimized charging control method for plug-in electric vehicles in LV distribution networks*. PhD thesis, 2016.

[20] J. García-Villalobos, I. Zamora, J. I. San Martín, F. J. Asensio, and V. Aperribay. Plug-in electric vehicles in electric distribution networks: A review of smart charging approaches. *Renewable and Sustainable Energy Reviews*, 38:717–731, 2014.

[21] K. Knezović, M. Marinelli, R.J. Moller, P.B. Andersen, C. Treaholt, and F. Sossan. Analysis of voltage support by electric vehicles and photovoltaic in a real Danish low voltage network. *Power Engineering Conference (UPEC), 2014 49th International Universities*, pages 1–6, Sept 2014.

[22] Z. Wang and S. Wang. Grid power peak shaving and valley filling using vehicle-to-grid systems. *Power Delivery, IEEE Transactions on*, 28(3):1822–1829, July 2013.

[23] S. Mocci, N. Natale, F. Pilo and S. Ruggeri. Demand side integration in LV smart grids with multi-agent control system. *Electric Power Systems Research*, 125:23 – 33, 2015.

[24] G. A. Putrus, P. Suwanapingkarl, D. Johnston, E. C. Bentley, and M. Narayana. Impact of electric vehicles on power distribution networks. In *2009 IEEE Vehicle Power and Propulsion Conference*, pages 827–831, Sept 2009.

[25] NIKOLA project website. http://www.nikola.droppages.com/.

[26] P.B. Andersen, M. Marinelli, O.J. Olesen, C.A. Andersen, G. Poilasne, B. Christensen, and O. Alm. The Nikola project Intelligent electric vehicle integration. *Innovative Smart Grid Technologies Conference Europe (ISGT-Europe), 2014 IEEE PES*, pages 1–6, Oct 2014.

[27] Charged EVs magazine. Tesla's batteries – past, present and future. https://chargedevs.com/features/teslas-batteries-past-present-and-future/.

[28] AC Propulsion: Vehicle to Grid Power. http://www.acpropulsion.com/products-v2g.html.

[29] W. Kempton, V. Udo, K. Huber, K. Komara, S. Letendre, S. Baker, D. Brunner, and N. Pearre. A Test of Vehicle-to-Grid (V2G) for Energy Storage and Frequency Regulation in the PJM System. Technical report, 2008.

[30] CHAdeMO V2X technology. https://www.chademo.com/technology/v2x/.

[31] A. Kieldsen, A. Thingvad, S. Martinenas, and T. M. Sørensen. *Efficiency Test Method for Electric Vehicle Chargers*. 2016.

[32] Qualcomm Demonstrates Dynamic Electric Vehicle Charging. https://www.qualcomm.com/news/releases/2017/05/18/qualcomm-demonstrates-dynamic-electric-vehicle-charging.

[33] Qualcomm Halo Wireless Charging. https://www.qualcomm.com/products/halo.

[34] C. Liu, C. Jiang, and C. Qiu. Overview of coil designs for wireless charging of electric vehicle. In *2017 IEEE PELS Workshop on Emerging Technologies: Wireless Power Transfer (WoW)*, pages 1–6, May 2017.

[35] D. J. Thrimawithana, U. K. Madawala, and Yu Shi. Design of a bi-directional inverter for a wireless V2G system. In *2010 IEEE International Conference on Sustainable Energy Technologies (ICSET)*, pages 1–5, Dec 2010.

[36] A. A. S. Mohamed, A. Berzoy, and O. Mohammed. Power Flow Modeling of Wireless Power Transfer for EVs Charging and Discharging in V2G Applications. In *2015 IEEE Vehicle Power and Propulsion Conference (VPPC)*, pages 1–6, Oct 2015.

[37] U. K. Madawala and D. J. Thrimawithana. A Bidirectional Inductive Power Interface for Electric Vehicles in V2G Systems. *IEEE Trans. Industrial Electronics*, 58(10):4789–4796, 2011.

[38] COTEVOS project website. http://www.cotevos.eu/.

[39] ElaadNL. EV Related Protocol Study v1.0, 2017.

[40] EV Connectors and EV Charging Cables. https://www.evse.com.au/ev-charging-cables-leads/.

[41] International Electrotechnical Commission. IEC 61851-1 ed2.0: Electric vehicle conductive charging system - Part 1: General requirements, 2010.

[42] International Electrotechnical Commission. IEC 61851-1:2017 Electric vehicle conductive charging system - Part 1: General requirements, 2017.

[43] C. Lewandowski, S. Gröning, J. Schmutzler, and C. Wietfeld. Interference analyses of Electric Vehicle charging using PLC on the Control Pilot. In *2012 IEEE International Symposium on Power Line Communications and Its Applications*, pages 350–355, March 2012.

[44] S. Ruthe, J. Schmutzler, C. Rehtanz, and C. Wietfeld. Study on V2G Protocols against the Background of Demand Side Management. In *IBIS - Interoperability in Business Information Systems*, volume Issue 1, 2011.

[45] ISO/IEC. ISO/IEC DIS 15118-3: Road vehicles - Vehicle to grid communication interface – Part 3: Physical and data link layer requirements, 2012.

[46] HomePlug Green PHY. http://www.homeplug.org/tech-resources/green-phy-iot/.

[47] ISO/IEC. ISO/IEC DIS 15118-2: Road vehicles - Vehicle to grid communication interface – Part 2: Network and application protocol requirements, 2012.

[48] ISO/IEC. ISO/IEC DIS 15118-1: Road vehicles - Vehicle to grid communication interface – Part 1: General information and use-case definition, 2012.

[49] OpenV2G project. http://openv2g.sourceforge.net/.

[50] C. Blach, S. Martinenas. Open source ISO/IEC 15118 communication implementation. https://github.com/Sergejus/cotevos-v2gstack.

[51] CHAdeMO celebrates 13500 fast chargers worldwide. http://insideevs.com/chademo-association-celebrates-13500-chademos-dc-fast-chargers-worldwide/.

[52] International Electrotechnical Commission. IEC 61851-23: Electric vehicle conductive charging system - Part 23: DC electric vehicle charging station, 2014.

[53] International Electrotechnical Commission. IEC 61851-24: Electric vehicle conductive charging system - Part 24: Digital communication between a d.c. EV charging station and an electric vehicle for control of d.c. charging, 2014.

[54] Open Charge Alliance. http://www.openchargealliance.org.

[55] OCA. Open Charge Point Protocol specification 1.6. http://www.openchargealliance.org/protocols/ocpp/ocpp-16/.

[56] V2G clarity. IEC 63110 - standardizing the management of electric vehicle (dis-)charging infrastructures. https://www.v2g-clarity.com/en/blog/iec-63110-standardizing-management-of-ev-charging-infrastructures/.

[57] OpenADR Alliance. http://www.openadr.org.

[58] International Electrotechnical Commission. IEC 61850-90-8:2016 ECommunication networks and systems for power utility automation - Part 90-8: Object model for E-mobility, 2016.

[59] J. Schmutzler, C. Wietfeld, and C. A. Andersen. Distributed energy resource management for electric vehicles using IEC 61850 and ISO/IEC 15118. In *2012 IEEE Vehicle Power and Propulsion Conference*, pages 1457–1462, Oct 2012.

[60] J. Schmutzler, C. A. Andersen, and C. Wietfeld. Evaluation of OCPP and IEC 61850 for smart charging electric vehicles. In *2013 World Electric Vehicle Symposium and Exhibition (EVS27)*, pages 1–12, Nov 2013.

[61] NKL. Open Charge Point Interface specification 2.1. http://en.nklnederland.nl/projects/our-current-projects/open-charge-point-interface-ocpi/.

[62] Hubject. Open InterCharge Protocol further development. https://www.hubject.com/en/further-development-of-the-eroaming-protocol-oicp-by-hubject-and-the-intercharge-partners/.

[63] e-clearing.net. Open Clearing House Protocol. http://www.ochp.eu/.

[64] OCA. Open Charge Point Protocol 2.0. http://openchargealliance.org/protocols/ocpp/ocpp-20/.

[65] Sachin Kamboj, Nathaniel Pearre, Keith Decker, Keith Trnka, and Colin Kern. Exploring the formation of electric vehicle coalitions for vehicle-to-grid power regulation. In *In Proc. 1st Int. Workshop on Agent Technologies for Energy Systems (ATES-2010), co-located with 9th Int. Conf. on Autonomous Agents and Multi-agent Systems (AAMAS-2010)*, pages 67–74, 2010.

[66] S. Kamboj and W. Kempton. Deploying power grid-integrated electric vehicles as a multi-agent system. *AAMAS*, 2011.

[67] S. Vandael, T. Holvoet, G. Deconinck, S. Kamboj, and W. Kempton. A comparison of two GIV mechanisms for providing ancillary services at the University of Delaware. In *2013 IEEE International Conference on Smart Grid Communications (SmartGridComm)*, pages 211–216, Oct 2013.

[68] X. Han, K. Heussen, O. Gehrke, H. W. Bindner, and B. Kroposki. Taxonomy for evaluation of distributed control strategies for distributed energy resources. *I E E E Transactions on Smart Grid*, 2017. (c) 2017 IEEE. Personal use of this material is permitted. Permission from IEEE must be obtained for all other users, including reprinting/ republishing this material for advertising or promotional purposes, creating new collective works for resale or redistribution to servers or lists, or reuse of any copyrighted components of this work in other works.

[69] ZeroMQ. http://zeromq.org/.

[70] OCA. Open Smart Charging Protocol 1.0. http://www.openchargealliance.org/protocols/oscp/oscp-10/.

[71] Parker project website. http://www.parker-project.com.

[72] SYSLAB PowerLabDK. http://www.powerlab.dk/facilities/syslab.aspx.

[73] M. M. N. Rezkalla, A. Zecchino, M. Pertl, and M. Marinelli. *Grid Frequency Support by Single-Phase Electric Vehicles Employing an Innovative Virtual Inertia Controller*. IEEE, 2016.

[74] A. Thingvad, S. Martinenas, P. B. Andersen, M. Marinelli, B. E. Christensen, and O. J. Olesen. *Economic Comparison of Electric Vehicles Performing Unidirectional and Bidirectional Frequency Control in Denmark with Practical Validation*. IEEE, 2016.

[75] M. Singh, I. Kar, and P. Kumar. Influence of EV on grid power quality and optimizing the charging schedule to mitigate voltage imbalance and reduce power loss. *Power Electronics and Motion Control Conference (EPE/PEMC), 2010 14th International*, pages 196–203, Sept 2010.

[76] J.A. Peças Lopes, Silvan A. Polenz, C.L. Moreira, and Rachid Cherkaoui. Identification of control and management strategies for LV unbalanced microgrids with plugged-in electric vehicles. *Electric Power Systems Research*, 80(8):898 – 906, 2010.

[77] K. Knezović and M. Marinelli. Phase-wise enhanced voltage support from electric vehicles in a Danish low-voltage distribution grid. *Electric Power Systems Research*, 140:274–283, 2016.

[78] K. Knezović, M. Marinelli, P. B. Andersen, and C. Træholt. Concurrent provision of frequency regulation and overvoltage support by electric vehicles in a real Danish low voltage network. In *Electric Vehicle Conference (IEVC), 2014 IEEE International*, pages 1–7. IEEE, 2014.

[79] P. Gnacinski. Windings Temperature and Loss of Life of an Induction Machine Under Voltage Unbalance Combined With Over- or Undervoltages. *Energy Conversion, IEEE Transactions on*, 23(2):363–371, June 2008.

[80] IEEE Recommended Practice for Monitoring Electric Power Quality. *IEEE Std 1159-1995*, 1995.

[81] H. Markiewicz and A. Klajn. Voltage disturbances standard EN 50160, 2004.

[82] K. Strunz, N. Hatziargyriou, and C. Andrieu. Benchmark systems for network integration of renewable and distributed energy resources. *Cigre Task Force C*, 6:04–02, 2009.

[83] F. Marra, G. Yang, and C Træholt. Demand profile study of battery electric vehicle under different charging options. *Power and Energy Society General Meeting, 2012 IEEE*, page 1–7, 2012.

[84] Deliverable 1.1: Report on the needs for interoperability between EVs and electrical power system. Technical report, COTEVOS project, 2014-06-30. http://cotevos.eu/wp-content/uploads/2014/08/D1.1-Report-on-the-needs-for-interoperability-between-EVs-and-electrical-power-system.pdf.

[85] New Zealand Electric Car Guide: Car Connectors And Inlets. http://www.cashbackcars.co.nz/electric-information.

[86] F. Lehfuß, M. Nöhrer, E. Werkman, J. A López, and E. Zabala. Reference architecture for interoperability testing of Electric Vehicle charging. In *Smart Electric Distribution Systems and Technologies (EDST), 2015 International Symposium on*, pages 341–346. IEEE, 2015.

[87] S. Gröning, C. Lewandowski, J. Schmutzler, and C. Wietfeld. Interoperability Testing Based on TTCN-3 for V2G Communication Interfaces. In *2012 International Conference on Connected Vehicles and Expo (ICCVE)*, pages 298–303, Dec 2012.

[88] Deliverable 4.3: Analysis of needs for on-going or incipient standards. Design of Round Robin tests and results of the performed tests. Recommendations for existing standards. Technical report, COTEVOS project, 2016-02-29. http://cotevos.eu/wp-content/uploads/2016/12/20160229_COTEVOS_IOP_tests_D4.3_v8.pdf.

[89] Business Opportunities for Interoperability Assessment of EV Integration. Technical report, COTEVOS project, 2016. http://cotevos.eu/wp-content/uploads/2016/11/COTEVOS-Whitebook-20161104-v4.0.pdf.

[90] World's first electric car fleet supplying electricity to the grid. http://www.dtu.dk/english/news/2016/09/worlds-first-electric-car-fleet-supplying-electricity-to-the-grid?id=ed132b88-be87-462e-a447-9843e450b157.

[91] D. Wang, J. Coignard, T. Zeng, C. Zhang, and S. Saxena. Quantifying electric vehicle battery degradation from driving vs. vehicle-to-grid services. *Journal of Power Sources*, 332:193 – 203, 2016.

[92] S. B. Peterson, J. Apt, and J.F. Whitacre. Lithium-ion battery cell degradation resulting from realistic vehicle and vehicle-to-grid utilization. *Journal of Power Sources*, 195(8):2385 – 2392, 2010.

[93] G. Lacey, G. Putrus, and E. Bentley. Smart ev charging schedules: supporting the grid and protecting battery life. *IET Electrical Systems in Transportation*, 7(1):84–91, 2017.

[94] "Cars are parked 95% of the time". Let's check! http://www.reinventingparking.org/2013/02/cars-are-parked-95-of-time-lets-check.html.

Collection of relevant publications

Pub. A S. Martinenas, S. Vandael, P.B. Andersen, B. Christensen, "Standards for EV charging and their usability for providing V2G services in the primary reserve market," in *Proceedings of International Battery, Hybrid and Fuel Cell Electric Vehicle Symposium (EVS29)*, Montreal, Canada, IEEE, Jun. 2016.

Pub. B S. Martinenas, "Implementation of E-mobility architecture for providing Smart Grid services using EVs," in *International Battery, Hybrid and Fuel Cell Electric Vehicle Symposium (EVS30)*, Stuttgart, Germany, 2017.

Pub. C S. Martinenas, M. Marinelli, P.B. Andersen, C. Træholt, "Implementation and Demonstration of Grid Frequency Support by V2G Enabled Electric Vehicle," in *Proceedings of the 49th International Universities Power Engineering Conference (UPEC) 2014*, Cluj-Napoca, Romania, Sep. 2014.

Pub. D M. Marinelli, S. Martinenas, K. Knezovic, P.B. Andersen, "Validating a centralized approach to primary frequency control with series-produced electric vehicles," in *Journal of Energy Storage*, Vol. 7, 2016, p. 63–73.

Pub. E S. Martinenas, M. Marinelli, P.B. Andersen, C. Træholt, "Evaluation of Electric Vehicle Charging Controllability for Provision of Time Critical Grid Services," in *Proceedings of the 51st International Universities Power Engineering Conference (UPEC) 2016*, Coimbra, Portugal, Sep. 2016.

Pub. F M. Rezkalla, A. Zecchino, S. Martinenas, A. Prostejovsky, M. Marinelli, "Comparison between Synthetic Inertia and Fast Frequency Containment Control Based on Single Phase EVs in a Microgrid," in *Applied Energy*, 2017.

Pub. G S. Martinenas, K. Knezovic, M. Marinelli, "Management of Power Quality Issues in Low Voltage Networks using Electric Vehicles: Experimental Validation," in *IEEE Transactions on Power Delivery*, IEEE, 2016.

Pub. H S. Martinenas, A.B. Pedersen, M. Marinelli, P.B. Andersen, C. Træholt, "Electric Vehicle Smart Charging using Dynamic Price Signal," in *Proceedings of IEEE International Electric Vehicle Conference (IEVC) 2014*, Florence, Italy, Dec. 2014.

Pub. I T.M. Sørensen, M.B. Jensen, S. Martinenas, "Analysis of needs for on-going or incipient standards. Design of Round Robin tests and results of the performed tests. Recommendations for existing standards" in *COTEVOS project deliverable*, 2016

Pub. A. Standards for EV charging and their usability for providing V2G services in the primary reserve market

EVS29 Symposium
Montréal, Québec, Canada, June 19 - 22, 2016

Standards for EV charging and their usability for providing V2G services in the primary reserve market

Sergejus Martinenas[1], Stijn Vandael[2], Peter Bach Andersen[1], Bjoern Christensen[3]

[1]*Center for Electric Power and Energy, Department of Electrical Engineering, Technical University of Denmark*

[2]*University of Delaware*

[3]*NUVVE Corporation*

Summary

Transition to sustainable energy and transport is inevitable, which brings new challenges for the existing power grid. Meanwhile, electric vehicles (EVs) are becoming more widespread and their potential for grid support services is becoming more evident. However, such intelligent integration of EVs into a smart grid is highly dependent on infrastructure and communication. This work overviews and analyses the current state of available standards in the field of eMobility. It particularly focuses on their usability for enabling V2G services such as primary frequency regulation.

Keywords: smart grid, V2G (vehicle to grid), standardization, electric vehicle, communication

1 Introduction

As electric vehicles are becoming widespread, the future of transportation is becoming sustainable and emission-less. However, this transition in the transportation sector could create problems of increased loads in power systems. At the same time, power systems are transitioning to accommodate more stochastic renewable energy sources, which add the need for additional balancing power in the grid. One challenge could be turned into a solution to the other one: if intelligently integrated, EVs can provide solutions to existing and future grid problems, aiding renewable energy integration. EVs could support multiple grid services in both, transmission and distribution level, such as frequency regulation or local network balancing [1][2]. These services are identified and investigated in the NIKOLA project [3]. Some standards have already been analyzed for their ability to be used in grid services such as smart charging [4][5][6][7]. The goal of this paper is to give an overview of how well existing eMobility standards are suited for providing grid services by looking at the example of primary frequency regulation in Denmark and US. The paper is divided into following sections: firstly, the existing standards and specification in the eMobility infrastructure are introduced in Section 2; secondly, the protocols and implementations of V2G service provision are described in Section 3; thirdly, the V2G services are matched against the eMobility standards and specifications in Section 4; lastly the gaps and improvements are identified and summarized in the conclusion.

2 Standards for eMobility infrastructure

While active eMobility development has started not too long ago, each communication link in the infrastructure is already covered by a standard or a specification. This section will introduce and describe all charging related standards and specifications shown in the Figure 1. The figure represents a part of eMobility infrastructure that is relevant for grid service provision i.e. only the actors that are able directly influence the charging process. It consists of electric vehicle (EV) connected to the charging point electric vehicle supply equipment (EVSE). An EVSE is electrically connected to the grid and has a communication link to the charging point operator and aggregator. The role of the aggregator is to combine and control (dis)charging of a large number of EVs to provide grid services, while still satisfying individual user driving goals.

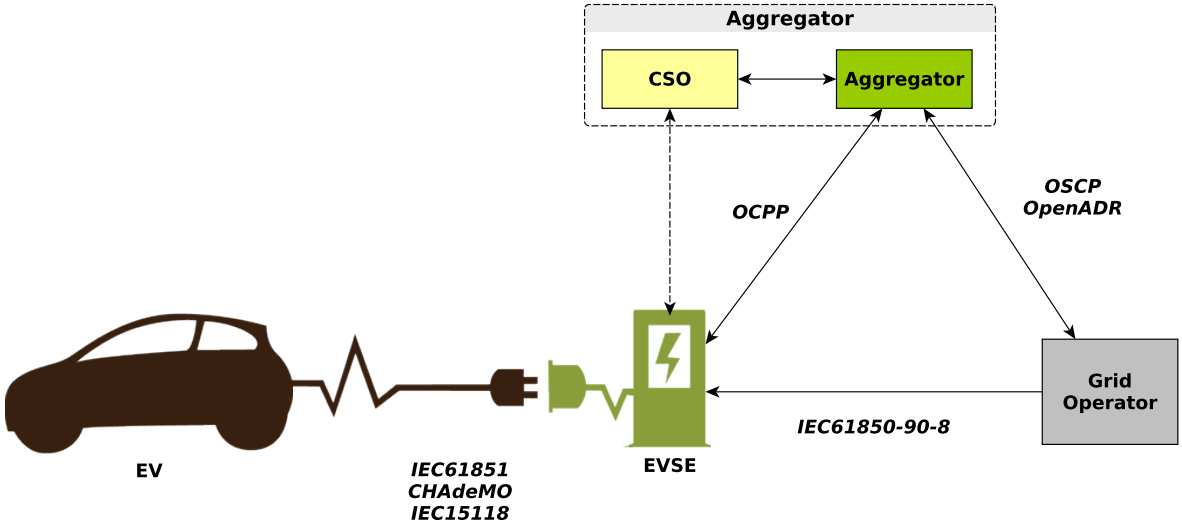

Figure 1: EV charging infrastructure with communication standards and specifications

2.1 EV to EVSE communication

The only physical communication link in the eMobility infrastructure is the link between EV and electric vehicle supply equipment (EVSE). It is mainly covered by IEC 61851 standard for AC charging and CHAdeMO specification for fast DC charging. Meanwhile, a new emerging standard called IEC/ISO 15118 is covering both AC and DC charging.

The IEC 61851 is a basic EV to EVSE communication standard defining the basic physical and safety requirements to enable EV charging. The communication according to this standard is done using a low level pulse width modulation (PWM) signal and voltage levels on a control pilot (CP) pin. After the vehicle has connected, the duty cycle of the PWM signal is indicating the maximum charging current in amperes the EV can charge with. This current limit can be dynamically adjusted by changing the duty cycle of the signal and the vehicle has to respond within 3 seconds. Additionally, the cable presence is indicated by plug present (PP) pin, which contains a resistor connecting to protective earth (PE) pin. The value of this resistor indicates the maximum current rating for that cable. It should be noted that there is an extension of this standard - IEC 61815-1 Edition 3 Annex-D, which extends the physical layer and adds minimal higher level communication descriptions. The US counterpart of this standard is called SAE J1772.

The ISO 15118 standard emerged to close the gap in communication requirements between EV and EVSE, defining the information transfer from EV to EVSE. The standard builds on top of the IEC 61851 and uses it as a fallback communication option if either party does not support the new protocol. The communication link is established using powerline communication (PLC) on top of the PWM signal running on the CP pin, that is the physical layer of the standard. On top of that an elaborate high level communication takes place, based on TCP/IP network setup with possible security features like transport layer security (TLS). The application layer of the communication protocol includes many information objects for existing and future eMobility services. Current implementations of the standard include such features as charging scheduling and identification for automated billing. Future implementations will include important features for grid service provision such as reactive power compensation and V2G support.

CHAdeMO is a protocol for a quick charging for electric vehicles, delivering up to 62.5 kW of high-voltage direct current (DC) via a special electrical connector. This protocol is the most widely deployed

DC (charging mode 4) fast charging protocol in the world. The communication is done using a familiar control area network (CAN) bus. Latest edition of the CHAdeMO specification added the possibility for bidirectional power transfer thus allowing V2G support.
As IEC 61851 was designed primarily to enable safe operation of EVs and EVSE while charging, it can only indicate the maximum limit of the charging current. Currently, only CHAdeMO specification actively allows bi-directional power flow thus enabling the use of EV battery for V2G services. Meanwhile, the future version of IEC/ISO 15118 will also expand the protocol to support such services.

2.2 Back-end communications

Communication between EVSE and EVSE operator (charging spot operator (CSO)) is not standardized yet. However, a popular specification called open charging point protocol (OCPP) is becoming a de-facto industry standard for this communication link. Additionally, an extension of a popular smart grid communication standard IEC 61850-90-8 has been made to extend a communication link from grid operators directly to EVSE. Multiple other specifications such as open smart charging protocol (OSCP) and open charge point interface (OCPI) are emerging to cover some missing links in eMobility back-end communications.
OCPP specification is developed by Open Charge Alliance (OCA) and meant for charging point to charging point operator communication [8]. It is primarily developed for charging point maintenance and operation, thus supporting many features like diagnostics, reservation, charging authorization and scheduling. This analysis is based on OCPP 1.6 specification.
A recent extension of a substation automation standard IEC61850 defines the information objects to control EV charging as distributed energy resource. A big part of IEC61850 and IEC61850-7-420 already covers eMobility domain, therefore IEC61850-90-8 mostly brings missing information objects such as EV and the EVSE nodes and means for charging scheduling.
As communication between EV aggregators/charging point operators and grid operators is a relatively new link, it is not yet covered by a standard. OSCP is also developed by OCA and is one of the first specifications that define the communication between CSO and grid operator e.g. distribution system operator (DSO). The DSO indicates the available grid capacity as a 24 hour prediction to the Charging Point Operator, which then distributes it by adjusting the charging rates.
Another specification that fits the needs of link is OpenADR [9]. It is developed to provide standardized communication protocol between grid utilities, operators and demand response (DR) providers helping facilitate automated demand response. It is not specifically meant for eMobility applications, but is designed to be generic enough to support many DR resources.
While back-end communications are a relatively new but actively developed area, with the most protocols being produced as specifications and are frequently updated. Such dynamic development allows for easy new feature introduction and bug fixing. Therefore back-end protocols are quickly enabling the features needed for V2G service provision.

3 EVs providing V2G services in Denmark and the US

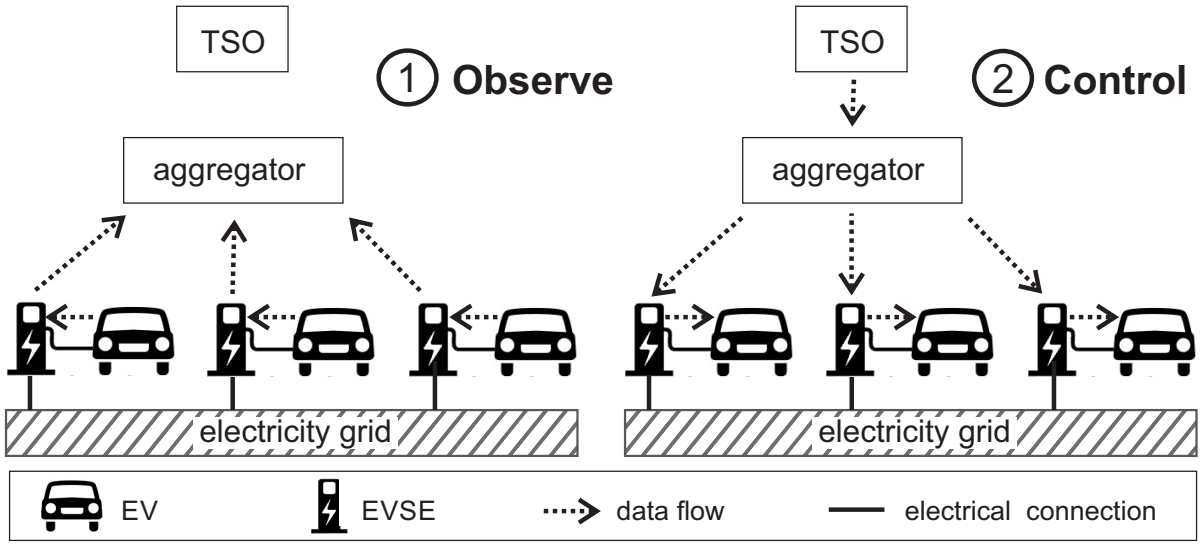

Figure 2: Interactions between aggregator, EVs and grid operator

At the University of Delaware (UDel) and Technical University of Denmark (DTU), researchers are providing regulation as ancillary service for the transmission system operator (TSO) by controlling the bidirectional power transfer between a fleet of EVs and the grid. At DTU the primary frequency reserve is provided in Energinet.DK grid [10]. At University of Delaware the synchronous reserve is provided in the PJM grid. To operate an EV fleet as regulation reserve, an aggregator uses 2 steps: (1) collect data from individual EVs and (2) control their (dis)charging power based on a TSO signal, see Figure 2. This TSO signal represents the imbalance on the grid, which needs to be restored by up-regulation (charge less or inject more) or down-regulation (charge more or inject less). At DTU, the TSO signal is a grid frequency measurement, where a value below 50Hz requires up-regulation, while a value above 50Hz requires down-regulation.
In the rest of this section, each step is described, together with the key properties required from the used communication protocols.

3.1 Collect data from EVs

In order to calculate optimal control signals in step 2, the aggregator needs to gather as much information as possible from individual EVs. In this paper, we divide EV parameters in three groups: essential, quality-improving and optional parameters. These three categories of parameters are presented below:
Essential parameters:

- Min. and max (dis)charging power
- State of charge in kWh
- Indication of plugged-in car
- Vehicle Identification Number

Quality-improving parameters:

- Required energy for driving
- Departure time

Optional parameters

- Car make and model
- Odometer reading
- Battery temperature

Essential parameters are required to provide regulation services. Without these parameters, even a basic operation is not possible. Quality-improving parameters are parameters that improve the quality of the provided regulation services. These parameters can improve the quality of service up to 25% [11]. Optional parameters are used for improving overall operation of the EV fleet, but have little influence on the quality of the provided regulation services.

3.2 Control EV (dis)charging

To control EV (dis)charging, the aggregator calculates control signals based on the information observed in step 1. For each EV a control signal is calculated, which is typically expressed in Watt. The main goal in this step is transferring the control signal, calculated by the aggregator, to each individual EV in a minimal time interval. In general, this time interval can be expressed as:

$$\tau_{total} = \tau_1 + \tau_2 + \tau_3 + \tau_4 \tag{1}$$

,where:
τ_1 is the time required for transferring the TSO signal to the aggregator.
τ_2 is the time required for communicating the EV control signal from aggregator to EVSE.
τ_3 is the time required for communicating the EV control signal from EVSE to EV.
τ_4 is the time required for the converter to ramp up or down the EV (dis)charging power.

The response delay directly influences the quality of service at both Energinet.DK and PJM. For providing the service at Energinet.DK grid, a response between 15-30 seconds is required. At least half of the reserve needs to be deployed within 15 seconds, while the rest of the reserve can be linearly interpolated response between 15 and 30 seconds Figure 3.

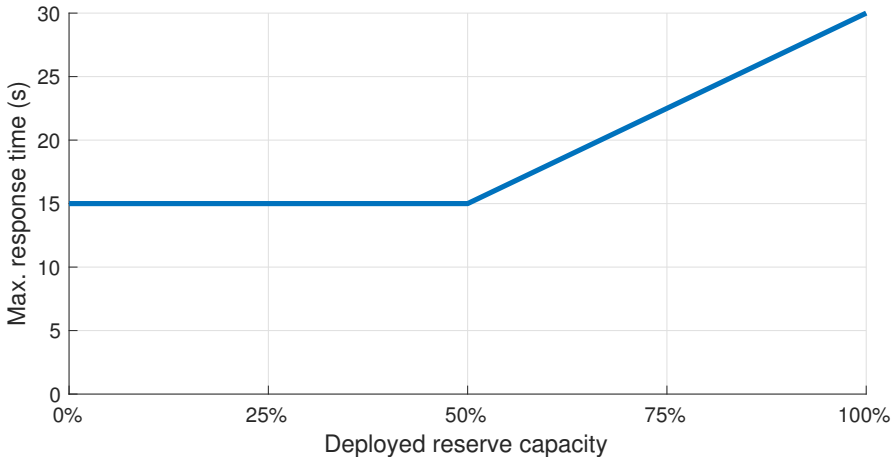

Figure 3: Ramping rate for a primary frequency reserve in DK2

When providing the service in the PJM grid, a performance score is calculated, which is used to measure the quality of service. This performance score consists of three components:

Correlation Quantifies the correlation between the requested regulation and the response of an EV fleet.

Time delay The time delay between requested regulation and a change in the response of the EV fleet.

Precision The difference between the requested regulation power and the provided regulation power.

The performance score is a scalar in the interval [0..1], calculated every hour by PJM and reported back to the University of Delaware. At the university, researchers are seeking to have a score above 0.9 to maximize their earnings. This entails a highly correlated response, 1-3 seconds delay and 1-5% difference between request and response Figure 4.

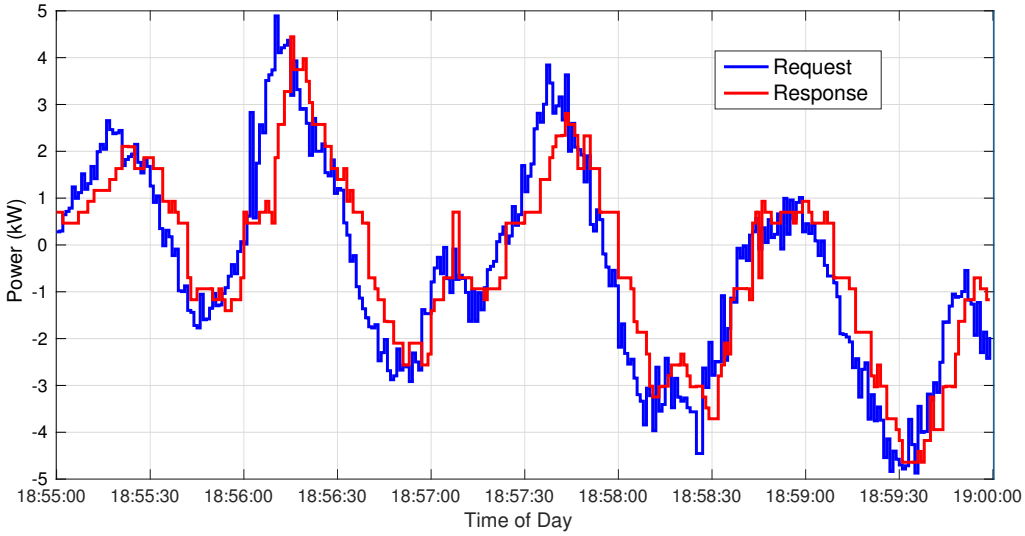

Figure 4: Example request and response curve for PJM grid service

4 Usage of standards for EV charging to provide V2G services in a primary reserve market

This section describes how the above mentioned standards can be used for providing V2G services in a primary reserve market. An overview of EV to EVSE communication standards with the highlighted features for grid service provision is shown in Table 1 and the same overview for EVSE to Aggregator in Table 2. Some parameters such as required energy for charging and departure time are implicit as part of the charging schedule feature. The values in brackets indicate that the feature is partially present or optional. The response times are maximum values taken from the standards.

Table 1: EV to EVSE communication standard/specification overview

Standard/ Specification	Power Control	V2G	SOC	Charging Schedule	Identification	Response Time
IEC61851	+	-	-	-	-	$< 3s$
IEC15118	+	(+)	(+)	+	+	$< 60s$
CHAdeMO	+	(+)	+	-	-	$< 1s$

Currently widespread, IEC61851 charging standard is not well suited for providing precise grid services as it is missing almost all required features, because most implementations do not include digital communication. While IEC15118 appears to be almost ideal for grid service provision, the response time specifications for most requests in the current revision is way too slow. Additionally, SOC field is only optional, therefore not included in most implementations, and V2G specific fields are still left to be defined in the future revisions. Similarly, latest CHAdeMO version includes V2G messages allowing bidirectional power flow, which enables it to provide symmetrical power services. However, it is missing such important features as build-in vehicle identification, possibility for charging schedule negotiation and communication security. Therefore it heavily relies on the need of user interaction and security of the physical connection.

Table 2: EVSE to aggregator communication standard/specification overview

Standard/ Specification	Power Control	V2G	SOC	Charging Schedule	Identification
OCPP	+	-	-	+	-
IEC61850-90-8	+	(+)	(+)	+	-

On the EVSE to aggregator communication side, the protocols are not as mature and developed as in the EV to EVSE link as this link is relatively new. OCPP was primarily developed by charging station operators. Additionally, OCPP is a specification developed by industrial alliance, therefore it is updated more often than a standard. Meanwhile, IEC61850-90-8 looks like it was developed to provide electrical services as it includes many electrical properties and a scheduling possibility.
As communication between the grid operators and aggregators is not standardized, in addition to more generic OpenADR, the EV specific OSCP was developed as one of the first attempts to make a specification for this link. Although it primarily covers only grid overload problem it is a good example of how the rest of grid services could be implemented.

5 Conclusion

As described in this work, most V2G services already provided in the real electricity grid are using existing eMobility standards to some extend. However, a unified approach that could incorporate the needed informational objects while being lightweight is still missing. As shown in Section 4, none of the standards cover all the required features to provide grid services. This issue is actively addressed in the research and demonstration projects like NIKOLA, where the findings are then forwarded to standardization committees such as IEC TC69. It should be noted that transition to smart grid and larger share of renewable energy sources is only starting, therefore current definitions of grid services will change. Meanwhile, it can already be predicted that the services will become more dynamic i.e. requiring faster

response and better precision. The analysis of the existing standards shows that only fast DC charging currently has the ability to provide future services. However, slower AC charging should not be dismissed, while the timing constraints for AC chargers are more relaxed, technically the built-in chargers are able to show the same timing performance as the DC charging systems. Another important issue, that is currently hindering the grid service provision by the EVs, is a lack of V2G protocol support in the charging communication. However, as noted in this paper, most standards are starting to incorporate the missing information objects in the latest revisions. Additionally to existing solutions from other emerging smart grid technologies like OpenADR, new EV focused specifications are starting to emerge e.g. OSCP and fill the communication gaps in the eMobility infrastructure. Finally, as most communication protocols become high level, data security problem arises. So far, only a few standards e.g. IEC15118 include security requirements as a part of the protocol specification, where most rely on implicit security of the communication link, which cannot always be guaranteed. Overall, the provision of existing grid services using EVs has already started and is largely implemented using current standards and their modifications that bridge the existing gaps. However, as the share of renewable energy in the grid will grow, the regulation services will become more dynamic and the standardization has to lead this change.

Acknowledgments

This work is supported by the Danish Research Project “NIKOLA - Intelligent Electric Vehicle Integration” under ForskEL kontrakt nr. 2013-1-12088. More information at www.nikolaproject.info.

References

[1] S. Martinenas, M. Marinelli, P.B. Andersen, C. Træholt, *Implementation and Demonstration of Grid Frequency Support by V2G Enabled Electric Vehicle*, , IEEE UPEC, 2014.

[2] K. Knezovic, M. Marinelli, P.B. Andersen, C. Træholt, *Concurrent Provision of Frequency Regulation and Overvoltage Support by Electric Vehicles in a Real Danish Low Voltage Network*, IEEE IEVC, 2014.

[3] P.B. Andersen, M. Marinelli, O.J. Olesen, C.A. Andersen, G. Poilasne, B. Christensen, O. Alm, *The Nikola project - Intelligent Electric Vehicle Integration*, IEEE ISGT Europe, 2014.

[4] J. Schmutzler and C. Wietfeld and C. A. Andersen *Distributed energy resource management for electric vehicles using IEC 61850 and ISO/IEC 15118*, IEEE Vehicle Power and Propulsion Conference (VPPC), 2012.

[5] J. Schmutzler and C. A. Andersen and C. Wietfeld *Evaluation of OCPP and IEC 61850 for smart charging electric vehicles*, World Electric Vehicle Symposium and Exhibition (EVS27), 2013.

[6] C. Lewandowski and S. Bcker and C. Wietfeld *An ICT solution for integration of Electric Vehicles in grid balancing services*, International Conference on Connected Vehicles and Expo (ICCVE), 2013.

[7] S. Bcker and C. Lewandowski and C. Wietfeld and T. Schlter and C. Rehtanz *ICT based performance evaluation of control reserve provision using electric vehicles*, IEEE PES Innovative Smart Grid Technologies Conference Europe (ISGT-Europe), 2014.

[8] *Open Charge Alliance*, http://www.openchargealliance.org.

[9] *OpenADR Alliance*, http://www.openadr.org.

[10] *Energinet.DK ancillary services provision*, http://www.energinet.dk/EN/El/Systemydelser-for-el/Sider/Systemydelserforel.aspx.

[11] S. Vandael and T. Holvoet and G. Deconinck and S. Kamboj and W. Kempton *A comparison of two GIV mechanisms for providing ancillary services at the University of Delaware*, IEEE International Conference on Smart Grid Communications (SmartGridComm), 2013.

Authors

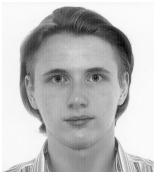

Sergejus Martinenas was born in Elektrenai, Lithuania, in 1989. He received a BSc degree in mechatronics engineering from the University of Southern Denmark in 2011, and an MSc degree in electrical engineering from the Technical University of Denmark in 2014. He is currently pursuing the Ph.D. degree in electrical engineering at DTU.
His research focuses on enabling technologies for electric vehicle integration into smart grids.

Stijn Vandael originates from Zonhoven, Belgium. He received the Master degree in industrial engineering from the Katholieke Hogeschool Limburg (KHLim), and the M.Sc. degree from the Katholieke Universiteit Leuven (KU Leuven). He received his PhD degree in 2015 at the department of Computer Science (KU Leuven). Currently, he is the principal software engineer in the V2G project at the University of Delaware (USA).

Peter Bach Andersen is a Researcher at the Technical University of Denmark (DTU). He holds a PhD from DTU and has participated in numerous EV-related projects and activities. His main focus is the application of informatics for electric vehicle integration. This includes software, communication technology, data analysis and optimization. Peter is currently managing a number of research projects and initiatives, including the establishment of the EV Lab, dedicated to this line of research.

Bjoern Christensen is a Chief Strategy Officer (CSO) at Nuvve with the responsibility to develop and implement strategies for Nuvves expansion into the world market. He has more than 30 years of international experience in Technology, Marketing, Business Development and Venture Capital.
He holds a Master of Science degree from the Technical University of Denmark .

Pub. B. Implementation of E-mobility architecture for providing Smart Grid services using EVs

EVS30 Symposium
Stuttgart, Germany, October 9 - 11, 2017

Implementation of E-mobility architecture for providing Smart Grid services using EVs

Sergejus Martinenas[1]
[1]*Center for Electric Power and Energy, Department of Electrical Engineering, Technical University of Denmark*
Kongens Lyngby, smar@elektro.dtu.dk

Abstract

This paper outlines the implementation and testing of a part of the e-mobility infrastructure relevant for providing smart grid services. The implementation is made using mainly open standards and protocols available in e-mobility field e.g. IEC61851 and Open Charging Point Protocol (OCPP). Implementation and testing results are described in detail emphasizing the shortcomings and needs for improvement. The testing is done using unmodified OEM vehicles participating in existing power grid services such as frequency regulation and load balancing.
Keywords: smart grid, V2G (vehicle to grid), standardization, electric vehicle, communication

1 Introduction

While EVs are largely viewed as additional loads on the transforming power grid, if intelligently integrated, they could provide solutions existing and future grid problems, e.g. aiding large scale renewable energy integration. EVs could provide higher quality grid services on transmission and distribution levels, such as faster frequency regulation and local grid balancing [1],[2]. These services were identified and implemented in the NIKOLA project [3]. Large scale application are currently being implemented in the Parker project [4]. To provide these grid services, various implementations of e-mobility charging architectures have been introduced. These charging and communication architectures are largely based on available e-mobility standards and specifications. Previous works have identified potential gaps in many of the communication standards and specifications for grid service provision [5], [6]. The goal of this work is to analyze an implementation of a part of e-mobility architecture using latest available open standards and specifications. Following the introduction the paper is divided into 4 sections. Section 2 presents the e-mobility architecture and discusses the relevant parts of it for implementation. Then in section 3 the implementation of the architecture is discussed. Section 4 discuses the the gaps in the used communication protocols and the way they are covered. Finally, the findings are summarized in the concluding section 5.

2 E-mobility architecture

E-mobility has a quite broad definition as it encompases all of the electric transportation. However, in the case of this work e-mobility is only concerned with electric vehicles also known as electric cars. An example of e-mobility architecture developed in COTEVOS project [7] is shown in Fig.1.

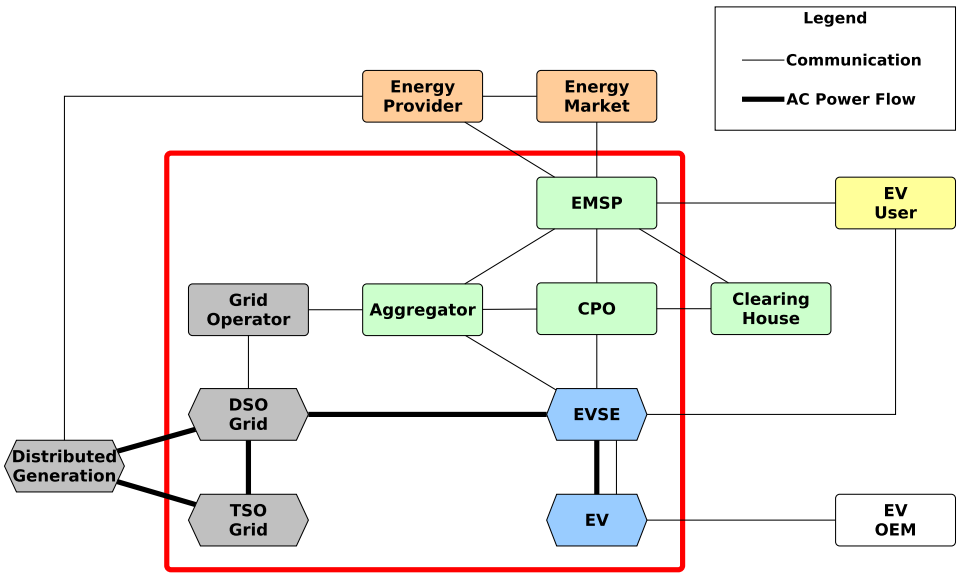

Figure 1: Updated E-mobility reference architecture from COTEVOS project showing actor/interface layer

The relevant part of the architecture for smart grid integration of EVs is highlighted in red. The communication protocols between the actors in the architecture are shown in Fig.2.

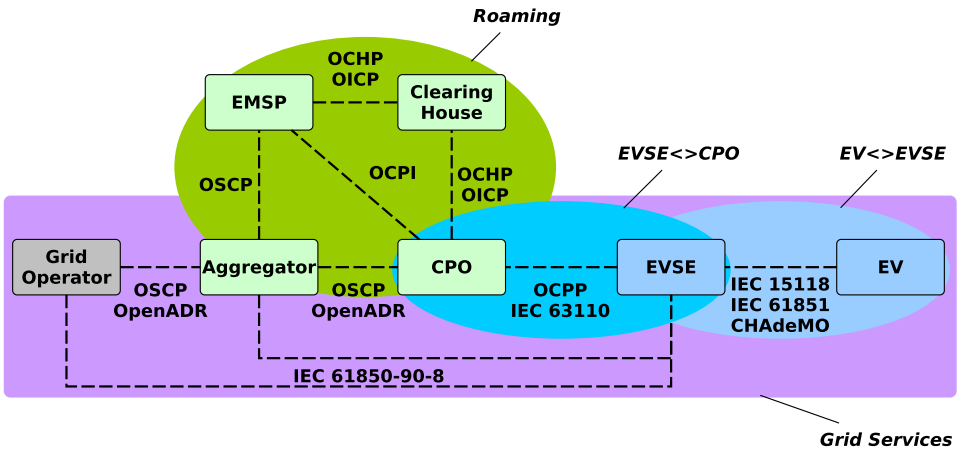

Figure 2: E-mobility architecture with communication protocols

The figure is an extension of overview presented in a EV related protocol study [8]. Here one can notice 4 main highlighted communication areas: EV to EVSE, EVSE to CPO, roaming related and grid service communication. This work is focusing on the grid service communication protocols. As can be seen in the architecture, most communication links are covered with multiple protocols defined by standards (e.g. IEC61851, IEC15118) or specifications (e.g. OCPP, OSCP, OpenADR). However, these protocols do not fully cover all the needed information and control features for the smart grid service provision using EVs.
The following section describes the implementation details of the grid service relevant part of the e-mobility architecture including component descriptions and communication protocols.

3 Implementation

The detailed implementation diagram can be seen in Fig.3.

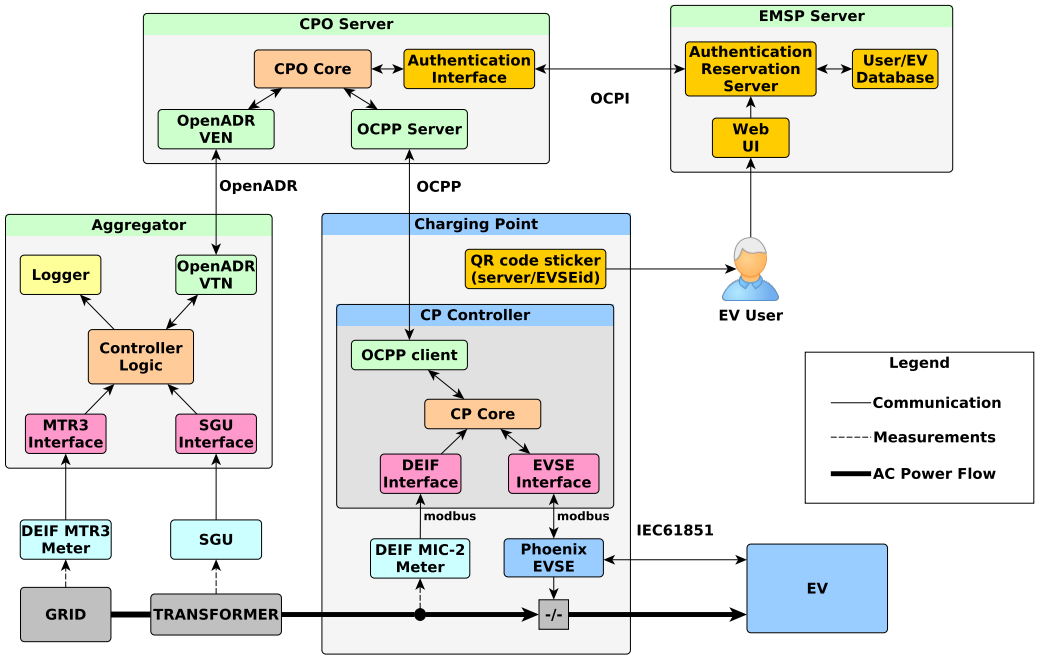

Figure 3: Detailed e-mobility architecture implementation diagram

The following actors of the architecture are used and implemented:

EV - Electric Vehicle - unmodified OEM vehicles with AC chargers using IEC61851 standard [9].

EVSE - Electric Vehicle Supply Equipment - custom made chargers assembled from off the shelf industrial components such as charge controller supporting IEC61851, relays and a microcomputer implementing OCPP version 1.6 support for the communication with CPO [10].

CPO - Charge Point Operator - controls and manages the EVSEs using OCPP protocol.

EMSP - E-mobility Service Provider - implements the actor between the EV user and a CPO, enabling charging spot reservation and charging authorization using OCPI protocol [11].

Aggregator - takes care of the communication with the grid operator and implements the smart grid service offered. The aggregator controls the vehicles via communication through CPO using OpenADR 2.0b specification [12].

The roles of the CPO, EMSP and the aggregator are split to provide modularity and ability to easily integrate with external actor e.g. another CPO.
The following communication standards are used in the implementation:

IEC 61851 - for EV to EVSE link - used as unmodified OEM vehicles, currently, only support IEC61851 standard for AC charging. The IEC61851 on the EVSE side is implemented by using Phoenix Contact EVSE controller.

OCPP 1.6 - for EVSE to CPO link - used as it is a de-facto standard for this link. Implemented in the microcomputer mounted inside the EVSE.

OCPI 2.1 - for CPO to EMSP link - chosen for the openness and maturity of the specification that covers the needs of the communication link. Implemented in the dedicated server, that also provides web interface for authorized EV users to login and enable the charging spot.

OpenADR 2.0b - for CPO to Aggregator link - chosen for maturity, openness and generic application capability. This allows for the aggregator to potentially combine EVs with other DERs to provide larger and more diverse grid services. The aggregator implements the role of the virtual top node (VTN) and the CPO implements the virtual end node (VEN). Another specification potentially fitting this link is Open Smart Charging Protocol (OSCP) [14]. However, it is mostly targeted at feeder capacity control thus limiting its' application for other grid services.

As the OCPI specification is primarily designed for roaming purposes, it is meant to support the communication between CPO and EMSP for providing grid services. Therefore, the CPO - EMSP link might use the OCPP message forwarding for communication purposes.
This setup will be used to test a few existing grid services.
The example smart grid services that are tested with the implementation are:

FCR-N - Frequency Controlled Normal operation Reserve - a DK2 reserve ensures that the equilibrium between production and consumption is restored, keeping the frequency close to 50 Hz, similar to primary frequency regulation [15].

Congestion Management - a modified charging service, used to prevent congestion on the feeder that EV is connected to.

Smart Charging - a modified charging service, meant for minimizing the charging price by accounting for actual and near future energy prices.

4 Communication

4.1 Communication requirements

It has been previously identified that the following information objects are essential for optimal grid service provision by EVs [5]. These information objects are:

(Dis)charging power limits - for estimation of EV controllability

State of charge - in kWh, for estimation of available flexibility.

Indication of plugged-in car - to determine if the charging point is occupied.

Vehicle Identification Number - or any other unique identifier needed for billing purposes.

Additionally, parameters like required energy for driving and estimated departure time are needed for estimating the available flexibility. This information greatly improves the quality of the service for the EV user.

4.2 Gaps in communication

The IEC61851 standard does not provide a digital communication link with the EV. It does however provide the indication of the plugged in vehicle and allows the EVSE to dynamically indicate the charging current limit. This functionality already enables the controllability needed for grid service provision. The lack of digital communication in IEC61851 requires alternative solutions for acquiring high level information from the EV. This functionality is important for reading the state of charge (SOC) and vehicle identification. The acquisition of the SOC information is solved by accessing it from the OEM backend. However, this feature is only available on the newer and higher end EVs. Vehicle identification is solved by prompting the user to login to enable the charging point. Vehicle model, battery size and maximum charging power is provided by the user when registering with the EMSP on the first use of the charging station. The quality improving parameters of desired battery SOC and estimated departure time may be implemented as additional user prompts in the EMSP web interface.
Actual charging rate is measured using a DEIF MIC-2 multi instrument device in the EVSE.

5 Discussion

Even though the implementation of the architecture for smart grid services currently requires many small workarounds for acquiring the necessary static and dynamic information, it is certainly possible. The standard that is posed to improve the situation and abolish the need for these workarounds is IEC15118. It enables high level communication link between the EV and EVSE and includes the majority of the use cases needed to provide grid services. However, the current edition of the standard does not position the necessary information objects e.g. SOC as a mandatory parameter. Nor does it support the time critical services by allowing for too long timeout values in the negotiation of the charging schedule.
Flexibility of the OCPP implementation permits for multiple fields in the communication messages to be optional, such as transaction identification is often a requirement from the EMSP and aggregator side. Moreover, OCPP version 1.6 still lacks the information fields to relay the necessary data from the EV to the aggregator e.g. SOC.
In addition to protocol gaps, current industrial implementations show, in contrast to architecture, no clear boundary between CPO and EMSP actors as their roles are often very much intertwined and performed by the same entity.

An important requirement that has not been in focus of this analysis is communication security. The protocols for each communication link have recommendations for securing the data exchange between the actors except for IEC61851 and OCPP. Improvements to the security of communication are promised in the OCPP version 2.0 [13].

Acknowledgments

This work is supported by the Danish Research Project "Parker" aimed at applying grid-balancing services to a fleet of electric vehicles and financed by ForskEL programme. More information at www.parker-project.com.

References

[1] S. Martinenas, M. Marinelli, P.B. Andersen, C. Træholt, *Implementation and Demonstration of Grid Frequency Support by V2G Enabled Electric Vehicle*, , IEEE UPEC, 2014.

[2] K. Knezovic, M. Marinelli, P.B. Andersen, C. Træholt, *Concurrent Provision of Frequency Regulation and Overvoltage Support by Electric Vehicles in a Real Danish Low Voltage Network*, IEEE IEVC, 2014.

[3] P.B. Andersen, M. Marinelli, O.J. Olesen, C.A. Andersen, G. Poilasne, B. Christensen, O. Alm, *The Nikola project - Intelligent Electric Vehicle Integration*, IEEE ISGT Europe, 2014.

[4] *Parker project website*, http://www.parker-project.com accessed on 2017-06-20.

[5] S. Martinenas, S. Vandael, P.B. Andersen, B. Christensen *Standards for EV charging and their usability for providing V2G services in the primary reserve market*, , Proceedings of International Battery, Hybrid and Fuel Cell Electric Vehicle Symposium (EVS29), 2016.

[6] J. Schmutzler and C. A. Andersen and C. Wietfeld *Evaluation of OCPP and IEC 61850 for smart charging electric vehicles*, World Electric Vehicle Symposium and Exhibition (EVS27), 2013.

[7] F. Lehfuß and M. Nöhrer, E. Werkman, J. A. Lópezz, E. Zabala, *Reference architecture for interoperability testing of Electric Vehicle charging*, International Symposium on Smart Electric Distribution Systems and Technologies (EDST), 2015.

[8] ElaadNL, *EV related protocol study*, https://www.elaad.nl/uploads/files/EV_related_protocol_study_v1.1.pdf accessed on 2017-06-27.

[9] International Electrotechnical Commission (IEC), *IEC 61851-1 ed2.0: Electric vehicle conductive charging system - Part 1: General requirements*, 2010.

[10] Open Charge Alliance (OCA), *Open Charge Point Protocol (OCPP) specification 1.6*, http://www.openchargealliance.org/protocols/ocpp/ocpp-16/ accessed on 2017-06-17.

[11] The Netherlands Knowledge Platform for Charging Infrastructure (NKL), *Open Charging Point Interface (OCPI) specification 2.1*, http://en.nklnederland.nl/projects/our-current-projects/open-charge-point-interface-ocpi/ accessed on 2017-06-17.

[12] OpenADR Alliance, *Open Automated Demand Response (OpenADR) specification 2.0b*, http://www.openadr.org/specification accessed on 2017-06-27.

[13] Open Charge Alliance (OCA), *Open Charge Point Protocol (OCPP) specification 2.0*, http://www.openchargealliance.org/protocols/ocpp/ocpp-20/ accessed on 2017-06-27.

[14] Open Charge Alliance (OCA), *Open Smart Charging Protocol (OSCP) specification 1.0*, http://www.openchargealliance.org/protocols/oscp/oscp-10/ accessed on 2017-06-27.

[15] Energinet.DK, *Ancillary services to be delivered in Denmark Tender conditions*, Technical Report, 2012.

Authors

Sergejus Martinenas was born in Elektrenai, Lithuania, in 1989. He received a B.Sc. degree in mechatronics engineering from the University of Southern Denmark in 2011, and an M.Sc. degree in electrical engineering from the Technical University of Denmark in 2014. He is currently pursuing the Ph.D. degree in electrical engineering at DTU.
His research focuses on analysis and implementation of enabling technologies for electric vehicle integration into smart grids.

Pub. C. Implementation and demonstration of grid frequency support by V2G enabled electric vehicle

Implementation and Demonstration of Grid Frequency Support by V2G Enabled Electric Vehicle

Sergejus Martinenas Mattia Marinelli, Peter Bach Andersen and Chresten Træholt
Center for Electric Power and Energy, DTU - Technical University of Denmark
Contact Person: Sergejus Martinenas, smar@elektro.dtu.dk

***Abstract*—Safe operation of the electric power system relies on conventional power stations. In addition to providing electrical energy to the network, some power stations also provide a number of ancillary services for the grid stability. These services could potentially be provided by the growing number of electric vehicles - faster and with better precision, using Vehicle-to-Grid technology. This paper explores the implementation of a system that demonstrates the use of the electric vehicles for providing frequency regulation in the Danish power grid. The system is tested with the use case of Primary Frequency Regulation. The service is implemented following the technical conditions for ancillary services in the Danish grid. The real life system is developed using web-centric communication technologies between the components. Communication and control functions of the system are validated through experiments. The response of the system is studied in terms of latency, precision and stability.**

Keywords – Vehicle-to-Grid, Smart Grid, Frequency Control, Electric Vehicles, Information and Communication Technology

I. Introduction

Power system frequency stability relies on the balance between power generation and consumption. Today, most of the power generation in the grid is provided by conventional power plants. Sudden generation losses and unexpected load increases require timely actions by the remaining generating units or by controllable loads in order to restore the power balance. Additionally, conventional generating units are displaced by renewable sources, such as wind and photovoltaic, which are not required to provide the same level of ancillary services, like the frequency regulation [1]. This leads to an increase of regulating power obligation among the remaining controllable resources.

Growing number of Electric Vehicles (EVs) is typically viewed as additional load on the grid from system operators perspective [2]. However, EVs are also one of the imminent candidates for providing grid regulation services. Especially, because most of the time (typically about 90%) they are plugged-in to a charging post and can provide fast regulating power in both directions. The ability of the vehicle to provide power back to the grid is called Vehicle-to-Grid (V2G) [3]. A noticeable amount of literature has already been written supporting the use of EVs with V2G capability for ancillary services [4], [5]. However, multiple technical challenges arise: the limited power and energy capacity of each individual unit and the need of having simple and effective measurement and control capabilities [6]. These problems are solved by aggregating a large number of V2G enabled vehicles [7] and connecting the aggregator to the high quality measurement device.

This work focuses on the system design and analysis of the issues that may arise when dealing with practical implementation of frequency response such as: communication latency, power and frequency measurements inaccuracies. Therefore, the implementation of the system and communication to the electric vehicle will be presented in detail.

The paper is organized as follows: Section II provides the background on grid frequency regulation services, with the example of Danish grid. Section III gives an overview on system implementation with focus on the communication implemented using a modern web-centric approach. Section IV shows the results of a frequency measurement and frequency regulation experiments. Section V presents discussion of the results.

II. Frequency Regulation Services

Generally, the grid frequency regulation reserves are divided into the three categories: primary, secondary and tertiary. The Danish power grid is located in two separate synchronous regions: DK1 and DK2. Jylland (continental part of Denmark) and island of Fyn are in DK1 region connected to the rest of Europe. The islands of Sjælland and Bornholm are in DK2 connected to most of Scandinavia. In each region, there are multiple levels of reserves providing frequency regulation services [8]. DK1 region has following frequency regulation reserves:

- Primary Reserve - regulation is restoring balance between production and consumption, stabilizing the frequency close to 50Hz. The regulation is automatic, power output of the reserve is controlled according to the frequency deviation, with the small permitted deadband.
- Secondary Reserve - regulation is enabled during major operational disturbance. It is used to indirectly restore frequency to 50.00Hz followed by stabilization by primary reserve. It also serves the purpose of releasing the

This work is supported by the Danish Research Project "NIKOLA - Intelligent Electric Vehicle Integration"- under ForskEL kontrakt nr. 2013-1-12088. More information (www.nikolaproject.info).

activated primary reserve. The regulation is automatic and controlled by a signal from Energinet.dk.
- Manual Reserve - manual power regulation used to restore system balance, acting as a tertiary reserve. It is activated manually from Energinet.dk's Control Center.

DK2 region also has corresponding reserves:

- Normal Operation Reserve - ensures that production and consumption equilibrium is restored. The regulation is automatic and responding to frequency deviation, without deadband.
- Disturbance Reserve - a fast reserve, activated in the event of major system disturbances. It is started automatically in the event of sudden frequency drop under 49.9Hz and remains active until frequency is restored or manual reserve takes over.
- Manual Reserve - manual power regulation used to restore system balance, acting as a tertiary reserve, manually activated from Energinet.dk's Control Center.

In this paper the primary reserve from DK1 is implemented and tested. It is chosen for experiments, as the reserve should directly respond to grid frequency deviations, it has a small optional deadband and requires a quick response time.

III. System Architecture

To implement the frequency regulation service the reserve has to have three main components: a controllable energy resource connected to the grid, fast and precise grid frequency measurements and a controller with appropriate control algorithm.

A. System Design

The system developed in this project, is split into three layers, shown in Fig. 1: power flow, data acquisition and intelligence.

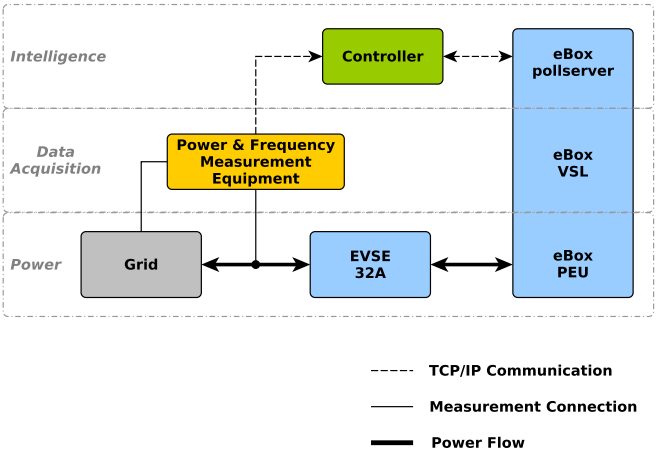

Fig. 1. System design for the frequency regulation service

The power layer consists of all the devices that contain power electronics or are used to generate or transmit electrical energy, e.g. EV battery, inverter, charging cables, breakers, etc. Data acquisition layer consists of the embedded and external measurement devices and their interfaces. The intelligence layer contains all the computers running higher level communication and control algorithms e.g. EV computer and controller server.

As shown in Fig. 1 the testing platform was build with following components:

- **EV** - DTU eBox with 35kWh battery and power electronics unit (PEU) unit capable of single phase bidirectional power transfer up to 20kW. It is controlled by the EV computer that interfaces with the PEU using build-in vehicle smart link (VSL) [9].
- **VSL** - an embedded computing interface, used for communication to eBox PEU and is located next to it. Additionally the VSL is responsible for handling IEC 61851 Control Pilot signal communication, when the vehicle is plugged in to the EVSE.
- **EV Computer** - build-in EV computer running the eBox pollserver application. It is connected to the network using wireless interface.
- **eBox Pollserver** - vehicle monitoring/control server with RESTful application programming interface (API). It is implemented on the vehicle computer and is used for remote and local control.
- **EVSE** - grid connected, 32A, three phase, custom charging spot with charging cable.
- **Frequency Measurement Device** - G4500 Power Analyzer from ELSPEC, highly accurate grid analysis unit, primarily used for grid frequency measurement, also connected to communication network.
- **Frequency Regulation Controller** - running on external computer, connected to network, performing following functions: reading data from measurement devices and dispatching control signals to the EV.

All of the system components have communication interfaces for control and data exchange.

B. Electric Vehicle Communication

The system layers: grid connected EV, frequency measurement device and controller, were distributed in the different places of the SYSLAB[1] laboratory and connected to the common communication network. The controller and measurement device are using wired network connection, the EV computer is connected using wireless communication. These physical layers are chosen for its robustness, flexibility and representation of the real field testing conditions. The full communication path from controller to the PEU is shown in Fig. 2.

The EV computer is running a pollserver application, which uses the connection to the VSL board to update the data values and control parameters. The pollserver receives and processes the requests from the controller into updated EV control commands or returns measurement data. The VSL is running an

[1]SYSLAB is laboratory for intelligent distributed power systems at Technical University of Denmark, part of PowerLabDK (www.powerlab.dk).

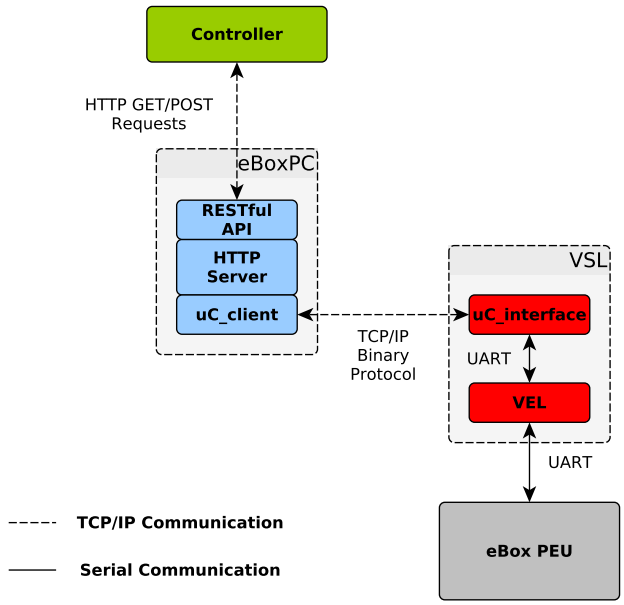

Fig. 2. Control message path from controller to the PEU

interface application, that sends those commands to the PEU unit. The higher level communication is implemented based on Hyper Text Transfer Protocol (HTTP). On the embedded side of the system (on the VSL and below) communication changes to serial UART, which is a common component used in industry for such applications.

As shown in the Fig. 2 high level communication has been implemented for communication with the EV using RESTful architecture. REpresentational State Transfer (REST) is a software architectural style rather than a communication protocol. It has first been described in the PhD thesis of R.Fielding [10]. REST description consist of a set of architectural constraints applied to components and data elements, within a system. It ignores the implementation details of the component and protocol syntax, focusing on the component roles, their interaction and interpretation of significant data elements. RESTful architecture have been used to map the IEC 61850 communication standard to web services [11]. The communication protocol is kept as simple and clear as possible to ease later expansion and higher level application such as IEC 15118. The structure of RESTful Unique Resource Identifier (URI) request, designed for this work, is shown in Fig. 3.

Fig. 3. RESTful URI request structure

Following is the RESTful API communication example: To read the measurements or parameters of the EV, an HTTP GET request is sent to the URI:

```
http://ebox:8080/getData/measurements
```

The response received is formatted in JavaScript Object Notation (JSON):

```
{ "System_Time": 1399382195,
  "Line_V": 229.000000, "SOC": 67,
  "Max_C_Amps": 31, "Max_D_Amps": 31,
  "Requested_Mode": 1, "Actual_Mode": 1,
  "Requested_Amps": -1.000000,
  "Actual_Amps": -1.200000, "Error": 0 }
```

For setting new control parameters, such as charging current or operation mode, a HTTP POST or PUT request is sent. For example, to update the charging current to -16A (negative values indicate charging, positive values indicate V2G mode, i.e. discharging into the grid), the HTTP POST request is sent to the following URI:

```
http://ebox:8080/setData/Requested_Amps=-16
```

To update the operation mode from charging (mode 1) to V2G (mode 2) following HTTP POST request is sent:

```
http://ebox:8080/setData/Requested_Mode=2
```

This communication API is used by the controller application to read the data and control the EV.

C. Primary Frequency Regulation Controller

The frequency regulation controller is running with the following algorithm:

while *true* **do**
  f = read current grid frequency;
  e = calculate the frequency error;
  P_{out} = calculate corresponding output power;
  actuate V2G power for the EV (P_{out});
  wait for sampling time
end

Algorithm 1: Frequency Droop Control

The Primary Frequency Regulation (PFR) controller was designed by following the technical specification of tender conditions for ancillary services in Danish power grid, see [8].

First the grid frequency is measured and the deviation from nominal frequency is calculated:

$$e = f_{nom} - f_m. \tag{1}$$

Here the e is the deviation i.e. the difference between nominal and measured frequency values. f_{nom} is a nominal grid frequency, in Europe it is $50.00Hz$. The f_m is the momentarily measured grid frequency, with $10mHz$ accuracy. Droop controller output is calculated as shown in (2).

$$P_{out} = \begin{cases} 0 & , |e| < \Delta f_{db} \\ P_{max} \cdot e \cdot \frac{100}{d_{pct}} & , \Delta f_{max} > |e| > \Delta f_{db} \\ P_{max} & , |e| > \Delta f_{max} \end{cases} \tag{2}$$

Here P_{out} is output power of the vehicle to the grid. P_{max} is the maximum output power of the vehicle, for a $32A$ charging spot at one phase it is $7kW$. Δf_{db} is a deadband used, in this case $20mHz$. Δf_{max} is a maximum frequency deviation, at which the maximum power should be output to the grid, in this case it is $200mHz$. The resulting droop control curve is shown in Fig. 4.

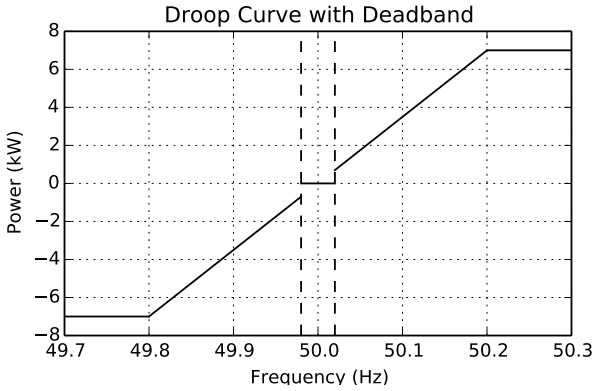

Fig. 4. Droop curve used for frequency regulation experiments

IV. Experimental Results

A. System Frequency Measurements

As specified in the ancillary service conditions, each frequency reserve must measure the grid frequency with accuracy better than 10mHz. Therefore a precise grid power analyzer was installed at the permanent grid connection in SYSLAB. The data from the measurement equipment was recorded from April 2nd to April 30th. All frequency values are plotted in Fig. 5.

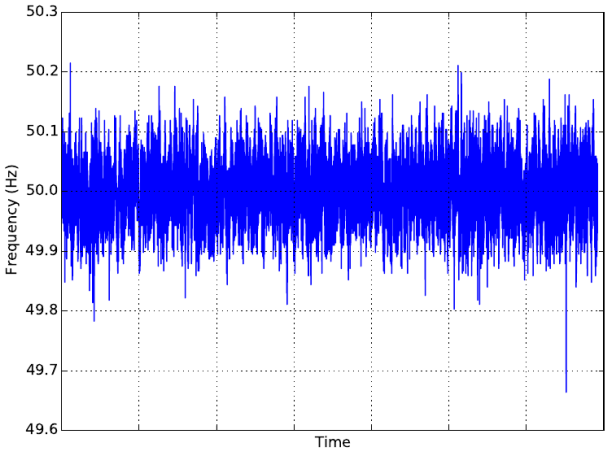

Fig. 5. Frequency data values plot for April 2 to April 30

Collected frequency data is analyzed with results shown in Table I.

TABLE I
Frequency data characteristics for April

Min Value	Max Value	Mean	Standard Deviation
49.664Hz	50.215Hz	50.001Hz	0.0425Hz

This analysis and frequency distribution in Fig. 6 shows that frequency is highly symmetric over longer periods of time, thus the amount of energy supplied by the EVs for up regulation should equal to the energy consumed by the vehicles for down regulation. However, the experimental example will show, that the energy taken and received back to the battery is not equal, due to efficiency of the charger, at lower current values being around 80%, and only up to 92% at higher charging power. This will result in significant drop of the battery SOC, on the longer symmetric regulation periods.

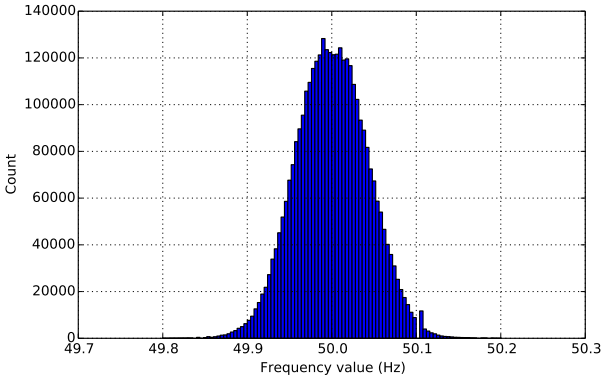

Fig. 6. Frequency data value distribution from April 2 to April 30

In the histogram in Fig. 6, the bin width is $4mHz$. Most of the frequency values - 99.99%, are between $49.8 - 50.2Hz$. The symmetrical spikes at bins $49.988 - 49.992Hz$ and $50.008 - 50.012Hz$ are corresponding to a metering-related deadband of some primary frequency regulation controllers. This deadband could occur because of the frequency measurement devices used to activate the controllers. The ancillary service conditions states, that the accuracy and sensitivity of the frequency meters must be better than $\pm 10mHz$ [8]. Therefore, it may happen that some power units, especially small ones which may be equipped with less sensitive metering devices, are not activated while the frequency is within $50.00Hz \pm 10mHz$.

B. Frequency Regulation

The results of the frequency regulation: each plot shows the grid frequency values, state of charge (SOC) of the EV battery and the V2G current from the EV to the grid. The positive current indicates that the vehicle is providing power to the grid and with the negative current values, EV is consuming power i.e. charging.

In the first experiment, the vehicle was plugged in overnight providing primary frequency regulation for 6 hours. Experiment result is shown in Fig. 7.

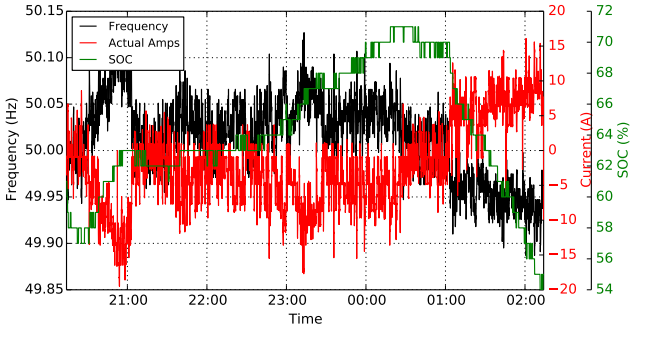

Fig. 7. Frequency regulation results for 6 night hours

Here one can observe that the frequency (marked in black) is above normal most of the night, thus the vehicle is charging at up to $20A$ (marked in red). The SOC of the vehicle (marked in green) is also balancing above the starting value, at the peak reaching 71%. However, at 3am the frequency drops below the nominal value and the vehicle switches to the V2G mode. At the end of the experiment the EV has 54% SOC.

A longer experiment was also performed with frequency regulation being active for 22 hours. The results are shown in Fig. 8.

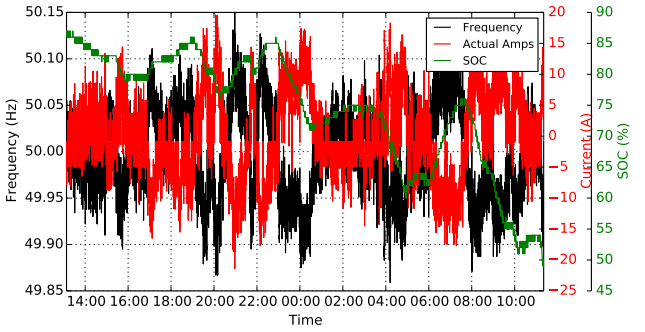

Fig. 8. Frequency regulation results for 22 hours

Here the average frequency value for the test period is $49.997Hz$. This indicates that the frequency is almost symmetric, with a slight bias towards the value below nominal. The SOC of the vehicle changes from 85% at the start to around 53% at the end of the test. The change can be explained by slight bias of the frequency and mainly by the V2G converter efficiency. The measured efficiency of vehicle PEU in V2G mode at these low current values is around 0.8, so the roundtrip efficiency results in around 0.64. This corresponds to the ratio of the end to start value of battery SOC in the example from Fig. 8.

Further, the close up from the 22 hour frequency regulation process is shown in Fig. 9.

In this plot the delay between the frequency measurement and response by the vehicle can be appreciated. Generally, the

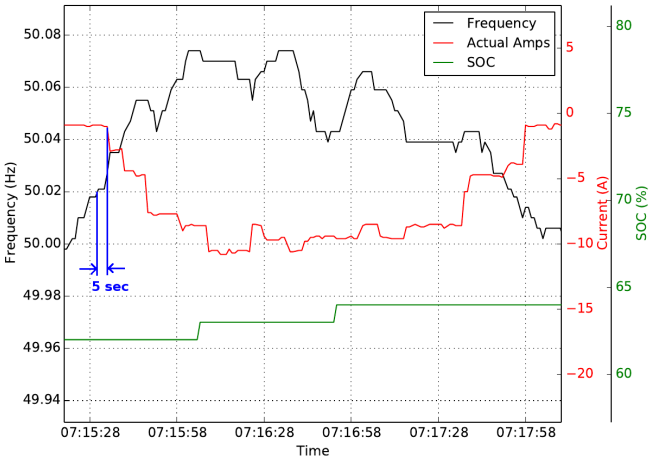

Fig. 9. Frequency regulation results close up with response delay

eBox is able to respond to the frequency change in 5 to 6 seconds on average. This delay consists of approximately: 1 second delay for frequency sampling time and control action in the controller, 1 second delay for communication and control parameter update in the pollserver, 3 to 4 seconds for PEU ramping time and 1 second delay for response data sampling in the measurement device.

All tests were performed in SYSLAB - a DTU research facility for intelligent, active and distributed power systems. SYSLAB is located at DTU Risø campus and is a part of the PowerLabDK experimental facilities.

V. Discussion

The primary frequency regulation based on an electric vehicle proved successful in operation. Web-centric communication protocols introduce application flexibility, platform independence and significantly speed up controller implementation. The response of the vehicle to the detected frequency deviation is much faster than the specified technical conditions for regulation: 5-6s versus 15s. This experimentally proves that bi-directional power exchange with electric vehicles are fast enough for providing this kind of grid support [12]. Even faster response times can be achieved by increasing data sampling and control parameter update frequency, however most of the delay is due to the slow ramping rate of the PEU unit. Overall the response delay could be reduced to less than half - around 2-3s. Several improvements are proposed for better EV integration for grid frequency support: the PEU efficiency should be improved to minimize the roundtrip energy losses; the battery degradation should be taken into account and studied in detail as different studies suggest contradictory results [13], [14]. However, it has been proven in multiple studies, that providing grid services using EVs is economically beneficial [15], [16]. Finally, this work has shown, that real-life application of the EV for grid frequency support is feasible and modern communication technologies help the intelligent integration of the EV for providing grid services [17].

REFERENCES

[1] M. Marinelli, S. Massucco, A. Mansoldo, and M. Norton, "Analysis of inertial response and primary power-frequency control provision by doubly fed induction generator wind turbines in a small power system," *Proceedings of the 17th Power Systems Computation Conference, Stockholm, 22-26 Aug. 2011*, 2011.

[2] K. Clement-Nyns, E. Haesen, and J. Driesen, "The impact of charging plug-in hybrid electric vehicles on a residential distribution grid," *Power Systems, IEEE Transactions on*, vol. 25, no. 1, pp. 371–380, Feb 2010.

[3] W. Kempton and J. Tomic, "Vehicle-to-grid power implementation: From stabilizing the grid to supporting large-scale renewable energy," *Journal of Power Sources*, vol. 144, no. 1, pp. 280 – 294, 2005.

[4] H. Lund and W. Kempton, "Integration of renewable energy into the transport and electricity sectors through V2G," *Energy Policy*, vol. 36, no. 9, pp. 3578–3587, 2008.

[5] J. Pillai, B. Bak-Jensen, and P. Thogersen, "Electric vehicles to support large wind power penetration in future danish power systems," in *Vehicle Power and Propulsion Conference (VPPC), Seoul, 09-12 Oct. 2012 IEEE*, Oct 2012, pp. 1475–1479.

[6] F. Marra, D. Sacchetti, A. Pedersen, P. Andersen, C. Træholt, and E. Larsen, "Implementation of an electric vehicle test bed controlled by a virtual power plant for contributing to regulating power reserves," *Power and Energy Society General Meeting, 2012 IEEE*, no. 081216, pp. 1–7, 2012.

[7] S. Han, S. H. Han, and K. Sezaki, "Design of an optimal aggregator for vehicle-to-grid regulation service," *Innovative Smart Grid Technologies (ISGT), 2010*, 2010.

[8] "Ancillary services to be delivered in Denmark Tender conditions," Tech. Rep. October, 2012.

[9] University of Delaware, "The Grid-Integrated Electric Vehicle," Tech. Rep.

[10] R. T. Fielding, "Architectural styles and the design of network-based software architectures," Ph.D. dissertation, 2000, AAI9980887.

[11] A. Pedersen, E. Hauksson, P. Andersen, B. Poulsen, C. Træholt, and D. Gantenbein, "Facilitating a Generic Communication Interface to Distributed Energy Resources: Mapping IEC 61850 to RESTful Services," in *Smart Grid Communications (SmartGridComm), 2010 First IEEE International Conference on, Maryland*, 17-20 Oct 2010, pp. 61–66.

[12] J. R. Pillai and B. Bak-Jensen, "Vehicle-to-grid systems for frequency regulation in an Islanded Danish distribution network," *2010 IEEE Vehicle Power and Propulsion Conference*, pp. 1–6, 2010.

[13] S. Peterson, J. Apt, and J. Whitacre, "Lithium-ion battery cell degradation resulting from realistic vehicle and vehicle-to-grid utilization," *Journal of Power Sources*, vol. 195, no. 8, pp. 2385–2392, Apr. 2010.

[14] S. You, J. Hu, A. Pedersen, P. Andersen, C. Rasmussen, and S.-T. Cha, "Numerical comparison of optimal charging schemes for electric vehicles," *Power and Energy Society General Meeting, 2012 IEEE*, pp. 1–6, 2012.

[15] W. Kempton and J. Tomić, "Vehicle-to-grid power fundamentals: calculating capacity and net revenue," *Journal of Power Sources*, vol. 144, no. 1, pp. 268–279, Jun. 2005.

[16] S. Han and K. Sezaki, "Economic assessment on V2G frequency regulation regarding the battery degradation," *Innovative Smart Grid Technologies (ISGT), 2012 IEEE PES*, pp. 1–6, 2012.

[17] A. Pedersen, P. Andersen, J. Skov Johansen, D. Rua, J. Ruela, and J. A. Pecas Lopes, *ICT Solutions to Support EV Deployment*, ser. Power Electronics and Power Systems. Springer-Verlag, New York, 2013, pp. 107–154.

Pub. D. Validating a centralized approach to primary frequency control with series-produced electric vehicles

Journal of Energy Storage 7 (2016) 63–73

Contents lists available at ScienceDirect

Journal of Energy Storage

journal homepage: www.elsevier.com/locate/est

Validating a centralized approach to primary frequency control with series-produced electric vehicles

Mattia Marinelli*, Sergejus Martinenas, Katarina Knezović, Peter Bach Andersen

Centre for Electric Power and Energy, Technical University of Denmark, Risø Campus, Roskilde, Denmark

ARTICLE INFO

Article history:
Received 19 March 2016
Received in revised form 16 May 2016
Accepted 17 May 2016
Available online 3 June 2016

Keywords:
Centralized control
Electric vehicles
Frequency control
Islanded systems
Testing

ABSTRACT

The aim of this work is twofold: on one hand it proposes a centralized approach to primary frequency control by using electric vehicles as controllable units; on the other hand, it experimentally validates whether series-produced EVs, adhering to contemporary standards, can be an effective resource for providing primary frequency control. The validation process is realized in an islanded system with renewable sources and it relies on verifying that the frequency values are within the desired limits following severe load steps or wind power fluctuations.

In order to reflect today's situation, the used EVs, three Nissan Leaf, are not taking advantage of any V2G capability, but rely solely on the possibility of limiting the charge between 6 A and 16 A. The centralized approach implies that the frequency is not measured locally as it is a common practice today, but is routed via the Internet in order to include potential communication delays that would take into account the presence of different entities for controlling the vehicles, such as aggregators and utilities.

The centralised approach is pursued to support aggregators in participating in current ancillary service markets. Ultimately, this paper aims to strengthen the applied research within EV integration through the practical validation of smart grid concepts on original manufactured equipment.

1. Introduction

With conventional units being replaced by renewable resources, there is an increased demand for additional ancillary services, such as frequency control. Due to their defining property of being quick-response high-power units, electric vehicles (EVs) emerge as a viable actor for providing frequency regulation. A noticeable amount of research efforts is put nowadays to investigate all different aspects needed to shift from the traditional power system, where frequency and voltages are controlled by a relatively small set of large units, into a futuristic system, where potentially all power devices can be involved in the controlling actions. For instance, in the ELECTRA project, innovative control schemes are being investigated in order to assess whether conventional frequency and voltage controlling approaches are still suitable, or which aspects need to be revised for scenarios with massive amounts of small distributed energy resources [1,2]. It is argued that TSOs alone will not be able to effectively manage the overall system balance and will have to partially delegate frequency control responsibility to DSOs as already happens today for congestions management and volt-reactive power provision [3–10].

Regardless of who will be responsible for frequency and voltage control, several technical challenges are ahead. For instance, will the aggregated provision of thousands of few kVA-units at low voltage level be as effective as the one of MVA-units response? Moreover, considering the traditional 3-phase system, will the response of groups of single-phase devices be as effective as the response of similar size 3-phase units? With a specific focus on frequency control, is it reasonable to expect millions of accurate local frequency measurements to be used for decentralized, traditional, droop controllers or is it rather better to have a limited set of centralized controllers, which rely on a few accurate

Abbreviations: DSO, distribution system operator; ENTSO-E, European Network of Transmission System Operators for Electricity; EV, electric vehicle; EVSE, electric vehicle supply equipment; FCR, frequency containment reserve; FRR, frequency restoration reserve; ICT, information and communications technology; OEM, original equipment manufacturer; OR, Operating reserve; PFC, primary frequency control; RES, renewable energy sources; RR, Replacement reserve; SOC, state-of-charge; TSO, transmission system operator; V2G, vehicle to grid.

* Corresponding author.
E-mail addresses: matm@elektro.dtu.dk, marinelli.mattia@gmail.com (M. Marinelli).

http://dx.doi.org/10.1016/j.est.2016.05.008
2352-152X/

measurements, sending out power set-points via normal Internet connection?

1.1. Background and literature analysis

Electric vehicles are one of the imminent candidates for providing ancillary services. Most of the time (typically about 90%) they are plugged into a charging post and can, in principle, provide fast-regulating power in both directions, or just modulate the charging power. A noticeable amount of literature has already been written supporting this statement [7–22].

It is argued that EVs with V2G capability can provide regulation services, and can compete in electricity markets, such as markets for ancillary services, where there is payment for available capacity, apart from the payment for the actual dispatch. Frequency control is one of the services which can be provided by EVs through this market. More specifically, primary frequency control (PFC) can be suitably provided by EVs due to their flexible operating mode and ability to seamlessly alter the consuming/producing power under the V2G concept [12–14]. The work described in [15] presents an aggregated PFC model, where a participation factor, dependent on the state-of-charge (SOC), is associated with each EV to determine its droop characteristic. It was shown that EVs can effectively improve the system frequency response, as well as that V2G-capable vehicles have better power response, due to more available primary reserves. Furthermore, a decentralized V2G control for primary frequency regulation is presented in [16]. The proposed method considers customer charging demands and adapts the frequency droop control to maintain or achieve the desired SOC. A comparative study is performed in [17], in order to evaluate benefits of EVs performing primary frequency control in an islanded system with high penetration of renewable resources. The presented study case argues that system frequency oscillates in a 0.3 Hz band if the EVs contribute to primary regulation, compared to 1 Hz in the case of only using available hydro units. Two studies, respectively from Japan and Great Britain, analyse participation in frequency control on large systems considering traveling constraints and including large amount of renewable sources [18,19]. However, even though the mentioned studies analysed different strategies for providing primary frequency control, rarely have they dealt with the experimental validation, but mostly remained on modelling and simulations. For example, the works described in [15–21] have implemented different droop controls and shown that EVs can be effective in primary frequency regulation, likewise in isolated microgrids and larger systems. Still, they assume an ideal EV response to the control signals, both in the reaction time and the provided power, and they omit communication and control latencies which may greatly impact the results.

In addition, technical challenges may arise due to the limited power and energy size of each individual unit, as well as the need to have simple and effective measuring and controlling capabilities for primary frequency regulation. Transmission systems operators may be sceptical about the possibility of having demand participating in the frequency regulation, mainly because of response uncertainties and metering inaccuracies. Therefore, an extensive experimental activity is required to prove the feasibility of these solutions. The activity described in this paper is carried out using series-produced vehicles and the universally supported IEC 61851 standard, to prove the applicability of the solution.

1.2. Objective of the manuscript

Most of the literature identified during the literature review focuses on modeling and simulating the EV primary frequency control, whereas the experimental validation is rarely touched upon. Therefore, this paper focuses on the evaluation of EVs' ability to provide primary frequency control in a centralized fashion. The frequency control analysis of three EVs connected to a small islanded power system is proposed. Having the system islanded gives the possibility of emulating realistic frequency events, which could hardly be appreciated if connected to the national grid. It is important to note that the experiments are carried out with commercially available vehicles without taking advantage of any V2G capability, but only with the possibility to modulate the unidirectional charging current. This limit is part of internal standards (IEC61851/J1772) for conductive AC charging and supported by the vast majority of EVs today.

A classical droop control function is utilized. However, contrary to today's practice, which relies on local measurement, the frequency measurement is routed via the Internet to the controller, which sends the current set-point to the EV. The authors believe that in the near future, it will be highly unlikely to equip each EV with a precise measurement device which meets the TSO requirements. This means that the used technology resembles that of an operational environment: a fleet of EVs providing frequency regulation on market terms through an aggregator who has the certified frequency measurement device. Such setup allows the inclusion and assessment of potential communication delays, especially their influence on system stability. This work does not take in consideration vehicle unavailability due to owner usage. However it has to be reminded that, due to the system wide nature of the service, the location of the resource providing frequency control is not extremely important. In that sense, it is the aggregator's best interest to rely on a higher number of vehicles to account for the plug-in uncertainties, whilst it is less important to know their exact location, as long as the utilized vehicles are connected to the grid and not used for other services.

Ultimately, the research question tackled in this paper is: can small size, single phase distributed energy resources, such as commercially available electric vehicles, effectively provide primary frequency control relying on a centralized controller which sends out current set-points?

The rest of the paper is structured as follows: Section 2 briefly recalls how the control of frequency is traditionally organized in Europe and in Denmark. Section 3 describes the controller characteristics, the communication architecture and the implementation in the laboratory. In Section 4 numerical and graphical results of the experiments are presented and discussed; several scenarios are investigated from load step, through steady state analysis to wind power balancing. Section 5 reports conclusions and lessons learned.

2. Current framework for frequency control in Europe and Denmark

2.1. Frequency services according to ENTSO-E division

Based on the European Network of Transmission System Operators for Electricity (ENTSO-E) definitions, reported in the Network Code and Operation Handbook, frequency control includes [23]:

- Primary frequency control;
- Secondary power-frequency control;
- Tertiary control.

ENTSO-E refers to the reserves for frequency control as Operating Reserves (OR), and specifically, indicates the above-mentioned controls as:

- Frequency Containment Reserves (FCR);
- Frequency Restoration Reserves (FRR);
- Replacement Reserves (RR).

The (automatic) primary frequency control aims at achieving the operational reliability of the synchronous area by stabilizing the system frequency after a disturbance or an incident at an acceptable stationary value in the second time frame, typically within 30 s. The minimum requirement for FCR is based on the maximum loss of power generation or demand, also called reference incident: within the Continental European synchronous area, the reference incident is defined as 3000 MW of generating capacity. FCR is shared among all control areas. The requirement of each control area is defined by contribution coefficients, calculated as the ratio between the energy generated in that area over a year and the energy generated in the entire synchronous area. The response has to be maintained for up to 15 min.

The secondary frequency control, which can be either automatic or manual, aims to restore the system frequency within a few minutes, typically up to 15 min after incident, by releasing system-wide activated frequency containment reserves. For large interconnected systems, where a decentralized frequency restoration control is implemented, frequency restoration also aims at restoring the balance between generation and load for each TSO, and consequently, restores power exchanges between TSOs to their set-point.

The tertiary control, activated manually and centrally at the TSO control centre, aims to restore the operating reserve, or to anticipate expected imbalances. Typically, the activation time is from 15 min up to several hours.

2.2. Frequency services in Denmark

The Danish power system has the particular feature of belonging to both the Continental European synchronous area and the Nordic (Scandinavian) power system. Specifically, Western Denmark (DK1) which comprises Jutland peninsula and Funen island, has several AC connections to Germany and is therefore subject to the frequency services mentioned previously in Section 2.1. With reference to the primary frequency control, the mandatory share assigned to Western Denmark is equal to 27 MW. Eastern Denmark (DK2) instead has several AC connections to Sweden and is therefore synchronous to the Scandinavian Region. In the current framework, there is no automatic secondary frequency control in the Nordic power system—although a manual/tertiary reserve is in place – and the primary frequency control is actually split in two separated services: frequency-controlled normal and frequency-controlled disturbance. The interested reader can get a more detailed overview on how the frequency control is organized in the Nordic system by consulting ref [24]. For what concerns the work described in this manuscript, it is interesting to analyse the technical conditions for providing the frequency-controlled disturbance service, which is actually rather demanding in term of response time:

- Supply inverse-linear power at frequencies between 49.9 and 49.5 Hz.
- Supply 50% of the response within 5 s.
- Supply the remaining 50% of the response within an additional 25 s.
- Accuracy and sensitivity of frequency measurements must be better than 10 mHz.
- SCADA system resolution must be better than 1 s.
- The listed requirements set the basis for benchmarking the performance of the experimental activity.

3. Controller characteristic and architecture and experimental layout

3.1. Primary frequency controller characteristics

Commonly, primary frequency control is achieved via droop controllers, so that synchronous machines operating in parallel can share the load, according to their power rating. The droop constant is generally intended as the measure of the machine sensitivity to frequency changes, and is the value that quantifies its contribution to primary frequency/power regulation. The frequency variation, Δf (in Hz), referred to the nominal frequency of the system is therefore given as a function of the relative power change ΔP (in W) or current change ΔI (in A) reported to the nominal machine power/current:

$$\text{a)}\,{}^{\Delta}\text{f}\big/_{f_{nom}} = \text{k}_{\text{droop}}\,{}^{\Delta}\text{P}\big/_{P_{nom}};\ \text{b)}\,{}^{\Delta}\text{f}\big/_{f_{nom}} = \text{k}_{\text{droop}}\,{}^{\Delta}\text{I}\big/_{I_{nom}} \tag{1}$$

For example, a 5% droop means that a 5% frequency change (2.5 Hz) causes 100% change in the machine output.

Defining a droop value for loads, on the other hand, may become less straightforward, as it may not be clear what the nominal power of the load – or of the set of loads – is. In this case, it has been considered that the available range of regulating power, that means 2.3 kW or 10 A per EV, is equal to the unit's nominal power, instead of the nominal charging power of 3.7 kW or 16 A per EV. Therefore, in the experimental setup that will be described in Section 3.2, the following parameters are used for the EVs' 4% droop control:

$$a)\begin{cases} \Delta f = 2Hz; f_{nom} = 50Hz \\ \Delta P = 2.3kW; P_{nom} = 2.3kW \\ k_{droop} = \dfrac{{}^{\Delta f}\big/_{f}\,nom}{{}^{\Delta P}\big/_{P}\,nom} = 4\%; \end{cases}$$

$$b)\begin{cases} \Delta f = 2Hz; f_{nom} = 50Hz \\ \Delta I = 10A; I_{nom} = 10A \\ k_{droop} = \dfrac{{}^{\Delta f}\big/_{f}\,nom}{{}^{\Delta I}\big/_{I}\,nom} = 4\% \end{cases} \tag{2}$$

Fig. 1 reports the individual EV controlling characteristic, which means the current set-point in function of the frequency, for two different droops: 4% and 2%. The 2% droop is realized by simply reducing the delta frequency to 1 Hz (i.e., 49.5 ÷ 50.5 Hz). It has to be reminded that the droop represent the slope of the curve if the plot reports the frequency in function of the current set-point. It is the inverse of the slope if the current is function of the frequency. The ideal droop curves, in dashed red and magenta in Fig. 1, spans respectively from 49.5 Hz to 50.5 Hz and 49 Hz to 51 Hz, and are linearly related to all the current values from 6 A to 16 A. The implemented ones, however, differ because the current values can be set with a discretization of 1 A. Therefore the ideal curve becomes quantized, and for every 0.05 Hz or 0.1 Hz, the current values are increased by 1 A. The minimum and maximum charging currents, respectively 6 A and 16 A, are maintained once the thresholds frequency are reached.

This is the first main outcome, since the current standard IEC61851 only allows 1A-discrete modulation, while Energinet.dk requirements specify a linear relationship. In case an aggregator would realize such control strategy, it would be necessary to have a sufficient pool of cars that, once aggregated, show an equivalent linear response.

A possible solution, which is left for further investigations, could be achieved by shifting the reported characteristics so that,

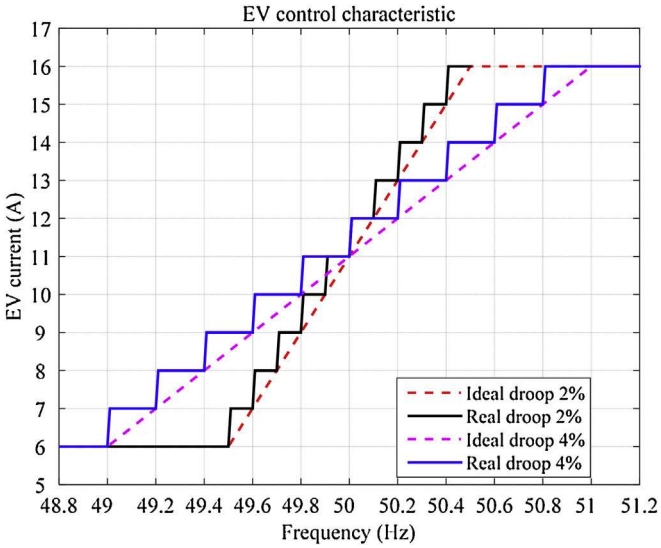

Fig. 1. EV ideal (dashed lines) and real (solid lines) control characteristic for 2 droop values (2% and 4%).

for instance, the current step between 6 A and 7 A is not realized for all the EVs at 49.00, but at 49.01 Hz for a certain set of EVs, at 49.02 Hz for another set and so on. Given the limited set of cars for the current experiments, the linearity requirement will not be fulfilled.

The careful reader will also notice that both droop curves are slightly asymmetric (i.e., the 11 A value is set between 49.8 and 50.0 Hz and not between 49.9 and 50.1 HZ), giving therefore a bit more controlling capability for the over-frequency situations. As it will become clearer while presenting the experimental results (see Section 4.2), this choice was made in order to compensate for recurring undershooting phenomenon of approximately 0.5 A in the effective charging current of the EVs.

3.2. Experimental layout

The experiments are executed using the hardware and ICT infrastructure of SYSLAB, which is a small-scale power system in the PowerLabDK platform. SYSLAB consists of a number of real power components interconnected by a three-phase 400 V AC power grid, and paralleled with communication and control nodes arranged in a dedicated network. The complete test bed is distributed (more than 1 km) over the Risø Campus of the Technical University of Denmark. The system may be connected to the local grid or can be islanded if desired [25]. The following components are used for the experiments, with their capabilities and operating points summarized in Table 1:

- Three controllable EVs (Nissan Leaf) each equipped with single phase 16 A (230 V) charger and 24 kWh lithium battery storage. The charger does not utilize any V2G capability, which means it is not allowed to inject power into the grid. The charging level can, however, be modulated between 6 and 16 A with steps of 1 A. Positive power means EV charging (i.e., consumption).
- Diesel genset equipped with a 60 kVA synchronous generator, capable of providing an active power output up to 48 kW. Positive power means generation.
- 15 kW ÷ 190 kWh Vanadium Redox Battery (VRB) storage system, equipped with an inverter capable of providing up to ±15 kW and ±12 kVAr. Positive power means battery charging, therefore consumption.
- 10 kW Aircon wind turbine equipped with full converter. Nominal wind speed 11 m/s, active stall power control. Positive power means generation. The Aircon is connected to the system only during the last set of experiments.

The diesel genset is used to provide inertia to the system. The governor of the genset, however, is disabled in order to avoid automatic frequency control. Frequency events are triggered by changing the VRB set-points. The three EV inverters are equipped with the droop controllers described in Section 3.1, and rely on frequency measurements routed via wired network connection. It means that the frequency measurement is not used for feeding a local controller, but is processed remotely, and sent via network to the computer controlling the charging post.

This aspect is extremely important because it is common practice for power plants to provide primary frequency control by using local frequency measurements. Moreover, as mentioned in Section 2.2, in order to participate in the frequency regulations, the usage of measurement devices with high accuracy (at least 10 mHz) and high sampling rate (at least 1 value every second) is required. This feasibility has already been proved in a grid-connected setup with just few seconds' latency [14].

The experimental setup, including both power components and communication architecture, is presented in Fig. 2. Since all the components are 3-phase except for the EVs, it has been necessary to create an intermediate phase splitter, shown in Fig. 3. The phases are permuted cyclically so that each EV is supplied on a different phase via a standard Mennekes (IEC 62196 Type 2) connector.

The operating set-points of different components are chosen in order to push the system to the limits. The EVs' initial charging level is chosen so that there is room to increase and decrease the charge level equally.

3.3. Centralized frequency communication architecture

The test setup used in this work consists of 3 electric vehicle supply equipment (EVSE), each connected to a different phase. The communication and control setup are shown in Fig. 4.

The control aggregator is connected to each EVSE by Ethernet, using the MODBUS protocol, and is used to set a maximum EV charging current. The aggregator is also connected to a measurement unit, also by Ethernet, using the MODBUS protocol, providing local frequency and power measurements. Each EVSE is connected to the EV following the IEC 61851 standard.

Table 1
Units' capabilities overview.

Units	Capability
Single Electric Vehicle (single phase charger)	6 ÷ 16 A per phase (equal to 1.4 ÷ 3.7 kW)
Set of 3 EVs	4 ÷ 11 kW
Vanadium Redox Battery	−15 ÷ 15 kW; −12 ÷ 12 kVAr
Diesel generator	0 ÷ 48 kW; −20 ÷ 30 kVAr
Aircon wind turbine	10 kW @11 m/s

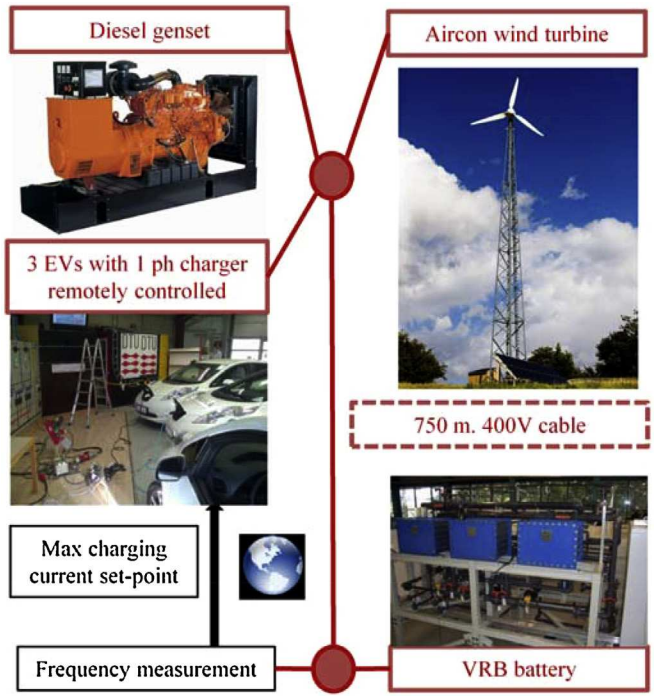

Fig. 2. Experimental setup: power components and electrical connections in red; communication architecture in black. (For interpretation of the references to color in this figure legend, the reader is referred to the web version of this article.)

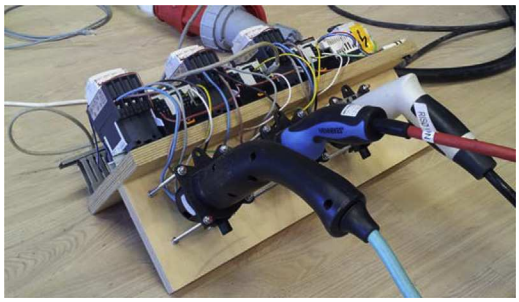

Fig. 3. 3-phase splitter: 3 Mennekes plugs used to connect each EV to a separate phase.

According to this standard, the EV listens to the communication line (called the Control Pilot line) from the EVSE, in the form of a PWM signal. The duty cycle of this signal indicates the maximum charging current limit the EV is allowed to draw. In this work currents from 6A to 16A with 1A steps are used, as indicated in Section 3.1. The frequency is measured using a DEIF MTR-3 meter connected to phase A. Measurements are polled every second with an accuracy of ±10 mHz and a maximum latency of 0.2 s.

4. Experimental investigation and results discussion

The experiments are intended to test the EVs' ability to modulate the charge level, in order to control the system frequency in the case of load variations and wind power fluctuations. The load events include an alternate load-increase and load-decrease so that both over- and under-frequency dynamics can be studied. The amplitude of the load event is equal to 30% of the initial load value; i.e., 3 kW. In the last set of experiments, an attempt to balance the variable wind production is performed. The diesel governor is always disabled so that it is entirely up to the 3 EVs to control the system frequency. System performance is evaluated by checking that the system does not black out, and that the frequency is kept within the prescribed droop control values. Voltage values are also observed during the whole length of the transients.

This analysis allows also the investigation of issues that may arise when dealing with the practical implementation of frequency response, such as: communication latency, robustness of service algorithm, power and frequency measurement inaccuracies, and coordination of more sources, such as more vehicles providing this service.

The tests scenarios are reported below:

a) Determination of diesel inertia and verification of lack of governor reaction (1 kW load variation and no frequency control).
b) Load power steps (alternatively ±3 kW VRB set-point).
c) Wind-power balancing. Aircon is connected to the system, and EVs have to balance wind variability.

4.1. Determination of diesel inertia and lack of governor reaction

The first test intends to prove that the diesel governor is effectively disabled, and also to evaluate the amount of inertia of the genset, which is not given in the datasheet. A 1 kW power imbalance is created at the 60th second of the test, by increasing the VRB power consumption from 4 to 5 kW so that the frequency starts to decline. The power flows of the three components – diesel, VRB and EVs – are reported in the first plot of Fig. 5.

EVs are not frequency responsive, but keep on consuming the pre-set maximum power. It can be seen that the diesel actually increases its electrical torque, so the generated power increases from 15.3 to 16.3 kW. It must be noted, however, that this increase in the electrical torque is not balanced by a corresponding increase in the mechanical torque, as would happen if the governor was enabled. This can be derived from the frequency trend shown in the second plot of Fig. 5. The frequency decreases till the diesel under-frequency protection, set to 47.5 Hz, opens the genset breaker, and the system blackouts.

Relevant information which can be derived from this experiment is the system inertia, calculated by measuring the frequency drop over a certain amount of time, given a certain power imbalance. Since the inverters that control the VRB and the EV chargers do not have any virtual inertia feature, it can be assumed that all the system inertia belongs to the combined rotating masses of the diesel genset, which means the reciprocating machine, flywheel, and synchronous generator.

According to the equation of motion indicated in (3a) and considering the parameters reported in Table 2, the system inertia can be calculated as reported in (4). Equation 3a is valid as long as the rotational speed, ω_m, does not differ too much from the nominal speed, ω_n.

$$\text{a)}\Delta P = J\omega_n \frac{\Delta\omega_m}{\Delta t}; \quad \text{b)}\omega_m = \frac{2\pi f}{p} \tag{3}$$

$$J = \frac{\Delta P \times \Delta t}{\omega_n \times \pi \times \Delta f} = \frac{1000\ \text{W} \times 120\ \text{s}}{157\frac{\text{rad}}{\text{s}} \times 3.14 \times 2\ \text{Hz}} = 122\ \text{kg m}^2 \tag{4}$$

Since the physical value may not provide an immediate indication, it may be useful to report the inertia in per unit:

$$2H = \frac{J(\omega_n)^2}{S_{nom}} = \frac{122\ \text{kg m}^2 \times \left(157\frac{\text{rad}}{\text{s}}\right)^2}{60000\ \text{VA}} = 50\ \text{s} \tag{5}$$

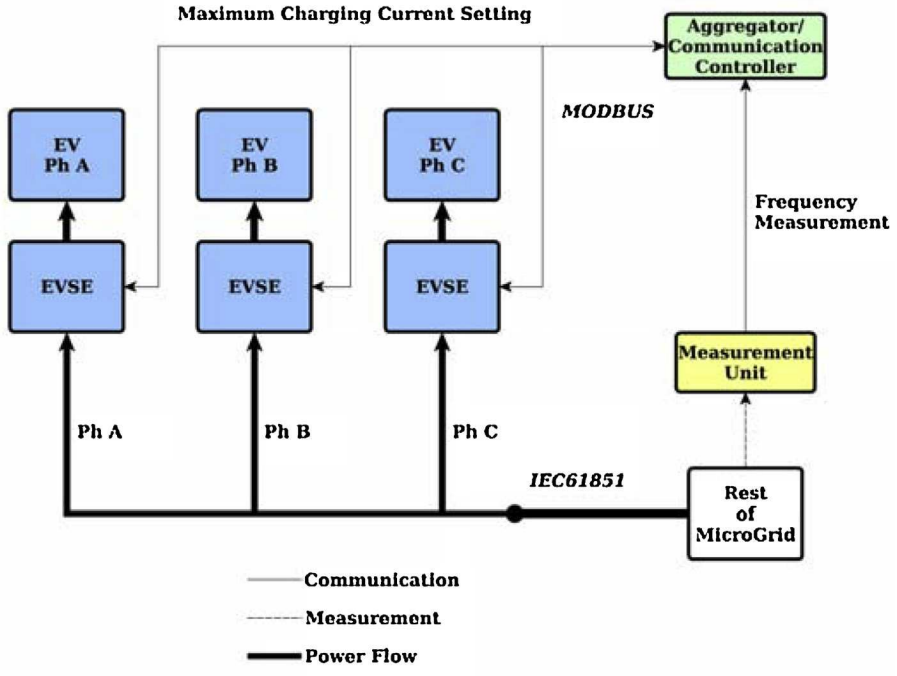

Fig. 4. Communication and control setup.

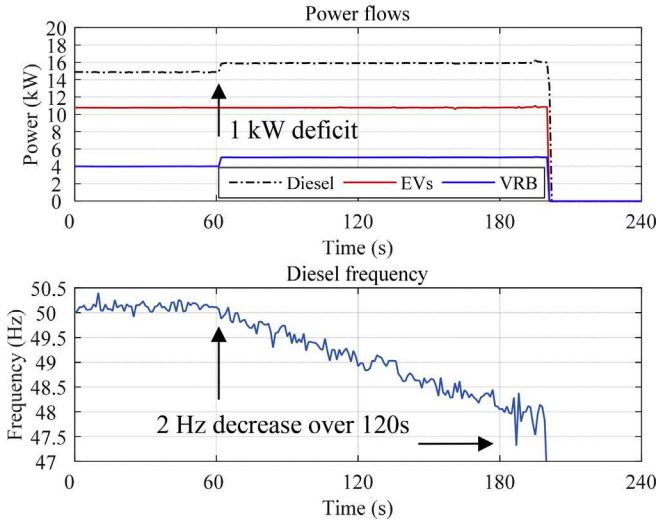

Fig. 5. First plot: Diesel, 3 EVs and VRB active power outputs. Second plot: frequency measured at Diesel power meter.

The 2H, or acceleration time constant, may seem rather large if compared to the typical values of conventional power plants, which generally span from 8 to 12 s [26]. It has to be kept in mind that this unit is designed for islanded operation, and has a reciprocating engine which needs proper balancing, in order to smooth out the natural pistons pulsations.

4.2. Load power steps

The second test is intended to assess whether the EVs can cope with large load variations, and to verify if their response follows the predefined droop characteristic illustrated in Fig. 1. The units' power outputs and the frequency measured at the diesel breaker are reported in Fig. 6 for the 2% droop controller. The initial conditions consist in: VRB consuming 2 kW, EVs consuming 7.2 kW (10.5 A each EV @ 230 V), diesel genset producing 9.6 kW (20% nominal power) and the rest accounts for system losses. As it will be better highlighted afterwards, even though the EVs are pre-set to consume 11 A, they actually draw less current. According to some discussions with OEM, the reason for this undershooting resides in the fact that OEM wants to be sure that if the PWM signal is limiting the charging current, the EV does not cross the set threshold even for few seconds.

It can be seen immediately in Fig. 6 that, despite the large load variations, which values around 30% of the initial load, the frequency is maintained between 49.5 and 50.5 Hz as expected from the 2% droop controlling characteristic. At the second 5400, when the first positive load step (VRB power from 2 kW to 5 kW) happens, the EVs quickly reduce their consumptions, and the frequency stabilises at around 49.4 Hz. The opposite situation is experienced at the second 5650, during the negative load step (VRB power from 2 kW to −1 kW), when the frequency stabilises at around 50.4 Hz.

Table 2
System values.

ΔP (power imbalance)	Δf/Δt (frequency drop in the time interval)	p (number of pair poles)	ω_n (generator nominal rotating speed)
1000 W	2 Hz/120 s	2	1500 rpm

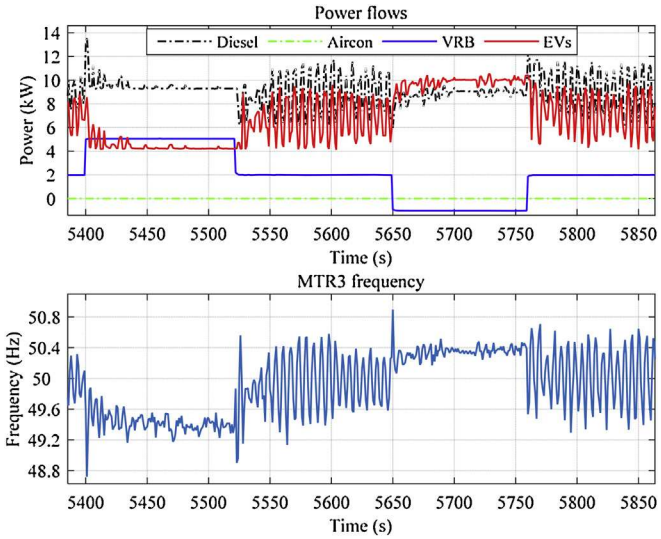

Fig. 6. First plot: Diesel, 3 EVs and VRB active power outputs (Aircon is disconnected). Second plot: frequency measured.

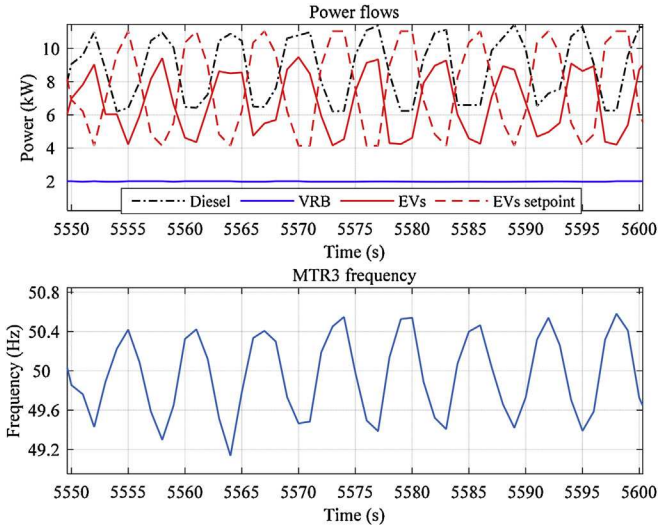

Fig. 7. First plot: Diesel, 3 EVs power and set-point and VRB active power outputs. Second plot: frequency measured.

Naturally, during the triggering events, the large system inertia plays a relevant role, which helps to slow down the frequency variations. As it can be seen from the equation of motion, the frequency variation depends on both the power variation (ΔP) and the inertia (J or 2H). Since it is not possible to change the system inertia, it has been decided to test the most challenging situation i.e., the largest power step which is equal to ± 3 kW in the VRB output. It has to be pointed out that the EV flexibility range, acting as the primary reserve available in the system, equals to ± 3450 W assuming the initial current set-point of 11 A per EV (that is ± 5 A per phase under the nominal voltage of 230 V). Frequency variations caused by a larger power steps, cannot be stabilized by the 3 EVs.

As mentioned in Section 4.1, the system inertia is around 5 times larger (in term of relative values) compared to the one of national power systems. However, it has to be noted that the load variation under test is extremely large, being 30% of the initial load value. If, for example, the Continental European power system is taken into consideration, the sizing accident for primary frequency control is estimated in a power step of around 3 GW. If this number is compared with the maximum load value, which is roughly 520 GW, the normalized load variation is equal to 0.6%. One could argue that the diesel used in this experiment also operates in a low-loaded situation (i.e., 9.6 kW production for a 60 kVA machine), so the load variation analysed in the test (i.e., 3 kW) should be referred to the nominal power of the diesel (i.e., 60 kVA). In this case, the normalized load variation is around 5% (i.e., 3/60), which is still 8 times larger compared to the value reported for Continental Europe.

Coming back to the transient behaviour of the system, it is interesting to observe in Fig. 7 that, when the load is equal to the initial conditions (i.e., VRB power at 2 kW), the frequency is oscillating around 50 Hz with a periodicity of around 6 s.

This means an oscillation with a frequency of 0.16 Hz that belongs to the group of local plant mode instability [27]. This is a clear indication that the controlling action of the EVs is too intense, leading the EVs to resonate with the diesel genset, which is naturally not a desirable operation. The 4% droop characteristic mentioned in Section 3.1 is investigated as well in order to verify whether a less intense proportional action would have been better. The wind balancing results, reported in Section 4.3, will evaluate system performances with both 2% and 4% droop.

Concerning the analysed load step test, it is also worthwhile focusing on the transient behaviour of the system right after the VRB power step. A 20-s time window is reported Fig. 8, where it is possible to notice the sudden frequency drop right after the 3 kW increase and the controlling action realised by the 3 EVs.

It can be noted in the third plot that the delay between the set and the calculated current is always around 1 s, at least in the time window displayed, while the delay between the measured and the set current is between 0 and 1 s. It is possible to notice few times that the measured and the set current are apparently synchronized. This is due to a limitation of the logging system that saves

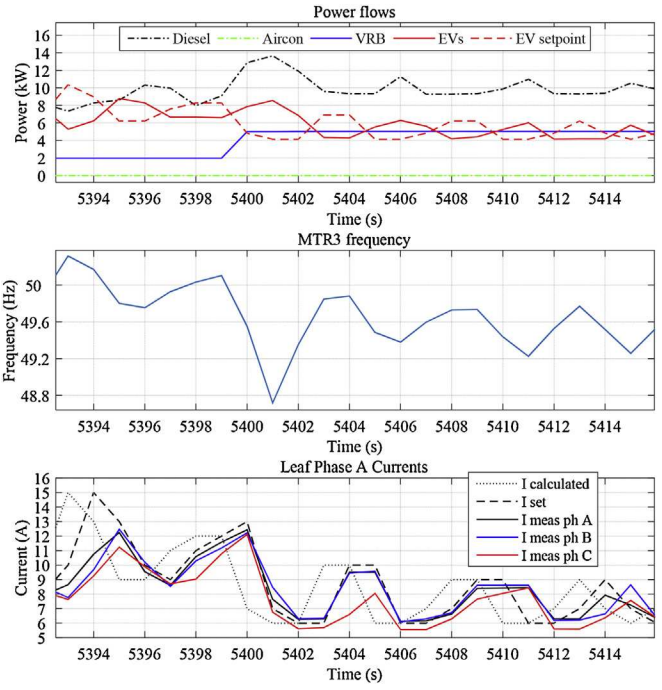

Fig. 8. First plot: Diesel, 3 EVs power and set-point and VRB active power outputs. Second plot: frequency measured. Third plot: calculated, set and measured current for each EV.

data every second making it difficult to appreciate faster dynamics: in this case, it is reasonable to assume that the EV response delay is within 0.5 s. However, it is possible to claim that most of the times the whole latency, starting from frequency measurement to EVs injected current into the grid, is between 2 and 3 s, which is certainly compatible with the requirements set by Energinet.dk for frequency controlled disturbance. An extensive and longer correlation analyses is conducted for the tests involving wind power balancing in order to support this finding.

Another relevant point concerns the current undershooting: as mentioned at the beginning of this section, the EVs almost never draw the current set by the controller, but steadily remain few decimal of ampere below the set value. This is due to the fact that the applied standard IEC 61851 defines a current limitation rather than a precise current set-point; therefore EVs are not required to follow the value, but just to limit the current. The reader will also notice that the EV connected to phase C (red line in the third plot of Fig. 8) is sometimes slightly slower than the other two and a bit more conservative when it comes to limiting the current drawn. The reason for this behaviour can be explained by the fact that, even though all cars are of the same type, the third one is actually two years older; therefore, the reason for the smaller delay could reside in a better design of the EV charging system. It has to be mentioned that the standard IEC 61851 specifies that this delay should be within 3 s.

4.3. Wind power balancing scenarios

In the final scenario, the effectiveness of EVs in balancing wind-power production is tested. Both droop characteristics are investigated in a similar setup, even though it has been necessary to reduce the VRB set-point during the 4% droop trial due to reduced wind speed. The initial values for both scenarios are summarized in Table 3.

Two 20-min time series results are reported in Fig. 9 for the two scenarios. The first impression is that the frequency is much more stable with the 4% droop; however, it has to be mentioned that wind conditions changed during the test and the wind turbine produced less power during the 4% test. However, in authors' opinion, this is not significantly impacting the controller's performance. In fact, as it was shown in the previous subsection, the EVs were marginally stable when following the load steps even without a variable power source in the system. In any case, tuning the controller is not the most important test objective at this stage, but rather verifying that EVs are able to sustain the system, and assessing their response time.

In order to get a more clear evaluation of the response time over the two tests, a correlation between phase A EV current and frequency measurements is reported. The left plot of Fig. 10 reports this correlation, highlighting also the applied control characteristic (red solid curve). The same correlation is moreover obtained by shifting the measured frequency respectively 1 s (middle plot) and 2 s (right plot) in the future.

A detailed numerical correlation analysis is reported in Table 4, by considering time shifts between 0 and 4 s and three classes of correlations are evaluated.

- I calculated—I set: correlation between the calculated current set-point, which is based on the measured frequency and the current set by the controller. This operation is done in parallel for all the machines therefore the correlation is the same. It can be seen that the highest correlation (97.5%) is obtained for 1 s shift, meaning that it is reasonable to assume this kind of delay between 0.5 and 1.5 s.

Table 3
System values during the wind power balancing scenarios.

Droop	Test duration	Diesel set-point (generation)	VRB set-point (consumption)	EV initial charging value (consumption)	Expected wind power (generation)
2% (6 ÷ 16 A; 49.5 ÷ 50.5 Hz)	1800 s	9.6 kW (20% nominal power)	7 kW	7.2 kW (11 A set per EV)	4 ÷ 7 kW
4% (6 ÷ 16 A; 49 ÷ 51 Hz)	1800 s	9.6 kW (20% nominal power)	4 kW	7.2 kW (11 A set per EV)	2 ÷ 5 kW

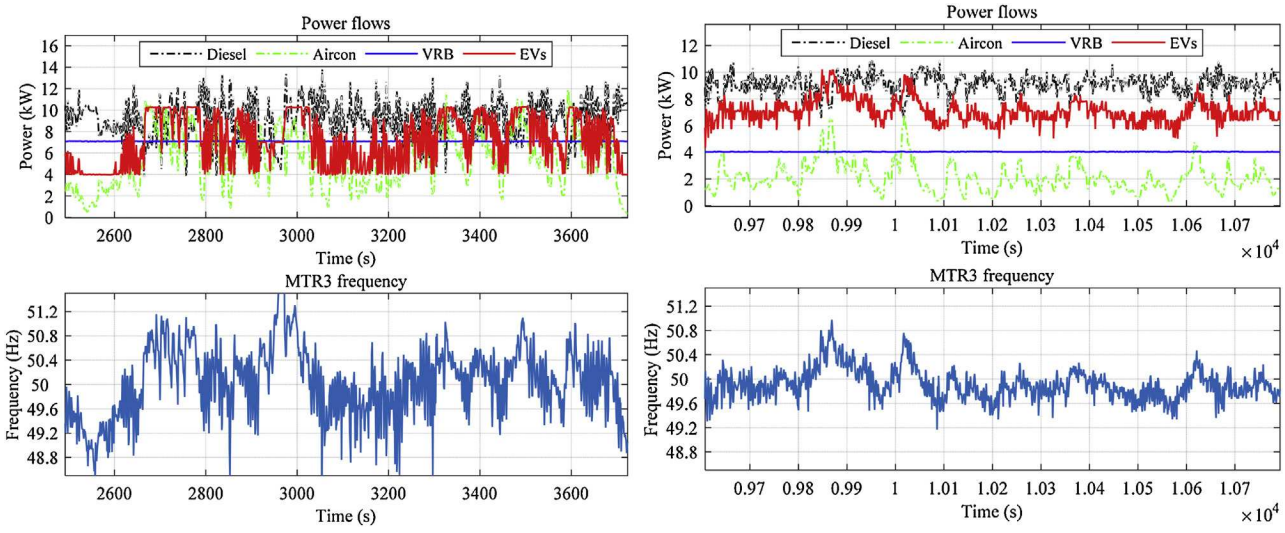

Fig. 9. First plot: Diesel, 3 EVs, VRB and Aircon active power outputs. Second plot: frequency. Dataset shown 20 min. EVs droop controller set to 2% (left plots) and to 4% (right plots).

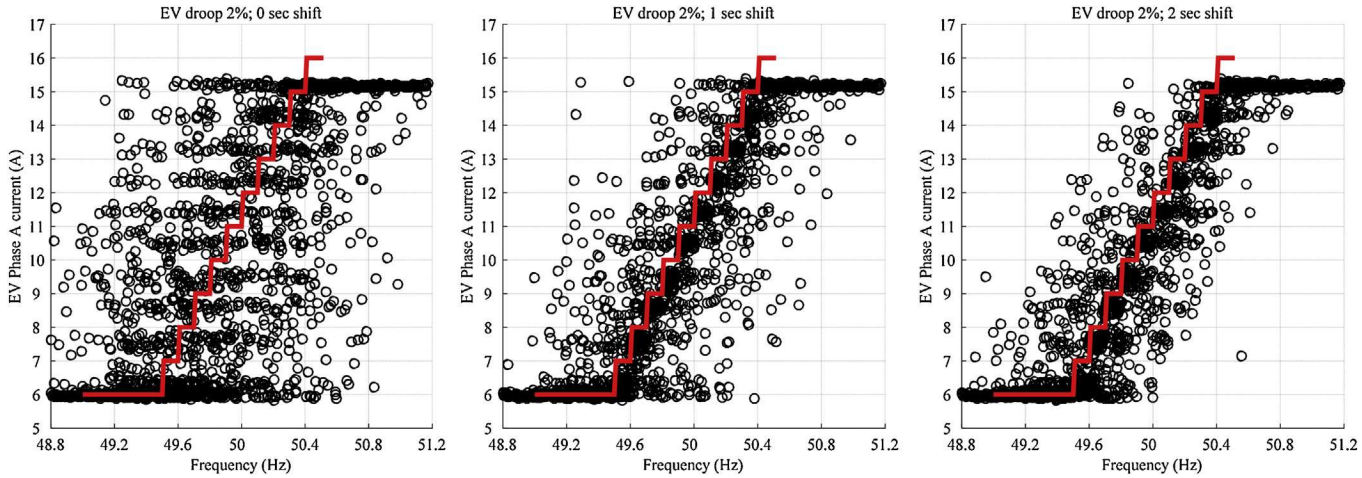

Fig. 10. Correlation between Phase A EV current and frequency measurements. Left plot: no time shift; middle plot: 1 s time shift; right plot: 2 s time shift. 2% droop controller.

Table 4
Correlation between calculated/set/measured phase currents – Droop 2% – wind balancing – data set 1800seconds.

	0 s shift	1 s shift	2 s shift	3 s shift	4 s shift
I calculated–I set	77.7%	97.5%	83.1%	57.4%	45.1%
I set–I measured (ph A; ph B; ph C)	91.7%	90.5%	67.4%	50.1%	53.9%
	93.3%	86.0%	62.2%	47.8%	57.9%
	62.6%	65.0%	53.6%	41.5%	40.9%
I calculated–I measured (ph A; ph B; ph C)	66.9%	90.7%	93.0%	70.0%	50.6%
	65.9%	89.9%	93.5%	70.9%	51.0%
	41.9%	59.0%	67.0%	58.2%	44.0%

- I set–I measured: correlation between the calculated current set-point and the current effectively consumed (and measured) by the EV. The highest correlation can be found in the first column (0 s shift), although also the second column (1 s shift) presents quite high correlation values. It is reasonable to assume that the average response time is within 1 s. It has to be stressed that this correlation, lower than the previous one, considers also the mismatching between measured and set current due to the undershooting phenomena, highlighted in Section 4.2. It can be also appreciated that the 3rd EV is actually the one presenting the poorest performance compared to the other two.
- I calculated–I measured: this correlation includes the two presented before and it is calculated in order to assess the overall EV response time. In this case the third column (2 s shift) is the one presenting the highest correlation, even though also the second one is rather large.

It can be concluded that the overall response time (from frequency measurement to EV current measurement) is between 1.5 and 2.5 s.

The same analysis is also performed for the 4% test case and the results are displayed in Fig. 11 and are reported analytically in

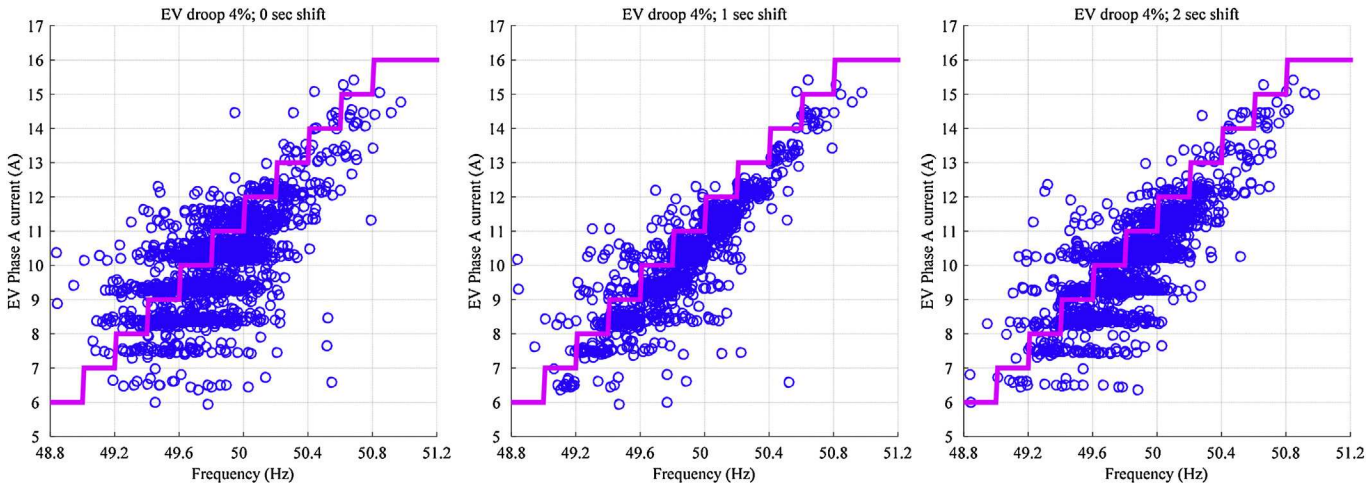

Fig. 11. Correlation between Phase A EV current and frequency measurements. Left plot: no time shift; middle plot: 1 s time shift; right plot: 2 s time shift. 4% droop controller.

Table 5
Correlation between calculated/set/measured phase currents – Droop 4% – wind balancing – data set 1800seconds.

	0 s shift	1 s shift	2 s shift	3 s shift	4 s shift
I calculated—I set	67.4%	99.5%	67.4%	56.7%	50.4%
I set—I measured (ph A; ph B; ph C)	89.6%	80.6%	60.9%	54.2%	61.5%
	92.1%	79.0%	61.7%	54.3%	62.9%
	87.2%	85.6%	67.3%	58.7%	63.1%
I calculated—I measured (ph A; ph B; ph C)	66.0%	89.2%	80.5%	61.0%	54.6%
	65.9%	91.2%	79.0%	61.8%	54.7%
	64.6%	86.8%	85.4%	67.3%	59.0%

Table 5. The results are consistent with the previous ones and due to better performances of the controller, it can be appreciated a higher correlation for the "I calculated—I measured" with 1 s shift instead of the 2 s shift.

Another important aspect relates to the quality of the frequency measurements. It is important to have a system robust against erroneous or missing information. In case faulty frequency measurements are detected, e.g. 0 Hz, the possibility of considering the last received frequency measurement as valid could be implemented, so EV control would be done according to that measurement. An alternative, although more expensive, could be the application of the 2 out of 3 logic often used in industrial processes. In this case it would be necessary for the aggregator to receive 3 different frequency measurements from separate instruments, possibly not electrically too far from each other, and then exclude the faulty one. In any case, similar approaches would still be cheaper compared than installing frequency meters in each EVSE.

A final consideration relates to the possibility of applying the same control structure also for deploying secondary frequency control. In fact, the EV current limitation set-point could be based on an integral effect of the frequency error similarly to what is currently done, where set-points are received by dedicated power stations. From the aggregator perspective, it could be foreseen that a certain amount of EVs are allocated to modulate their power outputs in order to restore frequency errors (in case the secondary frequency control is used for restoring the frequency) or restoring power exchanges between TSO control areas. Alternatively, other energy resources, characterized by slower dynamics, could be used for providing secondary control. For instance, experimental results reported in [28] proved the provision of secondary frequency control by using thermostatic controllable loads, such as domestic refrigerators. In any case, it is important to properly size the amount of reserve devoted to primary and secondary frequency reserve, as well as the frequency activation ranges in order to avoid lack of regulating power when needed.

5. Conclusions and future activities

The experimental results clearly show that frequency control from EVs is technically feasible with very fast response time. Therefore, coming back to the initial question, it is authors' opinion that EVs can be a reliable source for this kind of service and that providing primary frequency control with centralized communication architecture, relying on decentralized energy resources is technically feasible. The testing proved that already today, with existing commercial vehicles and standards without any particular V2G capability, it is possible to achieve this objective. Naturally, there is room for improvement and a few points that the authors think are necessary to tackle are listed.

Given the limited amount of regulating power, the chosen 2% droop value is rather small, meaning that the EVs' controlling action is rather intense, which is one source of oscillations. The less intense 4% controlling action proved better transient performances. The two new Leafs showed better performances, with the overall response delay always in the range of 2–3 s, while for the older one, the delay was sometimes a bit higher and the current undershooting slightly larger. Moreover, accuracy of the current limitation feature need to be better exploited in order to compensate the undershooting.

The observed communication delay is limited; therefore deploying this kind of strategy via the Internet is not seen as an obstacle to this approach. The granularity of the control, with the 1 A discretization, does not help to obtain a smooth response, as each EV can change its output with a 10% step. Naturally, this response could become smoother in the moment that an aggregated set of EVs is considered (i.e., 10 or more). The controller is actually setting a pure current reference: future work will also investigate a voltage-compensation loop, in order to take into account considerable voltage deviations as well as compensating for larger than expected undershooting. As a final remark, it was interesting to appreciate standard EV chargers withstanding frequency events spanning from 47 up to 52 Hz without any interruption.

Acknowledgments

This work is supported by the Danish Research Project "NIKOLA–Intelligent Electric Vehicle Integration"-under ForskEL kontrakt nr. 2013-1-12088. More information: www.nikolaproject.info.

The authors are grateful to Nissan Denmark for providing 2 of the 3 Leafs used in the experiments.

References

[1] L. Martini, L. Radaelli, H. Brunner, C. Caerts, A. Morch, S. Hanninen, C. Tornelli, Electra IRP approach to voltage and frequency control for future power systems with high der penetration, 23rd International Conference on Electricity Distribution CIRED, Lyon, 15–18 June 2015, 2015, pp. 1–5.
[2] K. Visscher, M. Marinelli, A.Z. Morch, S.H. Jakobsen, Identification of observables for future grids—The framework developed in the ELECTRA project, PowerTech, 2015 IEEE Eindhoven, June 29 2015–July 2 2015, 2016, pp. 1–6.
[3] M. Rezkalla, K. Heussen, M. Marinelli, J. Hu, H.W. Bindner, Identification of requirements for distribution management systems in the smart grid context, Power Engineering Conference (UPEC), 50th International Universities, 1–4 Sept. 2015, 2015, pp. 1–6.
[4] A. Zegers, H. Brunner, TSO-DSO interaction: an overview of current interaction between transmission and distribution system operators and an assessment of their cooperation in Smart Grids, ISGAN (International Smart Grid Action Network) Discussion Paper Annex 6 Power T&D Systems, Task 5, September, 2014.
[5] R. Yan, T.K. Saha, N. Modi, N.-A. Masood, M. Mosadeghy, The combined effects of high penetration of wind and PV on power system frequency response, Appl. Energy 145 (2015) 320–330, doi:http://dx.doi.org/10.1016/j.apenergy.2015.02.044.
[6] J. Fleer, P. Stenzel, Impact analysis of different operation strategies for battery energy storage systems providing primary control reserve, J. Energy Storage (2016), doi:http://dx.doi.org/10.1016/j.est.2016.02.003.
[7] E. Kaempf, H. Abele, S. Stepanescu, M. Braun, Reactive power provision by distribution system operators—optimizing use of available flexibility, Innovative Smart Grid Technologies Conference Europe (ISGT-Europe), IEEE PES, 12–15 Oct. 2014, 2014, pp. 1–5.
[8] J. García-Villalobos, I. Zamora, J.I. San Martín, F.J. Asensio, V. Aperribay, Plug-in electric vehicles in electric distribution networks: a review of smart charging

approaches, Renew. Sustain. Energy Rev. 38 (2014) 717–731, doi:http://dx.doi.org/10.1016/j.rser.2014.07.040.
[9] J. Hu, S. You, M. Lind, J. Østergaard, Coordinated charging of electric vehicles for congestion prevention in the distribution grid, IEEE Trans. Smart Grid 5 (2014) 703–711, doi:http://dx.doi.org/10.1109/TSG.2013.2279007.
[10] F. Mwasilu, J.J. Justo, E.K. Kim, T.D. Do, J.W. Jung, Electric vehicles and smart grid interaction: a review on vehicle to grid and renewable energy sources integration, Renew. Sustain. Energy Rev. 34 (2014) 501–516, doi:http://dx.doi.org/10.1016/j.rser.2014.03.031.
[11] K. Knezović, M. Marinelli, P. Codani, Y. Perez, Distribution grid services and flexibility provision by electric vehicles: a review of options, Power Engineering Conference (UPEC), 50th International Universities, 1–4 Sept. 2015, 2015, pp. 1–6.
[12] C. Gouveia, C.L. Moreira, J.A.P. Lopes, D. Varajao, R.E. Araujo, Microgrid service restoration: the role of plugged-in electric vehicles, IEEE Industrial Electronics Magazine, vol. 7, no. 4, Dec., 2013, pp. 26–41, doi:http://dx.doi.org/10.1109/MIE.2013.2272337.
[13] W. Kempton, J. Tomić, Vehicle-to-grid power implementation: from stabilizing the grid to supporting large-scale renewable energy, J. Power Sources 144 (2005) 280–294, doi:http://dx.doi.org/10.1016/j.jpowsour.2004.12.022.
[14] S. Martinenas, M. Marinelli, P.B. Andersen, C. Træholt, Implementation and demonstration of grid frequency support by V2G enabled electric vehicle, Proc 49th Int Univ Power Eng Conf IEEE (2014) 1–6, doi:http://dx.doi.org/10.1109/UPEC.2014.6934760.
[15] S. Izadkhast, P. Garcia-Gonzalez, P. Frias, An aggregate model of plug-in electric vehicles for primary frequency control, IEEE Trans. Power Syst. 30 (2015) 1475–1482, doi:http://dx.doi.org/10.1109/TPWRS.2014.2337373.
[16] H. Liu, Z. Hu, Y. Song, J. Lin, Decentralized vehicle-to-grid control for primary frequency regulation considering charging demands, IEEE Trans. Power Syst. 28 (2013) 3480–3489, doi:http://dx.doi.org/10.1109/TPWRS.2013.2252029.
[17] P.M.R. Almeida, J.A.P. Lopes, F.J. Soares, L. Seca, Electric vehicles participating in frequency control: operating islanded systems with large penetration of renewable power sources, 2011 IEEE PES Trondheim PowerTech Power Technol a Sustain Soc POWERTECH 1 (2011) 5–10, doi:http://dx.doi.org/10.1109/PTC.2011.6019424.
[18] T. Masuta, A. Yokoyama, Supplementary load frequency control by use of a number of both electric vehicles and heat pump water heaters, IEEE Trans. Smart Grid 3 (2012) 1253–1262, doi:http://dx.doi.org/10.1109/TSG.2012.2194746.
[19] J. Meng, Y. Mu, H. Jia, J. Wu, X. Yu, B. Qu, Dynamic frequency response from electric vehicles considering travelling behavior in the Great Britain power system, Appl. Energy 162 (2016) 966–979, doi:http://dx.doi.org/10.1016/j.apenergy.2015.10.159.
[20] J. Druitt, W.-G. Früh, Simulation of demand management and grid balancing with electric vehicles, J. Power Sources 216 (2012) 104–116, doi:http://dx.doi.org/10.1016/j.jpowsour.2012.05.033.
[21] X. Luo, S. Xia, K.W. Chan, A decentralized charging control strategy for plug-in electric vehicles to mitigate wind farm intermittency and enhance frequency regulation, J. Power Sources 248 (2014) 604–614, doi:http://dx.doi.org/10.1016/j.jpowsour.2013.09.116.
[22] P.B. Andersen, M. Marinelli, O.J. Olesen, C.A. Andersen, G. Poilasne, B. Christensen, et al., The Nikola project intelligent electric vehicle integration, IEEE PES Innov Smart Grid Technol Eur (2014) 1–6, doi:http://dx.doi.org/10.1109/ISGTEurope.2014.7028765.
[23] ENTSO-E, Continental Europe Operation Handbook. Available: https://www.entsoe.eu/publications/system-operations-reports/operation-handbook/Pages/default.aspx.
[24] Energinet.dk, Ancillary services to be delivered in Denmark—Tender conditions. Available: https://energinet.dk/EN/Soeg/Sider/Publikationsvisning.aspx?Filter1Value=4812&Filter1Field=Id.
[25] M. Marinelli, F. Sossan, G.T. Costanzo, H.W. Bindner, Testing of a predictive control strategy for balancing renewable sources in a microgrid, Sustain. Energy IEEE Trans. 5 (2014) 1426–1433, doi:http://dx.doi.org/10.1109/TSTE.2013.2294194.
[26] P. Kundur, Power System Stability and Control, McGraw-Hill Education, 1994.
[27] L.L. Grigsby, Power System Stability and Control. The Electric Power Engineering Handbook, CRC Press/IEEE Press, 2001, 2016.
[28] V. Lakshmanan, M. Marinelli, J. Hu, H.W. Bindner, Provision of secondary frequency control via demand response activation on thermostatically controlled loads: solutions and experiences from Denmark, Appl. Energy 173 (2016) 470–480, doi:http://dx.doi.org/10.1016/j.apenergy.2016.04.054.

Pub. E. Evaluation of Electric Vehicle Charging Controllability for Provision of Time Critical Grid Services

Evaluation of Electric Vehicle Charging Controllability for Provision of Time Critical Grid Services

Sergejus Martinenas, Mattia Marinelli, Peter Bach Andersen, Chresten Træholt
Center for Electric Power and Energy, Department of Electrical Engineering, DTU – Technical University of Denmark
Contact Person: Sergejus Martinenas, smar@elektro.dtu.dk

***Abstract*—Replacement of conventional generation by more stochastic renewable generation sources leads to reduction of inertia and controllability in the power system. This introduces the need for more dynamic regulation services. These faster services could potentially be provided by the growing number of electric vehicles. EVs are a fast responding energy resource with high availability. This work evaluates and experimentally shows the limits of EV charging controllability using widely supported IEC 61851 standard. The focus is put on EVs suitability for providing ancillary grid services with time critical requirements. Three different series produced EVs are tested. The experimental testing is done by using charging current controllability of built-in AC charger to provide a primary frequency regulation service with very dynamic input frequency. The results show that the controllability of most EVs is more than suitable for providing time critical grid services. Meanwhile, charging current ramping rates of recently produced EVs are potentially suitable to even provide synthetic inertia.**

Keywords – Electric Vehicles, Charging Stations, Power Control, Smart Grid

I. Introduction

Year by year the share of renewable generation in the power system is increasing. This, mostly stochastic energy source and lack of directly coupled rotating machines, leads to reduced controllability and lower system inertia [1], [2]. Such change introduces the need for much faster regulation services. Current grid services are designed to be provided by conventional generation sources, thus timing requirements of these services are adhering to ramping rates of thermal power plants. Transition to more dynamic grid power flows will require faster regulation services [3].

Simultaneously, the share of a new fast responding, high availability energy resource - the electric vehicle (EV), is rapidly growing. While EVs are viewed as a solution to the environmental problems in transportation sector, they are treated as additional loads that will require grid upgrades in the energy sector. However, with intelligent integration of the EV charging infrastructure they become a potential grid balancing resource [4], [5], [6]. When aggregated in large numbers, vehicles could provide the services including current ancillary services defined by grid operators, as well as ones addressing future issues of the grid, such as defined in the NIKOLA project [7]. EVs could provide a large range of grid services from local voltage control to system-wide frequency regulation [8]. This work focuses on the most time critical services with tight response time limitations such as primary frequency regulation and synthetic inertia.

Technically, service provision is possible by controlling the charging current limit of the build-in EV charger as defined by IEC 61851 standard [9]. Meanwhile, additional parameters such as state of charge (SOC), plug-in and plug-out times could improve the quality of the provided service [10]. However, the response times and precision for EVs of different make or model are not identical even though it is defined by the standard. Depending on the EV model, the speed of EV response can vary from under a second to few seconds. Such difference in timing, although being small, means that only some vehicles could provide time critical services such as synthetic inertia or very fast frequency regulation. In this work three separate vehicles of different brand and model are tested for speed and precision of response.

This work is mainly focusing on AC charging as DC charging is typically used for short high-power charging sessions meant to extend the vehicles operational range, thus not suitable for grid service provision due to short session duration. It should be mentioned that vehicle to grid (V2G) technology could greatly improve the grid service provision [11], however at the time of writing it is still in development phase and therefore is not considered in this work.

The paper is structured as follows: Section II describes potential grid services that EVs could provide. Section III presents the method and experimental test setup used for assessing EV charging controllability. Section IV shows and analyses the results of the experimental validation. Section V summarizes the conclusions and further discusses the evaluation as well as potential alternative solutions.

II. Grid ancillary services

This work focuses on evaluating the potential of electric vehicles to provide different grid support services for the current and future smart grid. Therefore the grid service definitions are taken from the Danish Transmission System Operator (TSO) - Energinet.DK ancillary service provision requirements [12]

This work is supported by the Danish Research Project "NIKOLA - Intelligent Electric Vehicle Integration"- under ForskEL kontrakt nr. 2013-1-12088. More information (www.nikolaproject.info).

and NIKOLA project service catalog [7]. The examples of grid services considered are primary frequency regulation, very fast frequency regulation, synthetic inertia, etc. All of these services are time critical but have very different response time constrains.

The Danish power grid is uniquely split into two separate synchronous regions: DK1 and DK2. Jylland peninsula and island of Fyn are in DK1 region connected continental part of Europe. The islands of Sjælland and Bornholm are in DK2 region connected Nordic synchronous area.

The definitions of services relevant to primary frequency regulation ancillary service from Energinet.DK:

- **Primary Reserve** in DK1 region - restores balance between production and consumption, stabilizing the frequency at close to, but deviating from $50Hz$. The regulation is automatic and responding to frequency deviation, with a small permitted dead-band. The first half of the activated reserve must be supplied within 15 seconds, while the last half must be supplied in full within 30 seconds.
- **Normal Operation Reserve** in DK2 region - ensures that production and consumption equilibrium is restored. The regulation is automatic and responding to frequency deviation, without dead-band. The reserve must be supplied within 150 seconds.
- **Disturbance Reserve** in DK2 region - a fast reserve, activated in the event of major system disturbances. It is started automatically in the event of sudden frequency drop under $49.9Hz$ and remains active until frequency is restored or manual reserve takes over. The first 50% of the response must be supplied within 5 seconds, the remaining 50% of the response within an additional 25 seconds.

In addition to these services the time critical grid services defined in NIKOLA project [7]:

- **Fast Frequency Reserve** - the time requirements are very similar to the one specified for the disturbance reserve in DK2, which is already a rather demanding service, but in this case the full reserve is required to be deployed in 10 seconds.
- **Synthetic Inertia** - the reserve that mimics rotational inertia of the generations. it requires full deployment of the reserve within 1 or 2 seconds. The time is highly influenced by the actual system inertia. The lower is the equivalent inertia of the system, the higher is the time criticality of this service. Moreover, what makes this service even more challenging, is the fact that the equivalent system inertia could change during the day, depending on the amount of inverter driven resources (such as photovoltaic or Type C and D wind turbines) are connected in the system.

It should be noted that different services have varying response time requirements from milliseconds to tens of seconds. The setup chosen for testing the EV response time is following the guidelines of primary frequency regulation service with simple droop control and no dead-band.

III. Methodology

The response time of the service is dependent on the whole control loop. Therefore, in this work, a typical control architecture for providing grid services is recreated. It consists of EV, charging spot, smart charging controller, measurement device and grid connection. The experimental test setup is shown in Fig. 1.

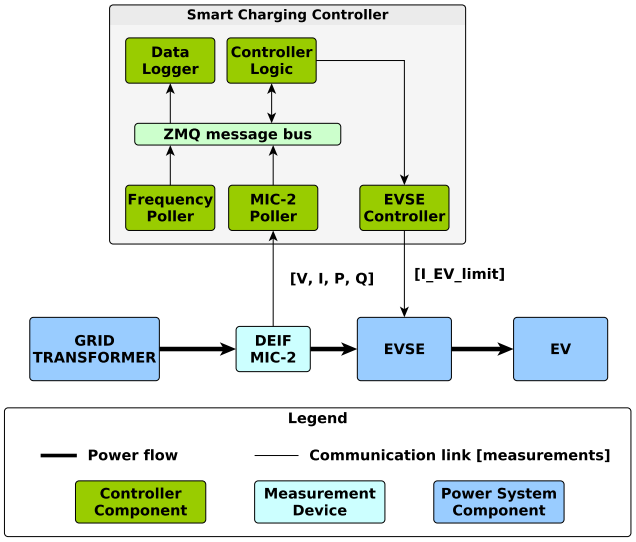

Fig. 1. Experimental test system setup

The details of the setup components are outlined here:

- **Smart charging controller** - receives the data from the measurement devices and sends control signals to the EVSE.
- **DEIF MIC-2** - multi-instrument measurement device for voltage, current and power measurements with 0.5% accuracy.
- **EVSE** - Electric Vehicle Supply Equipment, also known as the charging spot. The maximum charging current rating is $16A$.
- **EV** - one of the three different electric vehicles tested in this evaluation.
- **Grid** - grid connection at the SYSLAB experimental facility.

The smart charging controller consists of multiple subcomponents described here:

- **Controller logic** - reads the latest frequency measurements from the message bus, calculates the set-points and sends control signals directly to the EVSE controller.
- **EVSE controller** - acts as an abstraction interface between the physical EVSE and charging controller components.
- **Frequency poller** - interface to the frequency measurements. Commonly, DEIF MTR-3 measurement instru-

ment would be used for frequency sampling once a second with the accuracy of $\pm 10mHz$.

- **MIC-2 poller** - DEIF MIC-2 multi-instrument interface abstracting data collection from the measurement device. The poller polls the device every 0.2 seconds.
- **Data logger** - monitors the data on the message bus and logs the measurements and control parameters from each controller component into the database.
- **ZMQ message bus** - message bus developed for easier data exchange between controller components. ZeroMQ communication framework is used to establish a message bus, this is done to minimize the delay and ease the integration of additional controller components [13].

The control loop runs as follows: Firstly, the frequency measurement is read by the frequency poller and published to the message bus. Secondly, the controller logic reads the new frequency measurement and calculates the corresponding control signal. Thirdly, the control signal is sent to the EVSE controller that converts it to the analog signal read by the EV. Lastly, the EV adjusts its charging current according to the newly set limit.

The computer running smart charging controller and the measurement devices are connected to the same wired network. As the communication between these components has small latency of only a few milliseconds, this delay is disregarded in further analysis. However, in some field scenarios for remote charging location the communication to the charging point could be wireless, which would significantly increase the control latency. This could disqualify such charging locations from providing the most time critical grid services.

Typically, the slowest part of the whole communication-control loop is the EV power response time [14]. In most modern EVs, communication between a vehicle and a charging point is defined by IEC 61851 standard. The standard states that in case a charging current limit is changed, the vehicle should respond within 3 seconds. Additionally, the standard specifies the lowest current limit is $6A$ with a step of $1A$, while upper current limit is defined by a minimum function of the charging cable and the fuse rating of the EVSE. The charging power adjustment response time and precision of multiple commercially available EVs are compared. The EVs used in the test are EV I - Peugeot Ion (2011 model), EV II - Nissan Leaf (2015 model), and EV III - Renault Kangoo (2012 model). All of these EVs are equipped with 3.7 kW AC chargers which can be controlled between 6 to $16A$ - providing a $2.3kW$ flexibility window. This window is split in half, by setting nominal EV charging rate to $11A$ at the frequency of $50.00Hz$. This way EVs can provide symmetrical up and down regulation as detailed in [6]. As the grid frequency from real grid is rather stable, a symmetrical, randomized input frequency was designed that would force the controller to change the set-point at each iteration. This way the controllability of each EV is pushed to the limit and the ramping rates can be assessed. The input frequency used in this experimental testing is shown in Fig. 2.

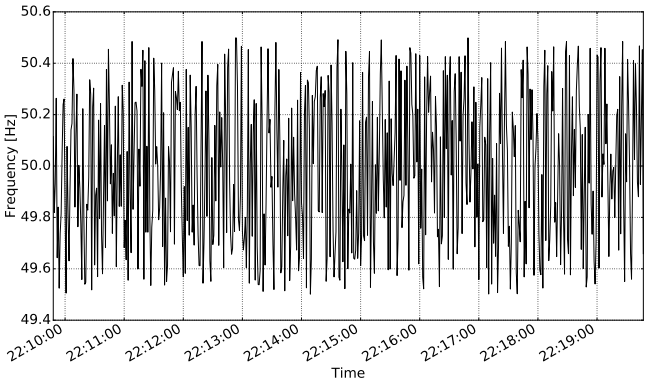

Fig. 2. Input frequency for controller logic

IV. Results

Here the response of the full control loop, with focus on EV power adjustment time and precision are evaluated and compared. Technically, response time is the major factor for grid service provision as response precision always improves with aggregation of multiple vehicles. Typical inaccuracy of the response is less than the step of $1A$, which only corresponds to approximately $200W$ in power. Such error is below the accuracy limit of typical multi-hundred kilowatt response power for an ancillary service and can be easily corrected by adjusting the charging current for the part of the aggregated EVs.

The control signal and response of the vehicle to the changes in the charging current limits are shown in Fig. 3, Fig. 4 and Fig. 5. The graphs are showing only the first 2 minutes of the experimental data to better appreciate the difference between the control and response.

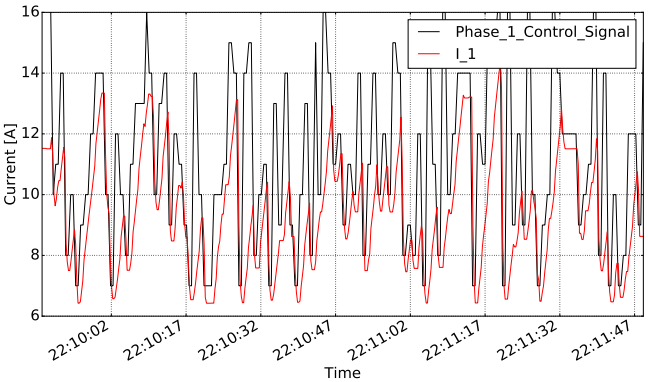

Fig. 3. Response precision and timing of EV I

As can be seen in Fig. 3, ramping speeds of the EV I on phase 1 are different for up and down modulation. While increasing the charging current to the new higher limit might take up to 2 seconds, decreasing the charging current to the lowered limit only takes up to 1 second.

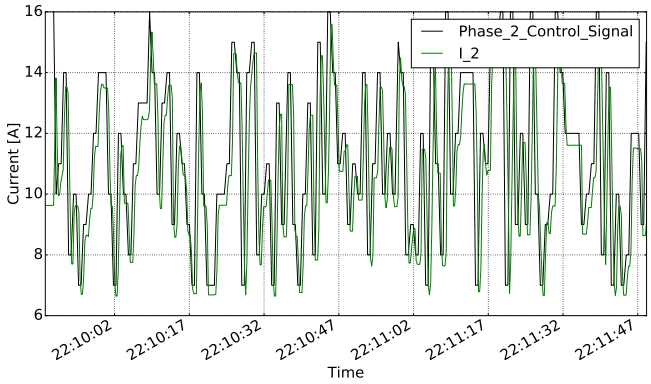

Fig. 4. Response precision and timing of EV II

As shown in Fig. 4, the EV II on phase 2 has much faster ramping rates. Both up and down modulation of charging current is performed in less than around 0.5 seconds.

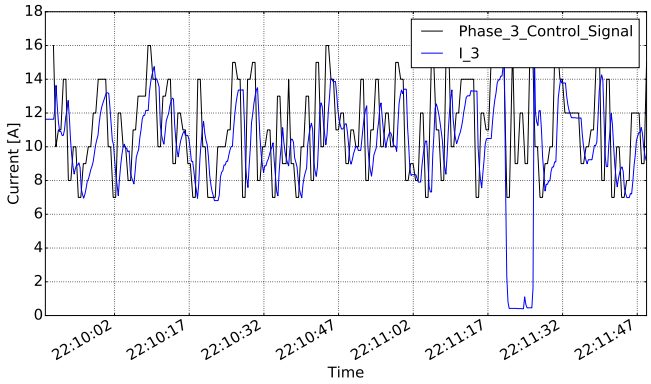

Fig. 5. Response precision and timing of EV III

Response plot in Fig. 5, shows that the EV III on phase 3 has a bit slower ramping rates for up and down modulation. It takes up to 1 second to lower the charging current and up to 2 - 3 seconds to increase the charging current to the higher limit. Additionally, the EV also shows occasional current drop to under $1A$ for a about 5 seconds, which could affect the quality of the provided service. This drop could be caused by the battery management system balancing the battery cell voltages or for passive battery cooling.

To better compare the responses of three EVs, zoomed in plot of the first minute of the experiment with control signal and response of all three vehicles is shown in Fig. 6.

Such difference in timing and response precision can be explained by advancement in power electronics of the EV chargers as EVs I and III are 5 years old and EV II is a recently produced 2015 model.

The timing performance and response precision of the three EVs is summarized in Table I.

While all EVs are well within the timing limits of the IEC 61851 standard for charging current regulation, EV I and

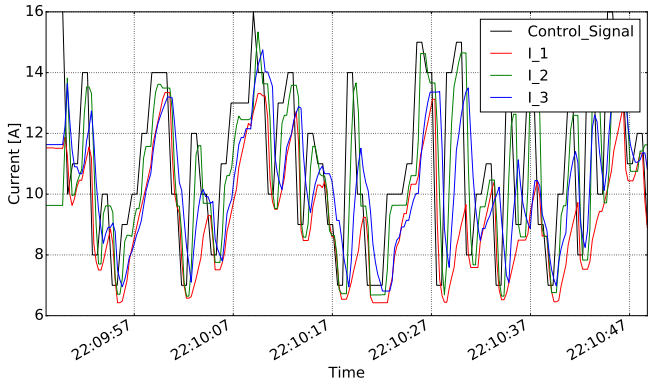

Fig. 6. Control and response comparison of all three EVs

TABLE I
SUMMARY OF EV RESPONSE TIMING AND PRECISION

EV nr.	Minimum delay	Average delay	Maximum delay	Average Response Error
I	0.4 s	1.1 s	2.0 s	0.8 A
II	0.2 s	0.3 s	0.6 s	0.4 A
III	0.5 s	1.5 s	2.5 s	1.0 A

III have similar response times closer to a few seconds, where EV II stands out by having sub-second response time.

To appreciate the response of the speed and precision of the vehicle response, correlations between control and actual charging currents were calculated for the whole experimental period, the results are shown in Table II.

TABLE II
CORRELATION BETWEEN CONTROL SIGNAL AND MEASURED RESPONSE

EV nr.	I	II	III
Correlation	0.56	0.73	0.23

The correlation values of all three EVs are quite different, that is due to multiple factors. Firstly, correlation factor of EV II is the highest due to its fast and precise response. Secondly, the correlation of the EV III is quite low due to frequent drop outs and slower response time. Lastly, EV I has average response time and lower precision, therefore it's correlation value is between EV II and EV III.

EV suitability for providing grid services is summarized in Table III.

As shown in this section, the EV response time to a control signal is quite fast compared to conventional generation. All EVs are suitable for performing even very fast frequency regulation. However only recently produced EVs with sub-second response times have potential to provide the synthetic inertia service. That is partly due to good adherence to IEC 61851 charging standard. The standard specifies the response time

TABLE III
SUMMARY OF EV ABILITY TO PROVIDE FAST GRID SERVICES

EV nr.	Primary Reserve ($< 15s$)	Normal Operation Reserve ($< 150s$)	Disturbance Reserve ($< 5s$)	Fast Frequency Reserve ($< 10s$)	Synthetic Inertia ($< 1s$)
I	+	+	+	+	-
II	+	+	+	+	+
III	+	+	+	+	-

to be below 3 seconds, however as shown, recently produced EVs can throttle the charging current in less than a second.

All tests were performed in SYSLAB - a DTU research facility for intelligent, active and distributed power systems. SYSLAB is located at DTU Risø campus and is a part of the PowerLabDK experimental facilities.

V. CONCLUSION

This evaluation provides a real analysis of currently available EVs readiness to provide grid services now and in the near future.

While the response times of the EVs are quite suitable even for fast grid services, they also have a few problems that might influence the quality of the delivered service. One such problem is inability of some EVs to resume the charging process after charging process was interrupted by disabling and re-enabling the charging spot. Some vehicles even require physical re-plugging of the charging cable or door opening to continue charging, which interferes with user comfort. Additionally, the speed of re-enabling the charging process is rather slow and takes multiple seconds. Another potential quality influencing problem is fluctuating undershoot of the EV charging current response to the limit set from the charging spot, typically the undershooting is up to 1 A.

While proportional control of EV charging according to control input as exemplified in this paper seems to be suitable for providing grid services it does not account for the efficiency of the EV charger [15]. This can be improved by charging the bulk of the aggregated EVs at maximum power and using only a few in proportional control to get a precise aggregated response. Another possible obstacle for grid service provision is the $6A$ minimum charging rate as defined in IEC 61851. If $6A$ charging rate is too high for some application, the charging could also be disabled and then re-enabled when needed. Finally, state of charge (SOC) of the EV should be considered while providing grid services for multiple reasons. Firstly, the charging controller should always allow appropriate time for the EV to charge to the level defined by the EV user, before departure time. Secondly, at high values of SOC, typically above 90 % EV batteries start balancing individual cell voltages, which leads to drop in the charging current, losing the controllability.

While this work only considered AC charging control, developments are being made to provide grid services using external V2G chargers utilizing the CHAdeMO fast charging protocol, that was extended to support bidirectional power flow. In that case the power response depends on the ramping rate of the V2G charger as the EV is only utilized as a battery. Actual barriers for commercial grid service provision, using AC charging or V2G technology, are incomplete communication protocols that lack information objects or response speed for this task [10]. An EV communication standard IEC 15118 that extends IEC 61851 by adding high level communication and necessary information objects could enable the EVs to provide grid services. However, current revisions of the standard specify the response times in tens of seconds, that are too slow for providing time critical grid services.

All in all, most EVs are technically capable of providing even most time critical grid services, while commercial applications still need harmonization in communication and regulatory areas.

REFERENCES

[1] P. Tielens and D. Van Hertem, "Grid inertia and frequency control in power systems with high penetration of renewables," *Young Researchers Symposium in Electrical Power Engineering*, pp. 1–6, 2012.

[2] A. Ulbig, T. S. Borsche, and G. Andersson, "Impact of low rotational inertia on power system stability and operation," *IFAC Proceedings Volumes (ifac-papersonline), Ifac Proceedings Volumes, Ifac Proc. Vol. (ifac-papersonline)*, vol. 19, pp. 7290–7297, 2014.

[3] G. Delille, B. Francois, and G. Malarange, "Dynamic Frequency Control Support by Energy Storage to Reduce the Impact of Wind and Solar Generation on Isolated Power System's Inertia," *IEEE Transactions on Sustainable Energy*, vol. 3, no. 4, pp. 931–939, Oct 2012.

[4] K. Clement-Nyns, E. Haesen, and J. Driesen, "The Impact of Charging Plug-In Hybrid Electric Vehicles on a Residential Distribution Grid," *Power Systems, IEEE Transactions on*, vol. 25, no. 1, pp. 371–380, Feb 2010.

[5] W. Kempton and J. Tomić, "Vehicle-to-grid power implementation: From stabilizing the grid to supporting large-scale renewable energy," *Journal of Power Sources*, vol. 144, no. 1, pp. 280 – 294, 2005.

[6] M. Marinelli, S. Martinenas, K. Knezović, and P. B. Andersen, "Validating a centralized approach to primary frequency control with series-produced electric vehicles," *Journal of Energy Storage*, vol. 7, pp. 63 – 73, 2016.

[7] P. Andersen, M. Marinelli, O. Olesen, C. Andersen, G. Poilasne, B. Christensen, and O. Alm, "The nikola project intelligent electric vehicle integration," *Proceedings of ISGT 2014*, 2014.

[8] K. Knezovic, M. Marinelli, P. Andersen, and C. Træholt, "Concurrent provision of frequency regulation and overvoltage support by electric vehicles in a real danish low voltage network," *Proceedings of IEEE International Electric Vehicle Conference 2014*, 2014.

[9] IEC TC69, "IS 61851-1:2010 Ed. 2.0," *IEC Standard*, 2010.

[10] S. Martinenas, S. Vandael, P. Andersen, and B. Christensen, "Standards for EV charging and their usability for providing V2G services in the primary reserve market," *Proceedings of International Battery, Hybrid and Fuel Cell Electric Vehicle Symposium 2016*, 2016.

[11] H. Lund and W. Kempton, "Integration of renewable energy into the transport and electricity sectors through V2G," *Energy Policy*, vol. 36, no. 9, pp. 3578 – 3587, 2008.

[12] "Ancillary services to be delivered in Denmark Tender conditions," Tech. Rep. October, 2012.

[13] P. Hintjens, *ZeroMQ: Messaging for Many Applications*. O'Reilly Media, 2013.

[14] S. Martinenas, M. Marinelli, P. Andersen, and C. Træholt, "Implementation and Demonstration of Grid Frequency Support by V2G Enabled Electric Vehicle," *Proceedings of the 49th International Universities Power Engineering Conference (UPEC), 2014*, pp. 1–6, 2014.

[15] A. Kieldsen, A. Thingvad, S. Martinenas, and T. Sørensen, "Efficiency Test Method for Electric Vehicle Chargers," *Proceedings of EVS29 - International Battery, Hybrid and Fuel Cell Electric Vehicle Symposium*, 2016.

Pub. F. Comparison between Synthetic Inertia and Fast Frequency Containment Control Based on Single Phase EVs in a Microgrid

Applied Energy xxx (2017) xxx–xxx

Contents lists available at ScienceDirect

Applied Energy

journal homepage: www.elsevier.com/locate/apenergy

Comparison between synthetic inertia and fast frequency containment control based on single phase EVs in a microgrid

Michel Rezkalla, Antonio Zecchino, Sergejus Martinenas, Alexander M. Prostejovsky, Mattia Marinelli *

Center for Electric Power and Energy, Department of Electrical Engineering, Technical University of Denmark, Denmark

HIGHLIGHTS

- Enhancing frequency control via small scale distributed energy resources.
- Analytical interdependency between fast frequency containment and synthetic inertia.
- System balancing by mean of unidirectional electric vehicles as flexibility resources.
- Experimental validation of theoretical findings with series produced EVs.

ARTICLE INFO

Article history:
Received 1 April 2017
Received in revised form 1 June 2017
Accepted 15 June 2017
Available online xxxx

Keywords:
Electric vehicles
Experimental validation
Frequency containment control
Frequency stability
Synthetic inertia

ABSTRACT

The increasing share of distributed and inertia-less resources entails an upsurge in balancing and system stabilisation services. In particular, the displacement of conventional generation reduces the available rotational inertia in the power system, leading to high interest in synthetic inertia solutions. The objective of this paper is twofold: first, it aims to implement and validate fast frequency control and synthetic (virtual) inertia control, employing single phase electric vehicles as flexibility resources. Second, it proposes a trade-off analysis between the two controllers. The interdependency between frequency containment and synthetic inertia control on the transient frequency variation is shown analytically. The capabilities and limits of series produced EVs in providing such services are investigated, first on a simulation based approach and subsequently by using real hardware. The results show that fast frequency control can improve the transient frequency behaviour. However, both on the simulation and on the experimental level, the implementation of synthetic inertia control is more challenging. In fact, due its derivative nature and the system dynamics, its performance is limited. Furthermore, the crucial importance of the EVs' response time for both controllers is highlighted.

1. Introduction

The rising share of inverter-coupled distributed energy resources (DER) raises new challenges in maintaining stable grid operation. One of the main issues is the reduction of the system inertia due to the replacement of rotating generators by converter-connected resources, as well as the expansion of high-voltage direct current (HVDC) connections, which decouples the inertial response between the interconnected areas [1]. Thus, the system's ability to withstand frequency changes by releasing or absorbing the energy stored in the rotating masses is notably reduced, leading to faster frequency dynamics [2]. Moreover, the high volatility of renewable energy sources (RES) contributes to the frequency stability issue by changing the grid inertia over time and increasing the need for better planning due to higher uncertainty.

Inertia is the parameter that represents the capability of rotating machines (including loads, when applicable) to store and inject their kinetic energy into the system [3]. The amount of inertia influences the frequency gradient, which is generally addressed as the rate of change of frequency (RoCoF) and the transient frequency values during a system incident. The RoCoF and the transient frequency values have a fundamental role in maintaining and operating the power system in a secure state. A large RoCoF and/or transient frequency deviations can lead to the automatic tripping of conventional generators and DER units [4] because they are connected to the grid by means of RoCoF or frequency relays [3]. The RoCoF relay limit is established by the grid code, which varies among countries.

Several transmission system operators (TSOs) have started to address this challenge, recognising the potential value of the

* Corresponding author.
E-mail address: matm@elektro.dtu.dk (M. Marinelli).

http://dx.doi.org/10.1016/j.apenergy.2017.06.051
0306-2619/

Nomenclature

$\bar{T}_D$	frequency dependent loads	J	moment of inertia
$\bar{T}_{FCC}$	electric torque of devices participating in FCC	K_D	load damping factor
$\bar{T}_{SIC}$	electric torque of devices participating in SIC	K_{FCC}	FCC proportional control coefficient
δ	electrical rotor angle	K_{SIC}	SIC proportional control coefficient
δ_0	rotor angle at $t = 0$	P	EV absorbed active power
ω_e	angular velocity of the electrical rotor	p	number of pole pairs
ω_m	angular velocity	S_b	generator's rated power
ω_{0m}	rated angular velocity	t	time
f	frequency	T_a	acceleration or deceleration torque
H	kinetic energy in Watt-per-seconds at rated speed	T_e	electrical torque
I	EV absorbed current	T_m	mechanical torque

inertial response of wind power plants, synchronous condensers, and synthetic inertia [5,6]. One of the main concerns of TSOs is the RoCoF, which might lead to a cascade tripping of conventional and DER units connected by means of RoCoF relays [4,7]. According to [8], an RoCoF relay has a typical delay in the range of 50 ms to 500 ms.

Further, the growing number of electric vehicles (EVs) has concerned distribution system operators (DSOs). The uncertainty of EV driving patterns, high penetration levels and charging in the distribution network could result in new system peaks and negative distribution system impacts, exceeding the load capacities of distribution lines and transformers [9,10].

The effects of EVs on future power systems are investigated in several studies, such as in [11,12]. In [11], the negative effects of uncoordinated charging of EVs on the power system was addressed. The authors presented the impacts that EV charging can have in an actual working wholesale electricity market. In [12] it was analysed how a large scale implementation of plug-in hybrid electric vehicles and full electric vehicles would influence the power system. This study shows that smart management of EVs bidirectional charging can alleviate peak power demand.

On the other hand, unscheduled high penetration of EVs may have detrimental effects on power system performance. Reliability and stability are the aspects of the grid that face the most challenges when EVs are used widely. Consequently, there is an exigent need to predict the EVs' customers in order to avoid irreparable effects, especially for the distribution network. Several studies have investigated these challenges, such as in [13,14]. In [13] the authors propose a simultaneous approach for allocation of EV parking lots and DRRs in a power distribution network to achieve a more reliable supply of the load demand. A probabilistic modelling of EVs' charging demand is presented in [14].

A noticeable amount of research has focused on the transition from the traditional system, where frequency is controlled by a small set of large generating units, to the future where it is controlled by a vast amount of small distributed resources [15,16].

Given that EVs are essentially battery storages with a seconds-range response time, the TSO can greatly benefit from EV participation in frequency service provision. As analysed in [17], EV participation in the ancillary service market appears to be one of the most promising applications because it can offer substantial earnings to EV aggregators and EV owners. Ref. [18] concluded that although V2G capable EVs can provide great benefits to the ancillary service market, battery degradation may represent a challenge for their viability [19,20].

EVs are able to provide fast regulating power bidirectionally using Vehicle-to-Grid or just by modulating the charging power unidirectionally [21,22]. In this context, EVs can play a fundamental role in the future ancillary service market. Although the potential benefits of exploiting the V2G capability for ancillary services was introduced in [23], this study did not investigate unidirection EVs charging in providing such services.

Due to the reduced system inertia, various studies have shown the techno-economic benefits and challenges of primary frequency provision from EVs, such as in [24–26]. In [24] the authors present the impact of declining system inertia on the primary frequency control (PFC) and future requirements. It also presents the impact of PFC provision from EVs on the system frequency performance. In [25] the authors present the general ability of EV fleets to utilize fluctuating renewable energy sources for charging and their effects on the power system. The authors in [26] summarise the challenges to control a system with low inertia. In this study, unlike in [11,12,23], EVs have been controlled by only modulating the charging current between 6 and 16 A with steps of 1 A to comply with the technical constraints imposed by the IEC 61851 standard [27,28].

Simultaneously, very few studies have investigated the EV's ability in providing synthetic inertia services. In [29] the authors presented a single-phase virtual synchronous machine (VSM) and its possible application for providing V2G services from an EV's batteries, this work was supported by an experimental setup that is based on the Opal-RT platform. In contrast, this paper presents a different approach in providing synthetic inertia services supported by an experimental investigation using series produced EVs.

The scope of this study is twofold: First, the EV's capabilities as flexibility resources are investigated. In particular, this study looks at synthetic inertia control (SIC) and frequency containment control (FCC) as exemplary services. Second, it analyses and evaluates the pros and cons of SIC and FCC on the frequency dynamics (e.g. RoCoF and frequency nadir and zenith). The general objective is to determine if SIC and FCC delivered by converter connected resources, which are relatively fast compared to conventional units, can replace or at least reduce the need for a conventional inertial response.

Ultimately, the research question that this study addresses is: *given the trend of decreasing system inertia, can fast frequency containment compensate or replace the need for synthetic inertia?*

The method and the results presented in this study are part of the EU-funded project ELECTRA IRP, which proposes novel frequency and voltage control concepts to maintain and operate the power system in a secure state [30]. It considers the grid inertia (i.e. the synchronous and synthetic inertia) to be an active part of the frequency control process and it is addressed by inertia response power control (IRPC). In this study, the synthetic inertia is considered to be an active part of the IRPC process.

Please cite this article in press as: Rezkalla M et al. Comparison between synthetic inertia and fast frequency containment control based on single phase EVs in a microgrid. Appl Energy (2017), http://dx.doi.org/10.1016/j.apenergy.2017.06.051

This paper is divided into the following five sections: Section 2 presents the frequency control in Europe and the analytical interdependency between frequency containment and synthetic inertia. Section 3 presents the frequency containment and the synthetic inertia controllers, the EV dynamic model and the experimental layout. The simulations and experimental results are shown and discussed in Section 4. Lastly, Section 5 presents the conclusions and it outlines future research points.

2. Frequency control in Europe and analytical formulation

This section presents a summary of the current framework for frequency control in Europe and it gives an overview of synthetic inertia and frequency assessment.

2.1. Framework for frequency control in Europe

Based on the network code that was defined by the European Network of Transmission System Operators for Electricity (ENTSO-E), frequency control is divided into the following three phases: (i) Primary frequency control, (ii) Secondary power-frequency control, and (iii) Tertiary control. ENTSO-E refers to the reserves for frequency control as operating reserves, and it specifically indicates the previously mentioned controls, respectively, as: (i) Frequency Containment Reserves (FCR), (ii) Frequency Restoration Reserves (FRR), and (iii) Replacement Reserves (RR).

The frequency containment stabilises the frequency, after a disturbance, at a steady-state value within the permissible maximum steady-state frequency deviation. This is done by a joint action of FCR within the synchronous area [31]. The frequency restoration process controls the frequency towards its set-point value by activation of FRR and it replaces the activated FCR. The reserve replacement process replaces the activated FRR and/or supports the FRR activation by activation of RR. One can notice that the inertial response is considered to be a natural characteristic of the power system.

2.2. Analytical interdependency between frequency containment and synthetic inertia

According to IEEE/CIGRE task force, frequency stability is the ability of the power system to maintain steady state frequency following a severe system upset, resulting in a significant imbalance between generation and load [32]. Frequency stability depends on the system's ability to restore the equilibrium between generation and load demand.

During any disturbance that causes an imbalance between the torques acting on the rotor (i.e. active power imbalance between generation and consumption), the net torque causing acceleration or deceleration is $T_a = T_m - T_e$, where T_m is the mechanical torque applied on the rotor, T_e is the electrical torque on the rotor. The simplest model of electro-mechanical swings in a power system is based on the so called swing equation:

$$T_a = T_m - T_e = J\frac{d\omega_m}{dt} \tag{1}$$

where J is the combined moment of inertia of the generator and the turbine (kg m^2), and ω_m is the angular velocity of the rotor (rad/s).

Following an imbalance between the torques (i.e. imbalance between generation and demand), the kinetic energy stored in the rotating masses of the generator and the prime mover is released. The kinetic energy at rated speed is expressed as $E_{kin} = \frac{1}{2}J\omega_{0m}^2$, where ω_{0m} is the rated angular velocity [33]. By normalising the previous equation in terms of the rated power of the generator S_b, the inertia constant H can be defined as the kinetic energy in Watt-per-seconds at rated speed:

$$H = \frac{J\omega_{0m}^2}{2S_b} \quad \Rightarrow \quad J = \frac{2HS_b}{\omega_{0m}^2} \tag{2}$$

Eq. (1) can be reformulated as:

$$\frac{T_m - T_e}{S_b/\omega_{0m}} = 2H\frac{d}{dt}\left(\frac{\omega_m}{\omega_{0m}}\right) \tag{3}$$

Since S_B/ω_{0m} is the base torque T_{base}, the (3) can be expressed in p.u. as:

$$\bar{T}_m - \bar{T}_e = 2H\frac{d\bar{\omega}_r}{dt} \tag{4}$$

$$\bar{\omega}_r = \frac{\omega_m}{\omega_{0m}} = \frac{\omega_e/p}{\omega_0/p} = \frac{\omega_e}{\omega_0} = \bar{\omega}_e \tag{5}$$

where ω_e is the angular velocity of the electrical rotor, ω_0 is the rated one and p is the number of pole pairs.

The previous equations can be reformulated in terms of the electrical rotor angle. Assuming δ as the electrical rotor angle with respect to a synchronously rotating reference and δ_0 is the rotor angle at $t = 0$, δ can be formulated as:

$$\delta = \omega_e t - \omega_0 t + \delta_0 \tag{6}$$

Therefore, the first and second derivatives of (6) are:

$$\frac{d\delta}{dt} = \omega_e - \omega_0 = \Delta\omega_e \tag{7}$$

$$\frac{d^2\delta}{dt^2} = \frac{d\omega_e}{dt} = \omega_0\frac{d\bar{\omega}_r}{dt} \tag{8}$$

Eq. (1) can be reformulated in terms of the rotor angle:

$$\bar{T}_m - \bar{T}_e = \frac{2H}{\omega_0}\frac{d^2\delta}{dt^2} \tag{9}$$

Reformulating (9) in terms of $\bar{\omega}_e$:

$$\bar{T}_m - \bar{T}_e = 2H\frac{d\bar{\omega}_e}{dt} \tag{10}$$

Assuming that $\bar{T}_m$ is constant and that the frequency regulation is only from the load side, then one can assume that $\bar{T}_e$ is composed by: the frequency dependent loads ($\bar{T}_D$), devices participating in FCC ($\bar{T}_{FCC}$) and devices participating in SIC ($\bar{T}_{SIC}$):

$$\bar{T}_e = \bar{T}_D + \bar{T}_{FCC} + \bar{T}_{SIC} \tag{11}$$

where each is composed by a base value and frequency dependent value:

$$\bar{T}_D = \bar{T}_{D_0} + K_D\Delta\bar{\omega}_e \tag{12}$$

$$\bar{T}_{FCC} = \bar{T}_{FCC_0} + K_{FCC}\Delta\bar{\omega}_e \tag{13}$$

$$\bar{T}_{SIC} = \bar{T}_{SIC_0} + K_{SIC}\frac{d\bar{\omega}_e}{dt} \tag{14}$$

$\bar{T}_{D_0}, \bar{T}_{FCC_0}$ and $\bar{T}_{SIC_0}$ represent the base electric torques in steady state and is addressed further as $\bar{T}_{e_0} = \bar{T}_{D_0} + \bar{T}_{FCC_0} + \bar{T}_{SIC_0}$. K_D is a damping factor in pu, which considers the electrical loads which change the active power consumption due to frequency changes. $K_{FCC} = K_{FCC}(t - t0)$ is the FCC proportional control coefficient. $K_{SIC} = K_{SIC}(t - t0)$ is the SIC proportional control coefficient. K_{FCC} and K_{SIC} are represented in function of the time to represent the time required from those devices to get activated (i.e. time delay). Therefore, the swing equation can be formulated as:

$$\bar{T}_m - \bar{T}_{e_0} = (2H + K_{SIC})\frac{d\bar{\omega}_e}{dt} + (K_D + K_{FCC})\Delta\bar{\omega}_e \tag{15}$$

Please cite this article in press as: Rezkalla M et al. Comparison between synthetic inertia and fast frequency containment control based on single phase EVs in a microgrid. Appl Energy (2017), http://dx.doi.org/10.1016/j.apenergy.2017.06.051

Eq. (15) can be expressed as a function of $\frac{d\bar{\omega}_e}{dt}$ and $\Delta\bar{\omega}_e$:

$$\frac{d\bar{\omega}_e}{dt} = \frac{\bar{T}_m - \bar{T}_{e_0} - (K_D + K_{FCC})\Delta\bar{\omega}_e}{2H + K_{SIC}} \quad (16)$$

$$\Delta\bar{\omega}_e = \frac{\bar{T}_m - \bar{T}_{e_0} - (2H + K_{SIC})\frac{d\bar{\omega}_e}{dt}}{K_D + K_{FCC}} \quad (17)$$

From (16), one can notice that FCC and SIC can affect the RoCoF variation during a transient. Meanwhile, (17) shows that the frequency deviation from steady state can be affected by introducing SIC and FCC. In this regard, the following investigation aims to assess the effects of the two controllers on frequency and RoCoF, by means of simulations and experimental validation.

3. Methodology

In this section, the mathematical formulation and characteristic of the implemented controllers as well as the experimental layout is presented.

3.1. Frequency containment control

Frequency containment control (FCC) is achieved by a joint action of FCC providing units within the whole synchronous area with respect to the frequency deviation. Generally, it is achieved using droop controllers, so that governors operating in parallel can share the load variation according to their rated power. The droop of the generator represents the ratio of frequency deviation to change in power output. The frequency variation, Δf, referred to the nominal frequency of the system and is given as a function of the relative power change ΔP or current change ΔI reported to the nominal machine power or current, respectively.

$$\text{(a)}\ \frac{1}{K_{FCC}} = \frac{\Delta f/f_{nom}}{\Delta P/P_{nom}}; \quad \text{(b)}\ \frac{1}{K_{FCC}} = \frac{\Delta f/f_{nom}}{\Delta I/I_{nom}} \quad (18)$$

For example, a 5% droop ($\frac{1}{K_{FCC}}$) means that a 5% frequency deviation causes 100% change in valve position or power output.

In this study, EVs are used to provide frequency support in terms of FCC by modulating the EV's charging current. Defining a droop value for loads may not be straightforward because the nominal power may not always be determined unequivocally. To comply with the IEC 61851 standard, the EV's charging current can be modulated with a granularity of 1 A, and in this case between 6 and 16 A. This available range of regulating current of 10 A has been assumed as the EV's I_{nom} [34]. EV charging is controlled by charging controller with a 8% frequency-current droop with frequency limits of 48–52 Hz.

The droop is presented in Fig. 1a, where the dash line represents the ideal droop and the solid line represents the real droop with 1 A granularity. To have an up and down regulation capability of ±5 A, the EV's initial current set-point is set at 11 A. Due to the 1 A granularity and the established operating point, the EV's current set-point oscillated between 11 and 12 A. To avoid this oscillation, the droop characteristic was shifted; so that the frequency limits became 48.2–52.2 Hz. The control diagram for the FCC is presented in Fig. 2a. Following various experiments, it was noticed that the EV's current was under-shooting [22]. To compensate for this phenomena, it has been used the ceil function for the different controllers instead of the rounding.

3.2. Synthetic inertia control

Although no direct coupling from converter connected generators to the grid is made, a large amount of kinetic energy is stored in these units (e.g. kinetic energy stored in a wind turbine's blades and gearbox). Together with different forms of energy storage in other units, this can be used to deliver synthetic inertia. This means that these units could mimic synchronous generators by delivering an active power response that is proportional to the RoCoF [35,36].

A synthetic inertia controller (SIC) is implemented in this study, the control diagram is presented in Fig. 2b. The RoCoF is measured over 200 ms. This unit controls the EV's charging current as a function of a RoCoF-current droop characteristic. The droop is shown in Fig. 1b, the dashed line represents the ideal droop and the solid line represents the 1 A granularity. The droop is implemented by defining the RoCoF's low and high limits, with zero RoCoF corresponding to 11 A. The deadband of ±0.8 Hz/s was introduced during the tuning phase where smaller deadband values have led to frequency oscillation. Therefore, it results in a very limited contribution from the EVs.

3.3. EV dynamic model

To successfully integrate EVs into power systems, it is necessary to correctly understand and characterise their dynamic behaviour. A detailed model is, therefore, derived considering the EV users' driving requirements, the battery charging and discharging characteristics, the battery dynamics (e.g. time response, ramping time, etc.) and the control/communication delays.

Since this study aims to investigate the EV's capabilities and limits in providing fast primary control and synthetic inertia control, the battery charge state was neglected. The EV model is presented in Fig. 3. From the dynamic point of view, it is possible to identify two main latencies between the set and the actual current:

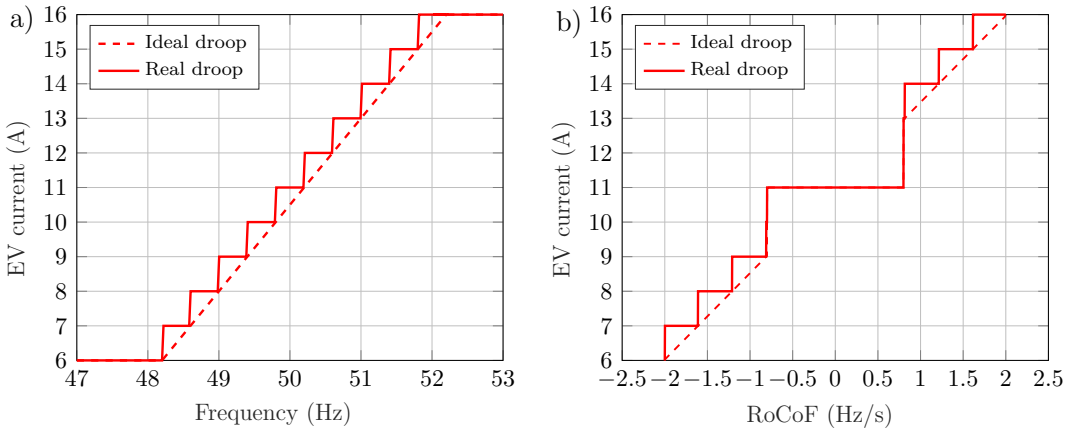

Fig. 1. (a) FCC droop characteristic, (b) SIC droop characteristic.

Please cite this article in press as: Rezkalla M et al. Comparison between synthetic inertia and fast frequency containment control based on single phase EVs in a microgrid. Appl Energy (2017), http://dx.doi.org/10.1016/j.apenergy.2017.06.051

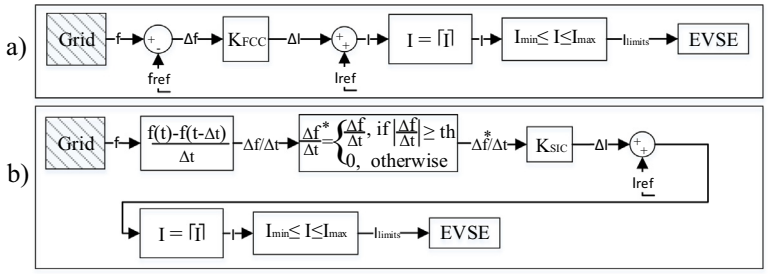

Fig. 2. (a) FCC control diagram, (b) SIC control diagram.

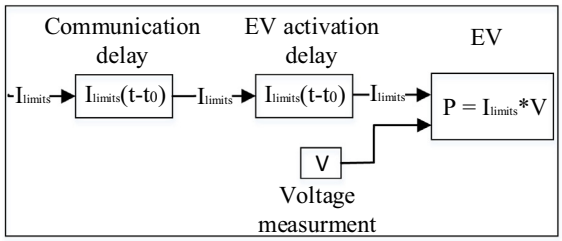

Fig. 3. EV dynamic model.

specifically, a communication delay and the EV activation delay, the sum of which varies between 150 ms and 2 s. The communication delay depends mainly on latencies in the IT infrastructure, which is in the range of tens of milliseconds. The EV activation delay varies among brands and heavily depends on the embedded power electronics. The most recent models show a faster response time. In any case, the current standard IEC61851 solely requires the car to respond within 3 s. The total delay observed in the experimental trials ranges between 200 and 400 ms. Therefore, in the simulation study the total delay is considered to be 250 ms. As a final note with respect to the voltage dependency, the EVs are modelled as constant current loads.

3.4. Experimental layout and power components

The experiments are executed in the experimental infrastructure SYSLAB, which is part of the PowerLabDK platform. SYSLAB represents a small scale low voltage power system. It consists of a number of real power components that are interconnected by a three-phase 400 V AC power grid, which is distributed over the Risø campus of the Technical University of Denmark [28]. SYSLAB is also characterised by its communication and control nodes, which allow a strong controllability over the grid. The system may be connected to the utility or it can be islanded if desired. The experimental layout is shown in Fig. 4.

The experimental setup is composed by two busbars that are connected by 675 m underground cable. The VRB is connected to busbar 2 and installed in building 2 where the busbar is located. The rest of the components are connected to busbar 1 and they are installed in the same building as the busbar. The Aircon wind turbine is installed around 10 m from building 1. The VRB, the Aircon and the Dump load are controlled through a Matlab/Java interface, while the EVs are controlled through a Python interface. Given that all of the components are 3-phase except the EVs, it has been necessary to create an intermediate phase splitter. Each EV is supplied on a different phase via a standard Mennekes (IEC 62196 Type 2) connector. The three Mennekes plugs are controlled separately by three different pieces of electric vehicle supply equipment (EVSE).

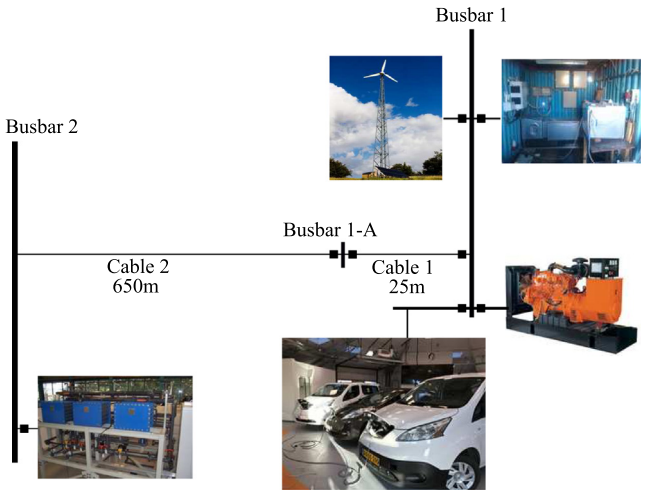

Fig. 4. Experimental layout.

The experiments are executed in an islanded configuration where the diesel generator-set acts as the grid forming unit and is the only synchronous inertia device. It also compensates for the small amount of reactive power drawn by each EV, corresponding to 200 VAr each. The different components used during the experiment are listed in Table 1 where *P*0 is the base operating point. SC1 and SC2 refer to Study Case 1 and Study Case 2, respectively.

3.5. EV charging controller and communication architecture

Each of the 3 single phase EVs is connected to a different phase of the grid by means of three EVSE. The control and communication setup is shown in Fig. 5.

This consists of the following components:

- The smart charging controller – receives the measurements from the multi-instrument, it calculates the response and it sends control signals to the EVSE.
- DEIF MIC-2 – is a multi-instrument measurement device that shows the voltage, current and power measurements with 0.5% accuracy. The device is only used for data logging.
- DEIF MTR-3 – is a multi-instrument measurement device that is used here for fast frequency measurements, which are polled every 200 ms.
- EVSE – is rated for 16 A
- EV – is the tested vehicle.
- Grid – is the grid connection at the SYSLAB experimental facility.

Please cite this article in press as: Rezkalla M et al. Comparison between synthetic inertia and fast frequency containment control based on single phase EVs in a microgrid. Appl Energy (2017), http://dx.doi.org/10.1016/j.apenergy.2017.06.051

Table 1
Properties of the devices used in the experiments.

Device	Capability	P0 (kW) SC1	P0 (kW) SC2	Description
Diesel	0–48 kW −20–30 kVAr	24	24	IVECO genset S = 60 kVA, 2 pole pairs
Aircon	10 kW @ 11 ms	–	∼4	Wind turbine type 4
Battery	±15 kW ±12 kVA	9	–	Vanadium redox battery, 120 kW h
Dumpload	0–78 kW	7	21	Resistor load bank
EV1	6–16 A (1.4–3.7 kW)	2.5	2.5	Nissan leaf 2016, 30 kW h lithium battery
EV2	6–16 A (1.4–3.7 kW)	2.5	2.5	Nissan e-NV200 2014, 24 kW h lithium battery
EV3	6–16 A (1.4–3.7 kW)	2.5	2.5	Nissan e-NV200 2015, 24 kW h lithium battery

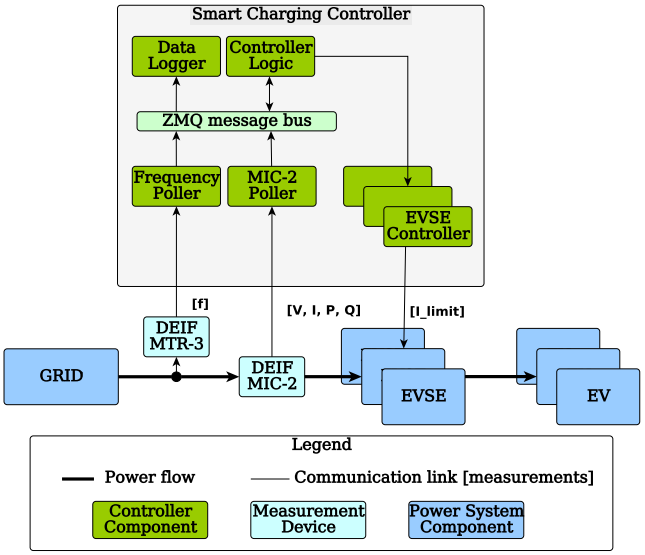

Fig. 5. The communication architecture for the implemented smart charging controller.

The smart charging controller consists of many sub-components, as follows:

- Controller logic – reads the latest frequency measurements from the message bus and calculates the $\Delta f/\Delta t$ and the Δf. Calculated set-points are directly sent to the EVSE controller.
- EVSE controller – acts as an interface between the physical EVSE and the controller logic.
- Frequency poller – acts as an interface to the frequency measurement device. In this case DEIF MTR-3 instrument used for frequency sampling every 0.2 s with accuracy of 10 mHz.
- MIC-2 poller – multi instrument device interface.
- Data logger – monitors the data exchange on the message bus and logs it to the database.
- ZMQ message bus – is the message bus that is used to represent the data exchange between the previously mentioned controller components.

The timing of the response is crucial for the provision of synthetic inertia. Therefore, the timing of each component in the control loop is important: frequency and RoCoF are measured every 200 ms, the controllers' response is almost instantaneous and communication delay (10–20 ms) to each EV/EVSE pair is optimised by controlling them independently. It uses multi-threading and each EVSE only receives a new control signal if the set-point has changed. Finally, the EV's reaction time is approximately 200–300 ms and, therefore, the whole control and actuator chain has an overall latency equal to 400–500 ms. According to this number, it is expected that the device could positively influence the whole frequency dynamic.

4. Results and discussion

This section is composed by two subsections, in which the simulations and experimental validation are presented. Two study cases are analysed. In the first study case (SC1), the system is studied involving a set of load steps. An alternate load-increase and load-decrease are applied, so that both over and under frequency dynamics can be analysed. In the second study case (SC2), wind power generation is added to the system. It adds random power fluctuations over the tested period and it allows the possibility of investigating the behaviour of the two controllers and the EVs in a more realistic and challenging situation.

The two study cases are each composed of three scenarios: in the first scenario, the EVs are treated as a constant load; that is, constant current set-point equal to 11 A (Base scenario). In the second scenario, the EVs participate with a synthetic inertia response; that is, SIC. In the third scenario, the EVs participate with a fast frequency response; that is, FCC. An overview of the different scenarios is given in Table 2. During the simulation, only SC1 was analysed.

4.1. Simulations

In this section a simulation study in DigSilent PowerFactory is carried out. It aims to investigate the effects of synthetic inertia control and frequency containment control, and it aims to achieve preliminary results before experimentally validating the controllers. To explore the effects of the 1 A granularity that is imposed by the standard, a sensitivity analysis of different granularity values is conducted.

The same components and grid configuration that are presented in Fig. 4 have been modelled, with the operating conditions of SC1, as shown in Table 1.

To make this study as realistic as possible, an oscillatory frequency has been induced in the system by means of a fictitious zero-mean variable load by means of fluctuating active power absorbed by the three-phase resistive load. In this way, it has been

Table 2
Study cases overview.

	Study Case 1	Study Case 2
Scenario 1	Base case	Base case + Wind
Scenario 2	SIC	SIC + Wind
Scenario 3	FCC	FCC + Wind

Please cite this article in press as: Rezkalla M et al. Comparison between synthetic inertia and fast frequency containment control based on single phase EVs in a microgrid. Appl Energy (2017), http://dx.doi.org/10.1016/j.apenergy.2017.06.051

possible to emulate the realistic frequency oscillation that the real diesel synchronous generator would generate in such an islanded grid configuration.

First, a load event with amplitude of 2 kW (8.7% of the total consumption) is applied at $t = 10$ s and three scenarios are analysed. The first scenario is considered as a base case where the EVs are treated as a constant load; that is, constant current set-point equal to 11 A. In the second scenario, the EVs participate with a SIC. In the third scenario, the EVs are equipped with the FCC controller. Both the SIC and FCC controllers are implemented according to the control diagrams in Fig. 2, thus applying integer EV current set-points to assure standard-compliance. Fig. 6 shows the grid frequency, the RoCoF and the EVs' current set-point.

As expected, Fig. 6a shows that FCC improves the frequency behaviour in terms of frequency nadir and steady state value. It also shows that SIC ameliorates the frequency slope, which is a typical behaviour of introducing more synchronous and/or synthetic inertia into the system. On the other hand, unexpectedly, Fig. 6b shows that FCC has a better performance in terms of RoCoF compared to SIC.

However, a steeper droop and/or smaller deadband for SIC would have led to better performance regarding the RoCoF and the frequency slope. To demonstrate this point, the same simulations were executed changing the deadband of SIC to ±0.5 Hz instead of ±0.8 Hz. The results are presented in Fig. 7.

Fig. 7a shows an improvement regarding the frequency slope compared to the previous case. On the other hand, Fig. 7b shows a marginal improvement regarding the RoCoF. Compared to the previous scenario, Fig. 7c shows that the EVs were participating more by changing the current set-point.

A sensitivity analysis is performed to better understand the effects of the 1 A granularity imposed by the standard IEC 61851 [27] on the performance of the two controllers. A series of simulations are carried out employing different load steps and different granularities. Frequency drops have been obtained by increasing the active power absorbed by the VRB by 20%, 40%, and 60%. They represent a load event of 8.7%, 15.7% and 23.5% of the total consumption, respectively. For the evaluation of the influence of the granularity, the following values of granularity have been applied, which are expressed as fraction of the actual granularity of 1 A: $\frac{1}{4}, \frac{1}{2}$ and 1. Moreover, for the sake of completeness, the case of continuous regulation (no granularity) and the uncontrolled case have also been included in the analysis.

Fig. 8 reports 3D bar plots of the results for all of the performed simulations. The results are reported by means of standard deviations (SD) for both Frequency and RoCoF for FCC and SIC.

As expected, Fig. 8 shows that in all of the cases the standard deviations depend on the size of the load step. On one hand, they are mostly constant for the different considered granularity, on the other hand higher values are found in the uncontrolled cases. Moreover, it is noticeable that beneficial effects on the frequency are found in case of FCC. As presented in Fig. 6, the EVs' effect makes the frequency rise to a higher steady-state value. Meanwhile, the SIC controller has an embedded reset logic, which makes the EV set-point go back to 11 A right after the event. It is of interest to highlight that the FCC shows an unexpected better contribution to the RoCoF limitation in comparison to the SIC. This is due to the limited number of control actions that took place in case of SIC, which is due to the implemented RoCoF deadband (Fig. 1b). Instead, when providing primary regulation via FCC, no deadband is applied, which activates the controller more often, thus contributing more to the RoCoF containment.

This sensitivity analysis shows that, in this islanded microgrid, the granularity does not influence the results. However, one should note that under a certain combination of system attributes (system inertia and stiffness of the power system) and control units (amount of power involved in the regulation, droop, response/ramp time and granularity of the control actions), the granularity might lead to system instability or oscillation between two consequent set-points, as was experienced during the validation phase.

4.2. Experimental validation

Following the results obtained during the simulations, the authors investigate the EVs capability to provide synthetic inertia and frequency containment control in an islanded grid in real circumstances. The experiments are executed in the islanded configuration that is shown in Fig. 4, where the diesel is the grid forming unit.

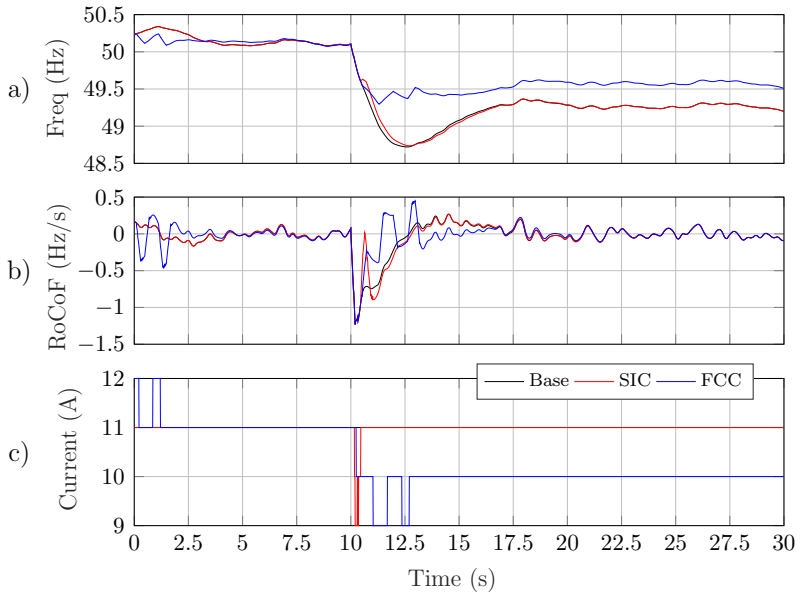

Fig. 6. Simulation results obtained by applying ±0.8 Hz/s deadband for SIC: (a) Frequency, (b) RoCoF and (c) EV current set-points for the three analysed scenarios, in case of granularity of 1 A.

Please cite this article in press as: Rezkalla M et al. Comparison between synthetic inertia and fast frequency containment control based on single phase EVs in a microgrid. Appl Energy (2017), http://dx.doi.org/10.1016/j.apenergy.2017.06.051

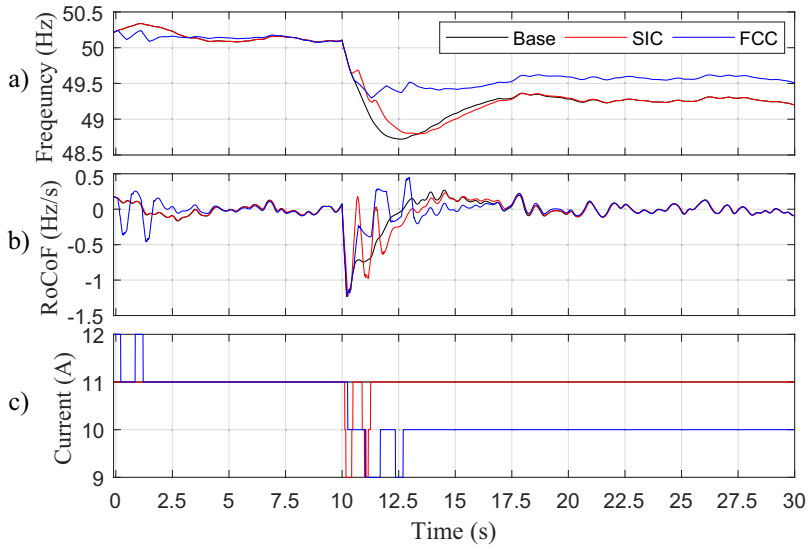

Fig. 7. Simulation results obtained by applying ±0.5 Hz/s deadband for SIC: (a) Frequency, (b) RoCoF and (c) EV current set-points for the three analysed scenarios, in case of granularity of 1 A.

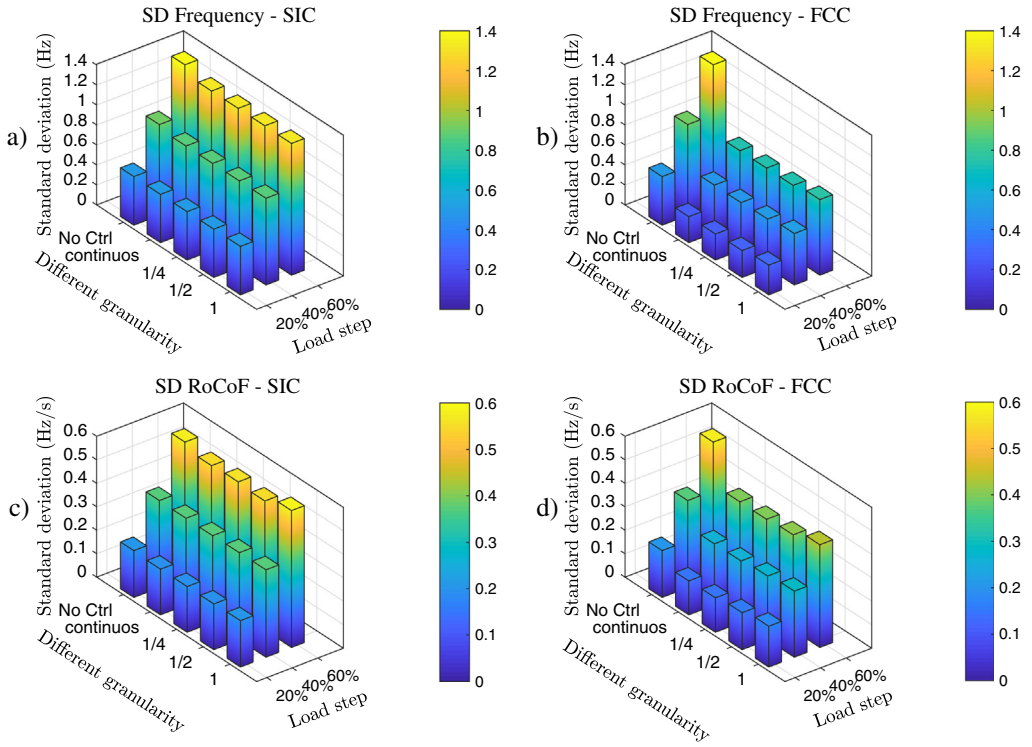

Fig. 8. (a) SD of the frequency applying SIC and (b) SD of the frequency applying FCC, (c) SD of the RoCoF applying SIC, (d) SD of the RoCoF applying FCC.

4.3. Study Case 1

In the first study case, the frequency variation is triggered by several load steps. A set of load events from the VRB of the same amplitude is applied (≈ ±2 kW), namely, 8.7% of the initial installed load. To better investigate the controllers as well as the frequency dynamics, an additional set of load events with a different amplitude is applied, specifically (≈ ±4 kW), 17% of the initial installed load. The grid units as well as the initial conditions are reported in Table 1.

The three scenarios are characterised by the same initial conditions and load steps. The first scenario (S1) is a base case, in which the EVs receive a constant current set-point; that is, 11 A absorbing around 2.5 kW. In the second scenario (S2), the EVs are controlled by the synthetic inertia controller, which modulates the charging level between 6 and 16 A with steps of 1 A in function of the RoCoF-current droop characteristic presented in Fig. 1b. In the third scenario (S3), the EVs are controlled by the frequency containment controller. The controller modulates the EVs' charging level between 6 and 16 A with steps of 1 A in

Please cite this article in press as: Rezkalla M et al. Comparison between synthetic inertia and fast frequency containment control based on single phase EVs in a microgrid. Appl Energy (2017), http://dx.doi.org/10.1016/j.apenergy.2017.06.051

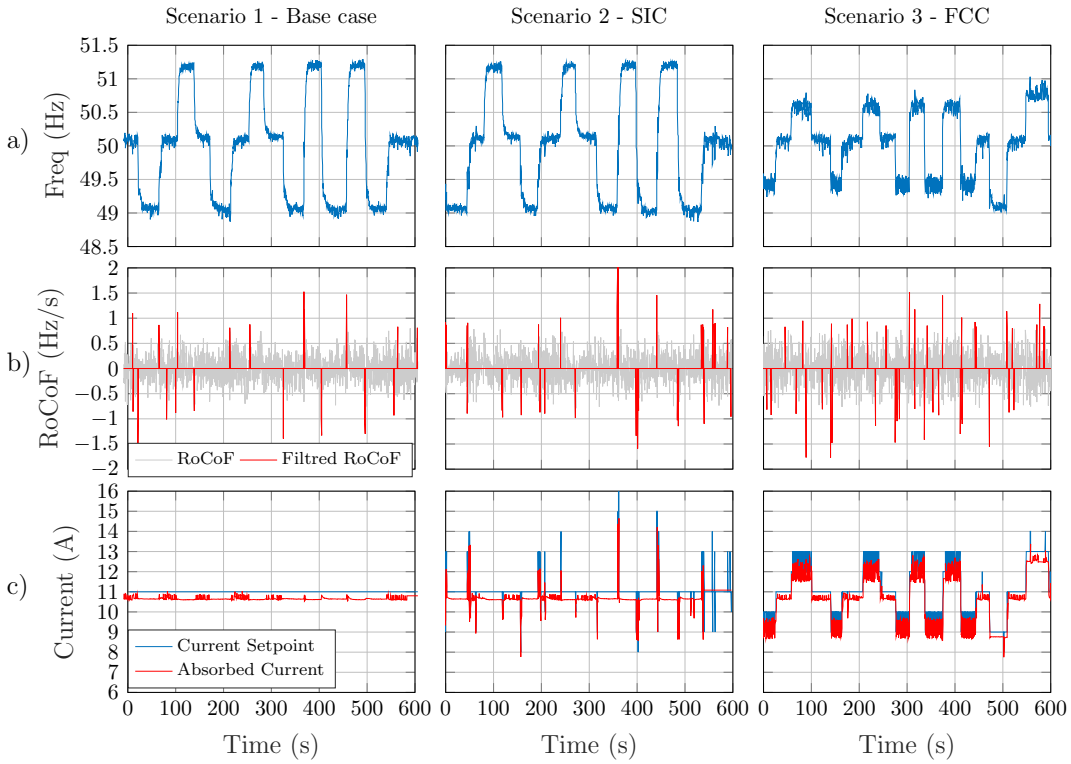

Fig. 9. Study Case 1 (load steps) – (a) Frequency, (b) RoCoF, (c) EV1's set-point vs absorbed current.

function of the frequency-current droop characteristic presented in Fig. 1a.

The results of the experiments are presented in Fig. 9. Fig. 9a shows the system frequency for the three scenarios. Fig. 9b shows the RoCoF measured over 200 ms in grey and the filtered signal after applying the deadband in red (±0.8 Hz/s deadband is considered). In Fig. 9c the controllers' current setpoint is plotted versus the EVs' absorbed current. Since the three EVs act similarly, only the current of EV1 is presented.

Fig. 9c shows that the EVs change the absorbed current as desired by the different controllers. However, due to the 1 A granularity, the implemented droop and the operating point, the 2 kW load event implies the FCC to oscillate between 12 and 13 A, and between 9 and 10 A. A 6 kW load event is only introduced for Scenario 3, at which a stable operating point was found. In fact, Fig. 9c shows that the EV's current did not oscillate for this load event (around $t = 450$ s). However, this oscillation can be reduced by implementing a hysteresis function.

Fig. 9a shows that FCC limits the maximum frequency deviation compared to the base case, while the SIC does not have an effect on it. On the other hand, due to the oscillation between the different set-points in case of FCC, Fig. 9b shows that the RoCoF was outside the deadband more frequently when compared to scenario 1 and 2.

Due to the response delay of the EVs and the dynamics of the diesel, which led to a continuous frequency oscillation, it is difficult to perceive a valuable improvement in terms of the RoCoF from SIC.

To better compare the performance of the two controllers in terms of RoCoF and frequency, the standard deviation and the energy contained in the signal (also addressed as normalised energy) is calculated and presented in Table 3. For a discrete signal $x(n)$, the normalised energy is calculated as $\frac{1}{N}\sum_{n=1}^{N} x(n)^2$, where N is the number of samples taken for computation. It shows that the two controllers do not improve the RoCoF when compared to the base case.

Table 3
SC1—Standard deviation and normalised energy.

	RoCoF		Frequency
	SD	Normalised Energy	SD
Base	0.29	0.083	0.77
SIC	0.31	0.093	0.79
FCC	0.33	0.11	0.48

To understand the effects of the SIC on the frequency compared to the base case, Fig. 10 shows a zoom of the frequency, the RoCoF and the EV's absorbed current for the three scenarios. In Fig. 10a, one can notice that the SIC has improved the frequency slope as expected and as experienced during the simulations.

Due to the embedded deadband, the SIC contribution is very limited. However, since the three EVs are characterised by the same delay and granularity (i.e. acting simultaneously with steps), one can observe the sharp change in frequency, which will lead to worse RoCoF compared to the base case as shown in Fig. 10b. To overcome this issue, it might be of interest to study different delays and droops among the EVs. This might induce a more smooth frequency change and, therefore, a better RoCoF. It is of interest to notice from Table 3, where the SD is reported, and Fig. 10b that the FCC has worsened the RoCoF when compared to the SIC and the base case.

4.4. Study Case 2

In the second study case, the two controllers are analysed during wind power production. The VRB set-point is set to zero during this study case. The same scenarios and droop characteristic as the previous study case are applied. Due to the random stochasticity of the wind generation and the diesel dynamics, the initial and boundary conditions are not exactly identical. Nevertheless, this

Please cite this article in press as: Rezkalla M et al. Comparison between synthetic inertia and fast frequency containment control based on single phase EVs in a microgrid. Appl Energy (2017), http://dx.doi.org/10.1016/j.apenergy.2017.06.051

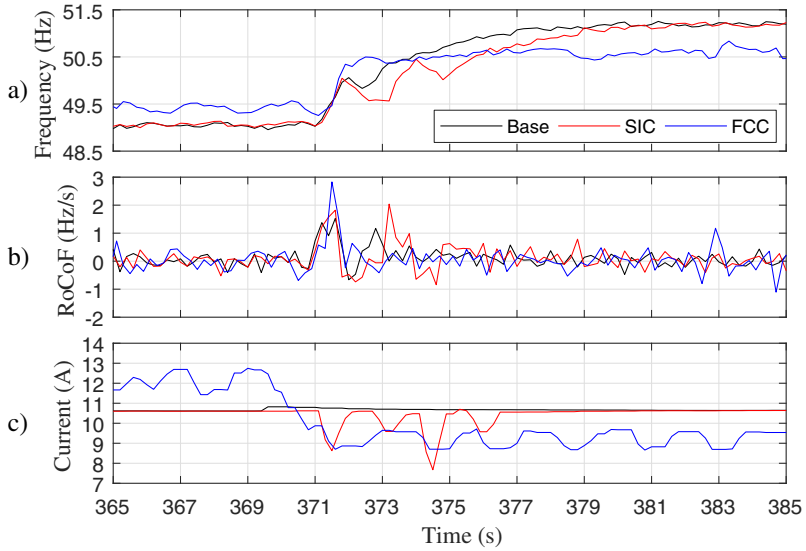

Fig. 10. (a) Frequency, (b) RoCoF, (c) EV1's absorbed current.

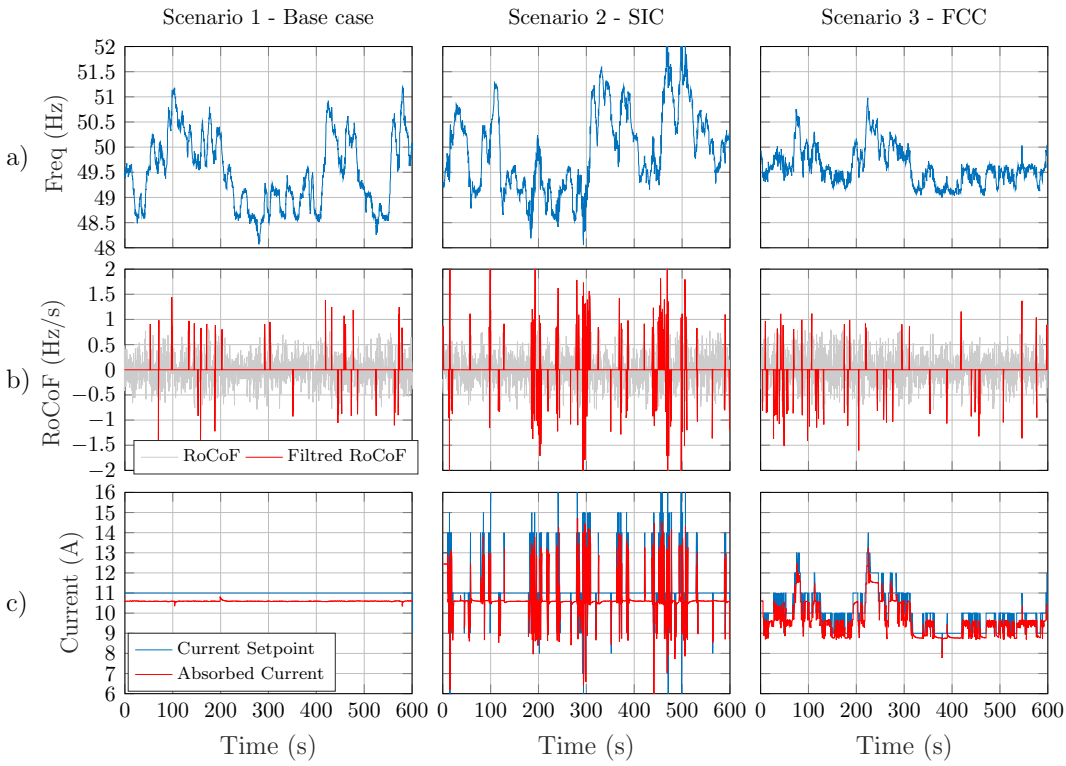

Fig. 11. Study Case 2 (wind power) – (a) Frequency, (b) RoCoF, (c) EV1's set-point vs absorbed current.

study case aims to investigate the performance of each controller and the EVs in a more challenging and realistic configuration rather than comparing the different scenarios. The results for SC2 are presented in Fig. 11.

Fig. 11a shows the grid frequency for the three scenarios. Fig. 11b shows the RoCoF measured over 200 ms in grey and the filtered signal after applying the deadband in red. In Fig. 11c the controllers' current set-point is plotted versus the EVs' absorbed current. Since the three EVs are acting similarly, only the current of EV1 is presented.

The three scenarios were executed over a total time of 30 min. The average wind production did not differ so much among the three scenarios: so that the different scenarios are still comparable. Fig. 11a shows that the FCC does have a remarkable effect in limiting the maximum frequency deviation. Fig. 11b shows that by applying the SIC, the RoCoF is outside the deadband more frequently.

To better compare the three scenarios, mean value and standard deviation of the wind production together with the standard deviation of the frequency and the RoCoF are calculated and presented in Table 4.

Please cite this article in press as: Rezkalla M et al. Comparison between synthetic inertia and fast frequency containment control based on single phase EVs in a microgrid. Appl Energy (2017), http://dx.doi.org/10.1016/j.apenergy.2017.06.051

Table 4
SC2—Standard deviation and normalised energy.

	Wind Generation		RoCoF		Frequency
	Mean	SD	SD	Normalised Energy	SD
Base	3.5 kW	1.4	0.31	0.098	0.71
SIC	4.6 kW	1.68	0.45	0.2	0.83
FCC	3.1 kW	1.28	0.34	0.11	

As mentioned previously, due to the random wind production and the non-replicability of the same conditions, the comparison is not perfect, especially in terms of RoCoF due to the continuous variation of the wind profile.

However, the mean value of the wind production among the three scenarios does not differ excessively, which allows the comparison of the standard deviation of the frequency among the scenarios. Table 4 and Fig. 11a show the remarkable positive effect of FCC on the frequency.

5. Conclusion and future work

Starting from the research question: given the trend of decreasing system inertia, can fast frequency containment compensate or replace the need for synthetic inertia? First, this work analytically showed the interdependence between frequency containment and synthetic inertia control on the transient frequency variation and the RoCoF. Second, on the simulation level, it presented the ability of fast frequency control in improving the frequency in terms of nadir, steady state value and RoCoF. It also presented the ability of synthetic inertia control to improve the frequency nadir and slope following an event. While it was acknowledged that EVs could quickly and almost precisely respond to fast changing current set-points, some technical limitations in employing EVs for such services were found. Finally, an experimental validation was conducted, presenting the capabilities and limitations of the two controllers under two different circumstances: following load events in both directions and exogenous wind generation profiles.

Employing the FCC, the simulations results showed a remarkable improvement of the frequency nadir and steady state value. It showed also a very limited improvement in terms of RoCoF. The controller did not limit the maximum RoCoF following the event but it did improve the overall behaviour compared to the base case. Similarly, the experiments showed the ability of FCC in limiting the maximum frequency deviation, both following a series of load events or considering a wind power generation. Although in simulation the sensitivity analysis showed a very limited effect of the granularity, in the experimental phase, due to the 1 A granularity, the FCC controller caused the EV absorbed current to oscillate between two consecutive set points, worsening the calculated RoCoF. It should be noted that this oscillation was due the combination of 1 A granularity, the implemented droop and the operating point. However, this effect can be limited by employing an hysteresis-based algorithm.

By applying the SIC, the simulations presented limited frequency improvements in terms of frequency nadir and frequency slope. They also showed that employing a smaller deadband allowed a better contribution, slightly improving frequency nadir and slope. On the other hand, the smaller deadband worsened the RoCoF trend when compared to the base case. However, in both cases, the controller did not limit the maximum RoCoF value. As mentioned, the SIC slightly improved the frequency slope but worsened the RoCoF. As interpretation of such unexpected phenomena, the authors believe that this might be due to the fact of using the same RoCoF signal for both control and examination purposes. In other words, the RoCoF used for control purpose should be calculated over a smaller time window to the one used by the RoCoF relay to detect the variations. Nevertheless, considering the derivative characteristic of the SIC, its implementation might easily lead to frequency oscillation and this limits the ability to exploit the resource (e.g. large deadband). For the SIC, the experiments were conducted for two cases: first, following load events; and second, considering wind power generation. In terms of frequency, the SIC effects were negligible for both cases. For the first case, even if the EVs were able to follow the desired set points, the SIC did not show a noticeable improvement in terms of RoCoF. On the other hand, considering wind power generation, the SIC had very remarkable negative effects in terms of RoCoF. It should be noted that this effect might have been limited by employing less steep droop parameters; on the other hand, this would have limited the EVs participation (i.e. flexibility margin).

In general, employing faster response devices will allow to better exploit the resource's capabilities. For example, this was shown in case of SIC where the smaller time response permitted the use of a narrower deadband. It can be concluded that the actual series produced EVs are able to provide ancillary services in terms of fast frequency response and synthetic inertia by solely relying on unidirectional charging. On the other hand, the experiments show that with the actual EV's response time, a large deadband was needed for the SIC and this limited its contribution. To achieve better performance, new requirements in terms of the EV's response time need to be set. In future work, the authors recognise the importance of extending the analytical formulation of the interdependence of the two controllers on the system frequency. Moreover, it is of interest to expand the analysis over a larger number of flexible units by employing different control attributes.

Acknowledgments

The work in this paper has been partly supported by the European Commission, under the FP7 project ELECTRA (Grant No.: 609687) and partly by the Danish research projects Parker (ForskEL kontrakt nr. 2016-1-12410) and Electra Top-up (grant: 3594756936313). The authors are also grateful to Nissan Denmark for providing the two Leafs that were used in the experiments.

References

[1] Adrees A, Papadopoulos PN, Milanovi JV. A framework to assess the effect of reduction in inertia on system frequency response. Power Energy Soc. Gen. Meet. 2016:1–5. http://dx.doi.org/10.1109/PESGM.2016.7741695.
[2] Ulbig A, Borsche T, Andersson G. Impact of low rotational inertia on power system stability and operation. In: The 19th world congress of the international federation of automatic control (IFAC14); 2014. p. 1–12. Available from: 1312.6435v2. interrefdoi:10.3182/20140824-6-ZA-1003.02615httphttp://dx.doi.org/10.3182/20140824-6-ZA-1003.02615.
[3] ENTSO-E. Frequency stability evaluation criteria for the synchronous zone of continental Europe. Tech. rep. ENTSOE; 2016.
[4] The commission for energy regulation. Rate of change of frequency modification to the grid code. Tech. rep. CER; 2014.
[5] Muljadi E, Gevorgian V, Singh M, Santoso S. Understanding inertial and frequency response of wind power plants. In: 2012 IEEE power electronics and machines in wind applications; 2012. 1–8. http://dx.doi.org/10.1109/PEMWA.2012.6316361.
[6] Sharma S, Huang SH, Sarma NDR. System inertial frequency response estimation and impact of renewable resources in ERCOT interconnection. In:

IEEE power and energy society general meeting; 2011. p. 1–6. http://dx.doi.org/10.1109/PES.2011.6038993.
[7] Walling RA, Miller NW. Distributed generation islanding implications on power system dynamic performance. In: Power engineering society summer meeting, Chicago; 2002. p. 92–6. http://dx.doi.org/10.1109/PESS.2002.1043183.
[8] Ten C, Crossley P. Evaluation of ROCOF relay performances on networks with distributed generation. In: IET 9th international conference on developments in power systems protection (DPSP 2008) 2008; 2008. p. 522–7. interrefdoi:10.1049/cp:20080092httphttp://dx.doi.org/10.1049/cp:20080092.
[9] Mu Y, Wu J, Jenkins N, Jia H, Wang C. A spatial-temporal model for grid impact analysis of plug-in electric vehicles. Appl Energy 2014;114(February):456–65. http://dx.doi.org/10.1016/j.apenergy.2013.10.006.
[10] Pillai JR, Bak-Jensen B. Impacts of electric vehicle loads on power distribution systems. In: IEEE vehicle power and propulsion conference, VPPC; 2010. p. 6–11. http://dx.doi.org/10.1109/VPPC.2010.5729191.
[11] Foley A, Tyther B, Calnan P, Gallachóir BÓ. Impacts of electric vehicle charging under electricity market operations. Appl Energy 2013;101:93–102. http://dx.doi.org/10.1016/j.apenergy.2012.06.052.
[12] Hedegaard K, Ravn H, Juul N, Meibom P. Effects of electric vehicles on power systems in Northern Europe. Energy 2012;48(1):356–68. http://dx.doi.org/10.1016/j.energy.2012.06.012.
[13] Amini MH, Parsa M, Karabasoglu O. Simultaneous allocation of electric vehicles' parking lots and distributed renewable resources in smart power distribution networks. Sustain Cities Soc 2017;28:332–42. http://dx.doi.org/10.1016/j.scs.2016.10.006.
[14] Amini MH, Moghaddam MP. Probabilistic modelling of electric vehicles' parking lots charging demand. In: Electrical engineering (ICEE), 2013 21st Iranian conference; 2013. p. 3–6. http://dx.doi.org/10.1109/IranianCEE.2013.6599716.
[15] Molina-garcía A, Bouffard F, Kirschen DS. Decentralized demand-side contribution to primary frequency control. IEEE Trans Power Syst 2011;26(1):411–9. http://dx.doi.org/10.1109/TPWRS.2010.2048223.
[16] Moghadam MRV, Member S, Ma RTB. Distributed frequency control in smart grids via randomized demand response. IEEE Trans Smart Grid 2014;5(6):2798–809.
[17] Kempton W, Tomić J. Vehicle-to-grid power implementation: from stabilizing the grid to supporting large-scale renewable energy. J Power Sources 2005;144(1):280–94. http://dx.doi.org/10.1016/j.jpowsour.2004.12.022.
[18] Sortomme E, El-sharkawi MA. Optimal scheduling of vehicle-to-grid energy and ancillary services. IEEE Trans Smart Grid 2012;3(1):351–9. http://dx.doi.org/10.1109/TSG.2011.2164099.
[19] Wang D, Coignard J, Zeng T, Zhang C, Saxena S. Quantifying electric vehicle battery degradation from driving vs. vehicle-to-grid services. J Power Sources 2016;332:193–203. http://dx.doi.org/10.1016/j.jpowsour.2016.09.116.
[20] Knezović K, Træholt C, Marinelli M, Andersen PB. Active integration of electric vehicles in the distribution network theory, modelling and practice [Phd thesis]. Technical University of Denmark; 2017. <http://orbit.dtu.dk/files/131995291/Knezovic_PhDthesis_final.pdf>.
[21] Mu Y, Wu J, Ekanayake J, Jenkins N, Jia H. Primary frequency response from electric vehicles in the Great Britain power system. IEEE Trans Smart Grid 2013;4(2):1142–50. http://dx.doi.org/10.1109/TSG.2012.2220867.
[22] Knezović K, Martinenas S, Andersen PB, Zecchino A, Marinelli M. Enhancing the role of electric vehicles in the power grid: field validation of multiple ancillary services. IEEE Trans Transp Electrif 2016;7782(c). http://dx.doi.org/10.1109/TTE.2016.2616864. 1–1.
[23] Kempton W, Tomic J. Vehicle-to-grid power implementation: from stabilizing the grid to supporting large-scale renewable energy. J Power Sources 2005;144(1):280–94. http://dx.doi.org/10.1016/j.jpowsour.2004.12.022.
[24] Teng F, Mu Y, Jia H, Wu J, Zeng P, Strbac G. Challenges on primary frequency control and potential solution from EVs in the future GB electricity system. Appl Energy 2016;194:353–62. http://dx.doi.org/10.1016/j.apenergy.2016.05.123.
[25] Schuller A, Flath CM, Gottwalt S. Quantifying load flexibility of electric vehicles for renewable energy integration. Appl Energy 2015;151:335–44. http://dx.doi.org/10.1016/j.apenergy.2015.04.004.
[26] Tielens P, Hertem DV. The relevance of inertia in power systems. Renew Sustain Energy Rev 2016;55:999–1009. http://dx.doi.org/10.1016/j.rser.2015.11.016.
[27] IEC 61851-1:2010. Electric vehicle conductive charging system Part 1: General requirements; 2010.
[28] Marinelli M, Martinenas S, Knezović K, Andersen PB. Validating a centralized approach to primary frequency control with series-produced electric vehicles. Adv Life Course Res 2016;7:63–73. http://dx.doi.org/10.1016/j.est.2016.05.008.
[29] Suul JA, Arco SD, Guidi G. Virtual synchronous machine-based control of a single-phase bi-directional battery charger for providing vehicle-to-grid services. IEEE Trans Ind Appl 2016;52(4):3234–44. http://dx.doi.org/10.1109/TIA.2016.2550588.
[30] Martini L, Morch A, Radaelli L, Caerts C, Tornelli C, Hänninen S, et al. Electra IRP approach to voltage and frequency control for future power systems with high DER penetration. In: 23rd international conference on electricity distribution CIRED; 2015. p. 1–5.
[31] ENTSO-E. ENTSO-E, Continental Europe Operation Handbook. Tech. rep. Cc, ENTSOE; 2009.
[32] Kundur P, Paserba J, Ajjarapu V, Andersson G, Bose A, Canizares C, et al. Definition and Classification of Power System Stability. IEEE Trans. Power Syst. 2004;21(3):1387–401. http://dx.doi.org/10.1109/TPWRS.2004.825981.
[33] Kundur P. Power system stability and control. McGraw-Hill; 1994.
[34] Zecchino A, Rezkalla M, Marinelli M. Grid Support by single-phase connected electric vehicles without V2G capability: fast primary frequency control. In: International universities' power engineering conference – UPEC, Coimbra; 2016. p. 6.
[35] Rezkalla M, Martinenas S, Zecchino A, Marinelli M, Rikos E. Implementation and validation of synthetic inertia support employing series produced electric vehicles. In: 24th International conference on electricity distribution CIRED, Glasgow, 14–15 Jun; 2017. p. 1–5.
[36] Rezkalla M, Marinelli M, Pertl M, Heussen K. Trade-off analysis of virtual inertia and fast primary frequency control during frequency transients in a converter dominated network. In: 2016 IEEE innovative smart grid technologies – Asia (ISGT-Asia); 2016. p. 890–5. interrefdoi:10.1109/ISGT-Asia.2016.7796503httphttp://dx.doi.org/10.1109/ISGT-Asia.2016.7796503.

Please cite this article in press as: Rezkalla M et al. Comparison between synthetic inertia and fast frequency containment control based on single phase EVs in a microgrid. Appl Energy (2017), http://dx.doi.org/10.1016/j.apenergy.2017.06.051

Pub. G. Management of Power Quality Issues in Low Voltage Networks using Electric Vehicles: Experimental Validation

Management of Power Quality Issues in Low Voltage Networks using Electric Vehicles: Experimental Validation

Sergejus Martinenas, *Student Member, IEEE,* Katarina Knezović, *Student Member, IEEE,* Mattia Marinelli, *Member, IEEE*

***Abstract*—As Electric Vehicles (EVs) are becoming more wide spread, their high power consumption presents challenges for the residential low voltage networks, especially when connected to long feeders with unevenly distributed loads. However, if intelligently integrated, EVs can also partially solve the existing and future power quality problems. One of the main aspects of the power quality relates to voltage quality. The aim of this work is to experimentally analyse whether series-produced EVs, adhering to contemporary standard and without relying on any V2G capability, can mitigate line voltage drops and voltage unbalances by a local smart charging algorithm based on a droop controller. In order to validate this capability, a low-voltage grid with a share of renewable resources is recreated in SYSLAB PowerLabDK. The experimental results demonstrate the advantages of the intelligent EV charging in improving the power quality of a highly unbalanced grid.**

***Index Terms*—Electric vehicles, power distribution testing, power quality, unbalanced distribution grids, voltage control.**

I. Introduction

DISTRIBUTION system operators (DSOs) have historically designed and operated their networks in order to follow a predicted demand with uni-direction power flows only. Nowadays, due to increased share of renewable energy resources, DSOs are confronted with changes in the low-voltage grid operation with even greater system complexity imposed by electric vehicle (EV) integration [1], [2]. Danish Energy Association predicts 47,000 EVs in Denmark by 2020 in a moderate penetration scenario [3], meaning that distribution networks will have to cope with overall voltage degradation, especially in unbalanced systems where voltage quality is already decreased. Unlike in other European countries, the three-phase connection in Denmark is not reserved only for industrial consumers, but is also available for residential customers. Therefore, Distribution System Operators (DSOs) experience high voltage unbalances due to the lack of regulation for per phase load connection [4]. Uncontrolled EV charging in such grids may result in large power quality deterioration, i.e., higher voltage unbalances [5], and the rise of neutral-to-ground voltage due to single-phase charging [6].

As an economic alternative to grid reinforcement, different EV charging strategies can be used for supporting the grid and enhancing both the efficiency and the reliability of the distribution system [7]. An extensive amount of research shows that intelligent integration, namely smart EV charging, can be used for lowering the impact on the power system or providing different ancillary services [8]–[14]. In order to integrate electric vehicles in the distribution grid, both centralised and decentralised charging strategies have been explored [15]–[17]. It has been found that centralised algorithms lead to the least cost solution and are easily extended to a hierarchical scheme, but they require great communication infrastructure for information exchange. On the other hand, decentralised control provided similar results to the centralised one without the complex communication infrastructure.

A decentralised voltage dependent charging strategy, which requires only local voltage measurements, can be used for mitigating the low EV-induced voltages [18], [19]. That is, EV charging power can be modulated in accordance to local voltage measurements in order to compensate the voltage unbalances and improve the overall power quality [20], [21]. However, technical challenges may arise and DSOs may be sceptical about the possibility of the distributed demand participating in the grid regulation. Therefore an extensive experimental activity is required for proving the feasibility of these solutions.

A. Objectives

As stated in [22], electric power quality is a term that refers to maintaining the near sinusoidal waveform of power distribution bus voltages and currents at rated magnitude and frequency. Thus power quality is often used to express voltage quality, current quality, reliability of service, etc. While frequency regulation is a system wide service, experimentally addressed in previous work [23], this paper is focusing on the other main aspect of power quality in LV networks i.e. voltage quality. To the authors' knowledge, most of the literature focuses on modelling the EV voltage support, whereas the experimental validation is rarely touched upon. Therefore, this work mainly focuses on the experimental evaluation of the real EV's ability to reduce voltage unbalances by modulating their charging current according to local voltage measurements. This autonomous control could partially solve voltage quality issues without the need for grid upgrades or costly communication infrastructure,

The authors are with the Centre for Electric Power and Energy, Department of Electrical Engineering, Technical University of Denmark (DTU), Roskilde, Denmark (e-mail: smar@elektro.dtu.dk; kknez@elektro.dtu.dk; matm@elektro.dtu.dk)

therefore enabling the integration of higher EV numbers in the existing power network. The experiment is carried out with commercially available vehicles without any Vehicle-to-Grid (V2G) capability, but with the possibility to modulate the charging current in steps according to the predefined droop control. Several scenarios differing in load unbalances and implemented droop controller have been tested in order to assess the influence of EV smart charging on improving power quality in the low voltage grid.

The paper is organised as follows. Section II briefly recalls the standards regarding the voltage power quality and the motivation for implemented voltage control. In Section III, the applied methodology and experimental setup are presented in details with a description of conducted scenarios. Finally, the results are discussed in Section IV followed by the conclusion in Section V.

II. Voltage control

The modern three-phase distribution systems supply a great diversity of customers imposing a permanent unbalanced running state. Contrary to other disturbances in the power system for which the performance is evident for the ordinary customers, voltage unbalance belongs to those disturbances whose perceptible effects are produced in the long run. Unsymmetrical consumption and production lead to voltage and current unbalances which imply greater system power losses, interference with the protection systems, components' performance degradation and overheating possibly to the point-of-burnout. Further on, the main effects of unbalanced voltages are mostly noticeable on the three-phase components e.g., transformers, synchronous machines and induction motors which are designed and manufactured so that all three phase windings are carefully balanced with respect to the number of turns, winding placement, and winding resistance [24]. Essentially, the unbalanced voltages are equivalent to the introduction of a negative sequence component with an opposite rotation to the one of the balanced voltages, resulting in reduced net torque and speed, as well as torque pulsations. In addition, large negative sequence currents introduce a complex problem in selecting the proper overloading protection. Particularly since devices selected for one set of unbalanced conditions may be inadequate for others.

To ensure that electric appliances are operated in a safe manner, the European standard EN50160 [25] defines acceptable limits for several grid parameters. More precisely, the standard defines the limits for Root Mean Square (RMS) phase-to-neutral voltage magnitude $|U_{pn}|$ and the Voltage Unbalance Factor (VUF) as follows:

$$0.9\ U_{nom} \leq |U_{pn}| \leq 1.1\ U_{nom} \tag{1}$$

$$VUF \leq 2\%, \tag{2}$$

for $> 95\%$ of all weekly 10 minute intervals, and

$$0.85\ U_{nom} \leq |U_{pn}| \leq 0.9\ U_{nom}, \tag{3}$$

for $< 5\%$ of all weekly 10 minute intervals. In addition, the standard defines the VUF as:

$$VUF[\%] = \frac{|U_{inverse}|}{|U_{direct}|} \times 100. \tag{4}$$

where $|U_{direct}|$, and $|U_{inverse}|$ are the direct (positive) and the inverse (negative) voltage symmetrical component respectively. Since the definition described in (4) involves voltage magnitudes and angles, i.e., complex algebra for calculating the positive and negative components, equations (5) and (6) give a good approximation while avoiding the use of complex algebra [26].

$$VUF[\%] = \frac{max\{\Delta|U_a^i|, \Delta|U_b^i|, \Delta|U_c^i|\}}{|U_{avg}^i|} \times 100 \tag{5}$$

$$|U_{avg}| = \frac{|U_{an}^i| + |U_{bn}^i| + |U_{cn}^i|}{3}, \tag{6}$$

where $\Delta|U_a|, \Delta|U_b|, \Delta|U_c|$ are deviations of the respective phase-to-neutral voltage magnitudes from the average phase-to-neutral voltage magnitude $|U_{avg}|$, for the observed time window i. These equations will be used later on for assessing the voltage unbalances in the tested study case.

A. Voltage controller implemented in the EVs

Generally droop controllers are used in power systems for distributing the regulation services among multiple machines regardless of the service purpose: frequency with active power control, voltage with reactive power control or voltage with active power control, etc. The chosen droop controller has been adjusted to the application needs by choosing the thresholds corresponding to the acceptable voltage limits. Three different threshold pairs have been tested, with two different proportional slope/gain values.

The used droop controllers have been inspired by the aforementioned standard. Firstly, an upper threshold for the droop controlled voltage is set to 0.95 U_{nom}, above which EVs charge at the maximum current I_{max} of 16 A. Secondly, they can either charge at minimum current I_{min} of 6 A or stop the charging process if the voltage drops below 0.9 U_{nom}, corresponding respectively to the *real droop 1* and *real droop 2* seen in Fig. 1a. The values in-between the EV charging limits would ideally be linear according to the voltage measurement. However, the current controller has the minimum charging current limit of 6 A and the steps of 1 A as defined in the IEC 61851 [27]. Therefore using a typical 3.7 kW EV charger, there are 10 current steps in total. In the implemented controller, these steps are equally distributed between 0.9 and 0.95 U_{nom}. In addition, a steeper droop control corresponding to *real droop 3* in Fig. 1b has also been tested. Similarly to the first droop control, this control also has 10 current steps equally distributed between the charging limits, but the lower voltage limit is set to 0.925 U_{nom}.

Defining an exact droop value for EVs or loads in general, may not be straightforward as it may not be clear what is the nominal power of the load. In this case, it has been considered that the available range of regulating power (i.e., 2.3 kW) is equal to the EV's nominal power instead of the overall EV charging power which amounts to 3.7 kW. The following parameters have been defined for the described droop controls, i.e., (7) for the droop control seen in Fig. 1a and (8) for the droop control seen in Fig. 1b:

$$\begin{cases} \Delta U = 11.5V; U_{nom} = 230V \\ \Delta P = 2.3kW; P_{nom} = 2.3kW \\ k_{droop} = \frac{\Delta U/U_{nom}}{\Delta P/P_{nom}} = 5\% \end{cases} \quad (7)$$

$$\begin{cases} \Delta U = 5.75V; U_{nom} = 230V \\ \Delta P = 2.3kW; P_{nom} = 2.3kW \\ k_{droop} = \frac{\Delta U/U_{nom}}{\Delta P/P_{nom}} = 2.5\% \end{cases} \quad (8)$$

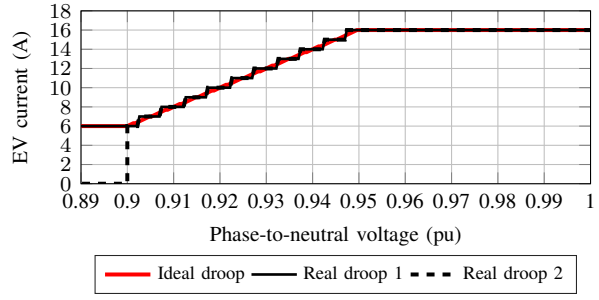

(a)

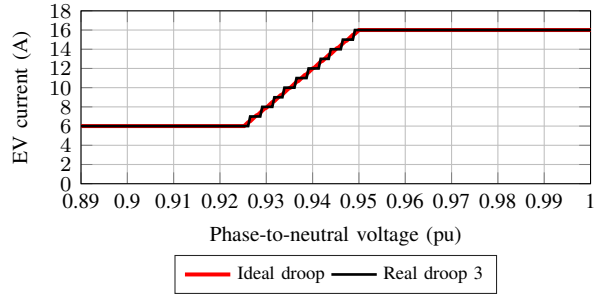

(b)

Fig. 1: Implemented droop controls: (a) k=5%, and (b) k=2.5%

Droop controller calculates the EV charging current limit I_{droop} using the following formula:

$$I_{droop} = \frac{(U_{meas} - U_{nom}) * (I_{max} - I_{min})}{(U_{nom} * k_{droop})} + I_{base} \quad (9)$$

where U_{meas} is the actual voltage measurement and I_{base} is a base EV charging current when voltage is at the nominal value and corresponds to 11A.

$$I_{EV} = \begin{cases} I_{droop}, & I_{min} \leq I_{droop} \leq I_{max} \\ I_{max}, & I_{droop} > I_{max} \\ I_{min}, & I_{droop} < I_{min} \end{cases} \quad (10)$$

I_{max} value represents the available power connection current rating at the consumer site, which is typically 16A, and can be further upgraded to 32A or higher. While I_{min} is chosen from lower charging current limit from IEC 61851 standard.

III. Methodology and Experimental Procedure

To validate the previously described controller in real EV charging processes, typical low voltage distribution feeder has been recreated in a laboratory environment. The feeder is grid connected through a typical MV/LV 200 kVA distribution transformer, whereas the EVs are connected in the end of the feeder next to the resistive load, representing a common home charging setup. Additionally, the feeder includes a set of renewable sources such as a wind turbine along with a controllable resistive load capable of modulating the consumption independently per phase.

The EV voltage support can theoretically be done by modulating the active and/or the reactive power. However, since the reactive power control is currently not available in commercial EVs, this experiment focuses on active power control for voltage support. Each electric vehicle supply equipment (EVSE) is equipped with a local smart charging controller which adjusts the EV charging power according to the droop control described in II-A. Since the controller is independent for each vehicle, the charging current is calculated based only on local voltage measurement meaning that the EVs connected to different phases will react differently. Therefore, the vehicles connected to heavy loaded phases will provide more voltage support due to lower measured voltages resulting in being a less burden to the already unbalanced grid.

A. Experimental setup

The experiments are performed in SYSLAB (part of PowerLabDK) which is a flexible laboratory for distributed energy resources consisted of real power components parallelled with communication infrastructure and control nodes in a dedicated network. The complete test setup is distributed over the Risø Campus of Technical University of Denmark. The studied experimental setup is depicted in Fig. 2 and Fig. 3. As seen in the figures, the setup consists of the following components:

- 3 commercially available EVs (Nissan Leaf) with single phase 16 A (230 V) charger and 24 kWh Li-Ion battery.
- 2-blade wind turbine Gaia with rated power $P_n = 11\ kW$.
- 45 kW resistive load (15 kW per phase) controllable per single-phase in 1 kW steps.
- set of Al 240 mm^2 underground cables approximately 1.95 km in length with AC resistance at 45^oC $R_{AC} = 0.14\Omega/km$ and series reactance $X = 0.078\Omega/km$
- 75 m of Cu 16 mm^2 cable with AC resistance at 45^oC $R_{AC} = 1.26\Omega/km$ and series reactance $X = 0.076\Omega/km$
- $10/0.4\ kV$, 200 kVA transformer.

The wind turbine connected to the test grid, although not significantly large as active power source, provides stochastic active and reactive power variation to the system. Additionally, it makes the test grid closer to a possible realistic distribution grid with more diverse components than just pure resistive loads.

From the line parameters above, the X/R ratio is calculated to highlight the impedance characteristic of the grid: X/R equals to 0.43. The X/R ratio of the test system is quite low i.e., in the range of the typical LV system and is comparable to CIGRE network [28] as well as other benchmark systems.

Therefore, active power modulation is the most effective way to control voltage levels although reactive power control could also be effective to a certain extent as shown in reference [11].

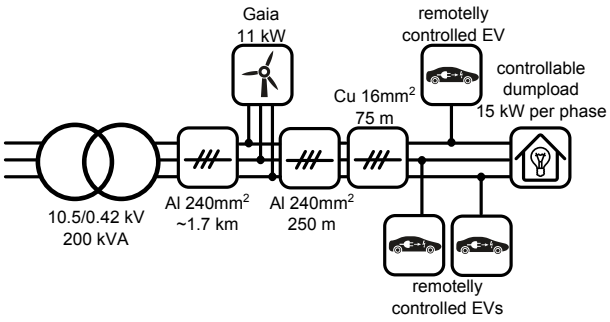

Fig. 2: Schematic overview of the experimental setup

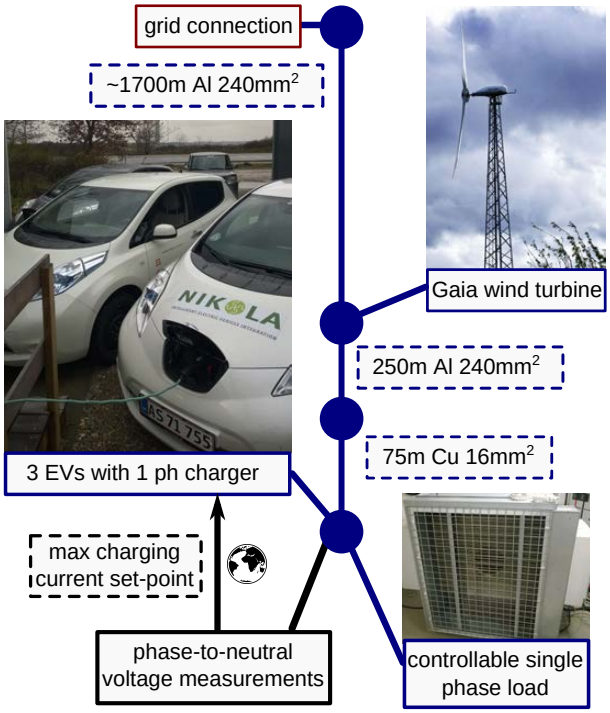

Fig. 3: Experimental setup for the voltage unbalance testing

The EV chargers are not equipped with Vehicle-to-Grid capability, but unidirectional charging rate can be remotely enabled and modulated between 6 A and 16 A with 1 A steps.

B. EV control algorithm

To enable EV smart charging, a control loop has to be established. The control loop typical consists of three components connected to the system: measurement device, controller and actuator. In this work, the measurement equipment providing the input for the controller is DEIF MIC-2 multi-instrument meter with 0.5% accuracy and 1 second sampling rate. The actuator that transfers the control signal to the system under control is Nissan Leaf EV with controllable charging current. The controller is designed as a simple, yet robust droop control algorithm, as described in II-A, and integrated to the following control loop:

1) Phase-to-neutral voltage is measured locally at each EVSE on second basis
2) The EV smart charging controller receives and evaluates:
   - Phase-to-neutral voltages at the connection point
   - The actual charging rate
3) The controller sends a control signal to the Electric Vehicle Supply Equipment (EVSE) for adjusting the EV charging current limit.

The control architecture, with the entire control loop, is shown in Fig. 4.

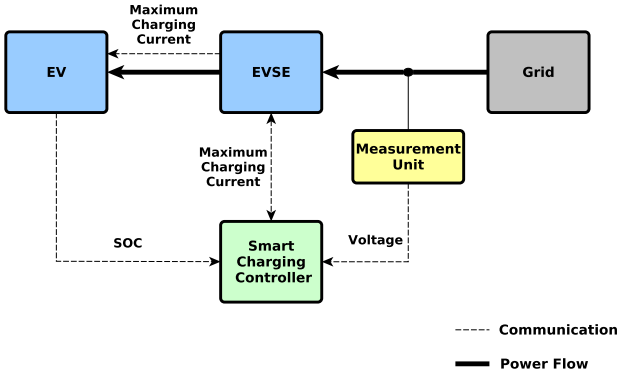

Fig. 4: Information and control flow for the smart charging of each vehicle

In this approach, the flexibility in the EV charging power could be exploited to preserve stable phase-to-neutral voltages while maintaining the user comfort since the EV is primarily used for transportation functions. The phase-to-neutral voltages are measured locally at the (EVSE) using the built-in power meter, which are then compared to the nominal voltage and chosen thresholds. Since the primary goal of this validation is proving that the controlled EV charging can improve the power quality, smart charging function for reaching the target State of Charge (SOC) by the scheduled time of departure has been omitted and left for future work.

C. Experimental procedure and result evaluation

The experiments are intended to test the EV capability to modulate the charge level according to the voltage measurements in order to provide voltage support and partially mitigate the voltage unbalances. The per-phase controllable load is used to represent a realistic variable household consumption, creating voltage unbalances due to different load fractions per phase.

Several test-cases will be analysed to evaluate the power quality in such a system. The full overview of conducted test scenarios is shown in Table I. The scenarios could be grouped into four main groups:

1) Uncontrolled charging scenario with no EV charging control - test scenario I.
2) Controlled charging scenario with 5% droop and minimum charging current of 6 A - test scenarios II to IV.

3) Controlled charging scenario with 5% droop and minimum charging current of 0 A - test scenarios V - VII.
4) Controlled charging scenario with 2.5% droop and minimum charging current of 6 A - test scenario VIII.

For each test scenario the single-phase load is increased from 0 up to 43 A in 5 steps.

The system performance is evaluated by measuring relevant phase-to-neutral voltages as well as VUFs. This analysis allows the investigation of issues arising when dealing with practical implementation of voltage support, such as communication latency, power and voltage measurement inaccuracies, and coordination of more sources. Additionally, it should be noted that the experimental setup is only using communication and control equipment that follows existing industry standards. Hence, tested control algorithms can be applied to any real grid operation, ensuring the interoperability and minimal integration effort.

IV. Results

To demonstrate the differences between uncontrolled and controlled EV charging, test scenarios shown in Table I were executed. Following subsections present the most relevant findings for each of the conducted scenarios.

A. Voltage quality using uncontrolled EV charging

Firstly, the setup is tested using the most occurring situation nowadays - uncontrolled EV charging, while the resistive load at the end of the feeder, representing the domestic consumption, is gradually increasing. Measured voltages at the EVSE, load increase steps and corresponding EV charging currents can be seen in Fig. 5.

Clearly, such voltage quality is unsatisfactory as phase-to-neutral voltages drop below 0.9 U_n on all phases for the maximum load step. Meanwhile, the EVs are steadily charging at the maximum current regardless of the grid status since there is no implemented control. It should be noted that one of the EVs is charging at 17 A even though the same 16 A rated current applies to all of the cars. This shows how even the same EV models differing only in the production year can have different impact on the power quality. Similar findings will be discussed later on for controlled charging scenarios. In addition, one can notice how the load steps are not completely synchronised for all three phases which will also apply to later on scenarios. The reason lies in the lack of automatic control, i.e., the steps had to be manually input into the device. However, this fact does not influence the EV behaviour.

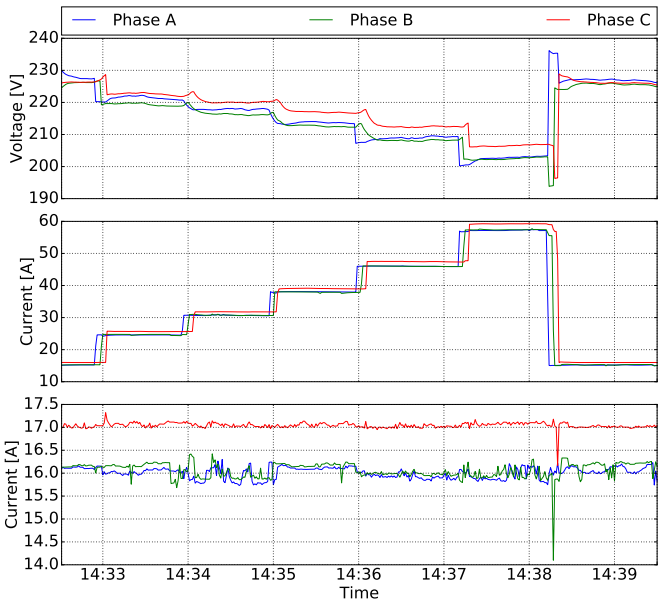

Fig. 5: Voltage and load current measurements for EV uncontrolled charging - test scenario I

B. Voltage quality using EV droop control

Firstly, the droop controller with a 5% droop and minimum charging current of 6 A, shown as *real droop 1* in Fig. 1a, is applied to the EV charging. Measured voltage at the EVSE, load increase steps and corresponding EV charging currents can be seen in Fig. 6, whereas Fig. 7 shows the correlation between the measured phase-to-neutral voltage and the measured EV response for each of the phases. The correlation plot closely resembles the droop characteristic shown in Fig. 1a.

It can be observed that the EVs already start responding at the second load step since the voltage exceeds the droop control boundary of 0.95 U_n. Even for the maximum loading, the voltages are kept above 0.9 U_n as EVs are reducing the charging currents to a minimum value of 6 A. Another interesting phenomena to notice is that the phase-to-neutral voltage on the unloaded phase is rising when the load is increased on the other phases. That is due to a floating, not grounded, neutral line, which introduces a greater voltage unbalance.

TABLE I: Overview of conducted scenarios

Scenario	I	II	III	IV	V	VI	VII	VIII
Load	3 phase	3 phase	2 phase	1 phase	3 phase	2 phase	1 phase	3 phase
Droop Control	-	5%	5%	5%	5%	5%	5%	2.5%
Min EV Current	16A	6A	6A	6A	0A	0A	0A	6A
Maximum load current on phase a [A]	43	43	43	0	43	43	0	43
Maximum load current on phase b [A]	43	43	43	0	43	43	0	43
Maximum load current on phase c [A]	43	43	0	43	43	0	43	43

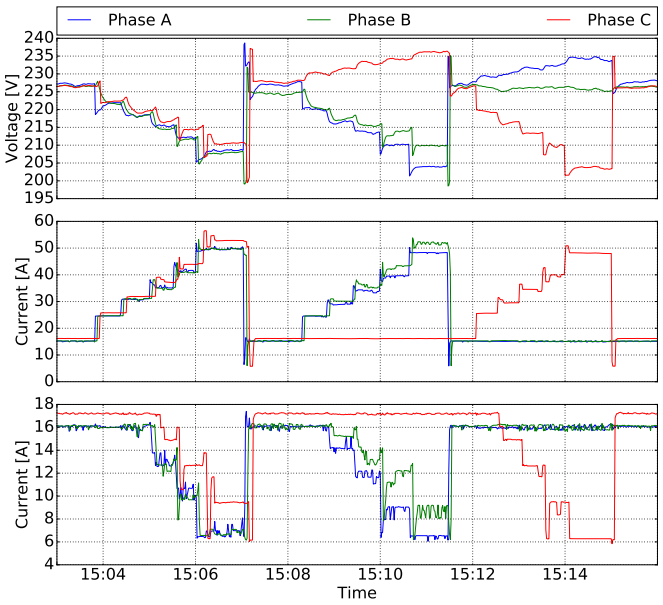

Fig. 6: Voltage, load and charging current measurements for EV smart charging test scenarios: II - 15:03 to 15:08, III - 15:08 to 15:12 and IV - 15:12 to 15:16

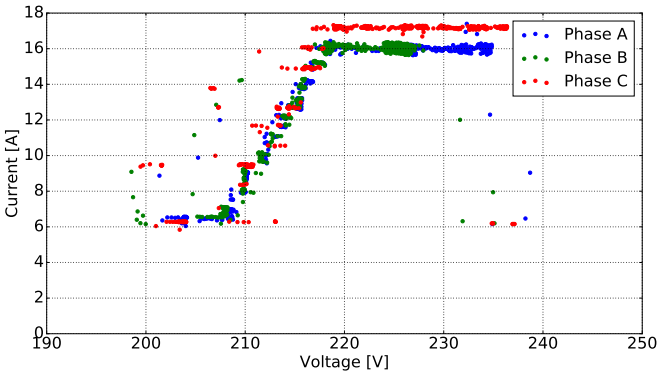

Fig. 7: Correlation plot between measured phase-to-neutral voltage and EV current for test scenarios II to V

C. Voltage quality using EV droop control with stopping the charge

Controlled EV charging according to IEC61851 also has the ability to stop and restart the charging of the vehicle. This function could potentially further improve the power quality in the system as the load from the EV could temporarily be removed. Therefore, the same droop controller with 5% slope, but minimum charging current of 0 A is studied. The modification of the droop curve is done as shown in Fig. 1a as *real droop 2*.

Similarly to previous scenarios, Fig. 8 shows the measured voltage at the EVSE, load increase steps and corresponding EV charging currents.

Fig. 9 presents the correlation between the controller's input voltage and the measured EV response. The relation pattern is partly resembling the curve shown on Fig. 1a as *real droop 2*. Although, unlike in the droop curve two clear drops at 6 and

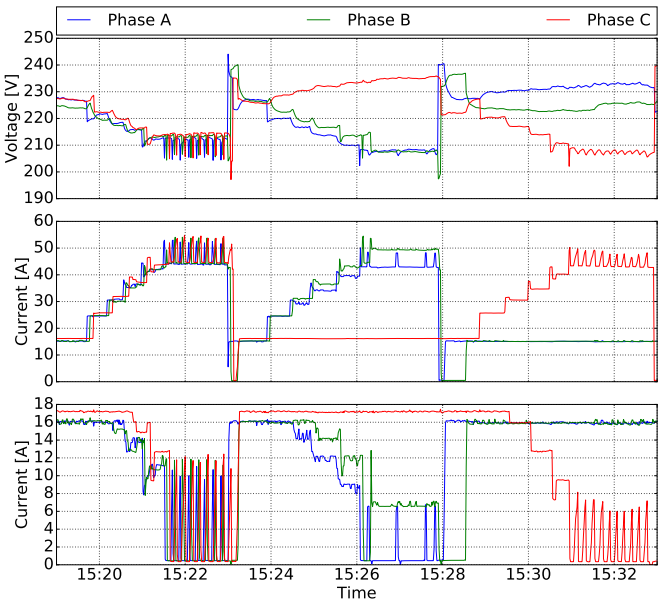

Fig. 8: Voltage, load and charging current measurements for EV smart charging test scenarios: V - 15:19 to 15:24, VI - 15:24 to 15:28 and VII 15:28 to 15:33

10 A are present. The second drop appears due to controller induced oscillation explained further.

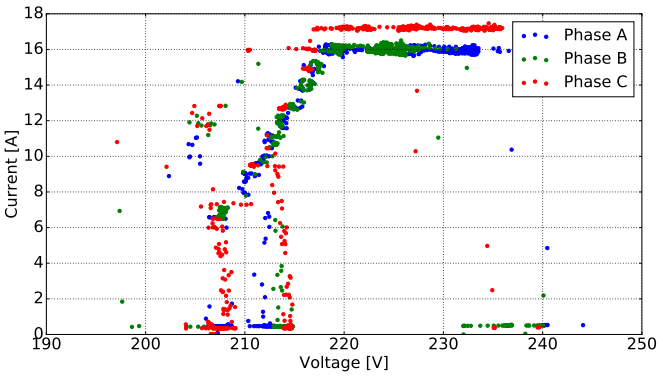

Fig. 9: Correlation plot between measured voltage and EV current for test scenarios V to VII

Fig. 8 shows that the system response is almost identical to the test scenarios II to IV, besides in the maximum loading case. At that point, one can notice oscillations in test scenario V and VII which occur due to the brief voltage dip for the last load step. This step briefly puts the voltage under 0.9 U_n, which triggers the controller to stop the charging of the EVs. As the EVs stop charging, the voltages rise to about 0.93 U_n, which makes the controller restart the EV charging since the voltage is now high enough. The restarting process takes about 8 seconds. However, as the EVs restart the charging, the voltage briefly dips under 0.9 U_n again making the controller to stop the charging. This instability repeats as long as the voltage level stays close to 0.9 U_n. In scenario VI, EV on phase a stably mitigates the voltage unbalance by stopping the charge. At the same time, EV on phase b also stabilises the

charging current at 7 A, right at the lower limit of stopping the charge. The aforementioned oscillation issues could be solved by modifying the controller to detect the voltage transients and only react for the steady state voltage measurements. However, this has been omitted from the conducted study and left for future work.

D. Voltage quality using EV droop control with steeper droop characteristic

The droop control has then been modified, making it more steep as shown in Fig. 1b. As for the previous scenarios, measured voltage at the EVSE, load increase steps and corresponding EV charging currents can be seen in Fig. 10, whereas the correlation is depicted in Fig. 11. As the droop curve used in this scenario is more steep, minor oscillations are present on phase c due to a slower response of the EV on this phase.

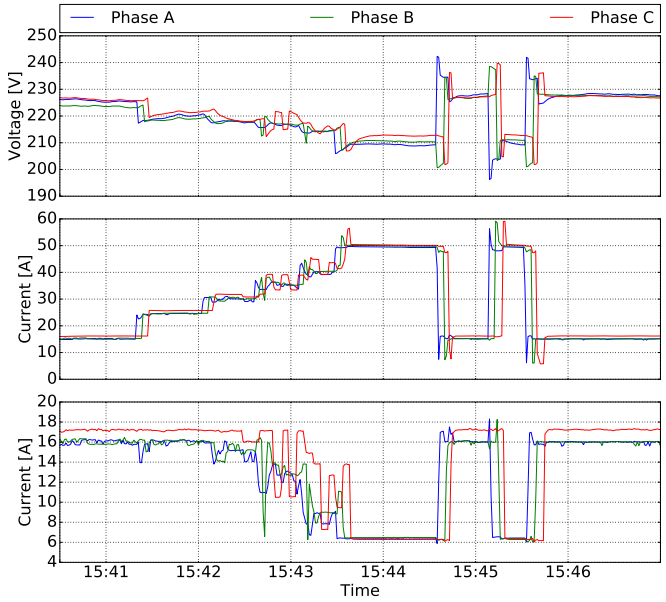

Fig. 10: Voltage, load and charging current measurements for EV smart charging - test scenario VIII

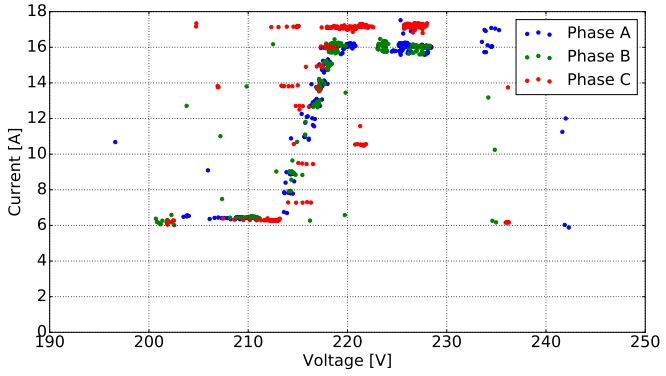

Fig. 11: Correlation plot between measured voltage and EV current for test scenario VIII

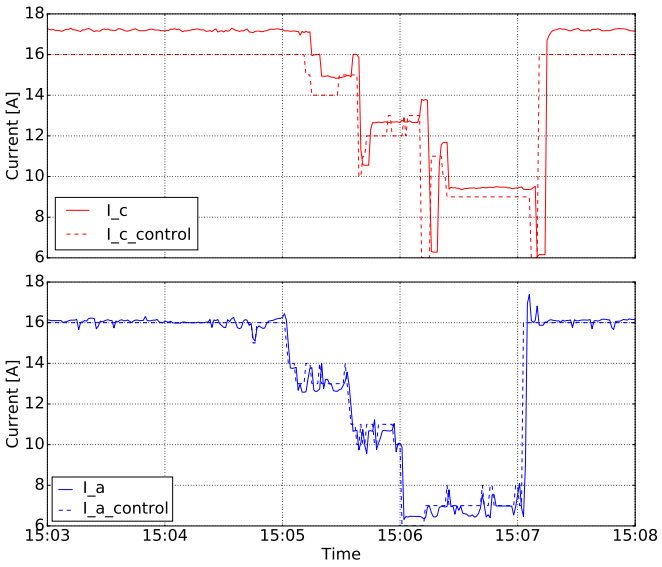

Fig. 12: Sample charging current control signal and measured value for EV smart charging - test scenario II

Moreover, Fig. 12 illustrates the difference between the control and the actual EV charging current. The EVs on phase a and b respond to the control signal in 1 to 2 seconds, while EV on phase c takes 4 to 5 seconds. The difference is due to a older production year for the EV connected to phase c. It is also important to note that the control signal sent to the EV is merely an upper limit for the charging current. Hence, the actual charging current of the vehicle should be below the set limit. However, EV on phase c is violating the set charging current limit by 1 A. It is an atypical behaviour possibly caused by a recent charger firmware update.

E. Result overview

According to EN50160, the voltage quality is typically assessed over a week with 10 minutes average intervals. However, the main reason to focus on a shorter period of time in this paper, is to evaluate the performance of the controller. The limited 10 minute intervals show the system response to the load event and control actions taken, in this period the voltage in the system stabilizes to new steady states, therefore this experimental time window can be extrapolated to longer time periods. Additionally, vehicles are solving the problem partly caused by themselves thus, it is reasonable to experience less voltage problems if EVs are not charging.

The setup was tested in 8 test scenarios with the result summary shown in Table II. Maximum VUF is calculated from the values observed at the maximum feeder loading. Steady state voltage values in the maximum load case are also shown for each test scenario. Finally, the voltage drops between the grid and EV connection points at the maximum load case are shown.

Firstly, one should note that smart charging when all 3 phases are evenly loaded (test scenarios I, II, V and VIII) improves the VUF. Secondly, VUF in heavily unbalanced scenarios is much beyond the standard limit for scenarios III,

TABLE II: Maximum VUF, steady state voltage values and voltage drop from grid connection to the EV connection point

Scenario	I	II	III	IV	V	VI	VII	VIII
Load	3 phase	3 phase	2 phase	1 phase	3 phase	2 phase	1 phase	3 phase
Droop Control	-	5%	5%	5%	5%	5%	5%	2.5%
Min EV Current	16A	6A	6A	6A	0A	0A	0A	6A
$\mathbf{VUF_{max}}[\%]$	1.3	0.8	9.0	7.9	0.6	8.4	6.4	1.0
$\mathbf{U_{an_{maxloadss}}}[\mathbf{V}]$	202.8	208.4	203.6	234.5	212.5	208.0	233.0	209.0
$\mathbf{U_{bn_{maxloadss}}}[\mathbf{V}]$	202.6	207.9	209.6	225.7	213.5	207.5	225.0	210.5
$\mathbf{U_{cn_{maxloadss}}}[\mathbf{V}]$	206.6	210.5	235.9	203.5	214.0	235.0	208.5	212.6
$\mathbf{\Delta U_{an}}[\mathbf{V}]$	33.0	27.4	32.1	1.6	23.5	27.8	3.0	27.0
$\mathbf{\Delta U_{bn}}[\mathbf{V}]$	30.3	25.1	23.1	7.3	20.7	25.4	7.2	22.6
$\mathbf{\Delta U_{cn}}[\mathbf{V}]$	28.3	24.4	-1.2	31.3	19.7	-0.1	27.5	22.3

IV, VI and VII. H ere, the controller tries to minimise the unbalance by setting EV charging current to the minimum value specified for each scenario. However, vehicles alone can not eliminate the unbalance in the case of maximum loading, since controllable EVs represent only 17 % of the total load. This flexibility could be extended to 25 % if the charging is stopped. It should be noted that values of smart charging scenarios V, and VII were calculated from the measurements of the steady states between the oscillations. Nevertheless, greater controllable power amount results in significant improvements in power quality for scenarios V to VII.

V. Conclusion

This work presented a method for improving the power quality of a low voltage network by intelligently controlling EV charging current. The validation showed how uncontrolled EV charging can significantly reduce the power quality of low voltage networks, especially in unbalanced networks with long feeder lines. It is shown that EV smart charging, even with a simple decentralised autonomous droop controller, can solve some of the power quality issues. The improvements include reduced voltage drops at the long feeder branches and potentially reduced VUFs in the cases of unbalanced loading. However, EVs should be integrated carefully, as shown in scenarios V and VII, since large power steps at the nodes with poor voltage quality could introduce even more severe problems like large voltage oscillations. Mitigating such problems requires more sophisticated control which accounts for transient voltage drops or introduces input filters. Nevertheless, it has been shown that local smart charging controllers can improve power quality in the distribution systems even in extreme cases. Consequently, this allows the integration of higher EV amount in the distribution grids without the need for unplanned and costly grid reinforcements. As the controller and the supporting infrastructure is made from standardised components, such control schemes could potentially be integrated in the EVSE with minimal development effort which makes such solution economically attractive.

Further research will continue to investigate the effects of the EV charging on the power quality by expanding the list of test scenarios, implementing more sophisticated control algorithms and exploring the effects on other power quality indicators, such as total harmonic distortion. Another topic not touched upon in this work is the user comfort. While controllable charging provides improvements in the power quality, it could potentially inconvenience the vehicle owner by not providing required state of charge level when EV is needed. This issue should be addressed as a part of the smart charging algorithm allowing the user to have a conveniently charged vehicle while still providing the voltage support service when EV is charging.

Acknowledgment

This work is supported by the Danish Research Project “NIKOLA - Intelligent Electric Vehicle Integration” under ForskEL kontrakt nr. 2013-1-12088. More information at www.nikolaproject.info.

References

[1] R. Walling, R. Saint, R. Dugan, J. Burke, and L. Kojovic, “Summary of distributed resources impact on power delivery systems,” *Power Delivery, IEEE Transactions on*, vol. 23, no. 3, pp. 1636–1644, July 2008.

[2] K. Clement-Nyns, E. Haesen, and J. Driesen, “The impact of vehicle-to-grid on the distribution grid,” *Electric Power Systems Research*, vol. 81, no. 1, pp. 185–192, Jan. 2011.

[3] Dansk Energi, Dong Energy, and Energinet.dk, “Analysis no. 5 – Scenarios for the deployment of electric vehicles (in Danish),” Tech. Rep., 2013. [Online]. Available: http://www.danskenergi.dk/Analyse/Analyser/

[4] M. Coppo, R. Turri, M. Marinelli, and X. Han, “Voltage management in unbalanced low voltage networks using a decoupled phase-tap-changer transformer,” *Power Engineering Conference (UPEC), 2014 49th International Universities*, pp. 1–6, Sept 2014.

[5] M. Gray and W. Morsi, “Power quality assessment in distribution systems embedded with plug-in hybrid and battery electric vehicles,” *Power Systems, IEEE Transactions on*, vol. 30, no. 2, pp. 663–671, March 2015.

[6] C. Jiang, R. Torquato, D. Salles, and W. Xu, “Method to assess the power-quality impact of plug-in electric vehicles,” *Power Delivery, IEEE Transactions on*, vol. 29, no. 2, pp. 958–965, April 2014.

[7] P. Andersen, M. Marinelli, O. Olesen, C. Andersen, G. Poilasne, B. Christensen, and O. Alm, “The Nikola project Intelligent electric vehicle integration,” pp. 1–6, Oct 2014.

[8] J. García-Villalobos, I. Zamora, J. I. San Martín, F. J. Asensio, and V. Aperribay, “Plug-in electric vehicles in electric distribution networks: A review of smart charging approaches,” *Renewable and Sustainable Energy Reviews*, vol. 38, pp. 717–731, 2014.

[9] W. Kempton and J. Tomić, “Vehicle-to-grid power implementation: From stabilizing the grid to supporting large-scale renewable energy,” *Journal of Power Sources*, vol. 144, pp. 280–294, 2005.

[10] S. Martinenas, A. Pedersen, M. Marinelli, P. Andersen, and C. Treaholt, “Electric vehicle smart charging using dynamic price signal,” *Electric Vehicle Conference (IEVC), 2014 IEEE International*, pp. 1–6, Dec 2014.

[11] K. Knezović, M. Marinelli, R. Moller, P. Andersen, C. Treaholt, and F. Sossan, "Analysis of voltage support by electric vehicles and photovoltaic in a real danish low voltage network," *Power Engineering Conference (UPEC), 2014 49th International Universities*, pp. 1–6, Sept 2014.
[12] K. Knezović, P. Codani, M. Marinelli, and Y. Perez, "Distribution grid services and flexibility provision by electric vehicles: a review of options," *Power Engineering Conference (UPEC), 2015 50th International Universities*, pp. 1–6, Sept 2015.
[13] Z. Wang and S. Wang, "Grid power peak shaving and valley filling using vehicle-to-grid systems," *Power Delivery, IEEE Transactions on*, vol. 28, no. 3, pp. 1822–1829, July 2013.
[14] S. Mocci, N. Natale, F. Pilo and S. Ruggeri, "Demand side integration in LV smart grids with multi-agent control system," *Electric Power Systems Research*, vol. 125, pp. 23 – 33, 2015.
[15] M. Gonzalez Vaya and G. Andersson, "Centralized and decentralized approaches to smart charging of plug-in vehicles," *Power and Energy Society General Meeting, 2012 IEEE*, pp. 1–8, July 2012.
[16] P. Richardson, D. Flynn, and A. Keane, "Local versus centralized charging strategies for electric vehicles in low voltage distribution systems," *Smart Grid, IEEE Transactions on*, vol. 3, no. 2, pp. 1020–1028, June 2012.
[17] S. Habib, M. Kamran, and U. Rashid, "Impact analysis of vehicle-to-grid technology and charging strategies of electric vehicles on distribution networks – a review," *Journal of Power Sources*, vol. 277, pp. 205 – 214, 2015.
[18] M. Singh, I. Kar, and P. Kumar, "Influence of EV on grid power quality and optimizing the charging schedule to mitigate voltage imbalance and reduce power loss," *Power Electronics and Motion Control Conference (EPE/PEMC), 2010 14th International*, pp. 196–203, Sept 2010.
[19] N. Leemput, F. Geth, J. Van Roy, A. Delnooz, J. Buscher, and J. Driesen, "Impact of electric vehicle on-board single-phase charging strategies on a Flemish residential grid," *Smart Grid, IEEE Transactions on*, vol. 5, no. 4, pp. 1815–1822, July 2014.
[20] S. Weckx and J. Driesen, "Load balancing with EV chargers and PV inverters in unbalanced distribution grids," *Sustainable Energy, IEEE Transactions on*, vol. 6, no. 2, pp. 635–643, April 2015.
[21] J. P. Lopes, S. A. Polenz, C. Moreira, and R. Cherkaoui, "Identification of control and management strategies for LV unbalanced microgrids with plugged-in electric vehicles," *Electric Power Systems Research*, vol. 80, no. 8, pp. 898 – 906, 2010.
[22] Chattopadhyay, Surajit. and Mitra, Madhuchhanda. and Sengupta, Samarjit., "Electric power quality," pp. 1 – 182, 2011.
[23] M. Marinelli, S. Martinenas, K. Knezović and P. B. Andersen, "Validating a centralized approach to primary frequency control with series-produced electric vehicles," *Journal of Energy Storage*, vol. 7, pp. 63–73, 2016.
[24] P. Gnacinski, "Windings temperature and loss of life of an induction machine under voltage unbalance combined with over- or undervoltages," *Energy Conversion, IEEE Transactions on*, vol. 23, no. 2, pp. 363–371, June 2008.
[25] H. Markiewicz and A. Klajn, "Voltage disturbances standard EN 50160," pp. 1–16, 2004.
[26] "IEEE Recommended Practice for Monitoring Electric Power Quality," *IEEE Std 1159-1995*, 1995.
[27] IEC TC69, "IS 61851-1:2010 Ed. 2.0," *IEC Standard*, 2010.
[28] K. Strunz, N. Hatziargyriou, and C. Andrieu, "Benchmark systems for network integration of renewable and distributed energy resources," *Cigre Task Force C*, vol. 6, pp. 04–02, 2009.

Sergejus Martinenas (S'14) was born in Elektrenai, Lithuania, in 1989. He received a BSc degree in mechatronics engineering from the University of Southern Denmark in 2011, and an MSc degree in electrical engineering from the Technical University of Denmark in 2014. He is currently pursuing the Ph.D. degree in electrical engineering at DTU.

His research focuses on enabling technologies for electric vehicle integration into smart grids.

Katarina Knezović (S'13) was born in Zagreb, Croatia, in 1989. She has received her BSc and MSc degrees in electrical engineering from the University of Zagreb, Croatia, in 2011 and 2013 respectively. She is currently pursuing a Ph.D. degree in electrical engineering at DTU.

Her research interests include power-system modeling, distribution networks, grid-coupling of electric vehicles, and the services they can provide, both in local and system-wide cases.

Mattia Marinelli (S'10-M'12) was born in Genova, Italy, in 1983. He received BSc and MSc degrees in electrical engineering from the University of Genova in 2005 and 2007. In March 2011 he achieved the European Ph.D. degree in power systems. Since September 2012 he has been with the Technical University of Denmark (DTU).

His research regards power system integration studies, wind and solar data analysis, electric vehicles and distributed energy resources modeling.

Pub. H. Electric Vehicle Smart Charging using Dynamic Price Signal

Electric Vehicle Smart Charging using Dynamic Price Signal

Sergejus Martinenas, Anders Bro Pedersen, Mattia Marinelli, Peter Bach Andersen and Chresten Træholt
Center for Electric Power and Energy, DTU - Technical University of Denmark
Contact Person: Sergejus Martinenas, smar@elektro.dtu.dk

***Abstract*—With yearly increases in Electric Vehicle (EV) sales, the future for electric mobility continues to brighten, and with more vehicles hitting the roads every day, the energy requirements on the grid will increase, potentially causing low-voltage distribution grid congestion. This problem can, however, be resolved by using intelligent EV charging strategies, commonly referred to as "Smart Charging". The basic approach involves modifying the default vehicle charging scheme of "immediate charging", to a more optimal one that is derived from insight into the current state of the grid. This work proposed in this paper, involves a real-time control strategy for charging the EV using a dynamic price tariff, with the objective of minimizing the charging cost. Two different charging scenario are investigated, and the results are verified by experiments on a real Electric Vehicle. Finally, the costs of the proposed solutions are compared to the default charging scheme.**

Keywords – Smart Charging, Smart Grid, Price Signal, Dynamic Tariff, Electric Vehicles, Information and Communication Technology

I. Introduction

The balance between production and consumption in the electrical grid has to be maintained at all times.With the number of EVs continuing to grow, their charging will keep adding to the load on the grid. To that effect, having too much uncontrolled charging could have a devastating impact on the grid balance, potentially increasing the load on the system to the level of congestion in some time periods. Today's Danish Low-Voltage 0.4 kV grid infrastructure is only capable of supporting only up to 30%-40% of EV penetration when charging at night [1]. Assuming that EVs are charging on a single phase and using 16A. Higher charging rates and number of vehicles would create grid congestion. Two immediate solutions exist to aid a higher penetration: to simply reinforce the grid along with the increase in load or intelligently integrate EVs by controlling their charging power, in order to even out the load on the grid. The method for modifying Electric Vehicle power consumption in response to grid dynamics is similar to the method, that is commonly used with other electric appliances: this method is known as "Demand Response" [2] [3]. A relatively new way to control the electricity demand is by using dynamic price signals. The price signal is based on the results of the EcoGrid EU project, that strives to create a real-time electricity price market based on actual renewable generation and power consumption. Controllers in the devices react to changes in a broadcasted electricity price and adjusts their consumption accordingly. This approach is especially viable for EVs, because their consumption is limited by the size of the battery and usage patterns are predictable.

This work focuses on the design and testing of a platform, using numerical simulation and real-world EV implementations.

The paper is organized as follows: Section II presents an overview of all the elements of the smart charging system. Section III describes the test cases used in the work. Section IV presents the simulation and testing results. Section V discusses the results as well as the potential commercial applications.

II. Smart Charging

Smart Charging is the ability of an EV to be charged according to predefined schedule [4] or in response to an external signal e.g. the electricity price. EVs could be charged in a smart way, taking into account the grid capacity and user demand. This would solve the biggest problem for EV integration into the power grid - grid congestion, thus allowing higher EV penetration rate. This would be possible without major grid reinforcements, which carries substantial economic benefits [5]. There are multiple ways to implement Smart Charging control: either by limiting the charging rate via the Electric Vehicle Supply Equipment (EVSE), using the IEC61851 standard pilot communication or by directly controlling the power of the vehicle charger. In this paper, the smart charging is achieved using direct EV build-in charger power control.

A. System Design

To implement the smart charging service, the system needs to include a controllable EV connected to the grid via an EVSE as well as a built-in smart charging controller.

The specific testing platform developed and described in this paper, was built using following components:

- **EV** - DTU and UD modified AC Propulsion eBox with 35kWh battery and Power Electronics Unit (PEU) capable of single phase bidirectional power transfers of up to 20kW [6]. It is controlled by the EV computer that interfaces with the PEU using a small build-in embedded

This work is supported by the Danish Research Project "NIKOLA - Intelligent Electric Vehicle Integration"- under ForskEL kontrakt nr. 2013-1-12088. More information (www.nikolaproject.info).

computer referred to as the Vehicle Smart Link (VSL) [7].

- **VSL** - an embedded computing interface, used for mediating the communication with the eBox PEU, in which it is housed. Additionally, the VSL is responsible for implementing IEC 61851 standard, allowing the vehicle to function with a standard EVSE.
- **eBox Pollserver** - vehicle monitoring/control server with RESTful Application Programming Interface (API). Runs on the vehicle computer and is used for remote and local control.
- **EVSE** - technical term for charging spot, in this case custom built with a maximum 32A charging current.
- **Smart Charging Controller** - runs on an external network connected computer, which performs the following functions:
  - monitoring the price stream and the EV status
  - calculating and updating the charging schedule
  - dispatching control signals to the EV
- **EcoGrid Price Streams** - dynamic tariff based on current and predicted future grid status. For simplicity, and replayability, this setup was implemented using a recording of the price signal streams for last year [8].

The testing system developed in this work, described in detail above, is shown the diagram in Fig. 1.

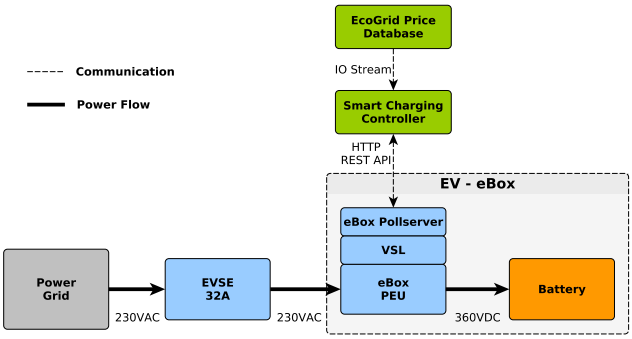

Fig. 1. Smart charging experimental setup

While not explicitly shown, all of the system components depicted in Fig. 1, have communication interfaces for control and data exchange.

B. EcoGrid Price Signal

Smart charging is implemented according to the EcoGrid price signal [9]. These prices are generated based on the Nord Pool spot, adjusted using the immediate as well as predicted grid state. Something which, especially in Denmark, is largely dictated by the wind conditions [10]. As previously stated as well as depicted in Fig. 1, the controller is getting the price updates from a prerecorded price stream. In this interface the live price update is emulated, by extracting new values from the price history using the moving window.

The EcoGrid price stream consists of three price streams:

- **Real-time price** - the actual electricity price, used for calculating the electricity bill, updated every 5 minutes
- **Hour ahead price** - a collection of 5 minute electricity price predictions for the next hour, updated once an hour
- **Day ahead price** - a collection of hourly price predictions for next 24 hours, updated once a day

Since the prices are provided for different time slots in three different streams, the combined price for the next 24 hours is composed as shown in Fig. 2. This combined price stream is useful for determining actual electricity price and predicting its' variation for next 24 hours.

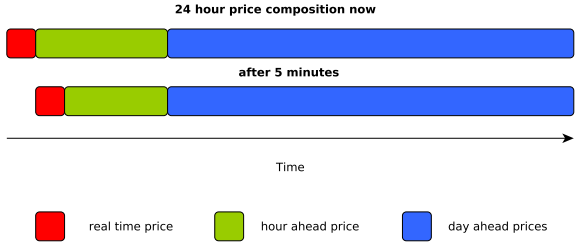

Fig. 2. EcoGrid price timing

The aggregated price signal consists of available price information from each price stream. As real-time price is only available and updated every 5 minutes it represents only a small part in the beginning of the signal. The other two price streams are updated once an hour and once a day. The first hour ahead price is placed right after the real-time price. The first value of a hour-ahead price is substituted by the real-time price, producing a combined price signal for following hour. Likewise, the day ahead price is added to the combined price signal extending it to the next day. This way each price stream occupies the time slot closest to real-time. The consumer pays the electricity bill according to the real-time price.

Figures 3 and 4 show samples of the EcoGrid price stream, from a zoomed out as well as a more detailed view.

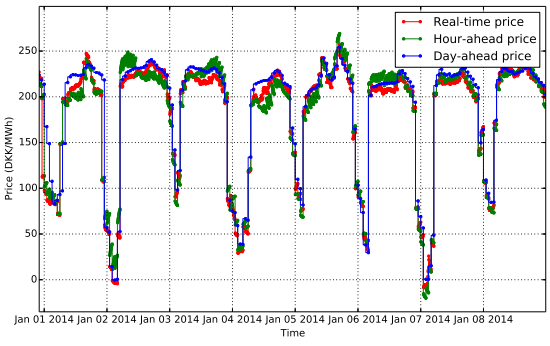

Fig. 3. EcoGrid price streams

The first trend noticeable in Fig. 3 is the periodic electricity price fluctuation: it is high during the day, then it falls in

the late evening and stays low until early morning. Another unusual detail is that, the electricity price sometimes goes below zero twice in the shown time period, specifically on January 2 and January 7. It can be explained by energy overproduction from renewable resources, particularly wind farms.

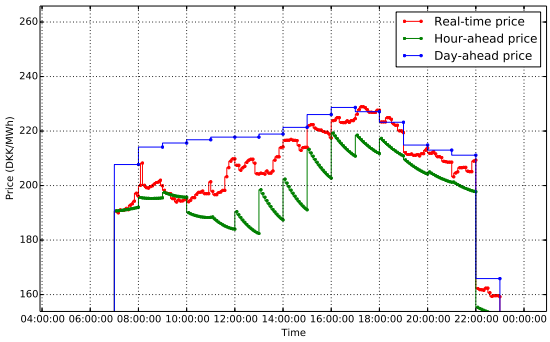

Fig. 4. EcoGrid price stream close up view

C. Electric Vehicle Communication

The EV computer is running an application, which either returns the measurement upon request or receives and processes requests from the controller into updated EV charge commands the VSL board. The VSL in turn is running an application, which acts as an interface, translating and forwarding those commands to the PEU unit. The higher level communication is implemented based on HyperText Transfer Protocol (HTTP). On the embedded side of the system (on the VSL and below) communication changes to serial UART, which is a common component used in industry for such applications.

The full communication path from the controller to the PEU is shown in Fig. 5.

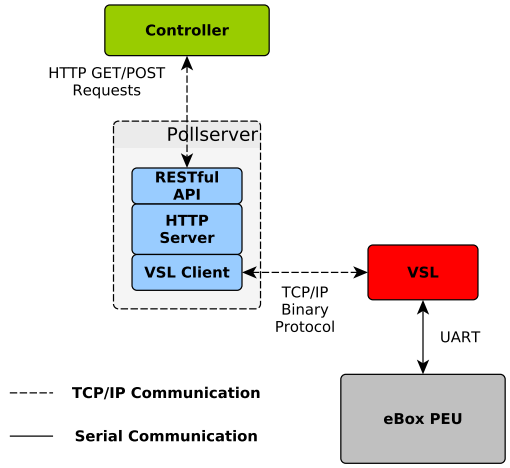

Fig. 5. Control message path from smart charging controller to the PEU

As shown in the Fig. 5, high level communication has been implemented for communication with the EV using RESTful architecture. REpresentational State Transfer (REST) is a software architectural style rather than a communication protocol. It was first described in the PhD thesis of R.Fielding back in 2000 [11]. The most profound difference between REST and other more traditional web services, is that data is presented strictly as a resource and not through a list of functions. It, in other words, ignores the implementation details of the component and protocol, focusing on their roles, interaction and interpretation. of significant data elements. RESTful services has successfully been used in power system architectures in the past, mapping existing standards such as IEC61850 [12].

The communication protocol is kept as simple and clear as possible to ease later expansion and higher level applications such as IEC15118.

The structure of the RESTful Unique Resource Identifier (URI) request, designed for this work, is shown in Fig. 6.

HTTP://	DeviceID:port/	Variable	=Value

Fig. 6. RESTful URI request structure

Following is the RESTful API communication example: To read the measurements or parameters of the EV, an HTTP GET request is sent to the URI:

```
http://ebox:8080/measurements
```

The response received is formatted in JavaScript Object Notation (JSON):

```
{ "System_Time": 1399382195,
  "Line_V": 229.000000, "SOC": 67,
  "Max_C_Amps": 31, "Max_D_Amps": 31,
  "Requested_Mode": 1, "Actual_Mode": 1,
  "Requested_Amps": -1.000000,
  "Actual_Amps": -1.200000, "Error": 0 }
```

For setting new control parameters, such as charging current or operation mode, a HTTP POST or PUT request is sent. For example, to update the charging current to -16A (negative values indicate charging), the HTTP POST request is sent to the following URI:

```
http://ebox:8080/Requested_Amps=-16
```

This RESTful API is used by the controller application to read the data and control the EV.

D. Charging Optimization

The Smart Charging simulation and experimental optimization code was written in Python using the PuLP linear optimization library [13].

The basic algorithm used for the smart charging controller, is outlined in Algorithm 1 below:

while *true* **do**
  read and process price stream data;
  read the actual EV State of Charge (SOC);
  calculate the optimal charging schedule;
  actuate charging power for the EV (P_{ch});
  wait for 5 minutes
end

Algorithm 1: Smart Charging Control

Prices for the charging period are read from the database with the structure presented in Fig. 2. The charging cost is then formulated as a linear programming problem for minimization, as shown in Equation 1. The constraints used are listed in Equations 2 and 3.

$$TotalPrice_{charge} = \sum_{i=1}^{N} \left(\frac{5}{60} \cdot power_i \cdot price_i \right) \quad (1)$$

$$E_{start} + \sum_{i=1}^{N} \left(\frac{5}{60} \cdot P_i \cdot \eta \right) \leq E_{capacity} \quad (2)$$

$$E_{end} + \sum_{i=1}^{N} \left(\frac{5}{60} \cdot P_i \cdot \eta \right) \geq E_{target} \quad (3)$$

where E_{start} and E_{end} represent energy in the battery at the plug-in and plug-out times respectively. E_{target} is the energy requirement for the battery at the time of plug-out. P_i is the charging power for the time interval i. N is number of 5 minute intervals from plug-in to plug-out. Because the experiments were run with a SOC between 30 to 90%, a linear model was sufficient, since the battery can be charged with constant power in that range [14].

III. Test Cases

The smart charging implementation was tested using two test cases. The input parameters for the two test cases, consisting of simulation and a real-world experiment, are summarized in Table I.

TABLE I
SMART CHARGING TEST PARAMETERS

Case	Plug-in Time	Plug-out Time	Start SOC	Target SOC
1	17:00	01:00	60%	90%
2	22:00	08:00	56%	90%

The two cases show smart charging performance for different time slots. In case one, the charging is done in the late evening hours and in case two it is done overnight. Similar starting SOC are used along with the same target SOC of 90%.

IV. Results

This section describes test results from the smart charging use cases. In both cases an optimal charging schedule was generated by the algorithm according to the supplied price signal.

A. Simulation

Simulation results for case one, where smart charging was performed in the evening, is shown in Fig. 7.

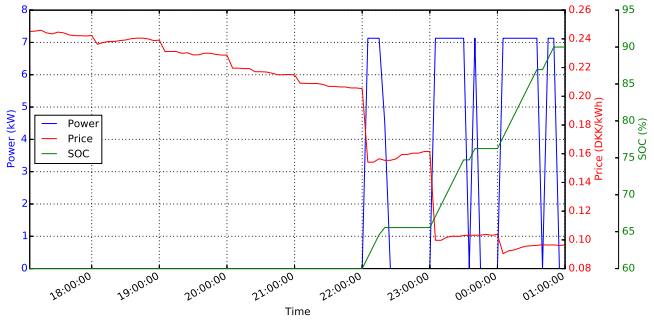

Fig. 7. Smart Charging simulation results for case 1

As can be seen from the figure, the vehicle is plugged in for a whole 7 hours and needs around 2 hours to charge to the target SOC. The smart charging optimization controller produced a schedule that charges the vehicle mainly in the end of the plugged-in time slot. That is due to lower electricity price in that period.

Similar simulation for case two, where smart charging was performed overnight, can be seen in Fig. 8.

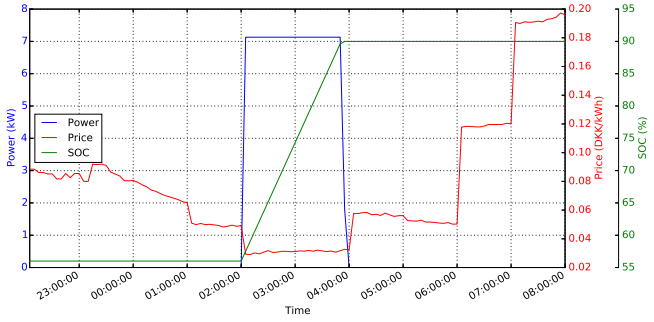

Fig. 8. Smart Charging simulation results for case 2

As can be seen form the results in Figures 7 and 8, the EV is being charged primarily at the lower price values. However, it can also be seen that ,for case one, the charging cost is not absolutely minimal, which is due to the fact that the real-time price differed from the day ahead- and hour ahead predictions, resulting in unexpected change to the original charging schedule.

B. Experiment

After the simulations were performed, a real-world test bench was set up, using the testing system diagram from Fig. 1.

The results of test case one, the evening charging experiment, are plotted in Fig. 9.

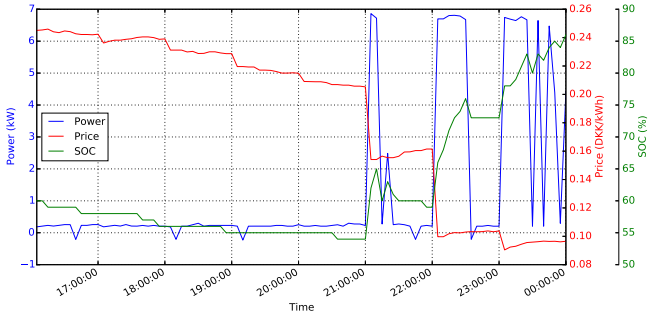

Fig. 9. Smart Charging experiment results for case 1

The final value of SOC in Fig. 9 shows that the vehicle did not reach the target, by plug-out time. It can be explained by the fact that charging efficiency of the real charger was not considered in the vehicle battery charger model. The charging pattern closely resembled the simulated case. The initial drop of in SOC before charging begins, can be explained by the idle power consumption of the PEU as well as the active cooling systems in the vehicle.

In the case two, the experiment with overnight charging, shown in Fig. 10, displays better results.

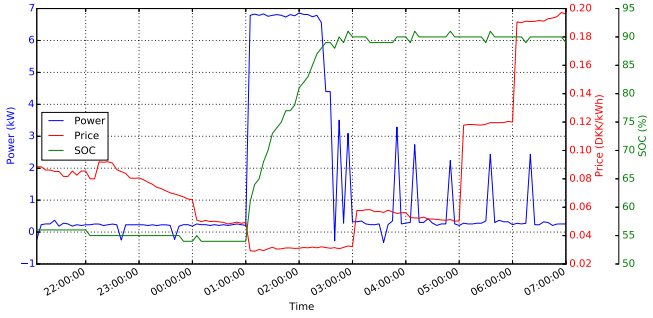

Fig. 10. Smart Charging experiment results for case 2

In this case, the battery model was improved to account for charger efficiency, which means the vehicle battery successfully reached the target SOC before plug-out time. The charging is happening during the cheapest time slots, which closely resembles the simulated case. The small charging peaks present after the vehicle has reached target SOC, is the controller trying to maintain the battery at the target SOC. The reason for the drops, are the same as previously mentioned regarding PEU idle consumption and active cooling system. The idle power consumption could be minimized by putting the vehicle into sleeping mode once the charging is complete, as well as adjusting the thermal regulation of the battery.

All tests were performed in SYSLAB[1] as part of NIKOLA project.

The energy required and charging cost results are summarized in Table II.

TABLE II
SMART CHARGING COST SUMMARY

Case	Energy Needed	Energy Used	Charging Cost
S1	11.66 kWh	9.88 kWh	1.043 DKK
S2	13.22 kWh	14.01 kWh	0.556 DKK
D1	11.66 kWh	11.66 kWh	2.682 DKK
D2	13.22 kWh	13.22 kWh	1.060 DKK

The first two rows, marked as S1 and S2, show the charging costs of smart charging. The last two lines, marked as D1 and D2, show the corresponding costs using the conventional "dumb charging". The first thing to notice, is that smart charging reduces the cost of charging with more than a factor two. The other noticeable thing is that charging in general is rather cheap. That is due to the fact that these prices are derived from bulk electricity prices, and therefore do not include various taxes. However, even after adding taxes, the economic benefit of smart charging versus regular charging, would be still noticeable.

V. DISCUSSION

The results of smart charging have shown that it is possible to effectively regulate EV charging rates, to avoid grid congestion and achieve lower charging costs compared to normal charging. At the same time, it is possible to maintain user comfort *i.e.,* making vehicle ready for the next trip with the desired SOC at the preferred time. However, as shown in this work, the comfort level can be reached only when using accurate estimation models for battery charger and user behavior [15]. This work brings the smart charging closest to real-commercial application. A few high-end EVs models already have a similar remote control interface for checking SOC and setting charging power [16].

Further developments of this work would enable this approach to be applied in real-world field tests. Improved charger and battery models with non-linear components, would allow for the smart charging of the battery all the way from 0 to 100% SOC. Realistic and sophisticated user behavior prediction model, would aid accurate prediction of plug-in and plug-out times. Accounting hour and day ahead price prediction quality would make even more optimal charging schedules and hence cheaper charging.

[1]SYSLAB is a laboratory for intelligent distributed power systems at Technical University of Denmark, Risø campus, it is a part of PowerLabDK (www.powerlab.dk).

REFERENCES

[1] F. Marra and M. Jensen, "Power quality issues into a Danish low-voltage grid with electric vehicles," *Electrical Power Quality and Utilisation (EPQU), 2011 11th International Conference on*, pp. 1–6, 2011.

[2] O. Ma, N. Alkadi, P. Cappers, P. Denholm, J. Dudley, S. Goli, M. Hummon, S. Kiliccote, J. MacDonald, N. Matson, D. Olsen, C. Rose, M. Sohn, M. Starke, B. Kirby, and M. O'Malley, "Demand response for ancillary services," *Smart Grid, IEEE Transactions on*, vol. 4, no. 4, pp. 1988–1995, Dec 2013.

[3] F. Sossan and M. Marinelli, "An auto tuning substation peak shaving controller for congestion management using flexible demand," in *Power Engineering Conference (UPEC), 2013 48th International Universities'*, Sept 2013, pp. 1–5.

[4] A. Aabrandt, P. Andersen, A. Pedersen, S. You, B. Poulsen, N. O'Connell, and J. Østergaard, "Prediction and optimization methods for electric vehicle charging schedules in the edison project," *2012 IEEE PES Innovative Smart Grid Technologies (ISGT)*, 2012.

[5] Energinet, "Smart Grid in Denmark," http://www.energinet.dk/en/forskning/energinet-dks-forskning-og-udvikling/Smart-Grid/Sider/default.aspx, Tech. Rep.

[6] "AC Propulsion eBox," http://www.futurecars.com/reviews/ebox.html.

[7] University of Delaware, "The Grid-Integrated Electric Vehicle," Tech. Rep.

[8] "EU EcoGrid Project," http://www.eu-ecogrid.net/.

[9] D. Gantenbein, C. Binding, B. Jansen, A. Mishra, and O. Sundstrom, "EcoGrid EU: An efficient ICT approach for a sustainable power system," in *Sustainable Internet and ICT for Sustainability (SustainIT), 2012*, Oct 2012, pp. 1–6.

[10] Z. Xu, M. Gordon, M. Lind, and J. Ostergaard, "Towards a Danish power system with 50% wind - Smart Grids activities in Denmark," in *Power Energy Society General Meeting, 2009. PES '09. IEEE*, July 2009, pp. 1–8.

[11] R. T. Fielding, "Architectural styles and the design of network-based software architectures," Ph.D. dissertation, 2000, AAI9980887.

[12] A. Pedersen, E. Hauksson, P. Andersen, B. Poulsen, C. Træholt, and D. Gantenbein, "Facilitating a Generic Communication Interface to Distributed Energy Resources: Mapping IEC 61850 to RESTful Services," in *Smart Grid Communications (SmartGridComm), 2010 First IEEE International Conference on, Maryland*, 17-20 Oct 2010, pp. 61–66.

[13] "Python PuLP," https://code.google.com/p/pulp-or/.

[14] F. Marra, G. Yang, and C. Træholt, "Demand profile study of battery electric vehicle under different charging options," *Power and Energy Society General Meeting, 2012 IEEE*, pp. 1–7, 2012.

[15] J. Iversen and J. Mø ller, "Inhomogeneous Markov Models for Describing Driving Patterns," 2013.

[16] "Unofficial Tesla Model S JSON REST API," http://docs.timdorr.apiary.io/.

Pub. I. Analysis of needs for on-going or incipient standards. Design of Round Robin tests and results of the performed tests. Recommendations for existing standards

COTEVOS

Deliverable D4.3

Analysis of needs for on-going or incipient standards. Design of Round Robin tests and results of the performed tests. Recommendations for existing standards

DTU
2016-02-29
V8.0

Project Full Title: COncepts, Capacities and Methods for Testing EV systems and their interOperability within the Smart grid

FP7-SMARTCITIES-2013, ENERGY 2013.7.3.2
Grant agreement no. 608934
Collaborative Project

Document information

Author(s)	Company
Thomas Meier Sørensen	DTU
Marianne Bruntt Jensen	DTU
Sergejus Martinenas	DTU
Additional authors	**Company**
F. Lehfuss	AIT
G. Mantovani	ALTRA
S. Misara	DERlab
J. Ratej	ETREL
C. Nölle	IWES
E. Karfopoulos	NTUA
F. Beloni, D. Pala	RSE
J.A. López, V. Sánchez, E. Zabala	TECNALIA
J. Laarakkers, R. Koffrie, E. Werkman	TNO
P. Kelm, B. Olek	TUL

WP no. and title	WP4 – Development of tests and procedures
WP leader	DTU
Task no. and title	4.3 – Analysis of needs for on-going or incipient standards. Design and performance of Round Robin tests. Analysis and proposal for procedures to be implemented within COTEVOS
Task leader	DTU

Dissemination level	
PU: Public	**X**
PP: Restricted to other program participants (including the Commission Services)	
RE: Restricted to other a group specified by the consortium (including the Commission Services)	
CO: Confidential, only for members of the consortium (including the Commission Services)	

Status	
For information	
Draft	
Final Version	**X**
Approved	

Revisions			
Version	**Date**	**Author**	**Comments**
0.0	20140606	Thomas Meier Sørensen	First Layout and Integrating of the detailed work plan
1.0	20150620	Thomas Meier Sørensen	2.layout
2.0	20151110	Thomas Meier Sørensen	3.version – new structure – new templates
3.0	20151123	Sergejus Martinenas	Implementing first review comments and improvements
3.1	20151126	Sergejus Martinenas Thomas Meier Sørensen	Further improvements after internal review
3.2	20151128	J.A. López, E. Zabala	Overal review
4.0	20151130	Sergejus Martinenas Thomas Meier Sørensen	Further improvements after internal review, for version delivered to EC

4.1	20160130	J.A. López	Overal review and proposal for improvements
5.0	20160211	Sergejus Martinenas Thomas Meier Sørensen	Updated input from partners
6.0	20160225	Sergejus Martinenas Thomas Meier Sørensen	Further improvements after internal review
7.0	20160229	Sergejus Martinenas Thomas Meier Sørensen	Updated input from partners
8.0	20160229	J.A. López, E. Zabala	Overal review

Executive Summary

This deliverable documents the procedures, for doing cost efficient interoperability testing on the COTEVOS unified infrastructure. It covers conformance testing based on standards and interoperability testing based on informational objects and functions where standards are not available.

To cover the whole scene of eMobility, a COTEVOS methodology for developing test cases was envisioned and developed. The methodology ensures that future input from eMobility stake holders can be processed and used for future test cases. Input can equally come from standardization activities or academia.

This deliverable describes several ways of validating the test cases. With the developed methodology, the set of test cases can be expanded to any level within the available test facilities. However the present test cases are not a complete set of interoperability test cases, since they are adapted to the available test infrastructure. Full interoperability calls for a longer period of testing combined with an ongoing process of adding relevant test cases when interoperability issues are reported.

A selection of test cases was developed to be a part of a round robin test. That means that when the round robin tests are accomplished successfully at all facilities, customers can get the relevant tests performed at any of the round robin test facilities/laboratories. With an identical result test matrix describing the available test at each participating laboratory is also developed.

Finally, the deliverable documents a plan for future expansion and validation of interoperability issues in the eMobility scene.

The main recommendation is that there is a need for a harmonized set of standards. These standards should cover all interfaces between actors on the eMobility scene. This will remove the root cause to most of the known interoperability issues at present.

Table of contents